Selective Induction of Apoptosis in HIV-infected Macrophages

by

Simon Xin Min Dong

A thesis submitted in partial fulfillment of the requirements for the

Doctorate in Philosophy degree in Microbiology and Immunology

Department of Biochemistry, Microbiology, and Immunology

Faculty of Medicine

University of Ottawa

uOttawa

Abstract

The eradication of Human Immunodeficiency Virus (HIV) from infected patients is one of the major medical problems of our time, primarily due to HIV reservoir formation. Macrophages play important roles in HIV reservoir formation: once infected, they shield HIV against host anti-viral immune responses and anti-retroviral therapies, help viral spread and establish infection in anatomically protected sites. Thus, it is imperative to selectively induce the apoptosis of HIV-infected macrophages for a complete cure of this disease.

I hypothesize that HIV infection dysregulates the expression of some specific genes, which is essential to the survival of infected host cells, and these genes can be targeted to selectively induce the apoptosis of HIV-infected macrophages. My objective is to identify the genes that can be targeted to eradicate HIV reservoir in macrophages, and to briefly elucidate the mechanism of cell death induced by targeting one of the identified genes.

A four-step strategy was proposed to reach the goal. First, 90k shRNA lentivirus pool technology and microarray analysis were employed in a genome-wide screen of genes and 28 promising genes were found. Second, siRNA silencing was applied to validate these genes with 2 different HIV-1 viruses; as a result, 4 genes, *Cox7a2*, *Znf484*, *Cdk2*, and *Cstf2t*, were identified to be novel gene targets. Third, the 4 validated genes were characterized by literature review. Lastly, I briefly elucidated the mechanism of apoptosis induced by targeting one of the identified gene, *Cox7a2*.

The results of this study can help to understand the mechanisms of HIV reservoir formation in macrophages and propose promising therapeutic targets for the eradication of HIV-infected macrophages from patients.

Acknowledgements

First of all, I would like to thank my supervisor, Dr. Ashok Kumar, for his mentorship of my PhD studies. It was his diligence, intelligence, and full support that made me step forward day by day. This study was also under the instructions of Dr. Franco Vizeacoumar from the University of Saskatchewan; his timely and patient guidance made applying a novel technology to this research possible. Dr. Angela Crawley, Dr. Tommy Alain, and Dr. Jonathan Angel, who were my Thesis Advisory Committee members, also gave me pertinent advice during this study; their encouragement allowed me to grow as an independent medical researcher.

In addition, Xiao Xiang, Niranjala Gajanayaka, Ramon Caballero, and Hamza Ali provided me everyday assistance. Duale Ahmed, David L. F. Roy, and Faria Ahmed also helped for some experiments and data analysis. Dr. Sandra Côte, Stephanie B. Schinkel, and Teslin Sandstrom at OHRI provided me assistance whenever I needed. Dr. Jason Fernandes, and Dr. Hapsa Mamady were my role models to be a medical researcher. Both Jasmine Huang and Ana Radar worked as part-time summer students for this project.

Finally, I would also like to say many thanks to Lynn Kelly, Martine St-Jean, Stephen Baird, Keith Wilson, and many other staff at the Apoptosis Research Center of Children's Hospital of Eastern Ontario. It was their timely assistance that made my work highly efficient so that I could progress rapidly. The selfless contributions from Katelynn J. Rowe (OHRI) were also indispensable to complete this research project.

Here I would like to express my sincere gratitude and respects to all of them.

Table of Contents

List of Abbreviations

AIDS	Acquired Immuno-deficiency Syndrome
ANT	Adenine Nucleotide Translocase
ART	Anti-retroviral Therapy
ATCC	American Type Culture Collection
BAD	BCL-2-associated Death protein
BAX	BCL2 Associated X protein
BBB	Blood-brain Barrier
BCL-2	B Cell Lymphoma 2
BSA	Bovine Serum Albumin
CDC	Centers for Disease Control
CDK2	Cyclin-Dependent Kinase 2
CNS	Central Nervous System
COX7A2	Cytochrome C Oxidase Subunit 7A2
CSTF2T	Cleavage Stimulation Factor subunit 2 tau variant
DCs	Dendritic Cells
dsDNA	double-stranded DNA
EDTA	Ethylenediamine Tetra-acetic Acid
ES	Elite controllers or Suppressors
FBS	Fetal Bovine Serum
GALT	Gut-associated Lymphoid Tissue
(e)GFP	(enhanced) Green Fluorescent Protein
HAART	Highly Active Antiretroviral Therapy
cART	Combination Antiretroviral Therapy
HPCs	Hematopoietic Progenitor Cells
HIV	Human Immunodeficiency Virus
HIV-1	Human Immunodeficiency Virus type 1
HIV-2	Human Immunodeficiency Virus type 2
HIV-HSA	HIV-1 virus produced from plasmid pNL4.3-BAL-IRES-HSA

HIV-eGFP	HIV-1 virus produced from plasmid HIV Gag-iGFP(envJRFL)
HSA	mouse Heat Stable Antigen, mouse CD24
IAP	Inhibitor of Apoptosis Protein
xIAP	X chromosome-linked Inhibitor of Apoptosis Protein; BIRC
cIAP1	cellular Inhibitor of Apoptosis Protein-1; BIRC 2
cIAP2	cellular Inhibitor of Apoptosis Protein-2; BIRC 3
cIAP1/2	cIAP1 + cIAP2, or BIRC2 + BIRC3
IAPs	xIAP + cIAP1 + cIAP2, or BIRC1 + BIRC2 + BIRC3
ICTV	International Committee on the Taxonomy of Viruses
IFN(s)	Interferon(s)
IMM	Inner Mitochondrial Membrane
IRES	Internal Ribosome Entry Site
LPS	Lipopolysaccharides
LTR(s)	Long Terminal Repeat(s)
LZhuTRAIL	Leucine Zipper Human TRAIL
LTNP(S)	Long-term Non-progressor(s) (of HIV-infected patients)
NK	Natural Killer cells
mAb	Monoclonal Antibody
MCS	Multiple Cloning Site
M-CSF	Macrophage Colony-stimulating Factor
MHC I	Major Histocompatibility Complex I
MMP	Mitochondrial Membrane Potential
Gd-Tex	Motexafin Gadolinium
mPTPC	mitochondrial Permeability Transition Pore Complex
mtDNA	mitochondrial DNA
NFκB	Nuclear Factor kappa B
NIH	National Institutes of Health
ORF(s)	Open Reading Frame(s)
PAGE	Polyacrylamide Gel Electrophoresis

PCR	Polymerase Chain Reaction
PBMC(s)	Peripheral Blood Mononuclear Cell(s)
PBS	Phosphate-buffered Saline
PMA	Phorbol 12-myristate 13-acetate
(primary) MDMs	(primary) Monocyte-derived Macrophages
PI	Propidium Iodide
RESV	Resveratrol
RIPK1	Receptor Interacting Protein Kinase 1
ROS	Reactive Oxygen Species
SDS	Sodium Dodecyl Sulfate
SMAC	Second Mitochondria-derived Activator of Caspase
SM(s)	SMAC Mimetic(s)
siRNA	small interfering RNA
SD	Standard Deviation
SOD	Superoxide Dismutase
Tat	(HIV) Trans-activator protein
TCR	T Cell Receptor
TNF-α	Tumour Necrosis Factor alpha
rTNF-a	Recombinant Tumor Necrosis Factor-alpha
TRAIL	TNF-related Apoptosis-inducing Ligand; CD253
TREM-1	Triggering Receptor Expressed on Myeloid cells 1
VCCs	Virus Containing Compartments
VDAC	Voltage-dependent Anion Channel
Vpr	(HIV) Virus Protein R
ZNF484	Zinc Finger Protein 484

List of Figures

List of Tables

1. General Introduction

1.1 A brief history on HIV/AIDS

The story of Acquired Immuno-deficiency Syndrome (AIDS) started in the summer of 1981, when the diagnosis of pneumocystis pneumonia in five previously healthy men was reported in the United States [1]. Numerous cases were reported with similar opportunistic infections by the end of this year [2,3], and the Centers for Disease Control of US received reports of 593 cases before September 15, 1982, reflecting the rapid increase in the clinical diagnosis of this disease [4]. This disease is characterized by the massive destruction of CD4+ T cells, causing progressive impairment of cellular immunity and increasing susceptibility to opportunistic infections [5]. A key milestone was reached in 1983, when Barré-Sinoussi et al and Gallo et al independently reported their isolations of a T-lymphotropic retrovirus from HIV-infected patients [6,7]. In 1986, the International Committee on the Taxonomy of Viruses (ICTV) proposed that the causative agents of AIDS be named Human Immuno-deficiency Virus (HIV) [8].

Since the discovery of the virus in 1983, governments, scientists, clinical doctors, and general public worldwide have dedicated considerable efforts to seek a cure for this disease. In the fiscal year of 2019, the US government invested $34.8 billion as the federal funding for HIV [9]. All the endeavors rapidly increased the basic knowledge on the virus, the molecular and behavioral aspects of transmission, the immune response to HIV infection, and the clinical course of AIDS [10]. Notably, the extensive research on HIV also led to remarkable progress in many other medical fields, such as Molecular Biology, Virology, Immunology, and Pharmacology [11]. The

full-length of the viral genome of many strains has been sequenced [12] and a universal strategy for amplifying and sequencing heterogeneous HIV whole genomes has been developed to identify newly emerging HIV strains [13]. Moreover, the molecular structure of HIV has been elucidated and the 3-dimensional crystal structure of viral proteins has been determined to 3Å resolution [14]. Another milestone in Anti-HIV research was the introduction of an anti-retroviral treatment, Highly Active Antiretroviral Therapy (HAART) in 1996, which could effectively control the clinical progression of this disease [15]. However, strict adherence is essential and an interruption causes a rebound of viremia and subsequent immune dysfunction [16]. The major issue in current treatment is that anti-HIV drugs cannot completely eradicate the viruses from human body, causing the need to search for novel cures for this disease [17].

1.2 General information about HIV/AIDS

1.2.1 The epidemiology of HIV infection

Currently, HIV infection is a worldwide epidemic, affecting approximately 36.9 million people all over the world in 2017 [18]. In 2016, it was estimated that there were 63,110 people living with HIV in Canada, but only 86% of those are diagnosed [19]. There are two types of HIV: HIV-1 and HIV-2. The predominant type is HIV-1, which accounts for approximately 95% of all infections worldwide. HIV-1 comprises three major groups (M, N, and O), and their genetic divergence can be as much as 40% [20]. 55% of HIV-2 genome is distinct from HIV-1, leading to a similar disease, but it is uncommon, less infectious, causes fewer deaths, and is mainly confined to West Africa [21,22].

1.2.2 HIV-1 viral genome and structure

HIV is an enveloped retrovirus ~100 nM in diameter, containing two copies of non-covalently linked, un-spliced positive-sense single-strand RNA enclosed by a conical capsid composed of viral protein p24 [23]. A haploid set of viral RNA is ~9.8kb, with multiple Open Reading Frames (ORFs) flanked by 5' and 3' Long Terminal Repeats (LTRs), and encodes 15 proteins in total [23]. LTRs are essential sequences for retrovirus to integrate its genetic material into host genomes, and they also act as promoters to drive viral gene expression [24]. Long ORFs encode structural proteins (Gag, Pol, and Env), whereas smaller ORFs encode regulatory proteins (Tat, Vpu, Vpr, Vif, Nef, and Rev) [25]. The HIV-1 genome and proteins are shown in **Figure 1**.

1.2.3 HIV-1 viral genes and proteins

The precursor of Gag is a p55 myristoylated protein, which is processed to p17 (Matrix), p24 (Capsid), p7 (NucleoCapsid), and p6 proteins by the viral protease [26]. The *pol* gene encodes 3 viral enzymes: protease, reverse transcriptase, and integrase. Protease cleaves precursor Gag into structural proteins, reverse transcriptase transcribes DNA from the viral RNA template, and integrase integrates double-stranded viral DNA into host genome [27]. The *env* Gene is translated to a precursor (gp160), which is processed by a host protease "furin" into an external glycoprotein (gp120) and a transmembrane glycoprotein (gp41) [28]. The glycoprotein gp120 acts as a ligand for CD4 receptor on CD4+ cells and couples with the seven transmembrane domains of its co-receptors [29]. The regulatory proteins can be grouped into essential regulatory elements (Tat and Rev) and accessory regulatory proteins (Vpu, Vpr, Vif, and Nef). Of all these HIV proteins, Trans-activator (Tat) and Virus Protein R (Vpr) are most relevant to this study. Tat has been identified to be an

Figure 1. The genomic structure and proteins of HIV-1.

HIV is an enveloped retrovirus with two copies of positive-sense genomic RNA, approximately 100 nM in diameter. A single set of viral RNA is ~9.8kb with multiple ORFs flanked by 5' and 3' LTRs and encodes 15 proteins in total. Long ORFs encode structural proteins (Gag, Pol and Env), whereas smaller ORFs encode regulatory proteins (Tat, Vpu, Vpr, Vif, Nef, and Rev). The *gag* gene is translated into a precursor protein p55, which is processed to p24, p17, p7, and p6 by viral protease (25). The *pol* gene encodes 3 viral enzymes, protease, reverse transcriptase, and integrase. The *env* gene is translated to a precursor protein gp160, which is processed by a host protease into an external glycoprotein gp120 and a transmembrane glycoprotein gp41. The regulatory proteins include essential regulatory elements (Tat and Rev) and accessory regulatory proteins (Vpu, Vpr, Vif, and Nef) [30].

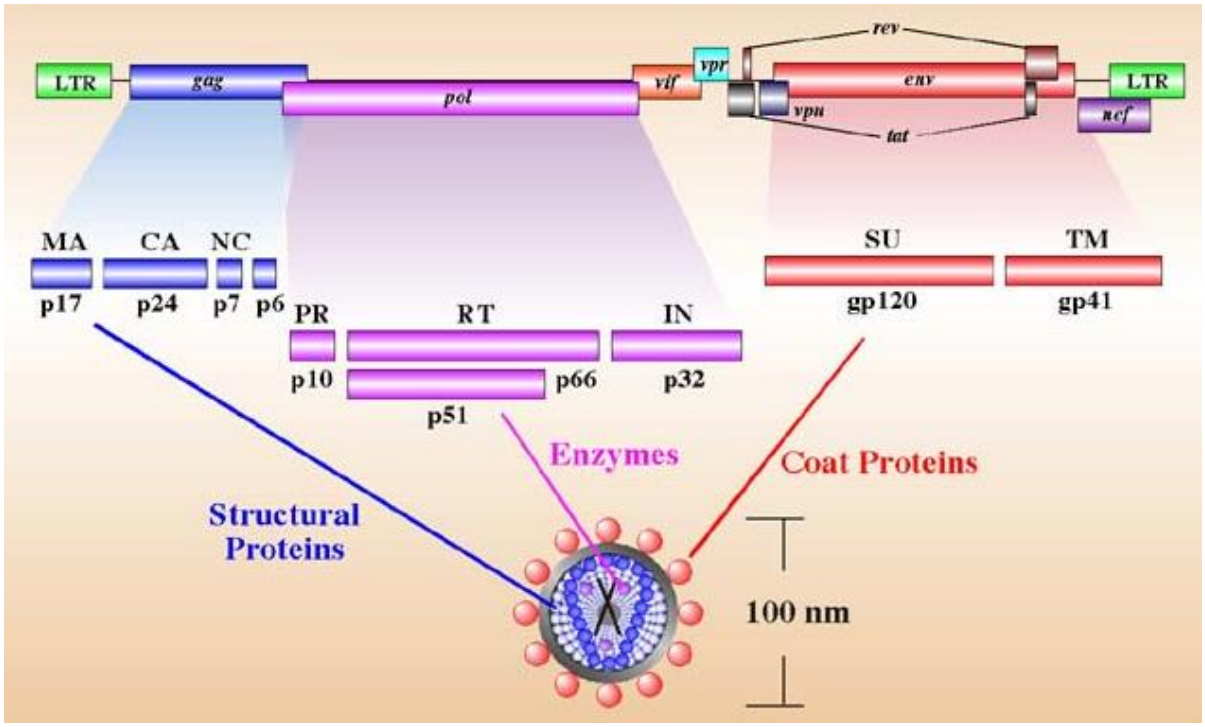

Adapted from website:
https://web.stanford.edu/group/virus/retro/2005gongishmail/HIV-1.jpg

essential regulatory element in activating the reverse transcription of viral genome RNA, ensuring efficient synthesis of viral mRNAs, and regulating the release of virions from host cells [31]. Vpr plays an important role in viral replication, especially the nuclear import of the pre-integration complex. In addition, Vpr arrests host cells in G2 phase, activating host DNA repair machinery, which enables the integration of viral genetic material into the genome of host cells [32].

1.3 Transmission, infection, integration, and life cycle of HIV

HIV is transmitted by three principal ways: blood, sexual contact, and mother-to-child [33]. The number of infectious viral particles and the area exposed to viruses greatly influence the transmission [34]. First, blood transfusion recipients could be infected by the viruses in blood and blood products. The study from Ho et al found that almost all the blood samples from HIV patients contain circulating infectious virus whether the individual is symptomatic or not, and HIV is readily found during acute infection, and the mean virus titers can be as high as 32,3500 infectious particles per ml [35]. Second, when the virus was first identified, it was believed to be transmitted by a sexual route. A high prevalence among homosexual men was initially reported, but now heterosexual activities were found to account for most of HIV infections worldwide, and the amount of virus in genital fluids is important for sexual transmission [36]. This route of transmission of HIV is likely through virus-infected cells since they can be present in larger numbers than free virus in bodily fluids [37]. During sexual transmission, HIV may enter the mucosal tissue and the viruses are endocytosed by epithelial Langerhans cells, which facilitate the cell-to-cell transfer of viruses to resident lymphocytes, macrophages, and other epithelial cells susceptible to HIV [38,39]. Third, Polymerase Chain Reaction (PCR) and virus culture studies indicate

that the mother-to-child transmission after birth is responsible for transmission to 11~60% of children born to HIV-positive mothers [40,41]. Clinical observations found that HIV could not be readily isolated from cord blood, but could be detected from virus-infected infants older than 1 month [42,43], indicating transmission can occur either in utero, or during or after delivery through contact with amniotic fluid, genital secretions, or blood of the mother [44].

Identification of the HIV receptor and co-receptors was crucial to understand the pathogenesis of AIDS. In 1984, CD4 on the cellular membrane was identified to be the HIV receptor [45], but CD4 is insufficient to trigger viral fusion at cellular membrane [46]. In 1996, the co-receptors essential for viral entry were identified to be CXCR4 for T-tropic strains, and CCR5 for M-tropic strains [47]. Some HIV strains use CCR2b, CCR3 and CCR8 as co-receptors for infections [48]. A genetic mutation known as CCR5-δ32 prevents infection of HIV-1, highlighting the roles of co-receptors in HIV infection [49]. T lymphocytes, macrophages, and astrocytes are the primary targets of HIV infection, whereas B lymphocytes, natural killer cells (NK), dendritic (including Langerhans) cells, hematopoietic stem cells, endothelial cells, and gastrointestinal epithelial cells are potential targets of HIV [50]. The HIV envelope glycoprotein gp120 binds to CD4 as its primary receptor, which is followed by a series of conformational changes that expose gp120's binding site for co-receptors [51]. The co-receptor then forms a complex with CD4 and HIV, leading to gp41-mediated fusion of viral and target cell membranes, which allows viral entry into the host cell and then releases the viral capsid into the cytosol [52].

After fusion, several intracellular events occur in succession, resulting in the integration of the viral genome into the host genome. The nucleocapsid is transported

to the late endosomes for uncoating and then delivered to the cytoplasm [53]. The viral RNA is then reversely transcribed by the viral reverse transcriptase, and eventually double-stranded DNA (dsDNA) is synthesized [54,55]. Subsequently, the dsDNA is imported into the nucleus and finally integrated into the cellular chromosome as a provirus [56]. The integration of viral DNA appears to be random and is previously believed to be essential for the cells to produce progeny virions [57]. However, in recent years, much evidence indicates that there are multiple forms of unintegrated viral DNA, which may help productive infection through the expression of early viral genes [58].

Although HIV has cytopathic effects in permissively infected cells, the virus may remain inactive (latent) in the permissively infected cells for long periods of time [59]. If host cells are quiescent or arrested in division, the infection is abortive; whereas in non-dividing cells, such as permissive activated T cells, macrophages or epithelia, progeny production takes place [60]. In permissive infections, the viral genome will be integrated, and viral replication starts within 24 hours in T cells [61], and after 48 hours in macrophages [62]. During replication, the earliest mRNA has a low molecular weight, indicating the transcription of regulatory genes, such as *tat*, *rev*, and *nef* [54,63,64]. *tat* is the earliest protein produced and subsequently upregulates the expression of Rev. Rev protein provides a balance in expression of *tat* and *nef*, which determines if the infection enters a productive or latent state: the predominance of Tat protein will lead to virus production, and the expression of Nef protein may induce viral latency [65]. In the early stage of replication, Rev upregulates unspliced mRNA, which is responsible for the other essential viral gene products to assemble new progeny particles. In the late stages, Rev downregulates its own expression, leading to

reduced replication and perhaps latency [66,67]. During productive infection, the cellular machinery transcribes proviral DNA into viral RNA, which is used as the template to produce viral proteins. Two copies of viral RNA with structural proteins are transported to the cellular membrane and then assembled into progeny virions. Mature virions bud from the cellular membrane and are released to the cellular milieu for new infections [68]. The life cycle of HIV-1 is summarized in **Figure 2**.

1.4 Immune dysregulation due to massive depletion of CD4+ T cells

The pathogenesis of AIDS is characterized by immune dysregulation. HIV specifically targets CD4+ cells, including T cells, macrophages, and dendritic cells; consequently, these cells are unable to fulfill their functions in immune signaling responses to foreign pathogens [60]. The progressive and massive depletion of CD4+ T cells is closely associated with immunological failure of HIV-infected patients [5]. There are two mechanisms accounting for the massive loss of CD4+ T cells: direct cytopathic effects (CPE) of HIV virus and the apoptosis of uninfected bystander cells [69]. The direct viral killing of HIV-infected cells is due to altered intracellular ion concentrations [70], cell lysis caused by increased cytosolic volume [71], cytolytic killing caused by viral fusion and budding [72,73], and natural killer (NK) cell-mediated cytotoxity [74,75]. However, in situ hybridization studies measuring viral RNA suggests that the number of productively HIV-infected CD4+ T cells are only 10% of the total CD4+ T cell pool [76], indicating other mechanisms are responsible for the massive loss of CD4+ T cells *in vivo*.

Further studies found that the apoptosis of uninfected bystander T cells was crucial in the pathogenesis of AIDS [5], and it was believed to be the driving force of the fast and selective depletion of CD4+ T cells leading to immunodeficiency [77]. However,

Figure 2. The life cycle of HIV

A typical HIV life cycle has eight stages: binding, fusion, reverse transcription, integration, transcription, replication, assembly, and budding. **1.** gp120-mediated binding to host cells; **2.** gp41-mediated fusion of viral and target cellular membranes; **3.** Reverse transcription of viral RNA into cDNA and dsDNA; **4.** Integration of viral origin dsDNA into cellular genome; **5.** Host cell activation and transcription of proviral DNA into RNA; **6.** Translation of viral RNA into viral proteins; **7.** Assembling two copies of viral RNA and structural proteins into progeny virions; **8.** budding from the cellular membrane and being released for new infections [78].

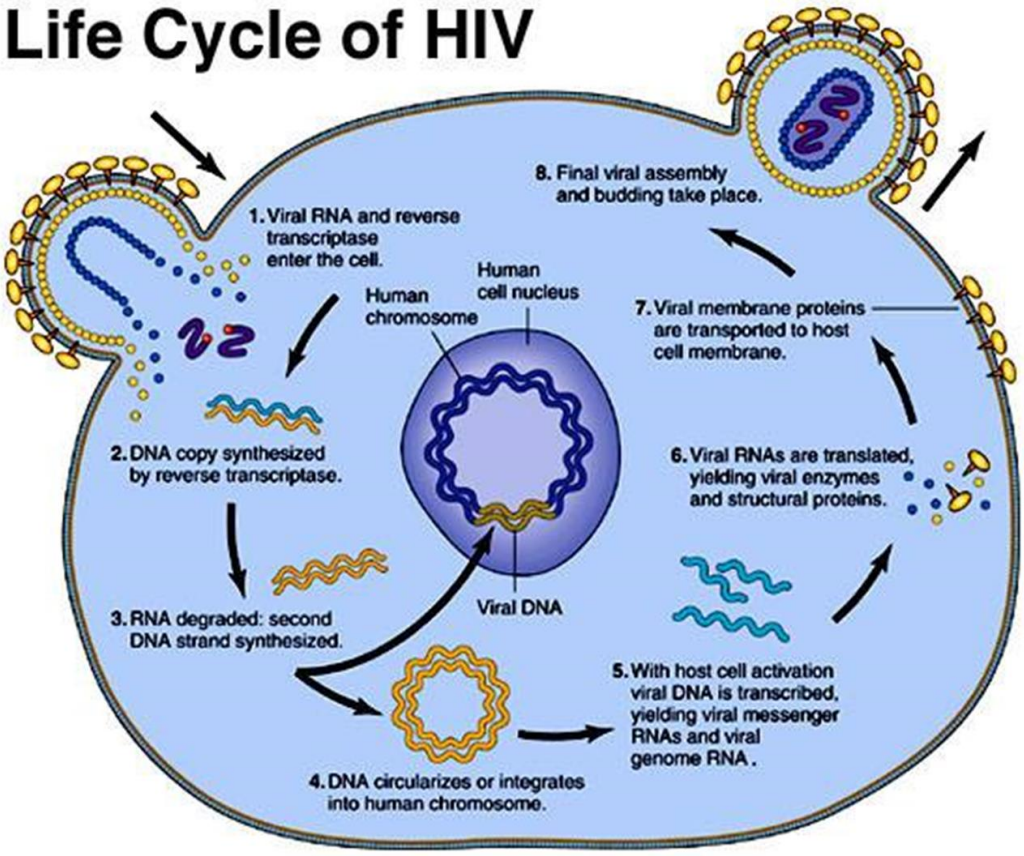

Byer CO., Galliano G, Shriver SP. Dimensions of human sexuality. McGraw-Hill Humanities Social. 2002.

the mechanisms governing the loss of CD4+ T cells are not fully understood. Existing literature indicates that viral proteins like Env, Tat, Nef, Vpu, Vpr may be involved in this pathological process [79]. Multiple factors have been found to be associated with HIV-induced uninfected bystander apoptosis, including Env glycoprotein phenotype, virus tropism, disease stage, co-receptor expression, immune activation, and therapies targeting the viral envelope [77]. Three major apoptotic pathways were postulated to elucidate the fast and massive loss of uninfected bystander T cells.

The first possible mechanism is Env-induced apoptosis of uninfected bystander cells due to repeated antigenic stimulation and interaction of the cell death receptor Fas and its ligand (Fas-L) [80]. Env is a soluble protein secreted from infected cells, and is able to directly induce the apoptosis of uninfected bystander T cells expressing receptor CD4, or co-receptors CCR5 or CXCR4 [80]. A transient contact between two interacting cells (one expresses Env and the other expresses receptor or co-receptors) causes the exchange of plasma membrane, leading to the rapid death of receptor or co-receptor expressing cells [81]. Ahr believed that it is very likely that CD4+ uninfected T cells from HIV-infected patients are continuously undergoing CD4 cross-linking through interaction with virions or via Env expressed at the surface of infected cells [80]. Tateyama et al demonstrated that cross-ligation of CD4 molecules prior to T cell receptor (TCR) stimulation triggers the upregulation of Fas on purified T cells and expression of Fas-L upon antigen, mitogen, and CD3 stimulation, sensitizing T cells to Fas-mediated apoptosis [82]. When the CD4-cross-linked uninfected T cells encounter antigen presenting cells in the local environment, they receive stimulatory signals through TCR, leading to increased apoptosis [82,83].

The second possible mechanism is the syncytia formation of neighboring cells, which then induces the apoptosis of uninfected bystander cells. The process of syncytia formation mediated by gp41 is a hallmark of HIV infection [77]. Murooka et al demonstrated that the syncytia formation in lymph nodes of HIV-infected humanized mice result from HIV-Env mediated fusion [84]. Syncytia formation starts from the fusion of two cellular membranes, followed by mixing of their cytoplasma and eventually the fusion of the two nuclei [85]. Syncytia formation activates Cdk1, Chk2, mTOR, p38 MAPK, and/or IKK, as well as NFκB and/or p53, resulting in the activation of intrinsic signaling pathway of apoptosis [81,86]. Perfettini et al. concluded that the consequence of syncytia formation was apoptosis [87]. Notably, syncytia formation has been found to be correlated with the progression and pathogenesis of AIDS, and viruses with syncytia inducing phenotype have been demonstrated to be associated with rapid CD4+ T cell decline [88].

The third mechanism is hemi-fusion of HIV-infected cells undergoing apoptosis with uninfected bystander CD4 or co-receptor expressing cells, leading to rapid transmission of apoptotic signals from one cell to the other; thus, apoptosis happens in a transmittable fashion [89]. The process of hemi-fusion is also mediated by gp41 [81,90–93], and involves transient fusion of cellular membranes resulting in a mixture of the outer leaflets of the plasma membrane bilayers [94]. Blanco et al found that apoptosis induced by Env requires intimate cell to cell contact and binding to the co-receptor CXCR4 that could be reversed by addition of the CXCR4 inhibitor AMD3100 [95]. Greg et al discovered that HIV gp41 mediated hemi-fusion initiates an apoptotic cascade that involves caspase 3 activation but is independent of FAS or other cell surface death receptor signaling like TNF or TRAIL [81,92]. Further studies using gp41

mutants with variable levels of fusion activity, including a hemi-fusion restricted mutant, indicated that bystander apoptosis was correlated with cell to cell hemi-fusion induction but not necessarily with virus infection or replication [96].

Therefore, existing studies strongly suggest that the apoptosis of uninfected bystander cells expressing receptor and co-receptors, is mediated primarily by Env gp41, causing a fast, selective, and massive depletion of CD4+ T cells. Although the intracellular and extracellular scenario of macrophages and T cells are quite different from each other, the mechanism of apoptosis in uninfected bystander T cells may help to understand the apoptosis of uninfected bystander macrophages.

1.5 The natural course of HIV infection without treatment

After infection, HIV targets the immune system and weakens the defense of the human body. Untreated individuals gradually become immunodeficient and susceptible to a wide range of infections, cancers and other diseases, resulting in death. In contrast, the life expectancy of individuals who are diagnosed and treated early is significantly increased. Therefore, understanding the natural courses of HIV infection helps to prevent this disease. The natural course of untreated HIV infection can be divided into three stages: acute primary infection, asymptomatic stage (clinical latency), and symptomatic HIV infection [97]. The symptoms of this disease at each stage vary from person-to-person and some individuals may not have any symptoms for many years [98].

The initial stage of HIV infection is called acute primary infection. Around two to four weeks after exposure, some individuals experience symptoms that feel like flu, while others have no obvious symptoms [98]. The symptoms are due to the immune response caused by primary infection [99]. It may take the immune system a couple

of weeks to a few months to produce HIV-specific antibodies as a response to the infection [99]. After exposure, the viral load in the blood starts with a short eclipse period of 8-10 days, during which the viral RNA is undetectable [100]. This period is followed by the appearance of HIV-1 markers (viral proteins and RNA) and HIV specific IgM in peripheral blood, along with various clinical symptoms, and a substantial drop in CD4+ T cell counts [99]. The viral load in the blood increases quickly and reaches a peak at 10^6-10^7 copies of RNA/ml, followed by a rapidly decrease to an average of 21 days after infection [101].

The asymptomatic stage begins after seroconversion, and the HIV-infected patients often feel better because the immune system starts to control the viral replication. Porter et al investigated 1202 HIV-infected patients, finding that for untreated individuals, the median time of this stage ranges from 8.1 to 10.8 years [102]. The viral load in blood at this stage is 5- to 50-fold lower than the peak in the first stage, and the number of T cells comes back to normal or near-normal levels [101]. Without treatment, some HIV-infected individuals can completely control viral replication. The viral load in their blood is undetectable (<50 copies/ml) and they do not show any clinical symptoms of AIDS for many years. Clinical observations found that there are two distinct subsets of patients: Elite controllers or suppressors (ES) are untreated patients, but they are able to completely control viral replication in their bodies [103]. Long term non-progressors (LTNPs) are the patients with stable CD4 counts for more than 5 years without antiretroviral therapy, but most of LTNPs have detectable levels of viremia and eventually progress to AIDS [104]. Sedaghat et al found that T cell counts in the majority of ES remained stable for more than 10 years after infection, but the gradual decline of CD4 cell counts could be observed in some

individuals [103]. However, the viruses are still active, continuously infect and kill new cells, produce progeny particles slowly, and gradually reduce the number of CD4 cells until the immune system is severely damaged, but the balance between cell death and proliferation is maintained due to immune activation at this stage [105].

The immune system cannot control the viral replication indefinitely. Thus, the natural course of HIV infection will finally enter the third stage, symptomatic HIV infection or AIDS, when the immune system is severely damaged [97]. CD4+ T cell counts in HIV-infected patients predicts the onset of immune-deficiency [106,107]. At this stage, the patients' CD4+ T cell count is lower than 350 cells/ml [108], and the infected individuals are more likely to get serious infections, cancers, or other diseases that the body would usually be able to fight off [109,110].

The natural course of HIV infection without treatment indicates that as the disease progresses, the virus will cause more and more damage to the immune system, suggesting that the earlier a person is diagnosed and treated, the better for her/his long-term health.

1.6 Anti-retroviral treatments after HIV infection

The identification of HIV in 1983 and the development of a diagnostic serologic test for the virus in 1985 have provided a good basis for early diagnosis of this disease. In addition, anti-HIV therapy changed dramatically with the introduction of antiretroviral drugs in 1987 and was revolutionized by combination antiretroviral therapy (cART) in 1996. As a result, HIV-infected individuals who are diagnosed and treated early can have normal life expectancy [111].

HIV infection is characterized by viremia, and the virus load in blood is highly related to disease progression [112]. In 1987, a powerful breakthrough in anti-HIV

treatment was achieved, when Azidothymidine, also known as Zidovudine, was introduced as the first treatment for HIV. This discovery was followed by the development of many other anti-HIV drugs [113]. In 1996, Highly Active Antiretroviral Therapy (HAART), which is a combination of three or more anti-retroviral drugs (inhibitors of protease, integrase, and reverse transcriptase) was recommended to treat HIV-infected patients [15]. This cocktail has been demonstrated to be highly effective at reducing viral replication and viral load in the blood can be suppressed to an undetectable level (50 copies/ml), but it rebounds once the drug treatment is stopped or interrupted [16]. Thus, HAART requires life-long adherence and does not completely eradicate HIV. On the other hand, although HIV vaccine trials have shown encouraging results, so far vaccines only provide partial protection [114]. To date, no HIV-vaccine has been approved due to the low overall efficacy as well as other reasons [114].

In the first three years after the introduction of HAART, the mortality of AIDS and hospitalizations decreased 60~80% (159). Suppressing HIV replication with HAART increased peripheral blood CD4+ T-cell counts rapidly and reversed immunodeficiency (160). Sedaghat's study found that HAART reduced immune activation in ES who have significant decline in CD4+ T cells, indicating viral suppression has long-term benefits for HIV carriers [115]. Therefore, the World Health Organization recommended that once the diagnosis is made, regardless of CD4+ T cell counts, the infected individuals, including pregnant women, start continuous, life-long antiretroviral treatments [116]. The expected clinical effect of HAART is that the long-term HIV-RNA count in the blood is below 50 copies/ml. If the HIV-RNA count in blood is greater than 400 copies/ml, the viral suppression is deemed to be inadequate

[110]. Based on these criteria, HAART is effective in more than 95% of infected patients [110,117].

1.7 Genetic diversity of HIV viruses

One of the remarkable characteristics of HIV is its rapid mutation [118]. The spontaneous mutations determine genetic diversity and viral evolution, which helps HIV escape the immune response, rapidly evolve drug resistance, and circumvent vaccination strategies [119]. Therefore, the rapid mutation of HIV is an important factor in the pathogenesis of AIDS.

By using intrapatient frequency of premature stop codons, Cuevas et al quantified the HIV-1 genome-wide rate of spontaneous mutations, finding an extremely high mutation rate of $4.1 \pm 1.7 \times 10^{3}$ per base per cell. They believed it was the highest reported for any biological entity [119]. The high mutation rate is believed to be due to the inability of the viral reverse transcriptase to accurately transcribe RNA to DNA, recombination, and short generation times, resulting in many genetically distinct subgroups [120]. However, Cuevas et al found that the HIV-1 reverse transcriptase contributes only 2% of mutations, whereas 98% result from editing by host cytidine deaminases of the APOBEC3 family [119], indicating that host factors play a more important role than reverse transcriptase in genetic diversity of the virus.

Due to rapid mutation and genetic diversity, some HIV subgroups show resistance to antiretroviral drugs and vaccines targeting viral proteins. Thus, a combination of different antiviral drugs has to be used for treatment [121]. After investigating the drug susceptibility from a random sample representative of 132,500 HIV-infected American adults, Richman et al found that among patients with viremia, the viruses in approximately 76% of the patients had resistance to one or more antiretroviral drugs

[121]. The drug-resistance of HIV viruses indicates that it is essential to search for potent new drugs that are vigorous against drug-resistant viral strains and that can safely be combined with other anti-retroviral drugs [122]. Fortunately, suppression of viremia can be achieved if a prolonged combination of different classes of drugs is used [15]. As a result, recent advances in drug development have significantly reduced patients who develop drug-resistant strains of HIV [123]. Nowadays, genetic mutation of HIV viruses is no longer a major challenge of Anti-HIV therapy [123].

1.8 HIV reservoir formation after infection

Currently, HIV infection is incurable primarily because HIV viruses escape the anti-viral immune response and drug treatments, because HIV hides itself in privileged sites and cells, termed as HIV reservoirs [16]. There are two types of HIV reservoirs: anatomical and cellular [124]. Understanding the mechanisms of HIV reservoir formation will help to treat HIV-infected patients.

1.8.1 Anatomical reservoirs

The anatomical reservoirs are tissues that are privileged, immune-tolerant or have poor penetration of anti-HIV drugs, so that HIV viruses can replicate despite the presence of immune response or anti-HIV therapy. The central nervous system (CNS), testes, and lymphoid organs are the three major anatomical HIV reservoirs in the human body.

HIV enters the CNS presumably due to the migration of infected monocytes or macrophages [124]. Comparative studies revealed that the viruses in the CNS are primarily non-syncytium-inducing and macrophage-tropic, while in the blood the viruses are syncytium-inducing and T cell-tropic, indicating CNS serves as an independent sanctuary for HIV viruses [124]. Moreover, the blood-brain barrier (BBB)

may not be penetrated by some anti-HIV drugs, protecting viral replication from treatments in the CNS [124]. As a result, some drugs cannot reach therapeutic concentrations to inhibit viral replications in the brain efficiently. Several strategies have been developed to enable anti-HIV drugs to penetrate BBB, such as bypassing BBB, inhibition of efflux transporters, or the use of active transporters and nanotechnology [125]. Despite potential side effects, these approaches may desirably increase the concentration of anti-HIV drugs in the CNS.

Viral suppression in the blood was achieved in some HIV-infected men, but viral particles were still detectable in their semen, indicating testes might be an immunologically privileged site and protect viruses from antiretroviral treatments [126]. Jenabian et al demonstrated that testes might be another important anatomical reservoir due to blood-testis barrier during anti-retroviral therapy (ART) [127]. The possible mechanism of HIV reservoir formation is that HIV-1 infected mononuclear cells in blood transiting through the testes tissue at the time of the orchiectomies [128]. In addition, Gantor et al found that urethral macrophages contain integrated HIV-1 DNA, RNA, proteins and intact virions in virus-containing compartment-like structures, and the viral components remain undetectable in HIV-1-infected individuals under antiretroviral treatment, indicating urethral tissue macrophages are one of a HIV-1 reservoir [129].

Lymphoid organs such as the spleen, lymph nodes and gut-associated lymphoid tissue (GALT), where the majority of virus replication takes place during untreated infection [130], could also acts as a reservoir for HIV during drug treatments. Chun et al demonstrated that the frequencies of infected cells in GALT is higher than that in Peripheral Blood Mononuclear Cells (PBMCs), and they found ongoing viral

replication as demonstrated by cross-infection in these organ or tissues during HAART, suggesting GALT is a reservoir for HIV during HAART [131]. Animal studies discovered that the fast and selective depletion of CD4+ T cells occurs in GALT within days of infection, which is earlier than that in peripheral lymphoid tissues, indicating that GALT is the major site of CD4+ T cell loss in early HIV infection [132]. The rapid and profound depletion of CD4+ T cells exclusively occurred in the lamina propria of the intestinal tract where the number of CD4+ T cells significantly declined at 7 days after infection and reached the lowest point by 14 to 21 days. The depletion of CD4+ T cells caused a decreased viral load in the tissue, however, new lymphocytes are recruited and serve as fresh host cells for viral infection and replication [132]. As a result, HIV infection induced anti-viral inflammation and decreased mucosal repair and regeneration in the gastrointestinal tract. This caused damage to mucosal surface and multiple deleterious sequelae [133] which is eventually replaced by fibrosis with complete destruction of the follicular architecture [134]. Although HAART can reduce plasma viral loads in blood to undetectable levels, it cannot completely suppress the viral replication in gastrointestinal tract, and only partially restore gastrointestinal CD4+ T cells [133]. Nevertheless, HAART significantly improved gastrointestinal symptoms such as abdominal cramping, bloating, and loose stools 7 days after initiation of treatment [135]. Guadalupe's study found that early treatment with HAART caused a twofold increase in the frequency of CD4+ T cells within the gastrointestinal tract, whereas antiviral treatment during chronic HIV infection rarely reconstituted gastrointestinal CD4+ T cells [136,137]. These studies indicate that GALT is an early target of HIV viruses, and existing anti-viral treatments do not restore its physiological functions once impacted, causing a challenge to current anti-HIV therapy.

1.8.2 Cellular reservoirs

There are three major cellular reservoirs of HIV: resting memory T cells, macrophages, and astrocytes. Existing data indicates that CD34+ hematopoietic progenitor cells (HPCs) [138], dendritic cells (DCs) [139], CD4+ NK cells [140], mast cells [141], neurons and oligodendrocytes are potential HIV reservoirs [142]. The mechanism of cellular reservoir formation is that HIV hides itself as provirus in the cellular genome. During immune response or drug treatments, HIV viruses become latent, or lower gene expression, and the phenotype of infected cells can be the same as uninfected normal cells [143]. However, once the drug treatment is interrupted or stopped, the provirus may be re-activated and infected host cells will release infectious viral particles again, causing a rapid viral rebound in the blood [144]. Moreover, these cells have a long lifespan, such as resting memory T cells, or their lifespan was prolonged due to HIV infection, such as macrophages, resulting in a major obstacle in the eradication of HIV viruses from the human body.

1.8.2.1 Resting memory T cells

Resting memory T cells are an ideal HIV reservoir due to their long lifespan, which ranges from months to several years [145], for the long-term maintenance of HIV proviral DNA. The latency of HIV in CD4+ T cells is established in the early course of this disease after primary infection [146]. However, during the asymptomatic period, the percentage of latently infected is estimated to be less than 0.05% of resting memory T cells [147], causing challenges in understanding the mechanism of HIV latency in this cell type [148,149]. When stimulated with their cognate antigen or other environmental factors, resting memory T cells may be reactivated, proliferate, and release infectious particles, causing a rebound of viremia [146]. Therefore, despite

the rarity of this infected population, they are still considered to be a major reservoir for the maintenance of HIV latency. Because resting state blocks viral reverse transcription and nuclear import [60], how the latency is established in resting memory T cells is still not well understood. It has been hypothesized that they were infected during the early course of infection in an activated state, and then switched into a resting memory state after proviral integration [142].

1.8.2.2 Macrophages

Macrophages play a particularly important role in HIV reservoir formation due to their wide distribution in the human body, ability to cross the blood-brain barrier and spread HIV-1 infection to immune-privileged sites, which are able to tolerate the introduction of antigens without eliciting inflammatory immune responses [124]. Using humanized myeloid only mice, Honeycutt et al demonstrated that HIV infection of tissue macrophages is rapidly suppressed by ART, as indicated by a rapid drop in plasma viral load as well as a dramatic drop in the levels of cell-associated viral RNA and DNA. In addition, no virus rebound was observed in 67% of the animals after 7 weeks of ART treatment, and no competent virus was released from the macrophages purified from these animals, representing a direct evidence of HIV persistence in tissue macrophages in vivo [150]. Like CD4+ T cells, monocyte/macrophages lineage cells express the receptor CD4 and co-receptor CCR5 of HIV. Thus, macrophages are one of the principle early targets of HIV, but the outcomes of the two cell types after infection are quite different [151]. The HIV infection results in cellular lysis and rapid depletion of CD4+ T cells, but does not cause cytopathic effects in macrophages [152]. Notably, macrophages are widely present in almost all tissues in the human body (although with different names), thus they disseminate HIV throughout the body,

including the brain [153]. Most importantly, macrophages have a life span extending from months to years [154,155], and HIV-infected macrophages become more resistant to cell death and live longer than uninfected normal macrophages [152,156].

Significantly, recent studies discovered that a subset of tissue resident macrophages are in fact derived from embryonic progenitors that could easily be detected in extravascular mesenchymal tissues and intravascular spaces before birth and they independently maintain the macrophage pool without being superseded by bone marrow-derived or blood monocyte-derived cells [157]. Therefore, each tissue has its own unique combination of long-lived embryonically derived macrophages and short-lived blood monocyte-derived macrophages (months to years as mentioned above) [158]. Existing data suggests that embryonic macrophages play roles in tissue remodeling, whereas monocyte-derived macrophages are primarily involved in host defense [159]. Unequivocally, because embryonically derived macrophages are long-lived and self-renewable, once infected, they are more likely to maintain HIV persistence and chronic infections than blood monocyte-derived macrophages [160]. Moreover, HIV-infected macrophages release soluble cytotoxic factors, which induce the apoptosis of uninfected bystander CD4+, CD8+ T cells and macrophages [107,161]. Thus, like memory T cells, macrophages have been identified to be another ideal HIV reservoir. After infection, the viral genomic RNA of HIV is reversely transcribed and integrated into the cellular genome and there is no viral protein expression during HAART [56]. As a result, the phenotype of infected macrophages can be the same as uninfected normal cells, causing the true latency responsible for HIV persistence [162]. However, once HAART is interrupted, the latent provirus may be activated and the infected cells will produce and release infectious HIV particles again for a long period of time [163,164].

In addition, macrophages accumulate and retain HIV virions within dedicated internal Virus Containing Compartments (VCCs), which are another forms of “viral reservoirs” inaccessible to antibodies and anti-retroviral drugs [165,166]. Thus, HIV-infected macrophages shield the viruses against host anti-viral immune responses and anti-retroviral therapies, and help spreading virus and establishing infection in anatomically protected sites such as the gastrointestinal tract, lymph nodes and brain [163]. Notably, Alveolar macrophages express CXCR4 and CCR5 as a result of which these cells can be infected by HIV-1. HIV reverse transcriptase has been detected in alveolar macrophages from HIV-infected patients, and during HAART, alveolar macrophages harbor HIV while plasma viral loads are undetectable, indicating that lung is an important cellular reservoir of HIV during suppressive antiretroviral therapy [167]. Interestingly, Szaniawski et al discovered that the susceptibility of macrophages to HIV-1 infection is sex-dependent: macrophages derived from males are more susceptible and this phenomenon was not observed in CD4+ T cells. Furthermore, their studies suggested that in male-derived macrophages, SAMHD1 is in less active state due to the higher levels of CDK1 expression, which is responsible for SAMHD1 phosphorylation [168]. Kandathil’s study found that HIV present in liver macrophages are defective or restricted during ART, but after stimulation ex vivo, they released infectious viral particles for more than 170 days, indicating liver macrophages are another important HIV reservoir [169]. Furthermore, infected macrophages also facilitate cell-to-cell transmission of HIV in tissues such as the genital mucosa and GALT, where immune cells are maintained within close cellular contacts [170,171]. In these locations, HIV-infected macrophages recruit CD4+ T cells via releasing soluble chemokines [172], and viruses can be transferred via direct cell-to-cell contacts [173].

This intracellular transmission also helps the viruses escape immune responses and anti-retroviral therapies [174,175], further indicating the critical roles of macrophages in HIV reservoir formation.

1.8.2.3 Astrocytes

Astrocytes, also known as astroglia, are the most abundant glial cells in the CNS and their roles are to establish and maintain an optimal microenvironment for the nourishment and function of neurons [176]. HIV DNA and RNA were frequently detected in the astrocytes of postmortem brain tissues from HIV-infected patients, suggesting that this cell type could be infected [177,178]. However, the results by northern blotting and in situ hybridization suggest that the expression of viral proteins in HIV-infected astrocytes is low and HIV RNA is <10 copies per cell, immunofluorescence assay results indicate that viral antigens were rarely detected in astrocytes, and HIV infection could not cause cytopathic effects in astrocytes [179]. In addition, astrocytes express HIV co-receptors CCR5 and CXCR4 [180], but they do not express CD4, and blocking CD4 does not affect the infection of astrocytes [181–183]. Several surface molecules, such as the mannose receptor, have been proposed to be the potential HIV-1 receptors of astrocytes [184]. Brack-Werner's study also found that viral proteins are rarely detected in brain tissue, indicating that HIV-infected astrocytes may not produce considerable HIV virus particles *in vivo* [185]. Astrocytes infected with HIV *in vitro* only have initial transient viral production, which peaks at around day 2-7 after infection and subsequently decreases to a low or undetectable level, indicating the establishment of persistence [186,187]. Persistently infected astrocytes were demonstrated to be able to transmit HIV viruses to other cell types such as T cells and macrophages [183] and cause productive infections, indicating

the important roles of astrocytes in HIV reservoir formation. Existing data has demonstrated that IFN-γ, TNF-α, and IL-1β can reactivate HIV in latently infected astrocytes [188–190]. Interestingly, astrocytes can engulf HIV viruses into vesicle-like structures and subsequently release them for the infection of CD4+ T cells, suggesting that astrocytes may disseminate HIV to other cells without viral replication [191].

In summary, both anatomical and cellular reservoirs help HIV escape host immune response and antiretroviral treatments, making anti-HIV a major medical challenge of our time. The mechanism of viral persistence in each cellular reservoir is quite different from each other. Despite great advances during the past decades, elucidating more precise mechanisms of HIV reservoir formation is still needed for a better understanding of the pathogenesis and a complete cure of HIV infections.

1.9 The interplay between HIV and macrophages

Notably, macrophages possess more restriction factors than other cell types in the human body, such as SamHD1, Apobec3, Tetherin, and Viperin, which may interfere with HIV infection and viral life circle [151]. SamHD1 has dNTPase and RNase activities, which block HIV infection by depleting the intracellular dNTP pool or degrading viral RNA [192]. Apobec triggers G-to-A hyper-mutation [193] and Tetherin prohibits the release of viral progeny from infected cells [162]. A series of host cell proteins were found to mediate subcellular trafficking of integration complexes, nuclear import, and integration target site selection, such as LEDGF/p75 and BET [194]. Furthermore, the activation of pro-virus is highly related to the integration site and governed by the cellular micro-environment [195,196], and both cellular transcriptional factors and viral proteins are involved in regulating pro-viral DNA expression [151].

Provirus, the reversely transcribed viral genome that is integrated into cellular genome, is believed to be a hallmark of retroviral replication [197]. However, in recent years, much evidence has indicated that there are multiple forms of unintegrated viral DNA, which may be another form of HIV reservoir and help productive infection through the expression of early viral genes [58]. There are three forms of unintegrated viral DNA: linear, 1-LTR circular, and 2-LTR circular [198]. 1-LTR circular is found to be predominant in *in vivo* infection [198]. Sloan and Wainberg believe that unintegrated viral DNA is due to a host DNA repair mechanism and may represent a form of host antiviral defence [58]. Kelly found that in macrophages cultured *in vitro*, the unintegrated linear DNA, 1-LTR, and 2-LTR circles were stable for at least 30 days with biological activity [199]. Brussel and Sonigo demonstrated that the circular forms of HIV-1 DNA were transcribed during HIV-1 infection, thus they were also involved in virus production [200]. Moreover, the viral gene transcription is persistent, selective and skewed towards viral early genes such as *nef* and *tat* [199]. The unintegrated viral DNAs, the transcription and translation of unintegrated DNAs prior to integration, also suggest that the interplay between HIV and macrophages is complicated.

All above information indicates that the interaction between HIV and macrophages is complicated. As a result, the frequency of HIV-infected macrophages is usually low [56,160,201,202], causing difficulties to elucidate the dynamics of HIV infection in macrophages [164].

1.10 HIV infection dysregulates the gene expression of macrophages

Macrophages are long-lived cells and have a life span extending from months to years [203,204]. HIV infection cause extensive biological effects due to gene dysregulation, which further elongates the lifespan of infected macrophages [205]. As

a result, HIV-infected macrophages become more resistant to cell death than uninfected cells, making it difficult to eradicate HIV reservoirs in this cell type.

Giralt et al reported that HIV infection substantially altered gene expression in adipose tissue, when naïve untreated patients were compared with un-infected controls [206]. Yeligar et al conducted a cross-sectional study of HIV-infected patients and uninfected controls; they found that HIV infection downregulates the gene expression of PPARc, whereas upregulates Nox1, Nox2, Nox4, and TGFb1, causing oxidative stress in alveolar macrophages [207]. Our lab has demonstrated that HIV-Tat significantly inhibits p38 MAPK and PI3K, which were implicated in HIV-Tat mediated inhibition of LPS-induced IL-23 and IL-27 production in macrophages [208].

Notably, the gene dysregulation caused by HIV infection may block the signaling pathway of apoptosis, making macrophages more resistant to apoptosis. For example, Castellano found that Bim, a highly pro-apoptotic negative regulator of *Bcl-2*, was up-regulated and recruited into mitochondria in HIV-infected macrophages (21). Yuan et al discovered that HIV Tat or gp120 upregulates TREM-1 and confers anti-apoptotic attributes Nuclear Factor kappa B (NFκB) p65 to prolong macrophage survival (22). After reviewing many studies on anti-apoptotic effects caused by HIV infection, Badley believed that a possible mechanism by which macrophages are resistant to the cytopathic effect of HIV-1 is the dysregulation of a variety of NFκB dependent apoptosis inhibitors, including BCL-2, cFLIP, xIAP and cIAP1/2 [209].

All above studies indicate that HIV infection causes extensive biological effects on macrophages, and the dysregulation of some specific genes might be the mechanism behind the prolonged lifespan of infected macrophages. Therefore, targeting these specific genes may selectively induce the apoptosis of HIV-infected macrophages.

1.11 Roles of HIV proteins in apoptosis

The above information suggests that HIV has evolved mechanisms to protect infected macrophages from the apoptotic effects due to infection. To further study the resistance to cell death of HIV-infected macrophages, it is crucial to understand the anti-apoptotic or pro-apoptotic effects exclusively caused by HIV single proteins. Herein, the biological functions and apoptotic effects of HIV-1 single proteins Tat, Vpu, Vpr, Vif, Nef and Env are presented.

Tat is produced early in the HIV life cycle and is secreted by infected cells, which significantly increases the transcription of viral dsDNA. The apoptotic effect of Tat is highly related to its level in host cells. At low levels during the early stage of infection in T cells, it is anti-apoptotic by decreasing host cells' vulnerability to TRAIL, TNF-a, and Fas by up-regulating BCL-2 and c-FLIP [210]. In contrast, a high level of Tat protein is expressed and secreted from infected cells during the late stages of infection and is taken up by uninfected bystander cells via endocytosis [211]. In this case, Tat induces apoptosis in infected and uninfected bystander CD4+ T cells by up-regulating Fas-L, BAX, caspase 8 and RCAS1 [212], causing increased oxidative stress [213]. In addition, Tat may trigger intrinsic apoptosis by targeting microtubules that are essential for cell structure and division [214].

Vpu is one of the accessory viral proteins. It is a small transmembrane protein encoded by HIV-1 that targets and degrades CD4 in the endoplasmic reticulum to prevent the superinfection of infected CD4+ cells and enhance the release of progeny virions from infected cells [215]. In a study on Jurkat T-cell line, Casella found that Vpu sensitized HIV-1 infected cells to Fas-induced cell death, which was not due to the expressions of *nef*, *vif*, *vpr*, and *tat* [216]. Strebel's review in 2013 also indicates

that in the late phase of infection, Vpu promotes Fas-mediated apoptosis of HIV-infected T cells by de-regulating the NFκB signaling pathway and assembling into cation-conducting cellular membrane pores [217]. Verma discovered that Vpu promotes p53–mediated apoptosis in human T cells by the inhibition of β-TrcP dependent ubiquitination of p53 [218]. These observations suggest that Vpu induces the apoptosis of HIV-infected cells by multiple signaling pathways.

Vpr is a multifunctional protein that remarkably enhances the efficiency of viral transcription [219]. Other roles of this protein include the nuclear import of pre-integration complex, modulation of T cell apoptosis, induction of G2 cell cycle arrest, and the regulation of NFκB activity [220,221]. Like Tat, the roles of Vpr in apoptosis also depend on its expression level in host cells. The low-level present during the early stages of the viral life cycle is anti-apoptotic due to the up-regulation of *Bcl-2* and down-regulation of *Bax*, along with the suppression of NFκB dependent pro-inflammatory cytokine production. However, after G2 cell arrest, Vpr is pro-apoptotic in lymphocytes when it binds to either BAX or Adenine Nucleotide Translocase (ANT), causing the release of cytochrome c, which activates caspases 9 and 3 [222].

Vif is a small basic protein essential for viral fitness and pathogenicity, and plays a critical role in the production of infectious virions [223]. Vif also contributes to the G2 cell cycle arrest and counteracts the innate antiviral activity of host APOBEC3F and APOBEC3G [224]. In 2006, Sakai et al identified that Vif and Vpr can independently cause T cell cytopathic effects [225]. Unfortunately, literature on the roles of Vif in the apoptosis of HIV-infected macrophages is quite limited.

Nef is also an early viral protein in the life cycle of HIV. During the early stage of infection, Nef inhibits apoptosis and T cell activation, and by endocytosis through CD4

receptor and class I Major Histocompatibility Complex I (MHC I), it enhances viral infectivity [226]. Olivetta and Federico discovered that Nef strongly counteracts HIV-1 induced apoptosis of macrophages by hyper-phosphorylation and consequent inactivation of the pro-apoptotic protein BAD [227]. Nef also inhibits the expression of p53 and pro-apoptotic serine/threonine kinase and apoptosis signal regulating kinase-1 [228]. In addition, Nef reduces the activity of the pro-apoptotic protein BCL-2-associated Death (BAD) by p21-activated kinase-mediated phosphorylation [229]. During the late stages of infection, Nef induces the apoptosis of HIV-infected CD4+ cells by up-regulating Fas/Fas-L and down-regulating BCL-2/BCL-XL [230]. It also increases the expression of PD-1 [231] and lysosomal permeabilization with the release of Cathepsin D into the cytosol, leading to cell death due to the rupture of outer mitochondrial membrane [232].

Env is the only surface viral protein required for binding and entry into host cells. HIV-*env* gene encodes a glycoprotein of 160kDa (gp160), which is cleaved into gp120 and gp41 after translation. The C-terminal subunit, gp41, is a transmembrane protein that mediates the conformational change needed for fusion [233]. The N-terminal subunit, gp120, is completely outside the viral membrane and interacts with the host receptor (CD4) and co-receptors (CCR5 and CXCR4) [80]. Env is a soluble protein secreted from HIV-infected cells, and both the soluble and membrane-bound forms are able to induce the apoptosis of uninfected bystander T cells expressing CD4 or CCR5 and CXCR4 [80]. Therefore, Env plays important roles in the fast and massive loss of uninfected bystander T cells [234].

The roles of HIV single proteins in host cells indicate that HIV has evolving strategies to protect infected cells from apoptotic clearance, and these single proteins

can be anti-apoptotic or pro-apoptotic at different stages of infection. Therefore, when we are studying the apoptosis induced by HIV-1 single proteins, the appropriate timing should be taken into consideration during the research.

1.12 Mitochondria in apoptosis of HIV-infected macrophages

Mitochondria are highly dynamic endosymbiotic organelles that play a pivotal role in apoptosis triggered by many different stimuli. Existing data indicates that mitochondria modulate cell death pathways in the pathogenesis of various infections including RNA viruses, DNA viruses, retroviruses, and microbes [235,236]. Mitochondria initiate cell death signals through the *Bcl-2* family and coordinate caspase activation through the release of cytochrome c as a result of their outer membrane permeability [237]. It has been demonstrated that mitochondria were closely correlated to the cell death after HIV infection, as a target of the deleterious effects of both HIV and ART [238–240]. Therefore, exploring the interaction between mitochondria and HIV in the apoptosis of infected macrophages is essential to understand the molecular mechanism of viral latency, and thus propose novel solutions for a complete eradication of HIV from HIV-infected patients.

It has been demonstrated that HIV infection has direct effects on mitochondria. After comparing the amount of mitochondrial DNA (mtDNA) obtained from 36 HIV-infected patients before and after seroconversion, Casula et al discovered that the mtDNA of PBMCs after HIV-1 infection was reduced in the absence of any antiretroviral therapy [241], indicating HIV infection alone may cause the loss of mitochondria. Buenz and Badley's review indicates that progressive HIV-infected patients have greater spontaneous apoptosis and loss of mitochondria membrane potential as well as the rate of reactive oxygen species (ROS) production than LTNPs

[104]. Moreover, Morse et al found that genes encoded by mtDNA were down-regulated in PBMCs and adipose tissue from HIV-infected, untreated HIV-infected patients compared to uninfected controls [242,243].

Existing data indicates that mitochondria play a central role in regulating apoptotic pathways, which determines the fate of HIV-infected cells: apoptosis or survival. HIV-1 proteins Env, Nef, Tat, Vpr, Vpu, and Protease are the major players for both apoptotic and anti-apoptotic effects induced by HIV infections [104,244]. At low expression level in the early stage of infection, these HIV proteins are anti-apoptotic [104,244]. Fernández Larrosa and colleagues found that the resistance to apoptosis in persistently infected lymphoid and monocytic cells is independent of active viral production and involves modulation of the apoptotic mitochondrial pathway [245]. The anti-apoptotic effect relies on the interaction between different HIV proteins and multiple cell compartments. For example, Olivette and Maurizio observed that Nef protection from HIV-induced apoptosis correlated with the hyper-phosphorylation and consequent inactivation of the pro-apoptotic protein, BAD [227]. However, at high expression level in the late stage of infection; they directly or indirectly change the mitochondrial membrane potential, causing the apoptosis of HIV-infected cells [246]. Apoptosis in HIV-infected patients is primarily associated with the lower expression of *Bcl-2*, which is an inhibitor of mitochondrial membrane permeability [246,247].

1.13 Vpr-induced apoptosis of macrophages

Vpr is one of the 6 HIV proteins that were found to play important roles in regulating apoptosis of HIV-infected cells. Based on the level of expression, the roles of Vpr in apoptosis can be anti-apoptotic or pro-apoptotic as reviewed above.

One of the most significant biological functions of HIV-Vpr is cell cycle arrest, which subsequently causes the apoptosis of HIV-infected cells [248,249]. Sakai et al found that HIV virus could not induce cell death and arrest cell cycle at G2 if the Vpr gene was deleted from viral genome, indicating Vpr is essential for HIV-induced cytopathogenic effect and cell cycle arrest [225]. The possible molecular mechanism of Vpr-mediated cell cycle arrest is its binding and inactivation of MOV34 [250], an upstream regulator of the p34-cyclin B complex that is important for G2/M transition [251,252], causing cell cycle arrest at G2. In this phase, the viral LTR was found to be the most active, and virus production was markedly increased, indicating cells delayed at G2 may be beneficial for virus replication [253].

How Vpr induces apoptosis through mitochondria is controversial. Jacotot found that Vpr directly targeted ANT, which was a component of the permeability transition pore [254]. Anderson found that Vpr bound to the Voltage-dependent Anion Channel (VDAC) in mitochondrial membrane [255]. Subsequently, mitochondria release cytochrome C, resulting in the activation of the caspase 3 [249], caspase 9 [256], and the downstream events of apoptosis. However, Anderson et al believed that Vpr-induced apoptosis was cell cycle dependent and requires BAX, but not ANT [257]. Their studies suggest that knockdown of ANT would not affect Vpr-induced apoptosis and Vpr triggered apoptosis via another mitochondrial pore protein, BAX. Moreover, their studies on certain mutants of Vpr supported their idea that the G2 arrest and apoptosis induction were correlated [257]. Despite the controversy, previous studies discovered the important roles of Vpr in mitochondria-mediated apoptosis of HIV-infected cells. HIV-Vpr also interacts with and suppress NFκB, which subsequently promotes pro-apoptotic signals by down-regulating *Bcl-2* family members, *Bcl-2* and

Bcl-xl [258]. Moreover, Huang et al found that Vpr Triggered mitochondrial destruction by impairing Mfn2-mediated ER-mitochondria interaction [239].

All the information above indicates that interplay between Vpr and host cells are multi-dimensional, and Vpr is a strong modifier of apoptosis in the pathogenesis of AIDS [32]. Notably, as reviewed above, free Vpr also contributes to the fast and selective depletion of uninfected bystander cells in the pathogenesis of AIDS [259].

1.14 Selective induction of apoptosis in HIV-infected macrophages

All above formation indicates that selective induction of HIV-infected macrophages is essential for a complete cure of the disease. Multiple previous studies specifically induced apoptosis of HIV-infected macrophages, indicating that the eradication of HIV reservoir in macrophages is achievable.

Perez and colleagues specifically killed HIV-infected CD4+ T cells by Motexafin Gadolinium (Gd-Tex), which is a compound that promotes intracellular ROS stress [260]. Although their study was not focused on macrophages, the research discovered that specific eradication of HIV-infected cells was possible and increasing intracellular ROS stress might selectively induce the apoptosis of HIV-infected cells. Cunyat et al reported that antagonists of Colony-Stimulating Factor 1 Receptor (CSF-1R) could selectively induce the cell death of HIV-infected macrophages *in vitro* [261]. Xue et al reported that Galectin-3, a potent apoptosis-inducing protein that regulates diverse cellular activities, could selectively induced the apoptosis of HIV-infected macrophages by promoting caspase-independent cell death [262].

Lum et al found that treatment with either Leucine Zipper human TRAIL (LZhuTRAIL) or agonistic anti-TRAIL receptor antibodies selectively induced apoptosis of HIV-infected MDMs *in vitro*, and LZhuTRAIL treated cells produced less

viral RNA and p24 than untreated controls [263]. Yunlong et al discovered that recombinant human TRAIL specifically induced apoptosis of HIV-infected macrophages and inhibited HIV replication via the inhibition of Akt-1 phosphorylation, which promoted cell survival by regulating caspase-mediated apoptosis [264]. Zheng's study found that Tat-treated monocytes developed TRAIL resistance by increasing *Bcl-2* expression, and the reduced apoptosis could be inhibited by polyclonal anti-Tat serum [265]. Schnepple et al discovered that Tat induced TRAIL resistance via producing a novel TRAIL splice variant, TRAILshort, which preferentially binds TRAIL receptor-2 to prevent the pro-apoptotic effects of TRAIL, and TRAILshort can be isolated from plasma and cells of HIV-infected patients [266].

Although TRAIL was found to preferentially induce apoptosis of HIV-infected macrophages and the mechanism has been partially elucidated, clinical observations since the mid-1990s found many cells were not sensitive to TRAIL and targeting TRAIL had no significant survival benefits [267], indicating targeting TRAIL is not sufficiently effective to cure HIV infection. This data suggest that it is imperative to search for other novel targets to specifically kill HIV-infected macrophages.

1.15 Targeting IAPs may induce apoptosis of HIV-infected macrophages

Members of the Inhibitor of Apoptosis Proteins (IAPs) family are known to play critical roles in regulating cell survival. Previous studies indicate that the expression of X-linked Inhibitor of Apoptosis Protein (xIAP, also termed as BIRC1), cellular Inhibitor of Apoptosis Protein-1 (cIAP1, also termed as BIRC2), cellular Inhibitor of Apoptosis Protein-2 (cIAP2, also termed as BIRC3), and Survivin (also termed as BIRC5) are upregulated to prolong the lifespan of HIV-infected macrophages. The results from our lab and other labs suggest that targeting IAPs may selectively induce apoptosis of HIV-infected macrophages.

Multiple studies implicated that IAPs played a key role in host cell survival after HIV infection. Berro et al identified that the expression of xIAP was up-regulated in latently HIV-1 infected model T-cell line ACH2 [268]. Pache et al found that cIAP1 is a negative regulator of early HIV-1 transcription and can be targeted by SMAC Mimetics (SM) to reverse viral latency [269]. López-Huertas confirmed that Tat up-regulated a variety of NFκB dependent apoptosis inhibitors including xIAP and cIAP2 [270]. Kuo et al reported that the expression of Survivin was upregulated in productively and latently infected CD4+ T cells and it was functionally involved in the survival of HIV-infected CD4+ T cells [271]. Our lab found that IAPs played a protective role in Vpr-induced apoptosis of macrophages, and down-regulating cIAP1/2 sensitized macrophage to Vpr-induced apoptosis [272–274]. Moreover, our lab also discovered that SM effectively induced apoptosis of macrophages from both treated and untreated HIV-infected patients. In addition, Ebert found that SM specifically promoted the elimination of HBV-infected hepatocytes [275], indicating that targeting IAPs may also selectively induce the apoptosis of HIV-infected macrophages.

Thus, numerous studies suggest that HIV infection may upregulate the gene expression of *IAPs* to enhance the survival of infected macrophages. I hypothesize that targeting IAPs may specifically induce the apoptosis of HIV-infected macrophages. However, the specific killing effects by targeting IAPs on HIV-infected macrophages has not been reported. Notably, IAPs were also known to be the last defender of normal cells; targeting them may kill uninfected normal cells, causing deleterious consequences for the immunity to infection [276,277].

1.16 90k shRNA lentivirus pool for a genome-wide screen of target genes

Studies on TRAIL and IAPs indicate that HIV infection alters the expression of some genes critical for the survival of infected cells; targeting these genes may

selectively induce the apoptosis of HIV-infected macrophages. I hypothesize that a screening of these genes may have practical application in search for novel Anti-HIV targets and help to understand the mechanism of HIV reservoir formation.

Unfortunately, it was estimated that there were approximately 19,000 genes in a complete haploid set of human genome [278], resulting in difficulties in screening target genes. Encouragingly, siRNA and shRNA technologies, which have been widely used for gene silencing in recent years, made a high-throughput screening of target genes possible [279]. Numerous studies on genome-wide screens using RNA-interference technologies have successfully identified multiple host factors that play important role in HIV-1 infection [280–283]. The shRNA lentivirus-based gene silencing technology, 90k shRNA lentivirus pool technology, which is an RNAi consortium library containing a pool of 90,408 unique shRNAs targeting ~18,000 human genes, allows a high-throughput screening of a large number of genes simultaneously. When this technology is applied, a large number of cells are infected with the lentivirus pool and the viral genomes are reversely transcribed and integrated into cellular genomes. The shRNA is amplified simultaneously when infected cells are proliferating. If the specific shRNA is lethal, cells infected with this specific shRNA will be killed, detached and finally removed from adherent cells. The lost specific shRNA in the later micro-array analysis indicates the target genes. This novel idea was applied to successfully screen target genes for breast cancer therapies in 2013 [284,285]. The workflow and mechanism of this technology are described in **Figure 3**.

In this study, I hypothesize that the 90k shRNA lentivirus pool technology may be customized for a fast screen of target genes to selectively induce the apoptosis of HIV-infected macrophages. Thus, this unbiased, pooled shRNA-based screening strategy [284,285] is applied to identify potential genes which can be targeted to specifically induce the apoptosis of HIV-infected macrophages.

Figure 3. Mechanism of 90k shRNA lentivirus pool technology

A. A large number of cells are infected with the 90k shRNA lentivirus pool. **B.** After infection, the lentiviral genomes are reversely transcribed and integrated into the cellular genome, and infected cells are selected with puromycin. To avoid duplicate infections, the infection rate is controlled to be between 30% to 40%. **C.** If the expression of a specific shRNA is lethal, the cells infected with this specific shRNA will be killed, detached, and finally washed away. **D.** If the expression of a specific shRNA is not lethal, the shRNA segments will stay in live cells and be amplified when infected cells are proliferating. **E.** shRNAs remained in live cells are amplified by PCR. **F.** The weak signals of specific shRNAs in micro-array analysis indicate target genes.

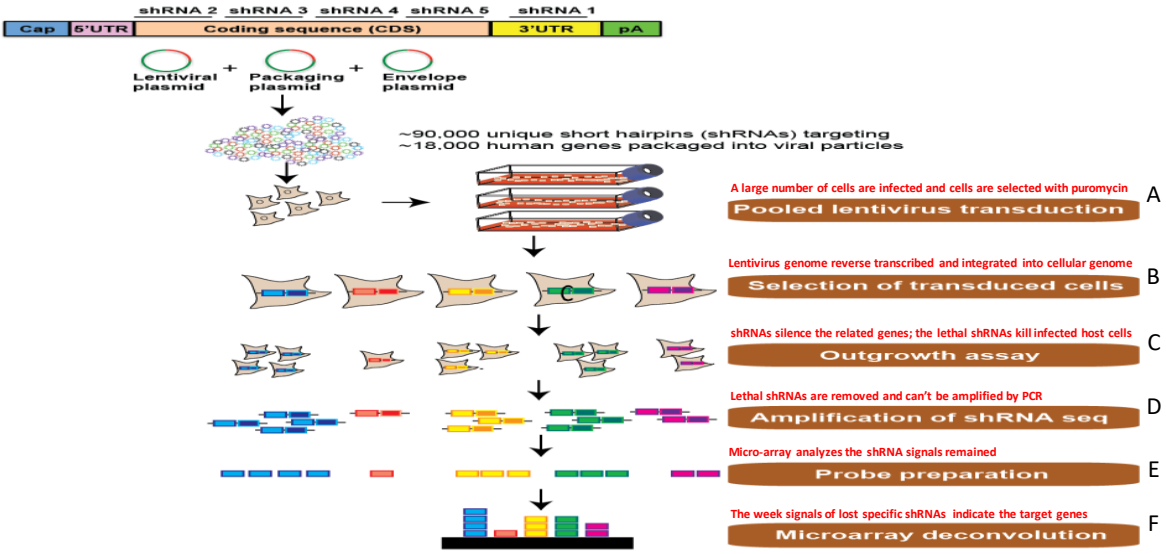
shRNA 2 shRNA 3 shRNA 4 shRNA 5 shRNA 1
Cap
5'UTR
Coding sequence (CDS)
3'UTR
pA
Lentiviral plasmid
Packaging plasmid
Envelope plasmid
~90,000 unique short hairpins (shRNAs) targeting
~18,000 human genes packaged into viral particles
A large number of cells are infected and cells are selected with puromycin
Pooled lentivirus transduction
A
Lentivirus genome reverse transcribed and integrated into cellular genome
Selection of transduced cells
B
shRNAs silence the related genes; the lethal shRNAs kill infected host cells
Outgrowth assay
C
Lethal shRNAs are removed and can't be amplified by PCR
Amplification of shRNA seq
D
Micro-array analyzes the shRNA signals remained
Probe preparation
E
The week signals of lost specific shRNAs indicate the target genes
Microarray deconvolution
F

1.17 Approaches of targeting genes in primary human macrophages

In this study, I am expecting a list of promising genes which can be targeted to selectively induce apoptosis of HIV-infected macrophages once the high throughput 90k shRNA lentivirus pool technology is applied to a fast screening of gene targets. In that case, validating promising target genes is an essential step to reach the goal of this study. Here I reviewed commonly used methods/technologies for targeting genes of interest in lab research.

1.17.1 Lentivirus

In recent years, lentiviruses, which are modified from HIV-1 with many of the viral genes removed, are widely used as a gene delivery tool. However, the lentiviral vectors contain HIV-LTRs with the packaging signals, but packaging genes are provided on separate plasmids. As a result, the pseudo lentiviral particles are replication deficient. The advantage of this approach is that it has a broad cell spectrum, high transduction efficiency, minimal need for optimization, and improved biosafety. shRNA lentivirus [286] or lentivirus-based CRISPR editing [287] are commonly used to knockout/silence genes of interest. Unfortunately, lentiviruses cannot be used to silence a specific gene in this study, which is focusing on HIV-infected macrophages, because after HIV infection, HIV-gp120, Nef, and Vpu will down-regulate the expression of MHC I & II, CD4 and CD28 in macrophages to avoid superinfection [151,244]. As a result, HIV-infected macrophages are activated and cannot be infected a second time by lentiviruses [288]. Consequently, lentiviruses which carry shRNA or CRISPR to target a specific gene cannot effectively infect HIV-infected macrophages. Therefore, lentiviruses which target specific host genes are excluded from validation purposes in this study.

1.17.2 siRNA transfection

Another approach is siRNA transfection, which is sequence-specific silencing of complementary target mRNA [289]. Although this way of targeting genes is very specific, for macrophages, particularly primary human macrophages, several technical issues have yet to be solved. First, macrophages are well-known to be hard-to-transfect cells because they are evolved to recognize foreign nucleic acids and may initiate immune responses to exogenous siRNA molecules [290,291]. Second, transfection reagents are usually toxic to cells, causing unreliable results in the case of studying cell death, despite achieving high transfection rates. Therefore, a balance between transfection rate and cell toxicity should be taken into consideration when selecting transfection reagents for human macrophages. Third, the HIV-1 infection rate of human macrophages is usually low [56,160,201,202], so if the siRNA transfection rate is also low, we may get ambiguous results which cannot distinguish the cell death induced by siRNA transfection of HIV-infected cells from mock infections.

1.17.3 Chemical inhibitors

Chemical inhibitors or small molecules are also a good approach to manipulate gene expression. The current goal of medical research is to develop new drugs that modulate gene expression of living cells for therapeutic purposes. Therefore, many natural products, artificial chemicals and compounds targeting various genes or gene products have been identified or designed. The major difference between siRNA targeting and chemical inhibitors is that siRNAs only target sequence-specific mRNA and thus they knock out the specific protein from cells, whereas chemical inhibitors may target any process of the translational machinery, including DNA, transcription, RNA processing, mRNA, and proteins [292]. The two approaches are different in

several ways. 1. Chemicals are usually not as specific as siRNA and in many circumstances only Pan inhibitors are available; 2. siRNA usually takes days to take effect, whereas pharmacological inhibition exhibits effects immediately within minutes or hours; 3. for some cell lines, siRNA silencing is easy to perform, whereas for others siRNA may be difficult, and pharmacological inhibition may be a better option. 4. When targeting a family of genes is a must, such as *IAPs*, usually a pool of siRNAs for all genes (*xIAP*, *IAP1*, and *IAP2*) is essential to completely interfere with the biological functions, but one compound (SM) is enough to effectively silence all genes. In that case, chemical inhibitors are a more suitable way for silencing than siRNA transfection.

In this study, we take advantage of the specificity of siRNA to validate promising target genes; whereas chemical inhibitors were selected to verify if the validated genes can be targeted to induce the apoptosis of HIV-infected macrophages.

1.18 HIV viruses for *in vitro* infection of primary human macrophages

Unfortunately, studies on selective induction of cell death in HIV-infected macrophage are rare, and which HIV viruses are appropriate to study the specific killing of HIV-infected macrophages has never been reported. Our analysis suggests that, to study specific killing of HIV-infected macrophages, the viruses should meet three prerequisites. 1. The virus should have a complete HIV-1 genome that expresses all the structural and non-structural viral proteins like wild type HIV-1 stains; 2. The virus should have a selection marker that is convenient to track HIV-infected cells for specific killing. Thus, commonly used wild-type HIV viruses without selection marker cannot be used in this study. 3. The infection rate in macrophages should be as high as possible to distinguish HIV-1 infected cells from mock infections.

Fortunately, 3 different viruses that can be produced from plasmid DNA, HIV Gag-iGFP(envJRFL) [293], pNL4.3-BAL-IRES-HSA [294], and pNL4.3-WT-IRES-HSA [294], are available and may meet the above prerequisites. Our pilot study suggested that the infection rate of the virus produced from pNL4.3-WT-IRES-HSA in primary human MDMs is lower than 5%. Thus, HIV-1 virus produced from this plasmid could not be used in this research. Eventually, the viruses made from HIV Gag-iGFP(envJRFL) and pNL4.3-BAL-IRES-HSA were selected to infected primary MDMs for this study. Maps of the two plasmids were displayed in **Figure 4**.

Herein we designate the virus produced from plasmid HIV Gag-iGFP(envJRFL) as HIV-eGFP, in which eGFP was inserted between MA and CA domains of Gag. The virus carries a Gag-internal or inter-domain green fluorescent protein (iGFP) fusion (Gag tagged with eGFP), which is packaged into virus-like particles but do not interfere with viral infectivity [295]. However, without untagged helper Gag, the virus cannot produce infectious virions. As a result, this recombinant HIV is as infectious as native HIV-1 in single-round infectivity assays. Moreover, a fragment of the *env* gene from JRFL is cloned into the NL4-3 *env* gene (NdeI to BamHI) to make the virus CCR5-tropic, which significantly increases its infection rate in human macrophages. The tagged eGFP facilitates the study of infection and was demonstrated to be very useful in monitoring virus transportation. In 2007, Hübner et al applied this artificial virus to reveal a natural progression of Gag trafficking during the viral gene expression program [293]. In 2011, Dale and colleagues used this virus to quantify cell-to-cell transmission of virus by flow cytometry and to track the proteins during assembly and transmission using live cell imaging [296]. In 2013, Padilla-Parra et al also applied this infection model to image the release of HIV upon virus maturation [297].

Figure 4. Maps of plasmid DNA to produce HIV-eGFP and HIV-HSA viruses

A. HIV Gag-iGFP(envJRFL) plasmid which was used to produce HIV-eGFP viruses. 1. *eGFP* gene was cloned between Matrix and Capsid genes; 2. It is a CCR5 Tropic virus; 3. It is one-time infection only; 4. It needs exogenous activations. This reagent and information were obtained through the NIH AIDS Reagent Program, Division of AIDS, NIAID, NIH: HIV Gag-iGFP_JRFL from Dr. Benjamin Chen [293].

B. pNL4.3 BAL IRES HSA plasmid which was used to produce HIV-HSA viruses. 1: Mouse HSA (60aa) inserted between *env* and IRES; 2. It is a CCR5 Tropic virus; 3. IRES was cloned before *tat* to make the virus always activate; 4. It doesn't need exogenous activation. This reagent and information were by the courtesy of Dr. Michel J. Tremblay, Laboratoire d'Immuno-Rétrovirologie Humaine, Centre de Recherche en Infectiologie (242).

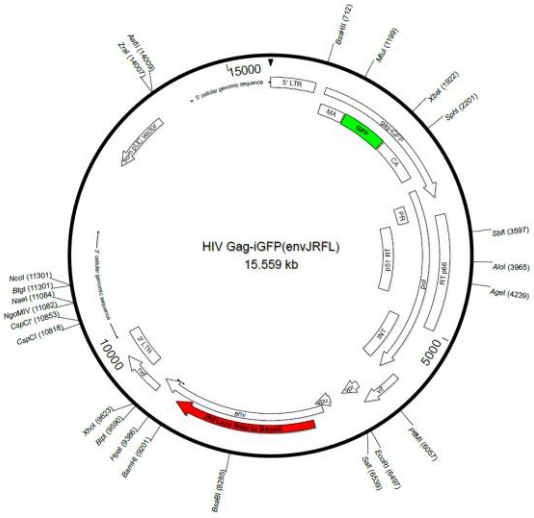

A. HIV Gag-iGFP(envJRFL) plasmid

From NIH AIDS Reagent Program, Division of AIDS, NIAID, NIH: HIV Gag-iGFP_JRFL, contribution by Dr. Benjamin Chen (Appendix 10.2).

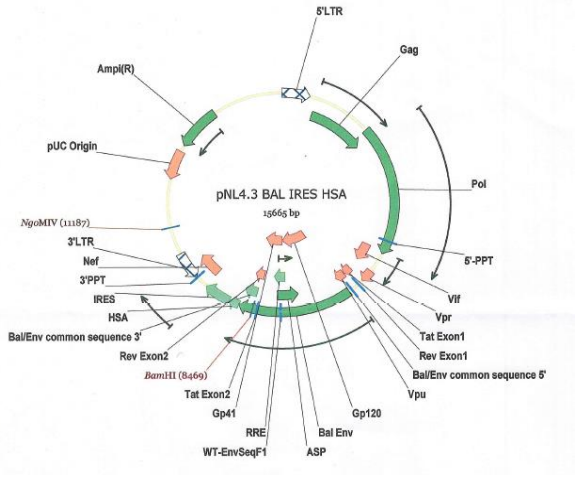

B. pNL4.3 BAL IRES HSA plasmid

By the courtesy of Dr. Michel J. Tremblay, Laboratoire d'Immuno-Rétrovirologie Humaine, Centre de Recherche en Infectiologie (Appendix 10.3).

Similarly, we designate the virus produced from plasmid pNL4.3-BAL-IRES-HSA as HIV-HSA in this study. The plasmid for this novel HIV-1 based reporter virus was constructed by Imbeault et al in 2009 [294], and the viral construct expresses all HIV-1 proteins with mouse Heat Stable Antigen (HSA, mouse CD24) as a reporter on the membrane of infected cells. HSA is a small protein with 60 amino acids, which minimizes the interference with viral replication and is convenient to track HIV-infected cells with anti-HSA monoclonal antibodies, or to separate infected cells using magnetic beads coated with an antibody specific for HSA. In addition, this tiny protein is expressed along with early virus genes upon productive infection. Moreover, the Internal Ribosome Entry Site (IRES) was cloned before *tat* gene, allowing the initiation of translation of *tat*, which enhances the efficiency of viral transcription [219,298]. Similar to HIV-eGFP, HIV-HSA virus is also CCR5-tropic (Bal), which is a co-receptor for HIV entry to increase the infection rate of the virus in macrophages [299]. This HIV-1 infection model has already been used in many studies on AIDS as well. For example, in 2017, Bolduc et al investigated the effect of Toll-like receptor 2 ligation on the permissiveness of activated $CD4^+$ T cells to HIV-1 infection by inoculating cells with HIV-HSA viral particles [300]. In 2019, Rao and colleagues applied this virus to study the roles of host mRNA decay proteins in regulating HIV-1 replication in infected macrophages [301].

In summary, both viruses I selected for this study express a reporter gene that is convenient for tracking HIV infections, and both are CCR5 tropic to significantly increase the infection rate in human primary macrophages. In this study, we took the advantages of these two HIV-1 viruses to search for novel genes which can be targeted to selectively induce the apoptosis of HIV-infected human macrophages.

2. Rationale

AIDS caused by HIV infections is an incurable disease primarily due to HIV reservoir formation and macrophages play important roles in HIV reservoir formation. Thus, it is imperative to selectively induce the apoptosis of HIV-infected macrophages for a complete cure of HIV-infected patients. Existing data suggests that HIV infection dysregulates some host genes critical for the survival of infected cells and targeting these genes may selectively induce the apoptosis of HIV-infected macrophages. Our lab discovered that down-regulating *cIAP1/2* sensitized macrophage to Vpr-induced apoptosis, indicating HIV infection may upregulate *IAPs* to enhance the survival of infected macrophages, and targeting IAPs may specifically induce the apoptosis of HIV-infected macrophages. In addition, although there is a large number of genes on human genome, the application of 90k shRNA lentivirus pool technology makes a fast screen of novel gene targets to remove HIV reservoirs in macrophages possible.

3. Hypothesis

I hypothesize that, 1) targeting IAPs selectively induces the apoptosis of HIV-infected macrophages, and 2) HIV infection upregulates the expression of other unknown host genes, which is essential for the survival of HIV-infected macrophages; targeting these genes selectively induces the apoptosis of HIV-infected macrophages.

4. Objectives

1. To select an optimal siRNA transfection reagent for primary human MDMs;

2. To determine if targeting IAPs selectively induces apoptosis of HIV-infected macrophages;

3. To search for novel genes which can be targeted to selectively induce apoptosis of HIV-infected macrophages;

4. To briefly elucidate the mechanism of one identified gene on the specific killing of *in vitro* HIV-infected macrophages.

5. Materials and Methods

5.1 Cell culture and differentiation of U937, THP-1, and U1 cell lines

U937 and THP-1 were purchased from American Type Culture Collection (ATCC, Cat. #: CRL-1593.2™ and Cat. #: TIB-202™). U1, which was HIV-1-infected U937, was purchased from National Institutes of Health (NIH, Cat. #: 165, Lot. #: 100218). All three cell lines were maintained at 37°C, 5% CO_2 in complete medium (DMEM from Wisent, Cat. #: 319-105-CL; 10% Fetal Bovine Serum (FBS) from Sigma, SKU: F1051; 100 U/ml penicillin G from Sigma, SKU: P3032; and 100 μg/ml streptomycin from Sigma, SKU: S9137) at the density of 10^5~10^6 cells/ml by the addition of fresh complete medium every 2 to 3 days. For the differentiation of U937, $5.0x10^5$ cells/well were cultured in costar 12-well plates (Sigma, SKU: CLS3513) with 1.0 ml complete medium supplemented with 50ng/ml Phorbol 12-myristate 13-acetate (PMA, Sigma, SKU: P1585). 3 days after differentiation of U937, the monolayer was washed with Phosphate-buffered Saline (PBS, Wisent, Cat. #: 311-425-CL) and maintained in complete medium with 50 ng/ml PMA for 2 more days before further experiments. For THP-1, $4.5x10^5$ cells/well were differentiated for 2 days in 1.0 ml of complete medium supplemented with 50 ng/ml PMA. The differentiation of U1 is the same as U937, but the medium was supplemented with 75ng/ml PMA, and the number of cells was increased to $7.5x10^5$ cells/well.

5.2 Preparation of primary human MDMs and M1 polarization

Peripheral Blood Mononuclear Cells (PBMCs) were prepared following the protocol of Lymphoprep Density Gradient (StemCell, Cat. #: 07851). Cells were counted and cultured in costar 12-well plates at the density of 1.5~$2.0x10^6$ cells/well

in DMEM medium without any supplement at 37°C, 5% CO_2 for three hours. Next, supernatant was removed, and the monolayer was washed twice with PBS, and cells were maintained at 37°C, 5% CO_2 in complete medium supplemented with 10 ng/ml Macrophage-colony Stimulating Factor (M-CSF, R&D, Cat. #: 216-MC-025) for 3 days. Cells were washed with PBS and maintained in complete medium containing 10 ng/ml M-CSF for 4 more days, allowing differentiation for 7 days in total before further experiments. For the experiments on subset M1 macrophages, primary MDMs were polarized into M1 by supplementation with 10ng/mL IFN-γ (R&D, Cat. #: 285-IF-100) for 48 hours [302].

5.3 HIV-1 production, *in vitro* infection of MDMs and HIV-p24 ELISA

MDMs were infected with dual tropic HIV_{CS204} viral stock supernatants containing 30 ng of HIV-p24 protein, supplemented with 8.0 µg/mL of polybrene (Sigma-Aldrich) for 2 hours as previously described [303]. The dual tropic HIV_{CS204} was a gift from Dr. J. Angel (The Ottawa Hospital, Ottawa, ON, Canada). HIV_{CS204} stocks were produced in CD8+ depleted PBMCs from healthy donors as described earlier [304]. Stocks of Mock were produced under similar conditions but in the absence of HIV. Following infection, MDMs were washed three times with PBS and cultured in complete medium. Supernatants were collected every 3 to 4 days for determining productive infection of MDMs by HIV-p24 ELISA. Aliquots of the mock and viral stocks or supernatants were inactivated for 1 hours at 37^{o}C in 1% Triton^{TM} X-100 (Sigma-Aldrich, SKU: 93443). HIV growth was determined by measuring p24 using HIV-1 p24CA capture kit as per the manufacturer's directions (AIDS & Cancer Virus Program, NCI, Fredrick, MD).

5.4 Preparation of 90k shRNA lentivirus pool

Pooled screening was done as previously described [284,285]. 90k shRNA lentivirus pool was generated by transfecting HEK293T cells (ATCC, CRL-1573™) with psPAX2, pMD2.G, and the 90K hairpin library in pLKO.1 vector in transfection mix containing FuGENE® HD Transfection Reagent (Promega, Cat. #: E2312) and Opti-MEM (ThermoFisher, Cat. #: 31985070) for 18 hours at 37°C, 5%CO_2. Subsequently, transfection media was replaced with high-Bovine Serum Albumin (BSA) growth media (DMEM, 100 U/ml penicillin G, and 100 µg/ml streptomycin). Supernatant was harvested at 24 and 48 hours, respectively, and the pooled media containing lentiviral were centrifuged at 1000RPM 3 minutes to remove cell debris. The supernatant containing lentiviral particles was aliquoted and stored at -80°C. Aliquoted viruses were thawed at room temperature only once before infection.

5.5 Infecting myeloid lineage cells with 90k shRNA lentivirus pool

To customize the protocol of 90k shRNA lentivirus pool technology for this study, $5.0x10^5$/well undifferentiated U937, THP-1 and U1 cells were seeded Corning® Costar® TC-treated 12-well plates. 100 µl, 150 µl, 200 µl of 90k shRNA lentivirus pool was used to infect undifferentiated or PMA-differentiated U937, THP-1, U1 and primary MDMs. 48 hours after infection, Puromycin (Sigma, SKU: P9620) was applied accordingly to select infected cells for another 48 hours. Undifferentiated cells were stained with Propidium Iodide (PI, Sigma, SKU: P4170-10MG) and cell death was analyzed by flow cytometer BD LSRFortessa™ X-20 at PI channel. Differentiated cells and primary MDMs was imaged under IX51 Olympus Fluorescence Microscope.

To apply 90k shRNA lentivirus pool to U937 and U1, $75.0x10^6$ cells of each cell line were infected with 30ml of 90k shRNA lentivirus pool, respectively. 48 hours after the infection, Puromycin (Sigma, SKU: P9620) was applied to select infected cells. 96 hours after the infection, live cells were collected and counted, $25.0x10^6$ cells were harvested as one cell pellet for a total of 2 pellets, which were designated as T0. Cells left were maintained in complete media without puromycin for 6 more days, and were harvested the same as T0, but were designated as T6. Cells left after T6 were differentiated with PMA for 6 days, then trypsinized, counted and harvested as T12. The genomic DNA was extracted using QIAamp Blood Maxi kit (Qiagen, Cat. #: 51194), quantitated by NanoDrop1000 Spectro-photometer (Thermo Scientific), and diluted to a final concentration of 400 ng/µl for further analysis.

5.6 Preparation of HIV-eGFP and HIV-HSA viruses from plasmid DNA

Plasmid HIV Gag-iGFP(envJRFL) was purchased from NIH (Cat. #: 12456, Lot. #: 130201). Plasmid pNL4.3-BAL-IRES-HSA was constructed by Tremblay's lab [305]. Plasmid pUC-19 (ThermoFisher, Cat. #: SD0061) was used to produce mock viruses. Endotoxin-Free plasmid DNA was transfected into chemically competent STBLE3 *E. coli* (Invitrogen, Cat. #: C7373-03). Single colonies were picked directly from agarose gel dish (100 mm TC-treated Culture Dish, Corning, Product #: 430167) for large volume culture in LB Medium (ThermoFisher, SKU: 12795-084) with 100 µg/ml Ampicillin (Sigma, SKU: A8351), and shaken horizontally at 30°C, 250RPM for 24-30 hours. Bacteria were harvested and plasmid DNA was extracted using QIAGEN Plasmid Giga Kits (Qiagen, Cat. #: 12191).

To produce HIV-1 and mock viruses, 50 µg plasmid DNA was transfected into 293T cells (ATCC® CRL-3216™) in complete medium (HyClone™ Dulbecco's High Glucose Modified Eagles Medium, ThermoFisher Scientific Cat. #: SH3002201; 10% Fetal Bovine Serum from Sigma, SKU: F1051; 100 U/ml penicillin G from Sigma, SKU: P3032; and 100 µg/ml streptomycin from Sigma, SKU: S9137) with 125 µl of Lipofectamine™ 2000 (Invitrogen, Cat. #: 11668019) at the density of $15.0x10^6$ cells/dish in 150 mm TC-treated Culture Dish (Corning, Product #: 430599). Viruses in supernatant were harvested at 48 and 96 hours, respectively, after transfection. To remove cell debris, supernatants were centrifuged at 2000g for 15 minutes and PEG-it™ virus precipitation solution (SBI, Cat. #: LV825A-1) was added to precipitate viruses at 4ºC for 24-48 hours. Subsequently, the supernatant with precipitation solution was centrifuged at 2000g for 30 minutes, and the precipitant was re-suspended in 4ºC PBS with 0.05M HEPES (Sigma, SKU: H3375) at 1/20 volume of original supernatants with viruses. Re-suspended viruses were aliquoted and stored at −80°C. p24 of virus stock were quantitated by ELISA according to the protocol (version 2) of HIV-1 $p24^{CA}$ Antigen Capture Assay Kit from Frederick National Laboratory for Cancer Research.

5.7 Infection of primary MDMs with HIV-eGFP and HIV-HSA

All virus stocks in frozen were thawed only once, and a master-mix was made before infections. For one well of 12-well plates, 150ng p24 of HIV-eGFP or HIV-HSA viruses in 400 µl complete DMEM medium was used to infect seven-day-old primary MDMs. The next day, cells were washed, and maintained in 1.0 ml fresh complete DMEM medium for 7-8 days before further experiments. To study the kinetics of eGFP expression, cells were harvested at day 1, 2, 3, 5, 7, 9 after infection, and the eGFP+

rates were analyzed by flow cytometer BD LSRFortessa™ X-20 at GFP channel. To study the kinetics of HSA expression, cells were harvested at day 3, 5, 7, 9, 11, 13 after infection, washed with PBS, blocked with 5.0 µl/sample FcR Blocking Reagent, human (MACS Miltenyl Biotec, Order #: 130-059-901), stained with anti-mouse HSA IgG antibody (M1/69) conjugated with FITC (MACS Miltenyl Biotec, Order #: 130-102-731), and HSA+ rates were analyzed by flow cytometer at FITC channel.

5.8 siRNA transfection for transfection reagent selection

At least two hours before siRNA transfection, U937 or primary MDMs were washed with PBS and maintained in 0.6 ml/well of antibiotic-free DMEM medium supplemented with 10% FBS, and in 37°C, 5% CO_2 incubator. A fixed amount of 20 nM *Bax* siRNA (Dharmacon, Accell Human *Bax* siRNA, Cat. #: E-003308-00-0005) or BLOCK-iT™ Alexa Fluor™ Red Fluorescent Non-targeting siRNA Control (ThermoFisher Scientific Invitrogen Cat. #: 14750100) in 200 µl transfection medium was used in all siRNA transfections unless specifically annotated. Accell Non-targeting siRNA #1 (Dharmacon, Cat. #: D-001910-01-05) was selected as control siRNA for western blotting. The 200 µl medium with siRNA and transfection reagents was added to the cells to make a final volume of 0.8 ml/well, and a total of 10 transfection reagents was tested following the protocols provided by the manufacturers, such as Lipofectamine RNAiMAX (ThermoFisher Scientific Invitrogen, Cat. #: 13778075), Lipofectamine 2000 (Invitrogen, Cat. #: 11668-019), siRNA Transfection Reagent (Santa Cruz, Cat. #: sc-29528), DarmaFect 3 (Dharmacon, Cat. #: T-2003-03), DarmaFect 4 (Dharmacon, Cat. #: T-2004-01), HiPerFect (Qiagen, Cat. #: 301704), and X-tremeGENE siRNA Transfection Reagent (Roche, Cat. #: 04 476 093 001). Cells were incubated at 37°C, 5% CO_2 before further experiments.

5.9 Detection of siRNA transfection rates

Primary human MDMs were transfected with 20 nM BLOCK-iT Alexa Fluor Red Fluorescent Control and transfection reagents for 16 hours, washed with PBS, trypsinized with 0.25% Trypsin-1.0 mM Ethylenediamine Tetra-acetic Acid (EDTA, StemCell, Cat. #: 07901) for 30 minutes. For each well, cells were pipetted up and down 16 times to detach cells, centrifuged, washed again with PBS, suspended in 500 µl of PBS with 0.5% BSA and the percentages of Alexa Fluor555 (siRNA) positive cells were analyzed by flow cytometer BD LSRFortessa™ X-20 at PE Channel (575/25). Only cells deeply stained were gated as Alexa Fluor555 (siRNA) positive cells.

5.10 Monitoring cell viability and GFP expression

Immediately after drugs (RESV or AEG40730 with PI) were added to the supernatant, or right after cells were infected with Lentivirus-eGFP, culture plates were incubated at 37°C, 5% CO_2 in Incucyte® (Essen Bioscience Incucyte™ Zoom). 10x objective lens was selected to scan cells at phase and red (for cell death) or green (for eGFP) channels and cells were scanned every 2 hours. Image collection and processing definition were completed following the Incucyte® manual, and only the objective area between 50 μM^2 and 2000 μM^2 were counted to be cells for data analysis. For image editing purposes, the digital data after auto-analysis was exported to Microsoft Excel for the generation of time-course cell death graphs; the kinetics of eGFP expression was auto-generated by Incucyte™ Zoom Software.

5.11 Localization of transfected siRNA in primary human MDMs

Primary human MDMs were transfected with 20 nM BLOCK-iT Alexa Fluor Red Fluorescent siRNA Control and 1.0 µl DarmaFect 3 for 6 hours. The supernatant was removed. The stock solution (10 mg/mL) of Hoechst 33342 (ThermoFisher Scientific Invitrogen, Cat. #: H1399) was diluted 2,000x in PBS, and 500 µl/well was added to cover all cells and incubate at 37ºC for 5 minutes. Cells were washed in PBS and imaged at DAPI Channel of EVOS FL Cell Imaging System.

5.12 Flow cytometry analysis of PI staining and GFP expression

For undifferentiated U937 and THP-1, cells were counted and $1.0x10^5$ cells were collected directly from the supernatant. For differentiated U937, THP-1 and primary MDMs, cells were washed with PBS, trypsinized, pelleted, with 0.4ml 0.25% Trypsin-EDTA for 30 minutes, neutralized with 0.6 ml complete medium, and pipetted up and down for 10 times; supernatants, washing PBS, and trypsinized cells from one well were combined into one sample. Samples are centrifuged at 800g for 5 minutes and washed once with PBS, and then re-suspended in 0.5ml PBS with 0.5% BSA (Sigma, SKU: A7030). Right before loading to flow cytometer, 1.0 µl PI (Propidium Iodide, Sigma, SKU: P4864) was added to the sample, vortexed and analyzed immediately at PI channel. For the infection of 90k shRNA lentivirus pool, differentiated or undifferentiated cells were infected for 48 hours. Then cells were treated with puromycin (Sigma, SKU: P9620) for another 48 hours and PI staining was used to analyze the cell death by flow cytometry. For the infection rate of lentivirus-eGFP, cells were infected for 24 hours, washed with PBS, trypsinized if they are differentiated, and re-suspended in 0.5 ml PBS with 0.5% BSA, and analyzed by flow cytometer at GFP channel.

5.13 siRNA transfection of primary human MDMs for validation

All siRNAs were purchased from Dharmacon (Cherry-pick Library, LP_22590 G-CUSTOM-234593, Appendix 10.1). Accell Non-targeting siRNA #1 (Cat. #: D-001910-01-05) was selected as control siRNA. A mixture of xIAP, cIAP1 and cIAP2 siRNA (Cat. #: E-004098-00-0005, E-004390-00-0005, E-004099-00-0005), and 5 μM AEG40730 (Tocris Bioscience, Cat. #: 5330) were selected as positive controls unless specifically suggested. At least two hours before siRNA transfection, HIV-infected cells were washed with PBS and maintained in 0.8 ml/well of antibiotic-free DMEM medium supplemented with 10% FBS. For each well, 20 nM siRNA and 1.0 μl DarmaFect 3 Transfection Reagent were mixed in 200 μl of Dharmacon Transfection Medium (Accell siRNA Delivery Media, Cat. #: B-005000) according to the manufacturer's manual and dropped wisely to primary MDMs prepared. Cells were incubated at 37°C, 5% CO_2 for further experiments.

5.14 siRNA transfection of respirasome complex genes

The study on apoptosis of HIV-infected MDMs induced by siRNA of respirasome genes followed the same procedure of siRNA validation of promising genes. All siRNAs were purchased from Dharmacon: Human *NDUFA11* (126328) siRNA (Dharmacon, Cat. #: L-018508-01-0005) was select to silence Complex I; Human *SDHA* (6389) siRNA (Dharmacon, Cat. #: L-009398-00-0005) was select to silence Complex II; Human *UQCRQ* (27089) siRNA (Dharmacon, Cat. #: L-012517-01-0005) was select to silence Complex III; Human *Cox7a2* (1347) siRNA (Dharmacon, Cat. #: L-011626-01-0005) was select to silence Complex IV, which was also used as a positive control for this experiment; Human *ATP5A1* (498) siRNA (Dharmacon, Cat. #: L-017064-01-0005) was select to silence Complex V.

5.15 Apoptosis of HIV-infected MDMs induced by siRNA silencing

siRNA transfected primary MDMs were maintained at 37°C, 5% CO_2 incubators for 48~72 hours, washed with PBS, trypsinized with 0.25% Trypsin-EDTA, and harvested for flow cytometry analysis. For HIV-eGFP-infected samples, cells were stained with Annex V conjugated with APC or BV711 for 10 minutes without wash, fixed with 1% PFA (Boster Biological Technology, SKU: AR1068), and cell death was analyzed by flow cytometry BD LSRFortessa^{TM} X-20. For HIV-HSA-infected samples, cells were wash with PBS, blocked with 5.0 µl/10^5cells of human FcR Blocking Reagent (Miltenyi Biotec, Order #:130-059-901), stained with Rat anti-mouse HSA IgG antibody (M1/69) conjugated with FITC, washed with PBS, and stained with APC- or BV711-Annex V (BD Biosciences, Catalog NO. 550475 or 563972), fixed with 1% PFA. The apoptosis was analyzed by flow cytometry BD LSRFortessa^{TM} X-20.

5.16 Propidium Iodide (PI) Staining to evaluate cell death

Cells were washed with PBS and fixed with methanol for 15 minutes at 4 °C. Subsequently, cells were treated with 25µl of 10 µg/ml RNase A, followed by staining with 25 µl of 1.0 mg/ml PI solution at 4°C for 1 hour. The DNA content was analyzed using a FACSCanto flow cytometer (BD Biosciences) and the FACSDiva software. The subdiploid DNA peak (<2N DNA), immediately adjacent to the G0/G1peak (2N DNA), represents apoptotic cells and was quantified by histogram analyses. PI histograms figures were obtained with WinMDI version 2.8 software (J. Trotter, Scripps Institute, San Diego, CA).

5.17 Isolation of HIV-HSA-infected MDMs

MDMs were infected with HIV-Bal-HSA for 9 days followed by magnetic sorting using HSA-CD24 beads (MACS Miltenyi Biotec.) through column separation, as previously described [294]**.** Briefly, infected MDMs were detached with accutase (Innovative Cell Technologies, San Diego, CA), FcRγII receptors were blocked with FcR blocker, stained with Biotin Anti-mouse CD24 Antibody M1/69 (Biolegend, Cat. # 101804) conjugated antibody and incubated with Anti-Biotin Microbeads UltraPure (MACS Miltenyi Biotec, Order #: 130-105-637). HSA+ cells were collected by positive selection in LS columns. The HSA-negative (negative fraction) cells were collected after passing the labelled cells through the column for the first time. The column was detached from the magnet and the HSA positively labelled cells were collected by plunging out the cells. Purity of the HSA-infected macrophages was assessed by flow cytometry using Anti-Biotin PECy7 Antibody (Abcore, Product #: AC15-0149-17).

5.18 Analysis of caspase activation

Activation of caspase-3, -8, and -9 was measured as per protocol of caspase-3, caspase-8 and caspase-9 Multiplex Activity Assay Kit (Fluorometric) (Abcam, Product Code: ab219915) by flow cytometry.

5.19 TNF-α ELISA and cytokine ELISA array

Human TNF-α DuoSet ELISA (R&D, Product Code: DY210) was used to quantify TNF-α as per the manufacturer's recommendation. Briefly, the 96-well plates were preincubated with TNF-α capture antibody for 16 hours followed by blocking with 1% FBS. TNF-α (1-1000 pg/mL) was used as standards. The samples were added to the plates for 16 hours followed by the detection antibodies for two hours. Next,

100µL/well of substrate solution was added. The enzymatic reaction was stopped with 50µl/well of BioFX® 450 nM Liquid Stop Solution (Surmodics, Product #: LSTP-1000-01). The plates were read at 490 nM using iMark Microplate Reader (Bio-Rad) using microplate manager 6 software. The levels of secreted cytokines were measured as per the directions in Milliplex® Map Kit (EMD Millipore). IL-17F, GM-CSF, IFN-γ, IL-10, CCL20/MIP3a, IL-12p70, IL-13, IL-15, IL-17a, IL-22, IL-9, IL-1β, IL-33, IL-21, IL-23, IL-5, IL-6, IL-17ε/IL-25, IL-27, IL-31, TNF-α, TNFβ, and IL-28A were detected using antibody-immobilized magnetic beads and were quantified by MAGPIX® multiplex with xPONENT® software (Luminex Corp.).

5.20 SDS-PAGE and Western blotting analyses

Cells were harvested and lysed in cell lysis buffer (Cell Signaling, Product #: 9803S). Proteins were quantitated following Bio-Rad Protein Assay (Bio-Rad, Cat. #: 5000006) manual and analyzed in 15% SDS-Polyacrylamide Gel Electrophoresis (PAGE). Subsequently, proteins were transferred onto PVDF membranes (Bio-Rad, Cat. #: 1620177), which were then blocked with 10% nonfat dried milk in PBS at 4ºC overnight. Membranes were probed with first antibody in 1% BSA in PBS for 1 hour at room temperature, followed by Rat Anti-mouse IgG conjugated with Horseradish Peroxidase (Bio-Rad, Cat. #: MCA152) in 1%BSA. Immunoblots were visualized using Clarity Max™ Western ECL Blotting Substrates (Bio-Rad, Cat. #: 1705060) and imaged with Chemigenius Bio-imaging System (Syngene) and GeneSnap Software (Syngene). Anti-BAX antibody was purchase from Santa Cruz (Cat. #: sc-20067); rabbit monoclonal Anti-CDK2 antibody (Product #: ab32147), rabbit monoclonal Anti-CSTF2T antibody (Product #: ab138486), rabbit polyclonal anti-ZNF484 antibody N-terminal end (Product #: ab173874), and rabbit polyclonal anti-COX7A2 antibody C-

terminal end (Product #: ab135432) were purchased from Abcam. All the following specific antibodies was purchased from Cell Signaling: cIAP1 (D5G9) rabbit mAb (Product #:7065), cIAP2 (58C7) rabbit mAb (Product #: 3130), xIAP (3B6) rabbit mAb (Product #: 2045), caspase-3 Antibody (Product #: 9662), caspase-8 (D35G2) rabbit mAb (Product #: 4790S), caspase-9 Antibody (human specific) (Product #: 9502), β-actin (13E5) rabbit mAb (Product #: 4970), PARP rabbit Antibody (Product #: 9542), Bid Antibody (human specific) (Product #: 2002), TRAF1 (45D3) rabbit mAb (Product #: 4715), TRAF-2 Antibody (Product #: 4712), RIP Antibody (Product #: 4926), and Phospho-RIP (Ser166) (D1L3S) Rabbit mAb (Product #: 65746). Anti-NDUFA11 Polyclonal Antibody (Cat. #: A16239) was purchased from Abclonal Technology; Anti-SDHA Polyclonal Antibody (Product #: HPA 064582) and Anti-ATP5A1 Polyclonal Antibody (Product #: HPA 044202) were purchased from Sigma Prestige Antibodies; Anti-UQCRQ Polyclonal Antibody (Product Code: ab136679) was purchased from Abcam Technology. ImageJ Software (developed by Wayne Rasband from National Institute of Health of USA) was used for the densitometric analysis of BAX and β-Actin protein bands, and the protein ratio (BAX/β-Actin) of each experiment was calculated independently. The results were summarized into bar diagrams.

5.21 Apoptosis of HIV-infected MDMs induced by chemical inhibitors

The study on apoptosis of HIV-infected MDMs induced by chemical inhibitors follow the same procedure as siRNA validation of promising genes, but the treatment was shortened to 24 hours. 5 μM AEG40730 (Tocris Bioscience, Cat. #: 5330) was selected as positive control. To target 4 validated genes, 0.375 μM Sodium Azide (Sigma, Sku: S2202) dissolved in ddH_2O was used to target *Cox7a2*; 0.3 μM CDK2

Inhibitor II (Santa Cruz: Cat. #: sc-221409) dissolved in DMSO (Sigma, Sku: 276855), was used to target CDK2; 0.16 µM Cordycepin (Sigma, Sku: C3394) dissolved in DMSO was used to target CSTF2T; 0.5 µM Azodicarbonamide (Sigma: Cat. #: W504718) dissolved in DMSO was used to target *Znf484*; For respirasome complexes, 10 µM Rotenone (Sigma, Sku: R8875), dissolved in 99.9% Ethanol (Fisher, Product Code: 11394054) was used to target Complex I; 2.0 µg/ml Carboxin (Honeywell, Product #: 45371) dissolved in 99.9% Ethanol was used to target Complex II; 10 µM Antimycin A (Sigma, Sku: A8674) dissolved in 99.9% Ethanol was used to target Complex III; 0.375 µM Sodium Azide was still used to target Complex IV, which was also used as a positive control (CO7A2) for this experiment; 2.5 µM Oligomycin A (Sigma, SKU: 75351) dissolved in 99.9% Ethanol was used to target Complex V. LCL161 was purchased from Active Biochem (Cat. #: A-1147); Necrostatin-1 was purchase from ApexBio (Cat. #: A4213), Staurosporine was purchased from ApexBio (Cat. #: A8192), and LPS was purchased from Sigma (SKU: L4391).

5.22 ROS production detection

To measure the ROS production in Mock- or HIV-infected primary human macrophages, seven-day old MDMs were infected with HIV-HSA viruses (150 ng p24) and maintained at 37°C, 5% CO_2 for 7 days. Cells were transfected with 20 nM siRNA for 48 hours, harvested, blocked with FCR blocking buffer, and then stained with CellROX® Deep Red Reagent (Life Technologies™, Cat. #: C10422) and mouse CD24-FITC for 30 minutes at 37°C. Cells were washed twice with 1.0 ml PBS, and then fixed with 500 µl of 1% PFA (pH 7.6). The ROS production were analyzed by flow cytometry (BD LSRFortessa™ X-20) at FITC and APC channel.

5.23 Microscopy

For transfection reagent optimization, images of cells treated with AEG40730 and RESV were retrieved directly from IncuCyte®. For the transfection efficiency of siRNA in Primary human MDMs, cells were transfected with 20 nM BLOCK-iT Alexa Fluor Red Fluorescent Control with various transfection reagents for 16 hours and imaged under at DAPI Channel of EVOS FL Cell Imaging System. For the customization of 90k shRNA lentivirus pool, differentiated U937, THP-1, and primary MDMs were washed once with PBS, fixed with 3.7% Formaldehyde (Fisher Scientific, Cat. #: F79P-4), imaged on IX51 Olympus Fluorescence Microscope.

5.24 Statistical analysis

Microsoft Excel 2016 was applied to compute Mean Value, Standard Deviation (SD) and plot kill curves; P values were calculated using Student t test, or One-way Anova, followed by Dunnett's posttest. * indicates $p \leqslant 0.05$, ** indicates $p \leqslant 0.01$; *** indicates $p \leqslant 0.001$. Plotted data represent the Mean value ± Standard Deviation (SD). GraphPad Prism 6.0 software was used to create bar diagrams. Each experiment was repeated at least three times independently (n=3). The apoptosis of HIV-infected MDMs induced by siRNA or chemical inhibitors was based on 4 independent experiments from different donors (n=4). ROS production induced by respirasome complexes was based on 8 independent experiments from different donors (n=8).

5.25 Ethics statement

HIV-infected individuals and healthy participants involved in the study gave informed written consent and the protocol for obtaining blood samples was approved by the Review Ethics Board of the Ottawa General Hospital and the Children's Hospital of Eastern Ontario, Ottawa, ON, Canada.

6. Results

Chapter 6.1: Optimizing siRNA transfection into primary human macrophages by reversing Resveratrol-induced apoptosis

1. Introduction

Macrophages, the multifunctional phagocytes, play crucial roles in many physiological activities, such as immune regulation, cleaning up exogenous antigens, clearance of endogenous cell debris, tissue repair, regeneration, and fibrosis [306–309]. In addition, macrophages are long-lived cells distributed all over the human body with a lifespan of months to years [203,204]. Thus, these cells play critical roles in innate immunity and in the pathogeneses of several chronic and inflammatory diseases through the induction or resolution of inflammation and tissue repair [310]. Recent evidence obtained by way of microarray analysis and conventional approaches of *in vivo* studies has suggested the involvement of M1 proinflammatory macrophages in gastrointestinal typhoid fever, tuberculoid leprosy and active tuberculosis. Anti-inflammatory M2 macrophages, however, are associated with lepromatous leprosy and chronic rhinosinusitis [310–316]. In addition, it has been shown that macrophages can be altered by the tumor microenvironment and can promote solid tumor progression and metastasis [317–320]. Moreover, macrophages have been shown to play a major role in HIV reservoir formation [16]. Targeting macrophages as a potential therapeutic strategy via induced apoptosis has been suggested, such as downregulating pro-inflammatory pathways and targeting tumor-associated or HIV-infected macrophages [319,321–323]. Small interfering RNA

(siRNA) silencing has been identified as a critical tool in inducing apoptosis in infected or neoplastic cells [324,325], but effective use of siRNA needs transfection technology to deliver siRNA into the correct subcellular location of target cells [326].

Primary human macrophages are well-known to be extremely hard to transfect [290,291,327], primarily due to their recognition of foreign nucleic acids, and their initiation of immune responses to exogenous siRNA molecules [290,291]. Moreover, in some infections, such as HIV, the infection rate of human macrophages *in vitro* or *in vivo* is usually low [56,160,201,202]. As a result, ambiguous results may be obtained if the transfection rate is also very low when studying specific killing of HIV-infected macrophages by siRNA silencing. These challenges may be overcome by optimizing the transfection technology for primary human macrophages. Transfection is a tug-of-war between transfection rate and cytotoxicity, however, and a higher transfection rate is generally accompanied with increased cytotoxicity, which may non-specifically activate certain genes and unfavorably affect experimental data [328]. Since cellular toxicity is correlated with the transfection reagent and cell type [328–330], an optimized method for siRNA transfection in primary human macrophages, which takes into consideration the balance between transfection rate and cytotoxicity, has not been reported.

In 2011, Guha et al reported that an anti-oxidant drug, Resveratrol (RESV), killed a monocytic cancer cell line, U937, by upregulating the gene expression of *Bax*, a component of the intrinsic apoptosis signaling pathway [331]. I hypothesize that an ideal siRNA transfection can effectively deliver *Bax* siRNA into human macrophages and protect cells against apoptosis induced by RESV. The IncuCyte® has been widely used in recent years to study cell viability without removing cells from incubators [332],

as it automatically analyzes and generates presentation-ready graphs. When dyes suitable for staining dead cells are applied, this technology can automatically report the time-course of cell death induced by drug treatments [333], allowing for a time and cost-effective way of selecting the optimal transfection reagent for adherent cells. Herein, I combined the protective effects of *Bax* siRNA to RESV-induced cell death and the auto-analysis function of the IncuCyte® for a fast selection of optimal siRNA transfection reagents for primary human macrophages. This novel method may be universally applied for a rapid optimization of siRNA transfection technology for adherent cells. Moreover, this method provides the comparison of transfection efficiency between multiple reagents that is simple, intuitive, visual, and objective. Most importantly, this strategy takes into consideration the balance between transfection rate and cytotoxicity.

Note: all the experiments in this chapter were performed by Simon Xin Min Dong.

Figure 5. Model for reversal of RESV-induced apoptosis in human MDMs using *Bax* siRNA

A. RESV-induced apoptosis of U937 by upregulating the expression of *Bax*, reported by Guha in 2011 [331]. **B.** Pretreating cells with *Bax* siRNA and transfection reagents reverses RESV-induced apoptosis in primary human macrophages; the better the transfection reagent, the less RESV-induced apoptosis. Based on this mechanism, the optimal transfection reagent for primary human MDMs can be identified.

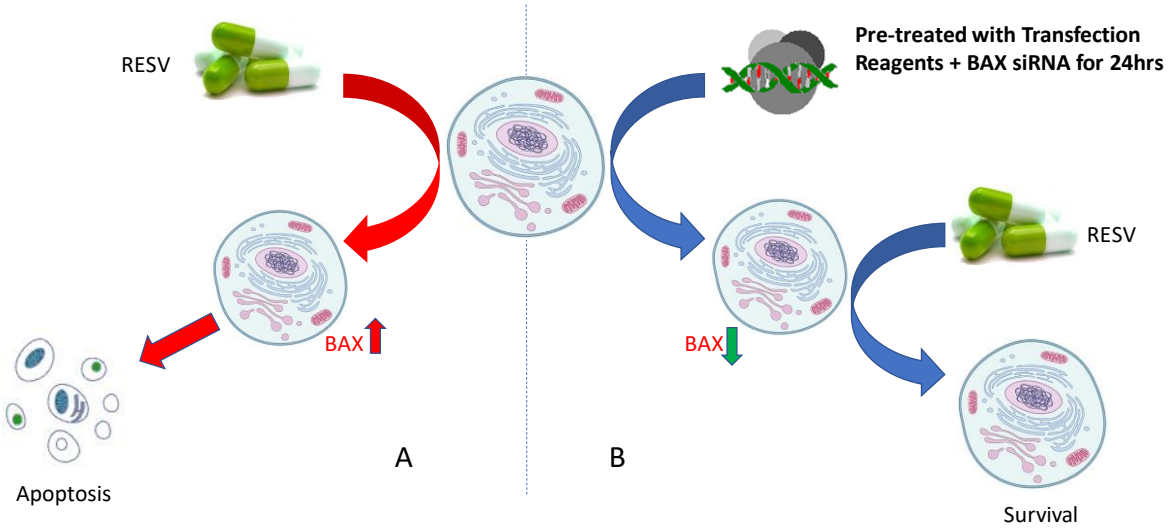

Guha. J of Pharmacolo Exp Thera 2011; 336(1): 206-14.

2. Results

2.1 RESV induces cell death of PMA-differentiated U937 and human MDMs

RESV has been shown to induce apoptosis in U937 cells [331]. To determine if RESV induces apoptosis in primary human monocytic cells, I first determined the suitable dose of RESV to induce cell death in Phorbol 12-myristate 13-acetate (PMA)-differentiated U937 cells and primary human monocyte-derived macrophages (MDMs). A second mitochondria-derived activator of caspase (SMAC) mimetics dimer, AEG40730, has previously been used in our laboratory to induce apoptosis in primary human MDMs. In this study AEG40730 was used as a reference drug to determine the suitable dose of RESV to moderately induce apoptosis of differentiated U937 and primary human MDMs. The suitable dose of RESV should be able to kill target cells effectively, but the killing effect should not be more than 10.0 µM AEG40730. Propidium Iodide (PI), which specifically stains RNA and DNA of dead cells, was employed to track cell death and the IncuCyte® was used for real-time imaging, data analyses, and generating time-course graphs of cell death.

PMA-differentiated U937 and primary human MDMs in cell culture plates were treated with various doses of RESV and PI was added to the complete medium simultaneously to track cell viability. Cells were incubated, imaged by IncuCyte®, and cell death was analyzed by IncuCyte® Zoom 2016B software to generate kill curves of AEG40730 and RESV. My results indicated that RESV at concentrations of 300 µM and 250 µM induced the ideal amounts of cell death in PMA-differentiated U937 (**Fig. 6A**) and primary human MDMs (**Fig. 6B**), respectively.

Figure 6. Optimal RESV dosage inducing apoptosis of U937 and MDMs

PMA-differentiated U937 and primary human MDMs were treated with 10 μM AEG40730 and various doses of RESV; 1.0 μl/ml Propidium Iodide (PI) was used to stain and identify dead cells. Cells were monitored and analyzed by IncuCyte®, and time-course graphs of cell death were automatically generated. **A.** time-course cell death of differentiated U937 induced by AEG40730 and RESV; **B.** time-course cell death of primary human MDMs induced by AEG40730 and RESV.

Fig. 1A: PMA-differentiated U937

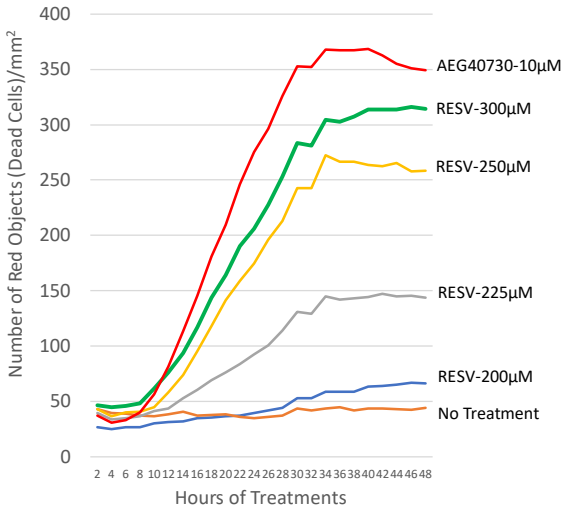

Fig. 1B: Primary human MDMs

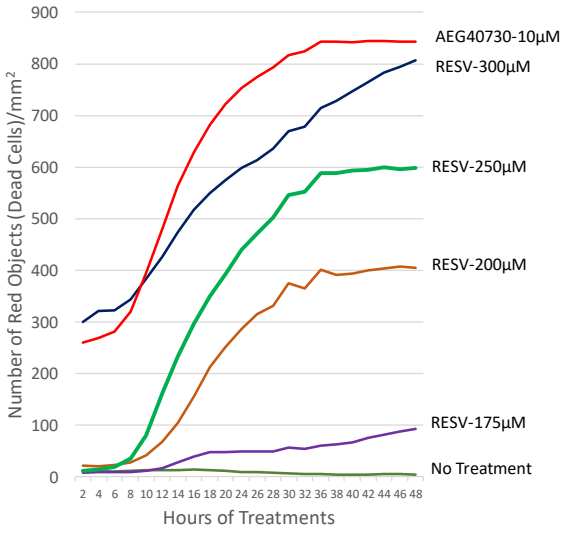

2.2 Selection of siRNA transfection reagent for PMA-differentiated U937 and primary human MDMs

To determine the protective effect of *Bax* siRNA, PMA-differentiated U937 cells and primary human MDMs were treated with 20 nM *Bax* siRNA and each of the 10 transfection reagents obtained from various biotechnology companies (DharmaFECT 3 and DharmaFECT 4 from Dharmacon, HiPerFect from Qiagen, Lipofectamine RNAiMAX, Lipofectamine 2000 and Lipofectamine 3000 from Invitrogen, PureFection™ from SBI System Bioscience, X-tremeGENE from Roche, siRNA Transfection Reagent from Santa Cruz, and Ambion siPORT Amine siRNA Transfection Reagent from ThermoFisher) for 24 hr as per the manufactures' protocols suggested. Subsequently, the transfected U937 cells and MDMs were treated with 300 µM and 250 µM RESV respectively, followed by incubation in the IncuCyte® for 48 hr. PI was added to the complete medium simultaneously. To achieve efficient transfection, I fixed the amount of siRNA at 20 nM/well but varied the amount of transfection reagents by ±25% of the dose recommended by the manufacturers. For example, Dharmacon recommended 0.8 µl/well DharmaFECT 3 transfection reagent for macrophages seeded in a 12-well plate. Therefore, 20 nM *Bax* siRNA was transfected with 0.6 µl, 0.8 µl, or 1.0 µl/well DharmaFECT 3 transfection reagent, respectively, for 24 hr before RESV treatment. Cells were imaged and analyzed by IncuCyte® at various time points post RESV treatment, and kill curves were generated to compare the protective effects of *Bax* siRNA with different transfection reagents. Using this approach, I was able to decipher, via IncuCyte, the level of cell death caused at each concentration of the reagents. The kill curves closest to the negative control (no RESV treatment, no siRNA, and no transfection reagent) would indicate the optimal transfection reagent with least cytotoxicity, as more efficient transfection should result in a greater protective effect of *Bax* siRNA with least cytotoxic effect of the transfection reagent (**Fig. 7A**

and 7B). The results show that of all the 10 transfection reagents examined, *Bax* siRNA transfected with DharmaFECT 3 transfection reagent prevented maximally RESV-induced cell death in both PMA-differentiated U937 cells and primary human MDMs. For clarity and ease of presentation, only the two best kill curves, which were closer to the "no treatment curve" for a transfection reagent, are shown. The kill curve with the concentration causing the most cell death was not shown. However, if the best two curves selected for a transfection reagent were very close to each other, only one curve was shown in the figure (e.g. Santa Cruz transfection reagent in **Fig. 7A**). The protective effect of *Bax* siRNA was detectable as early as 12 hr post-RESV treatment and the maximal protective effect was observed by 24 hr post-RESV treatment. In contrast, *Bax* siRNA transfected with X-tremeGENE from Roche caused the highest level of cell death. The transfection reagents from Santa Cruz, Lipofectamine RNAiMAX, and HiPerFect containing *Bax* siRNA moderately prevented RESV-induced cell death. **Fig. 7B** shows that for primary human MDMs, Lipofectamine 2000 was less toxic than other reagents but relatively more toxic than DharmaFECT 3 reagent. This was further confirmed via fluorescence microscopy. For this, 20 nM BLOCK-iT™ Alexa Fluor® Red Fluorescent Control siRNA was transfected with either 1.0 µl DharmaFECT 3 or 6.0 µl Lipofectamine 2000 for 16 hr following which the cells were imaged under fluorescent microscope. The results revealed altered cell morphology and extensive granulation in cells treated with Lipofectamine 2000 compared to the cells treated with DharmaFECT 3 transfection reagent (**Fig. 7C**), indicating Lipofectamine 2000 is more toxic than DharmaFECT 3 for primary human MDMs. These results suggest that DharmaFECT 3 is the most appropriate transfection reagent for primary human MDMs. Therefore, in the next series of experiments, I primarily focused on DharmaFECT 3 transfection reagent.

Figure 7. Transfection reagent selection for U937 and human macrophages

20 nM *Bax* siRNA was transfected with 3 different doses of each transfection reagent (the amount recommended by the manufacturer, +25% and -25% of the dose recommended by the manufacturer). For clarity and ease of presentation, the best two kill curves for the transfection reagents closest to the "no treatment curve" are shown. If the best two curves selected for a transfection reagent were very close to each other, however, only one curve is shown. Representative graph for the time-course cell death of PMA-differentiated U937 cells (A) and primary human MDMs (B) pretreated with *Bax* siRNA 24 hr before treatment with 300 μM RESV. (C) The cytotoxicity comparison between DharmaFECT 3 and Lipofectamine 2000 in primary human MDMs. 20 nM BLOCK-iT™ Alexa Fluor® Red Fluorescent control siRNA was transfected with either 1.0 μl DharmaFECT 3 or 6.0 μl Lipofectamine 2000 for 16 hr following which the cells were imaged under fluorescence microscope.

A: PMA-differentiated U937

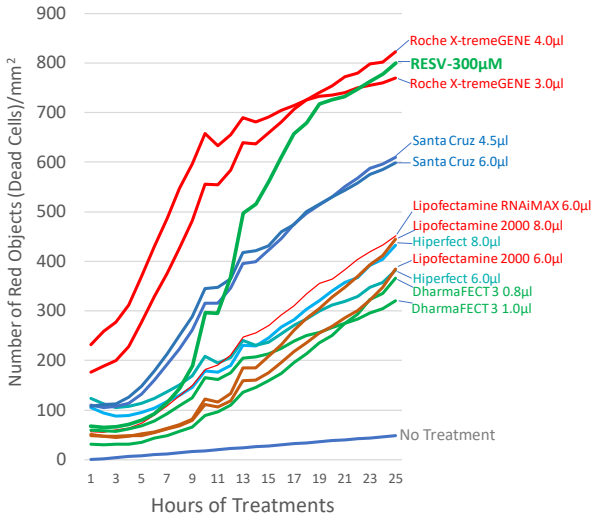

B: Primary human MDMs

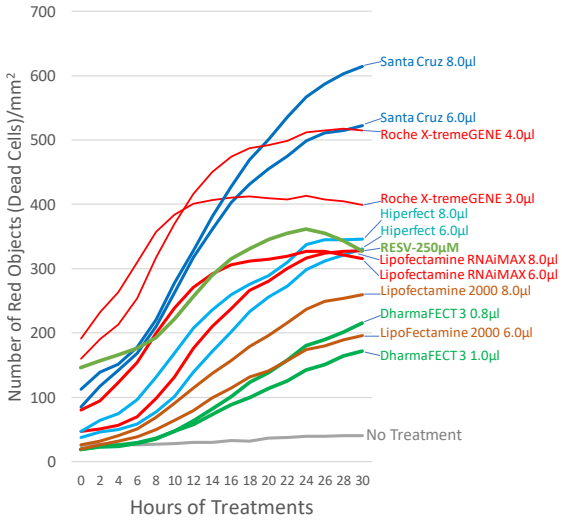

C: Primary human MDMs

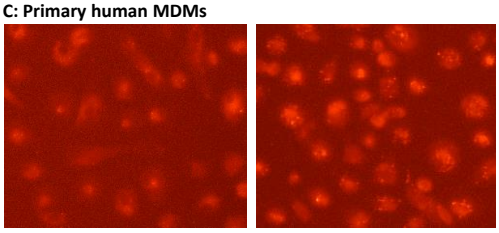

DharmaFECT3 1.0 µl LipoFectamine2000 6.0 µl

2.3 Determining optimal dose of siRNA and transfection reagent for primary human MDMs

To determine the optimal dose combination of siRNA and DharmaFECT 3 transfection reagent, various amounts of siRNA and DharmaFECT 3 transfection reagent were combined to pre-treat MDMs for 24 hours following which cells were treated with 250 µM RESV and PI was added to the complete medium simultaneously. Cell death was monitored by IncuCyte® and kill curves were generated (**Fig. 8A**). My results show that the most protective effects to RESV-induced cell death of primary human MDMs were achieved when the combination of 1.0 /well DharmaFECT 3 transfection reagent and 20 nM/well *Bax* siRNA were applied. In contrast, 30 nM/well siRNA along with 2.0 µl/well DharmaFECT 3 transfection reagent killed cells similar to that of the positive control (250 µM RESV without siRNA pretreatment), indicating that high doses of siRNA and transfection reagents are highly toxic to human MDMs.

To verify if siRNA was delivered into the correct location of target cells, I tracked siRNA in macrophages by transfecting 20 nM/well the BLOCK-iT™ Alexa Fluor® Red Fluorescent Control siRNA with DharmaFECT 3 transfection reagent. Cells were stained with Hoechst 33342 for 15 minutes, as a nuclear counterstain, and imaged under a microscope. I found that after 6 hours of transfection, red fluorescence, which suggested the location of transfected siRNA, was observed in the cytoplasm of primary MDMs (**Fig. 8B & 8C**), indicating that the transfection reagent I selected, DharmaFECT 3, and the dose I determined, 1.0 µl/well, successfully delivered siRNA into the cytoplasm of primary human MDMs.

Figure 8. Dosage combination of DharmaFect 3 and siRNA and localization of siRNA

A. time-course cell death of dosage combination of DharmaFect 3 and siRNA: MDMs pretreated with various dosage combination of *Bax* siRNA and transfection reagents for 24 hours; then treated with 250 μM RESV and PI. Cells were monitored, analyzed by IncuCyte®, and time-course graphs of cell death were generated. For the localization of siRNA in primary human MDMs, MDMs were transfected with BLOCK-iT Alexa Fluor Red Fluorescent Control and DarmaFect 3 for 6 hours and stained with Hoechst 33342. Cells were imaged with EVOS FL Cell Imaging System. **B.** MDMs without siRNA transfection. **C.** MDMs transfected with the BLOCK-iT™ Alexa Fluor Red Fluorescent Control.

A

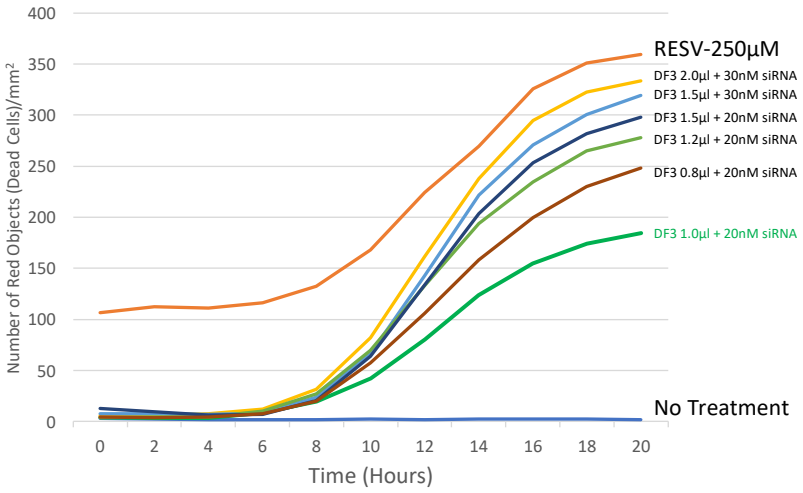

B

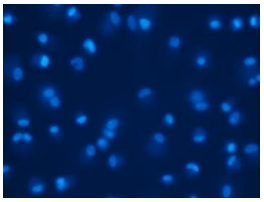

Negative Control

C

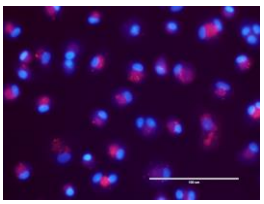

DF3 + NT siRNA-Alexa Fluo555

2.4 Efficiency of siRNA transfection into primary human MDMs

Next, I determined the efficiency of siRNA transfection in human MDMs using BLOCK-iT™ Alexa Fluor® Red Fluorescent Control siRNA (Alexa Fluor control siRNA) with DharmaFECT 3 transfection reagent and compared it with the transfection reagents from other manufacturers. 20 nM Alexa Fluor control siRNA was transfected into human MDMs with DharmaFECT 3 or X-tremeGENE for 16 hr. Cells were imaged (**Fig 9A1-Fig 9D1**), trypsinized, and the percentages of Alexa Fluor555 positive cells were analyzed by flow cytometry. Our results show that without treatment, none of the cells were stained **(Fig 9A1),** whereas cells treated with Alexa Fluor control siRNA in the absence of transfection reagent showed only few deeply stained macrophages **(Fig 9B1).** However, with DharmaFECT 3 and X-tremeGENE transfection reagents, most of the macrophages were deeply stained (**Fig 9C1, 9D1**). The lightly stained cells might be the macrophages in which the Alexa Fluor control siRNA is bound on the cell membranes but are not transfected. The quantification of cells transfected with the Alexa Fluor control siRNA by flow cytometric analysis indicated that ~83.9% of human MDMs were effectively transfected with 1.0 µl DharmaFECT 3 transfection reagent (**Fig 9C2**) compared to the 0% in untreated and un-transfected cells **(Fig 9A2)** and 15% in cells treated with Alexa Fluor control siRNA alone without transfection reagent **(Fig 9B2).** Similarly, approximately 95% cells were transfected with X-tremeGENE transfection reagent **(Fig 9D2)**. Although the transfection rate of X-tremeGENE was as high as 95% (**Fig 9D2**), this reagent exhibited significantly higher number of cell death (**Fig 7A and 7B**), suggesting that the X-tremeGENE transfection reagent from Roche was very toxic to primary human MDMs. In addition, the siRNA transfection efficiency of Lipofectamine 2000 was in the range of 85-90% (data not shown), but the high transfection rate was offset by its higher cytotoxicity compared to DharmaFECT 3 transfection reagent (**Fig 7B and 7C**). Thus, DharmaFECT 3 was identified as the optimal transfection reagent for primary human MDMs.

Figure 9. siRNA transfection efficiency in primary MDMs.

Primary human MDMs were transfected with 20 nM BLOCK-iT Alexa Fluor Red Fluorescent Control siRNA and various transfection reagents for 16 hr. **A1:** No siRNA, no transfection reagent; **B1:** 20 nM BLOCK-iT Alexa Fluor Red Fluorescent Control without transfection reagent; **C1:** 20 nM BLOCK-iT Alexa Fluor Red Fluorescent Control with 1.0 µl DharmaFECT 3; **D1:** 20 nM BLOCK-iT Alexa Fluor Red Fluorescent Control with 4.0 µl Roche X-tremeGENE. **A2:** Percentage of control siRNA+ at A1; **B2:** Percentage of control siRNA+ at B1; **C2:** Percentage of control siRNA+ at C1; **D2:** Percentage of control siRNA+ at D1.

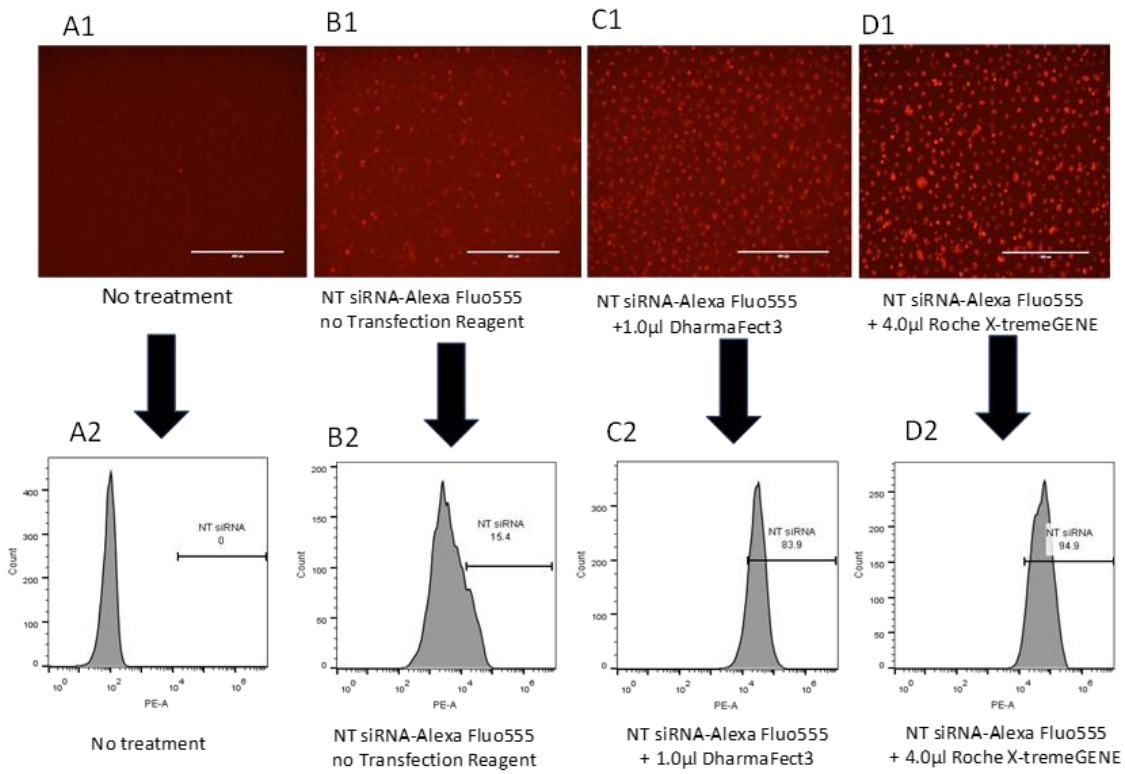
A1
B1
C1
D1
No treatment
NT siRNA-Alexa Fluo555
no Transfection Reagent
NT siRNA-Alexa Fluo555
+1.0µl DharmaFect3
NT siRNA-Alexa Fluo555
+ 4.0µl Roche X-tremeGENE
A2
B2
C2
D2
NT siRNA
0
NT siRNA
15.4
NT siRNA
83.9
NT siRNA
94.9
Count
PE-A
No treatment
NT siRNA-Alexa Fluo555
no Transfection Reagent
NT siRNA-Alexa Fluo555
+ 1.0µl DharmaFect3
NT siRNA-Alexa Fluo555
+ 4.0µl Roche X-tremeGENE

2.5 Protective effect of Bax siRNA with DharmaFECT 3 for PMA-differentiated U937

To quantify the protective effects of *Bax* siRNA transfected with DharmaFECT 3 transfection reagent for PMA-differentiated U937 cells against RESV-induced cell death, cells were treated with 20 nM *Bax* siRNA and 1.0 µl DharmaFECT 3 transfection reagent as before followed by RESV treatment along with PI for 24 or 48 hr. The images were retrieved from IncuCyte® for quantitative analysis. RESV treatment alone for 24 hr (**Fig. 10A1**) and 48 hr (**Fig. 10A2**) resulted in a large number of dead cells as indicated by red dots. In contrast, there was a significant reduction in the number of dead cells in PMA-differentiated U937 cells pretreated with 20 nM *Bax* siRNA and 1.0 µl DharmaFECT 3 transfection reagent followed by RESV treatment for 24 hr (**Fig. 10C1**) and 48 hr (**Fig. 10C2**) as revealed by staining with PI (red dots), suggesting that *Bax* siRNA transfection effectively protected U937 cells against RESV-induced cell death. As expected, very few dead cells were observed in negative controls without RESV treatment and siRNA transfection (**Fig. 10B1** and **10B2**). To quantify dead cells, I retrieved the data on "Red Object Counts" (dead cells stained with PI) recorded by IncuCyte® from the same images (**Fig. 10A1 to 10C1**, and **Fig. 10A2 to 10C2**), and converted the data into a bar diagram from one representative experiment (**Fig. 10D**). **Fig. 10E** shows the percentage of dead cells calculated from three independent experiments. In addition, our Western blot and densitometry analysis revealed that 20 nM *Bax* siRNA along with 1.0 µl DharmaFECT 3 transfection reagent significantly silenced the expression of *Bax* gene in PMA-differentiated U937 cells (**Fig 10F and 10G**).

Figure 10. Protective effects of Bax siRNA in PMA-differentiated U937 cells.

A1: RESV treated for 24 hr; **A2:** RESV treated for 48 hr; **B1:** No RESV treatment 24 hr; **B2:** No RESV treatment 48 hr; **C1:** Pretreated with 20 nM *Bax* siRNA and 1.0 µl DharmaFECT 3 for 24 hr then RESV treated for 24 hr; **C2:** Pretreated with 20 nM *Bax* siRNA and 1.0 µl DharmaFECT 3 for 24 hr then RESV treated for 48 hr. **D:** Number of dead cells in A1, B1, C1 and A2, B2, C2, information directly retrieved from Incucyte®. **E:** Percentage of dead cells compared to RESV treated; **F:** Representative Western blot analysis of PMA-differentiated U937 cells transfected with 20 nM Bax siRNA and 1.0 µl DharmaFECT 3 for 48 hr. G: Densitometry analysis of BAX and β-Actin protein bands from three independent Western blot experiments with results shown as mean ± SD (n=3). * indicates $p \leq 0.05$. ** indicates $p \leq 0.01$.

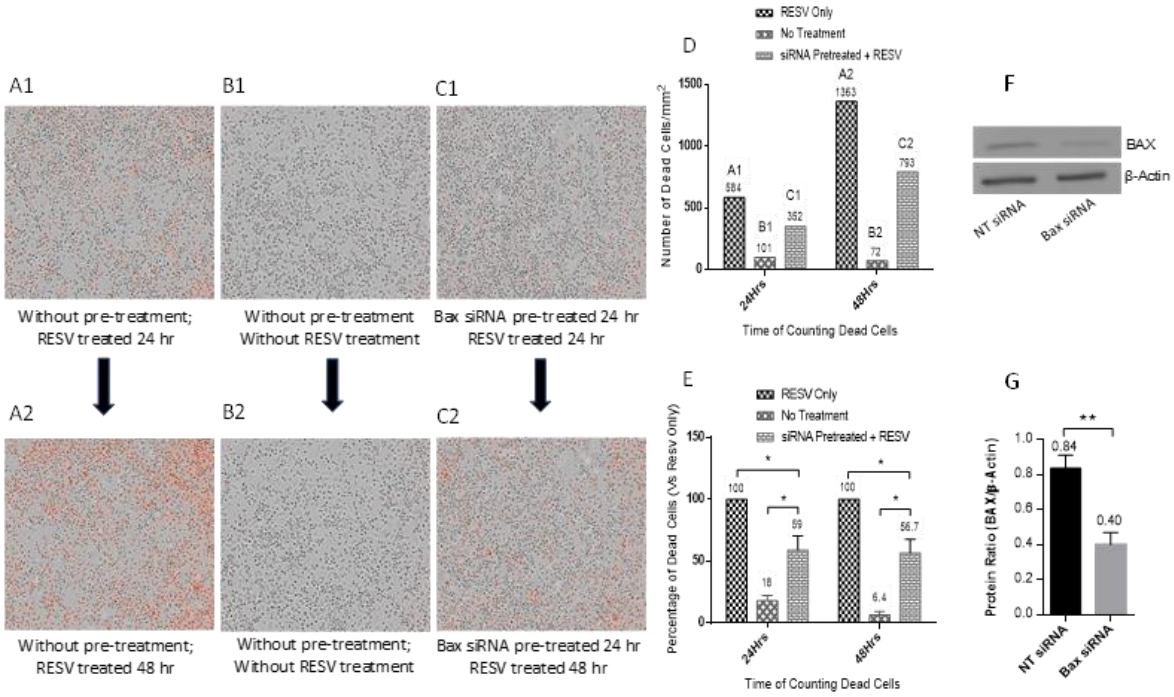
A1
B1
C1
Without pre-treatment; RESV treated 24 hr
Without pre-treatment Without RESV treatment
Bax siRNA pre-treated 24 hr RESV treated 24 hr
A2
B2
C2
Without pre-treatment; RESV treated 48 hr
Without pre-treatment; Without RESV treatment
Bax siRNA pre-treated 24 hr RESV treated 48 hr
D
RESV Only
No Treatment
siRNA Pretreated + RESV
Number of Dead Cells/mm2
1500
1000
500
0
A1
584
B1
101
C1
362
A2
1363
B2
72
C2
793
24Hrs
48Hrs
Time of Counting Dead Cells
F
BAX
β-Actin
NT siRNA
Bax siRNA
E
RESV Only
No Treatment
siRNA Pretreated + RESV
Percentage of Dead Cells (VS Resv Only)
150
100
50
0
100
18
59
100
6.4
56.7
*
*
*
*
24Hrs
48Hrs
Time of Counting Dead Cells
G
Protein Ratio (BAX/β-Actin)
1.0
0.8
0.6
0.4
0.2
0.0
0.84
0.40
**
NT siRNA
Bax siRNA

2.6 Protective effect of Bax siRNA with DharmaFECT 3 for human MDMs

The protective effects of *Bax* siRNA against RESV-induced cell death for primary human MDMs were also studied. Similar to the PMA-differentiated U937 cells, I pretreated primary human MDMs with 20 nM *Bax* siRNA and 1.0 µl DharmaFECT 3 transfection reagent for 24 hr, followed by RESV treatment along with PI for 24 or 48 hr. The images retrieved from IncuCyte® were analyzed. RESV treatment alone for 24 hr (**Fig. 11A1**) and 48 hr (**Fig. 11A2**) resulted in a large number of dead cells (red dots). In contrast, there was a significant reduction in the number of dead cells in MDMs pretreated with 20 nM *Bax* siRNA and 1.0 µl DharmaFECT 3 transfection reagent for 24 hr followed by RESV treatment for 24 (**Fig. 11C1**) and 48 hr (**Fig. 11C2**), indicating that *Bax* siRNA effectively protected MDMs against RESV-induced cell death. As expected, very few dead cells were observed in negative controls without RESV treatment and *Bax* siRNA transfection (**Fig. 11B1** and **11B2**). To quantify dead cells, I retrieved the data of MDMs on "Red Object Counts" recorded by IncuCyte® from the same images (**Fig. 11A1 to 11C1, and Fig. 6112 to 6112**), and converted the data into a bar diagram from one representative experiment (**Fig. 11D**). **Fig. 11E** shows the percentage of dead cells calculated from three different experiments. These results suggest that *Bax* siRNA significantly protected MDMs from RESV-induced cell death. In addition, Western blot (**Fig. 11F**) and densitometry analysis (**Fig. 11G**) revealed that 20 nM *Bax* siRNA along with 1.0 µl DharmaFECT 3 transfection reagent significantly silenced the expression of *Bax* gene in primary human MDMs. Overall, pretreating PMA-differentiated U937 and primary human MDMs with *Bax* siRNA and DharmaFECT 3 transfection reagent significantly reduced both the number and percentage of dead cells induced by RESV.

Figure 11. Protective effects of *Bax* siRNA in primary human MDMs.

A1: RESV treated for 24 hr; **A2:** RESV treated for 48 hr; **B1:** No RESV treatment 24 hr; **B2:** No RESV treatment 48 hr; **C1:** Pretreated with 20 nM *Bax* siRNA and 1.0 µl DharmaFECT 3 for 24 hr then RESV treated for 24 hr; **C2:** Pretreated with 20 nM *Bax* siRNA and 1.0 µl DharmaFECT 3 for 24 hr then RESV treated for 48 hr. **D:** Number of dead cells in A1, B1, C1 and A2, B2, C2; information was directly retrieved from IncuCyte®. **E:** Percentage of dead cells compared to RESV treated; the mean value and standard deviations were calculated using Microsoft Excel (n=3). **F:** Representative Western blot analysis of primary human MDMs transfected with 20 nM Bax siRNA and 1.0 µl DharmaFECT 3 for 48 hr. G: Densitometry analysis of BAX and β-Actin protein bands from three independent Western blot experiments. The results shown are mean ± SD (n=3). * indicates $p \leq 0.05$. ** indicates $p \leq 0.01$.

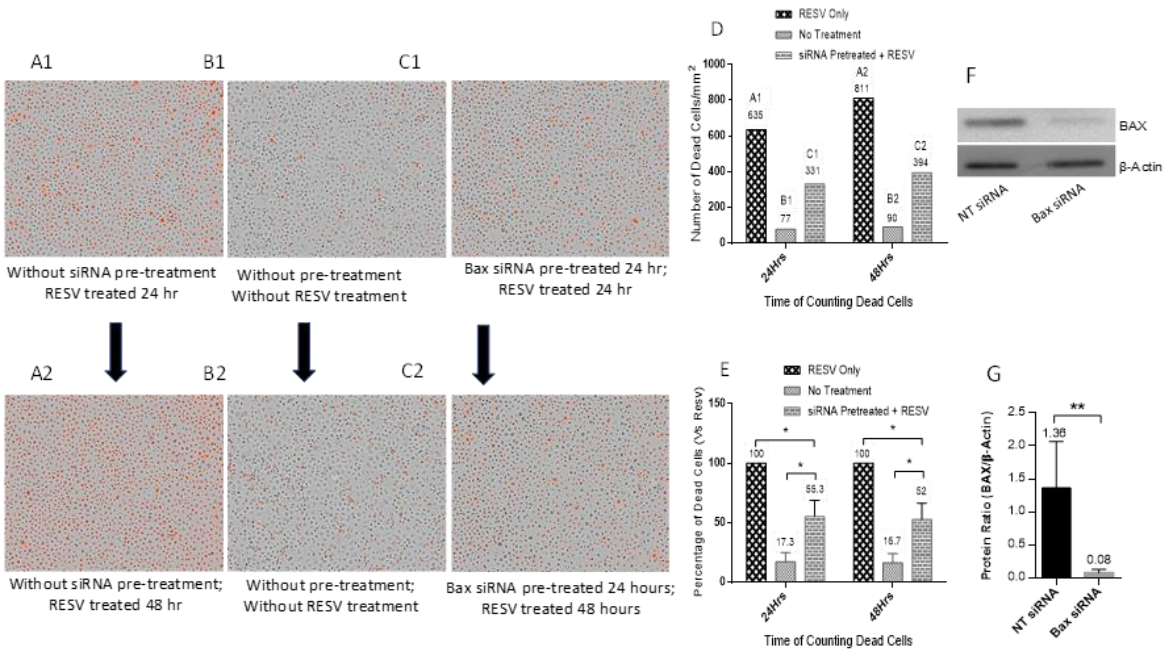
A1
B1
C1
Without siRNA pre-treatment
RESV treated 24 hr
Without pre-treatment
Without RESV treatment
Bax siRNA pre-treated 24 hr;
RESV treated 24 hr
A2
B2
C2
Without siRNA pre-treatment;
RESV treated 48 hr
Without pre-treatment;
Without RESV treatment
Bax siRNA pre-treated 24 hours;
RESV treated 48 hours
D
RESV Only
No Treatment
siRNA Pretreated + RESV
Number of Dead Cells/mm 2
A1 635
B1 77
C1 331
A2 811
B2 90
C2 394
24Hrs
48Hrs
Time of Counting Dead Cells
F
BAX
β-Actin
NT siRNA
Bax siRNA
E
RESV Only
No Treatment
siRNA Pretreated + RESV
Percentage of Dead Cells (Vs Resv)
100
17.3
55.3
100
16.7
52
24Hrs
48Hrs
Time of Counting Dead Cells
G
Protein Ratio (BAX/β-Actin)
1.36
0.08
NT siRNA
Bax siRNA

3. Discussion

siRNA is a critical loss-of-function tool for elucidating the roles of genes in experimental *in vitro* studies. Primary human macrophages are well-known to be hard-to-transfect cells with siRNA [290,291,327]. Currently, a fast, cost-saving, and easy-to-do method which can be used to select efficient siRNA transfection reagents for various adherent cell types, and in particular, primary human macrophages have not been reported. In this study, I took advantage of the protective effect of *Bax* siRNA and the auto-analysis function of IncuCyte® to select a transfection reagent that efficiently transfects siRNA into primary human macrophages and PMA-differentiated U937 cells. Our results suggest that DharmaFECT 3, a transfection reagent from Dharmacon, was the most efficient to transfect siRNA into both cell types, whereas most of the other transfection reagents were cytotoxic. Furthermore, ~85% of primary human MDMs can be transfected by this selected reagent. I also show that *Bax* siRNA effectively prevented RESV-induced cell death in primary human macrophages and PMA-differentiated U937 cells.

I observed that primary human MDMs from many individuals were not sensitive to siRNA transfection. The mechanisms responsible for resistance to transfection are not well understood. There are at least two factors that determine resistant phenotype of macrophages to siRNA transfection [290,291,327]. First, macrophages are professional immune cells; they have evolved to recognize foreign nucleic acids and may initiate immune responses to exogenous siRNA molecules [290,291]. Second, macrophages possess more restriction factors than other cell types which may interfere with intracellular machinery for siRNA silencing. For example, Li et al identified 114 restriction factors which significantly impact HIV replication in macrophages [334]. SamHD1, Apobec3, Tetherin, and Viperin are well-known restriction factors that affect multiple viruses at distinct stages of their life cycles [335]. SamHD1 has

RNase activity which may degrade exogenous siRNA [192], directly causing the failure of siRNA transfection into macrophages.

Efficiency of siRNA transfection may vary with the cell type and more so with the adherent cells depending upon the transfection reagents used. Reynolds emphasized the importance of selecting a transfection reagent for target cells [330], but a fast, cost-saving, and easy-to-do method for human macrophages has yet to be reported. Therefore, I analyzed 10 transfection reagents commercially available from 7 biotechnology companies to select the most suitable reagent for siRNA transfection in primary human MDMs. By employing *Bax* siRNA, I successfully selected the optimal transfection reagents for two hard-to-transfect cells, primary human macrophages [290,291,327] and PMA-differentiated U937 cells [336], suggesting that this novel method may be widely applied for the selection of an optimal siRNA transfection reagent for various adherent cells. Most importantly, the time-course graphs auto-generated by IncuCyte® software are an integrated readout of both transfection rate and cytotoxicity of the transfection reagents. Therefore, this strategy inherently takes the balance between transfection rate and cytotoxicity of the transfection reagents into consideration. The BLOCK-iT™ Alexa Fluor™ Red Fluorescent Non-targeting Control siRNA has been reported to be a useful reagent for assessing the transfection efficiency of siRNA [337]. This reagent alone, however, does not ascertain the cytotoxicity of the transfection reagents, and the higher transfection rate may be offset by the cytotoxicity of the transfection reagents. In addition, it also reports false positive siRNA signals caused by siRNA attaching to the outer cell membrane, without actually reaching the cytoplasm. Thus, this reagent can be used to track the location of siRNA but does not convey the optimal transfection reagent for target cells.

In summary, taking advantage of the protective effects of *Bax* siRNA to RESV-induced cell death and the auto-analysis function of IncuCyte®, I report that DharmaFECT 3 is the

optimal transfection reagent for both PMA-differentiated U937 and primary human MDMs. Although DharmaFECT 3 has been used for siRNA transfection of cell lines LNCaP (Prostate carcinoma) and SK-OV-3 (Ovarian adenocarcinoma), MCF7 [338], A2780 [339], SW480 and HT29 [340] cell lines, the novel method I describe herein is indeed a quick and effective strategy to select the optimal transfection reagent for adherent cells, and in particular, hard-to-transfect primary human macrophages. The kill curves are automatically generated by the IncuCyte®, avoiding human bias. Thus, it is easy to determine the optimal siRNA transfection reagent directly from the graphs auto-generated by the software. Moreover, the comparison of the transfection efficiency between multiple reagents is simple, intuitive, visual, and objective. This strategy takes into consideration the balance between transfection rate and cytotoxicity of the transfection reagents and can be widely applied to a fast and cost-saving selection of optimal siRNA transfection reagent for adherent cells. The limitations of this method are that the application requires the IncuCyte® Imaging System, familiarity with IncuCyte® data analysis, and high quality of cell monolayer seeded in culture plates.

Chapter 6.2: Smac Mimetics selectively induce apoptosis in primary human HIV-infected macrophages through RIPK1

1. Introduction

Macrophages are permissive to productive infection with HIV and a source of viral progeny for transmission to other cell types such as T cells [195,341–346]. HIV-infected macrophages are widely distributed in tissues such as gastrointestinal and other mucosal tissues, lymph nodes and within the central nervous system where they have a life span extending from months to years [203,204,347–350]. In contrast to the characteristic depletion of CD4+ T cells, macrophages do not decline in number, are resistant to apoptosis, survive active viral replication, and harbor unintegrated and integrated viral DNA in a state of latency [195,209,357,358,245,344,351–356]. In patients on effective antiretroviral therapy (ART), macrophages serve as reservoirs as HIV persists in these cells, shielded against various host anti-viral responses and respond poorly to ART [195,245,343,344,359]. Moreover, infected macrophages accumulate and retain virions within unique compartments designated as virus-containing compartments (VCCs) [360,361]. The virions present in VCC are protected from neutralizing antibodies and are inaccessible to anti-viral drugs [362–364]. Since HIV-infected macrophages are not cleared by CD8+ T cells, neither current ART nor the immune system is able to effectively eliminate this reservoir [359].

While several recent studies support that macrophages serve as a major non-T cell HIV reservoir [160,202,365–371], the role of macrophages in HIV infection and persistence has been conclusively demonstrated by employing humanized BLT and

myeloid only mice (MoM mice containing myeloid cells devoid of T cells). Honeycutt et al show that replication competent virus could be recovered from tissue macrophages, and the transfer of infected macrophages into uninfected animals resulted in sustained infection demonstrating that macrophages are genuine targets for HIV infection *in vivo* [343]. Further, they demonstrated that HIV persists in macrophages following suppressive ART *in vivo* in MoM model [150]. Therefore, to completely eradicate HIV in individuals on ART, it is imperative to eliminate both CD4+ T cells and myeloid tissue reservoirs. Most research to date has focused on eliminating the latent reservoir of CD4+ T cells by employing strategies to reactivate HIV in T cells and elimination of reactivated HIV-infected cells by host immunity [372–374]. However, approaches towards killing of HIV-infected macrophages *in vitro* or *in vivo* are not well studied. Two recent studies have attempted to clear macrophages reservoir by targeting infected macrophages with CSF-1 receptor antagonists and galactin-3 with some success [261,262].

In order to devise strategies to eliminate HIV-infected macrophages, it is imperative to identify apoptosis-related genes and signaling proteins involved in resistance of HIV-infected macrophages to apoptosis. The mechanism underlying resistance of infected macrophages to HIV-induced apoptosis may relate to the differential expression of pro- and anti-apoptotic genes including inhibitors of apoptosis (IAP) proteins [245,273]. The role of IAPs has been studied by employing antagonists of second mitochondria-derived activator of caspases (Smac), Smac Mimetics (SMs). SMs are a small molecule antagonist of IAPs that competitively inhibits Smac-IAP1/2 interactions and repress anti-apoptotic functions of IAP proteins. Recently, IAP1/2 and Survivin, another member of the IAP family were suggested to

be involved in survival of HIV-infected CD4+ T cells [271,375]. In addition, IAPs have been implicated in protection against hepatitis B infection and in the reversal of HIV latency in CD4+ T cells [269,376]. Using HIV-Vpr as an apoptosis-inducing agent, we have shown a protective role for IAP genes in resistance to cell death in macrophages [272,274,377]. CpG-induced protection against apoptosis and mitochondrial depolarization in monocytic cells was shown to be mediated by cIAP2 induction [272,274]. Moreover, down regulation of *IAP1/2*, by using siRNAs and SMs, sensitized macrophages to Vpr-induced apoptosis [377]. Therefore, strategies based on suppressing IAPs by employing SMs, may be useful in killing HIV-infected macrophages. Herein, I show that SMs induced apoptosis in *in vitro* HIV-infected macrophages and that this may occur through the concomitant down regulation of both *IAPs* and Receptor Interacting Protein Kinase-1 (*RIPK1*).

Note: for this chapter, I am the co-first author of this manuscript, and I performed 50% of the experiments. For the sake of coherence, I have included the experiments performed by other laboratory personnel. Their contribution has been acknowledged and recorded.

2. Results

2.1 SM induces cell death in HIV-infected myeloid U1 cells but not in counterpart uninfected U937 cells

SMs bind to cIAP1/2 and promote their E3 ligase activity which leads to their auto-ubiquitination, subsequent proteasome degradation and apoptosis [378,379]. We have previously shown that cIAP1/2 genes play a protective role in mediating survival of macrophages in response to Vpr-induced cell death [272,274,377,380]. We hypothesized that SMs will induce apoptosis in HIV-infected macrophages. U1 cells are chronically infected with two copies of proviral HIV DNA and show minimal constitutive expression of the virus. PMA stimulation of U1 cells induces HIV production and terminal differentiation along the mononuclear phagocytic lineage similar to HIV infection of primary macrophages [381,382]. Thus, we first determined the effects of SMs on apoptosis in undifferentiated and PMA-differentiated U937 and U1 cells. The chronically infected U1 cells and uninfected counterpart U937 cells were treated with SM-LCL161 followed by assessment of cell death by PI staining and flow cytometry. SM treatment induced significant cell death in U1 cells but not in U937 cells **(Fig. 12A).** To determine whether differentiation of U937 and U1 cells into primary macrophage-like cells render these cells susceptible to SM-induced apoptosis, U937 and U1 cells were differentiated with PMA. Similar to the effect of SM on undifferentiated U1 cells, SM -LCL161 induced significant cell death in differentiated U1 cells but not in differentiated U937 cells **(Fig. 12B).** Apoptosis of HIV-infected U1 cells was further confirmed by showing cleavage of caspase-3 in U1 but not in U937 cells by Western blot analysis using antibodies specific for caspase-3 **(Fig. 12C)**.

Figure 12. SM induces cell death of HIV-infected myeloid cells

A. U937 and chronically infected counterpart U1 cells were treated with SM-LCL161 at 1, 2, and 4μM for 48 hours. **B.** PMA-differentiated U937 and U1 cells were treated with SM-LCL161 at 1, 2, and 4μM for 48 hours. Cell death was assessed by intracellular PI staining. The p values were calculated using Mann-Whitney U test. (***p=<0.0001, **p=0.002). **C.** U937 and U1 were treated with increasing concentration of SM-LCL161 for 48 hours and cytosolic fractions were collected and subjected to western immunoblotting. 30 μg of total proteins were loaded to the protein gels. The membranes were probed with antibodies specific for caspase 3. The figure shown is a representative of three experiments *(These experiments were performed by Ramon Edwin Caballero)*.

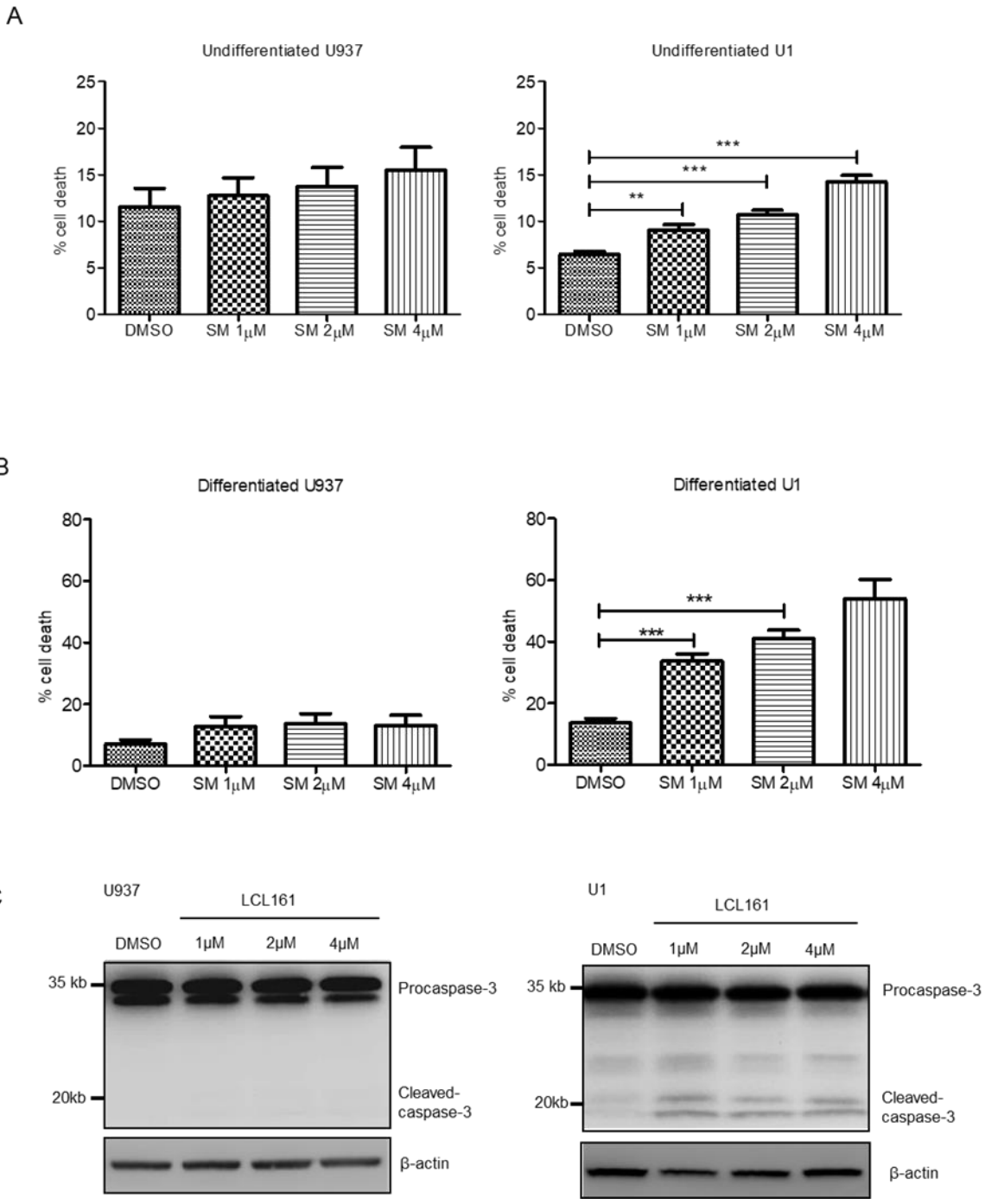
A
Undifferentiated U937
% cell death
25
20
15
10
5
0
DMSO
SM 1μM
SM 2μM
SM 4μM
Undifferentiated U1
% cell death
***
***
**
DMSO
SM 1μM
SM 2μM
SM 4μM
B
Differentiated U937
% cell death
80
60
40
20
0
DMSO
SM 1μM
SM 2μM
SM 4μM
Differentiated U1
% cell death
***
***
DMSO
SM 1μM
SM 2μM
SM 4μM
C
U937
LCL161
DMSO
1μM
2μM
4μM
35 kb
20kb
Procaspase-3
Cleaved-caspase-3
β-actin
U1
LCL161
DMSO
1μM
2μM
4μM
35 kb
20kb
Procaspase-3
Cleaved-caspase-3
β-actin

2.2 SM induces cell death in *in vitro* HIV-infected MDMs and MDMs derived from HIV-infected patients

To validate above findings in primary MDMs, we first verified the functional activity of SM by treating HIV-infected MDMs with LCL161 and observed degradation of both cIAP1 and cIAP2 **(Fig. 13A)** as reported earlier [377,380]. The *in vitro* HIV_{CS204}-infected MDMs were treated with SM-LCL161 followed by assessment of cell death by PI staining and flow cytometry. SM-LCL161 induced significant cell death of HIV_{CS204}-infected MDMs but not in mock-infected MDMs **(Fig. 13B).** Representative histograms of the intracellular PI staining are shown **(Fig. 13C).** The p24 values in MDMs infected with HIV_{CS204} for 7 days are shown in **Fig. 13D**. SM-induced cell death experiments were conducted at 48 hours post-treatment with SM as higher % of cell death was observed at 48 hours compared to 24 hours post treatment with SM-LCL161 (data not shown). To determine whether SM-induced cell death in *in vitro* HIV-infected MDMs is due to apoptosis, caspase activation was quantified based on the fluorescent signal of cleaved caspase substrates. Treatment of HIV_{cs204}-infected MDMs with SM-LCL161 showed activation of caspases 3, 8, and 9 in contrast to the mock-infected MDMs **(Fig. 13E).** A representative histogram for the induction of caspase 3, 8 and 9 following SM treatment of HIV-infected MDMs is shown **(Fig. 14).**

Figure 13. SM induces cell death of *in vitro* HIV-infected MDMs

A. The HIV-infected MDMs were treated with increasing concentration of SM-LCL161 for 48 hours. The cytosolic fractions were subjected to western immunoblotting. Membranes were probed with antibodies specific for human cIAP-1 and cIAP-2. **B.** Human MDMs were *in vitro* infected with HIV_{CS204} (100 ng p24/well) for 7 days. Cells were then treated with SM-LCL161 for 48 hours and cell death was assessed by PI staining and flow cytometry. **C.** Representative histograms of B. **D.** After 7-days of infection, supernatants were analyzed for p24 by ELISA. **E.** *In vitro* HIV-infected MDMs were treated with SM-LCL161 for 48 hours. The activation of caspases was detected by fluorescent caspase substrate (caspase-3, n=3; caspase-8, n=4; caspase-9, n=6). The p values were calculated using Mann-Whitney U test *(These experiments were performed by Ramon Edwin Caballero)*.

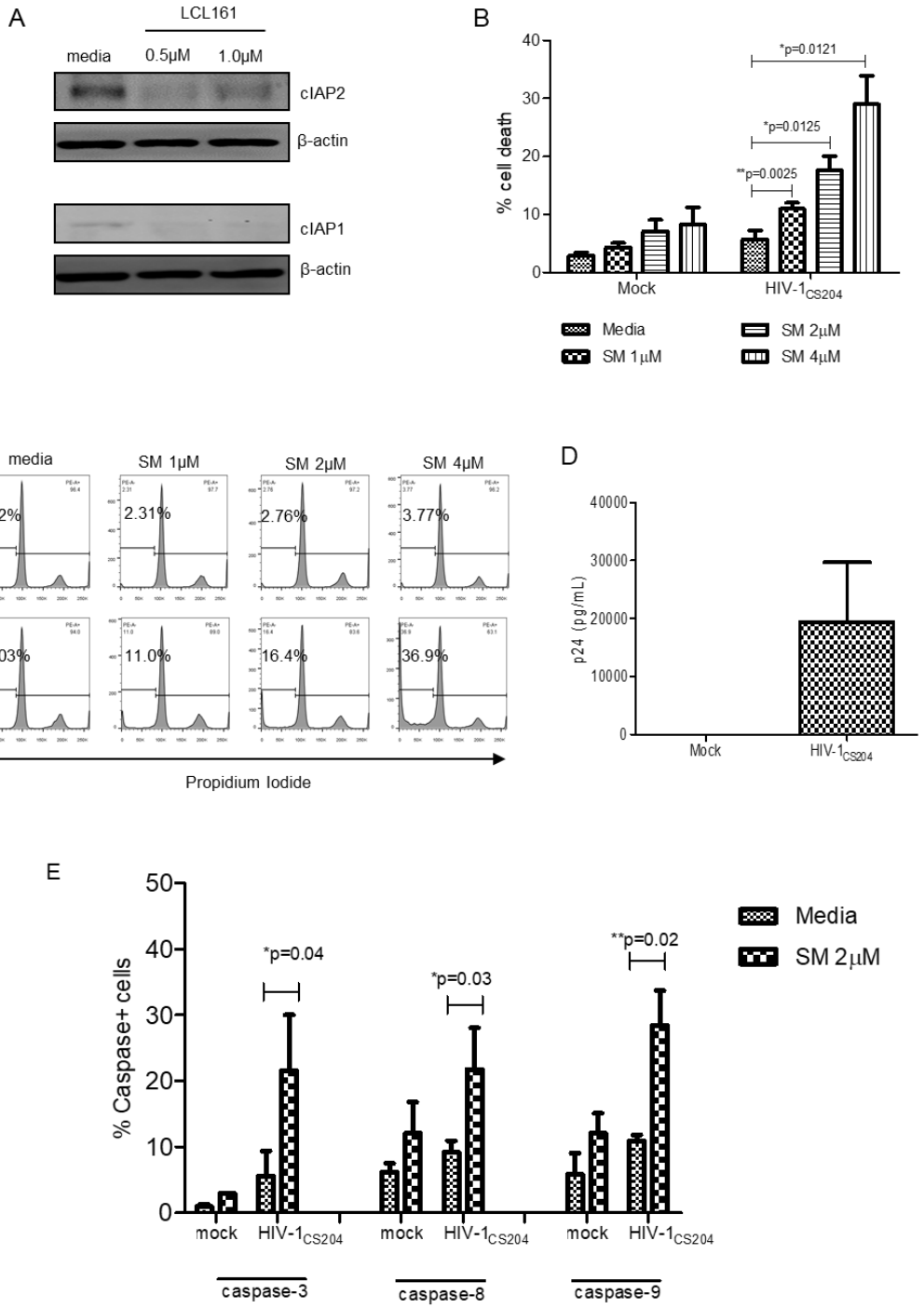
A
LCL161
media
0.5μM
1.0μM
cIAP2
β-actin
cIAP1
β-actin
B
% cell death
*p=0.0121
*p=0.0125
**p=0.0025
Mock
HIV-1CS204
Media
SM 1μM
SM 2μM
SM 4μM
C
media
SM 1μM
SM 2μM
SM 4μM
Mock
HIV-1CS204
Cell count
3.62%
2.31%
2.76%
3.77%
6.03%
11.0%
16.4%
36.9%
Propidium Iodide
D
p24 (pg/mL)
Mock
HIV-1CS204
E
% Caspase+ cells
*p=0.04
*p=0.03
**p=0.02
Media
SM 2μM
mock
HIV-1CS204
caspase-3
caspase-8
caspase-9

Figure 14. SM induces the activation of caspases in HIV-infected MDMs

Primary human MDMs were *in vitro* infected with HIV_{CS204} (100 ng p24/well) for 7 days. The cells were then treated with SM-LCL161 for 48 hours. The activation of the caspase 3, 8, and 9 were detected by intracellular caspase staining and analyzed flow cytometry. Representative histograms of 3 experiments are shown *(These experiments were performed by Ramon Edwin Caballero)*.

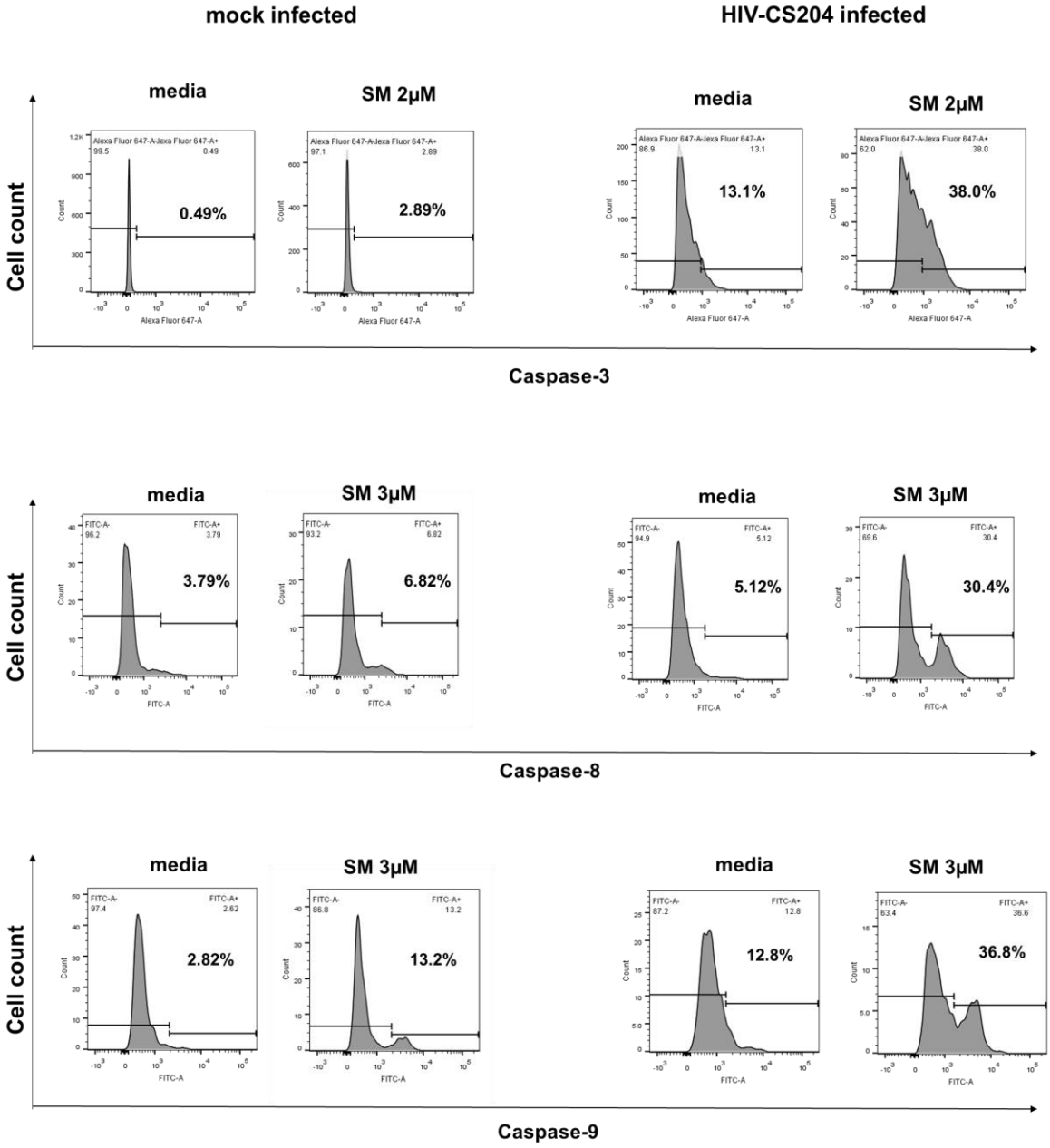
mock infected
HIV-CS204 infected
media
SM 2μM
media
SM 2μM
Cell count
0.49%
2.89%
13.1%
38.0%
Caspase-3
media
SM 3μM
media
SM 3μM
Cell count
3.79%
6.82%
5.12%
30.4%
Caspase-8
media
SM 3μM
media
SM 3μM
Cell count
2.82%
13.2%
12.8%
36.8%
Caspase-9

Further, to determine whether macrophages derived from HIV-infected individuals are similarly prone to SM-induced cell death, MDMs were generated from ART treated and ART naïve HIV-infected individuals and treated with SM-LCL161. Consistent with *in vitro* infection studies, *ex vivo* derived MDMs from treatment naïve and ART-treated HIV-infected individuals showed significantly increased susceptibility to SM-LCL161-induced cell death in a dose-dependent manner **(Fig. 15A)**. The level of SM-induced apoptosis in macrophages derived from ART naïve and ART treated patients was not very different. Moreover, ART treatment did not affect the expression of cIAP1 and cIAP2 in uninfected or HIV-infected macrophages (data not shown) suggesting that ART treatment did not affect the IAP pathway in uninfected or HIV-infected macrophages.

Apoptosis has been shown to induce viral activation and replication in latently infected U1 and ACH2 cell lines [383]. In addition, Pache et al have shown that SMs can affect viral transcription in infected $CD4^+$ T cells via NFκB dependent signalling [269]. To determine if SMs affect HIV replication in macrophages, *in vitro* HIV-infected MDMs were treated with SM-LCL161 for 48 hours followed by analysis of p24 secretion. Interestingly, virus replication in primary HIV-infected MDMs **(Fig. 15B)** and in HIV-infected U1 cells **(Fig. 15C)** was not affected by SM treatment.

Figure 15. SM induces cell death of MDMs generated from HIV-infected individuals

A. & **B.** Primary MDMs generated from untreated and ART-treated HIV-infected patients were treated with SM-LCL161 for 48 hours. Cell death was assessed by PI staining and flow cytometry. Supernatants from SM-treated *in vitro* HIV-infected MDMs. **C.** & **D.** SM treated primary MDMs and U1 cells were analyzed for p24 secretion. The p values were calculated using Mann-Whitney U test *(These experiments were performed by Niranjala Gajanayaka)*.

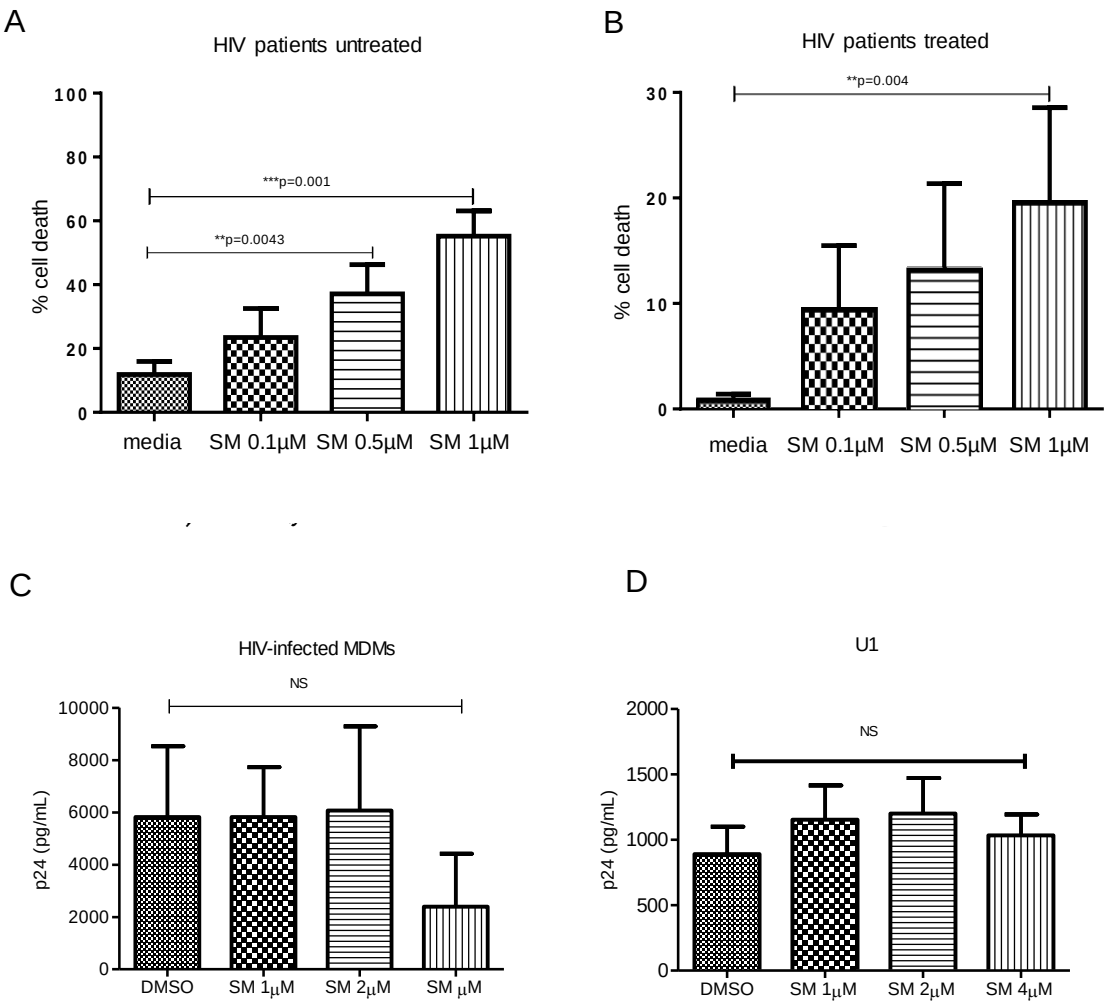
A
HIV patients untreated
% cell death
100
80
60
40
20
0
***p=0.001
**p=0.0043
media
SM 0.1μM
SM 0.5μM
SM 1μM
B
HIV patients treated
% cell death
30
20
10
0
**p=0.004
media
SM 0.1μM
SM 0.5μM
SM 1μM
C
HIV-infected MDMs
p24 (pg/mL)
10000
8000
6000
4000
2000
0
NS
DMSO
SM 1μM
SM 2μM
SM μM
D
U1
p24 (pg/mL)
2000
1500
1000
500
0
NS
DMSO
SM 1μM
SM 2μM
SM 4μM

2.3 SM specifically kills HIV-infected primary human MDMs

Based on above results, it is unclear if SMs are killing HIV-infected and/or bystander uninfected HIV-exposed MDMs. To examine this, we employed a R5 laboratory strain of HIV-1, HIV-Bal-HSA, expressing HSA (mouse CD24). Expression of CD24 by HIV-infected cells can be used to identify infected cells by flow cytometry using FITC-conjugated anti-mouse HSA antibody [294]. MDMs were infected with HIV-Bal-HSA for 7 days followed by treatment with SM-AEG40730 for another two days. HIV-HSA infection rate in MDMs ranged from 5-30 % over 15 days post infection depending upon the donor variability **(Fig. 16A).** Apoptosis of total HSA-expressing (HIV-infected) and HSA-negative (uninfected, HIV exposed bystander cells) cells by SM-AEG40730 was quantified by counter staining with Annexin-V labelled with BV711 expression. The gating strategy is shown in **Fig. 16B.** To rule out non-specific low-level fluorescence by dead cells/debris, highly intense FITC positive HSA-expressing cells were gated. Specific killing of intensely FITC-positive HSA-expressing (HIV-infected) cells was quantified for Annexin-V labelled with BV711 expression. The gating strategy is shown in **Fig. 16C.**

Quantification of Annexin-V positive, total (HSA+ and HSA-; **Fig. 16D, left panel**) and intensely HSA+ MDMs **(Fig. 16E, left panel**) revealed that SM-AEG40730 killed significantly higher number of total HIV-infected and uninfected (HSA+ and HSA-) and high HSA-expressing (HIV-infected) MDMs compared to the DMSO-treated HIV-infected cells. Representative histogram showing killing of total HSA+ and HSA- **(Fig. 16D, right panel**) and intensely positive **(Fig. 16E, right panel)** HSA-expressing cells is shown.

Figure 16. SM specifically induces cell death of HIV-HSA-infected MDMs

A. Primary human MDMs from healthy donors were infected with HIV-Bal-HSA over a period of time. Supernatants were collected at various days following infection and analyzed for p24 production by ELISA. **B. & C.** Gating strategy for the detection of apoptosis of HIV-infected total (HSA+ and HSA-) MDMs and high HSA expressing MDMs. **D.** MDMs were *in vitro* infected with HIV-Bal-HSA for 9 days. Cells were treated with DMSO or 5 µM AEG40730 for 72 hours. Cell death of total HSA+ and HSA- MDMs was detected by Annexin-V-BV711 and flow cytometry (left panel). Representative histogram shows HIV-HSA-infected cells (middle panel) and cell death of total HSA+ and HSA- cells (right panel). **E.** Intensely HSA positive HIV-infected cells were gated and analyzed for apoptosis by Annexin-V-BV711 staining and flow cytometry (left panel). Representative histogram shows intensely positive HIV-HSA-infected cells (middle panel) and cell death of high HSA+ cells (right panel). The p values in B & C were calculated using Mann-Whitney U test.

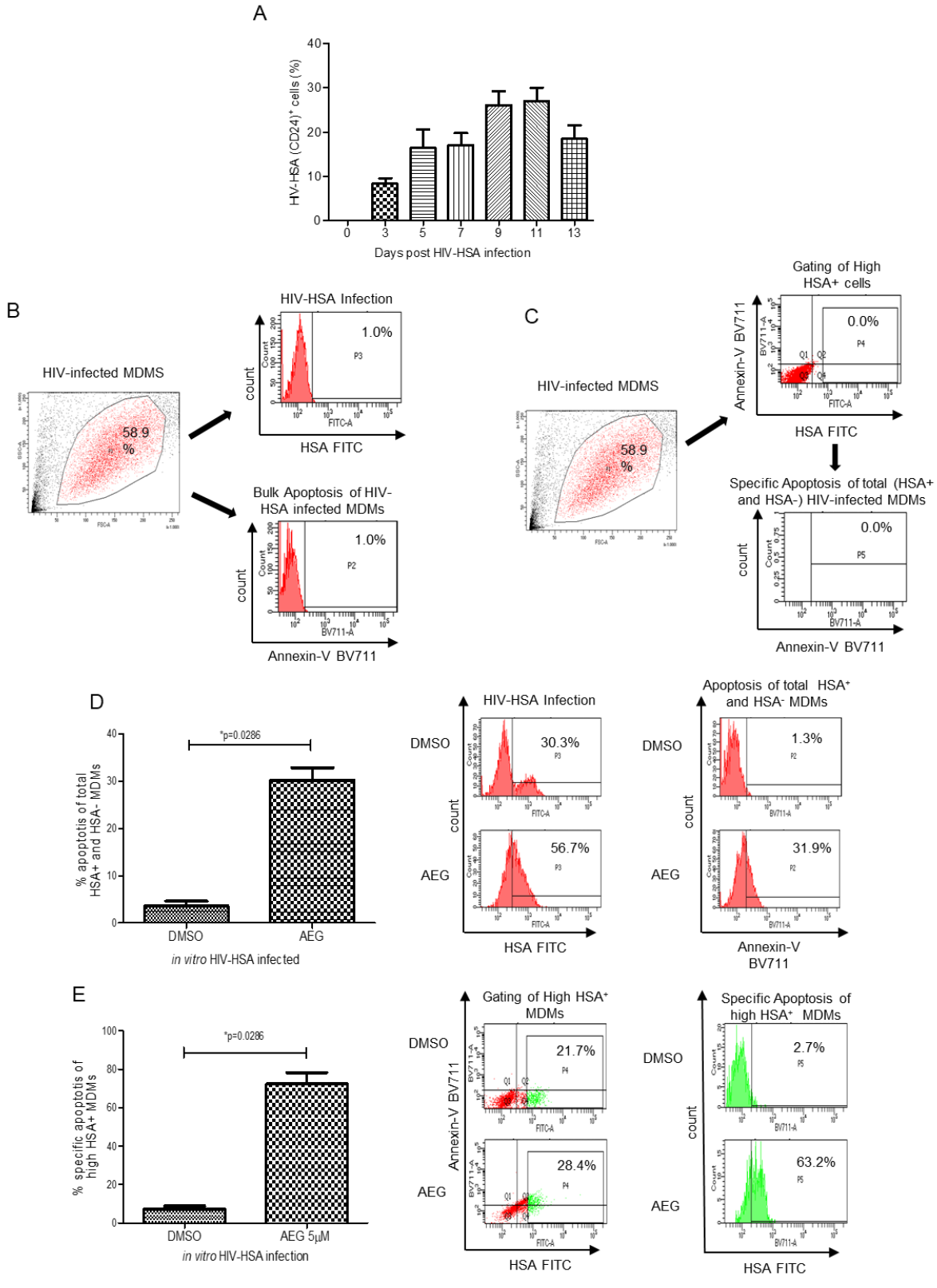
A
HV-HSA (CD24)+ cells (%)
Days post HIV-HSA infection
B
HIV-infected MDMS
58.9 %
HIV-HSA Infection
1.0%
HSA FITC
Bulk Apoptosis of HIV-HSA infected MDMs
1.0%
Annexin-V BV711
C
HIV-infected MDMS
58.9 %
Gating of High HSA+ cells
0.0%
Annexin-V BV711
HSA FITC
Specific Apoptosis of total (HSA+ and HSA-) HIV-infected MDMs
0.0%
Annexin-V BV711
D
*p=0.0286
% apoptotis of total HSA+ and HSA- MDMs
DMSO
AEG
in vitro HIV-HSA infected
HIV-HSA Infection
30.3%
56.7%
HSA FITC
Apoptosis of total HSA+ and HSA- MDMs
1.3%
31.9%
Annexin-V BV711
E
*p=0.0286
% specific apoptotis of high HSA+ MDMs
DMSO
AEG 5µM
in vitro HIV-HSA infection
Gating of High HSA+ MDMs
21.7%
28.4%
Annexin-V BV711
HSA FITC
Specific Apoptosis of high HSA+ MDMs
2.7%
63.2%
HSA FITC

The HIV exposed but uninfected bystander cells play a critical role in the HIV pathogenesis and disease progression by causing selective depletion of CD4+ T cells, leading to immunodeficiency [77]. Although HIV infection of T cells and macrophages differ with respect to cell death *in vivo* and *in vitro* [152,195], uninfected bystander macrophages may also play a crucial role in HIV pathogenesis. Therefore, we determined if SMs selectively induce apoptosis of HIV-infected or HIV-exposed uninfected bystander macrophages. For this, MDMs were infected with HIV-Bal-HSA for 7 days followed by treatment with either SM-AEG40730 or SM-LCL161 for another two days. Specific killing of HSA-expressing (ie HIV-infected) and HSA-negative (HIV uninfected) cells by SM-AEG40730 or SM-LCL161 was quantified by counter staining with BV711 labelled Annexin-V as above. SM-AEG40730 and SM-LCL161 killed significantly high numbers of HIV-HSA-expressing (HIV-infected) cells compared to either the mock or HSA-negative (HIV-uninfected/bystander, HIV-exposed) cells **(Fig. 17A, B).** However, killing of HSA-negative (HIV-uninfected/bystander) cells was relatively higher than mock-infected cells but was not significant suggesting that SMs specifically kill HIV-infected macrophages.

Similar experiments were performed with an eGFP-expressing HIV strain, HIV-eGFP. MDMs were infected with HIV-eGFP for 7 days followed by treatment with SM-AEG40730 for two days. Expression of eGFP by HIV-infected cells can be visualized by flow cytometry to identify infected cells. Specific killing of eGFP expressing (HIV-infected) cells by SM-AEG40730 was quantified by counter staining with Annexin-V labelled with BV711 expression. The gating strategy is similar to what is shown in **Fig. 16B**. To rule out non-specific low-level fluorescence by dead cells/debris, highly intense eGFP-positive cells were gated. Specific killing of intensely eGFP-positive (HIV-infected) cells was quantified for Annexin-V labelled with BV711 expression. The gating strategy is similar to as shown in **Fig. 16C**.

Figure 17. SM specifically induces cell death of HIV-HSA-infected MDMs but not in HIV-exposed uninfected MDMs

A. & B. SM-LCL161 and SM-AEG40730 specifically kill HIV-HSA-infected cells but not HSA-MDMs. MDMs were infected with HIV-HSA for 11 days followed by treatment with either SM-LCL161 (upper panel) or AEG40730 (lower panel) for another 2 hours followed by analysis of cell death by PI staining (n=5). The p values were calculated using paired t test *(These experiments were performed by Ramon Edwin Caballero)*.

A

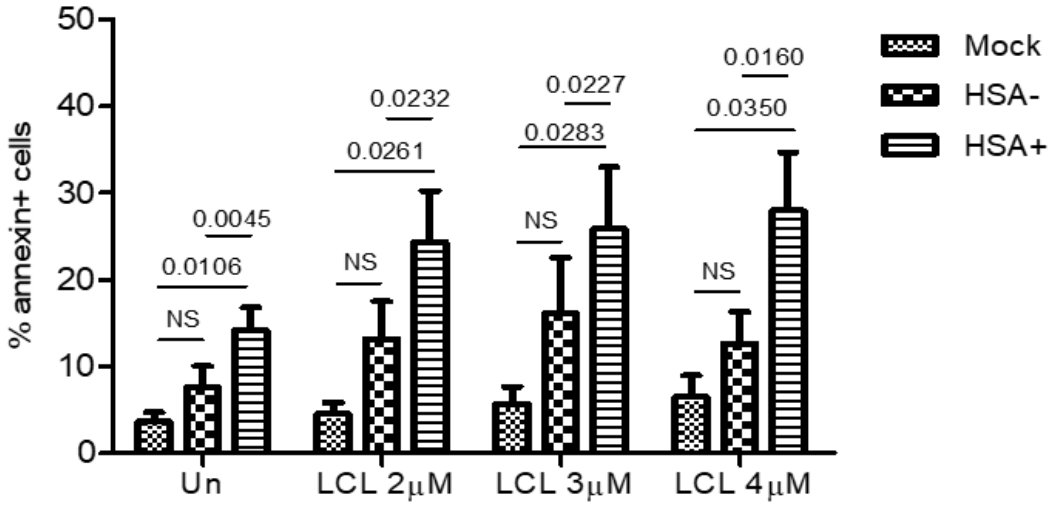
% annexin+ cells
50
40
30
20
10
0
Un
LCL 2μM
LCL 3μM
LCL 4μM
NS
0.0106
0.0045
NS
0.0261
0.0232
NS
0.0283
0.0227
NS
0.0350
0.0160
Mock
HSA-
HSA+

B

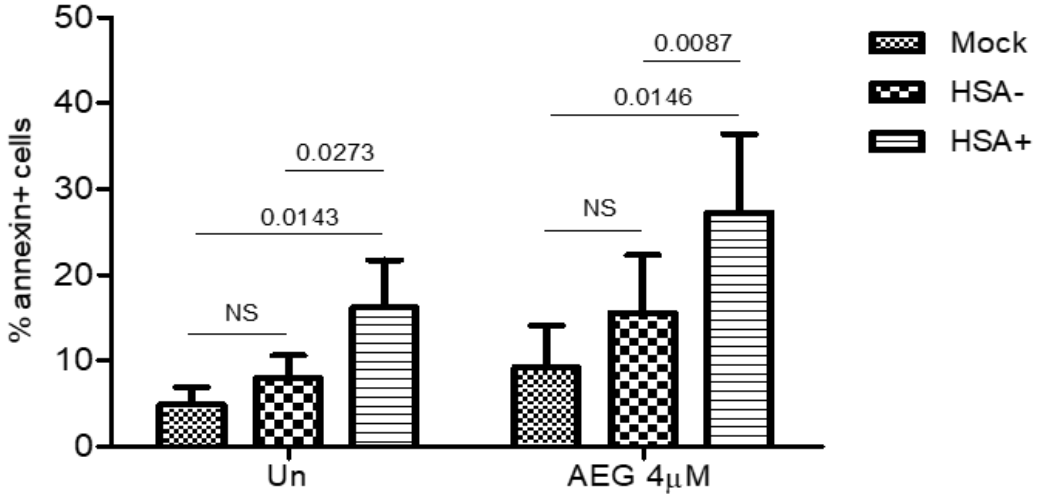
% annexin+ cells
50
40
30
20
10
0
Un
AEG 4μM
NS
0.0143
0.0273
NS
0.0146
0.0087
Mock
HSA-
HSA+

MDMs infected with HIV-eGFP for 1-2 days could be detected by flow cytometry; however, MDMs infected for 7 days could not be detected as the virus multiplied for one round only (data not shown). Interestingly, treatment of HIV-eGFP-infected cells with SM-AEG40730 revealed killing of significantly high number of total eGFP + and eGFP- MDMs compared to the DMSO-treated eGFP+ and eGFP- MDMs **(Fig. 18A, left panel).** It may be noted that the eGFP+ cells increased in number following SM treatment as SM is known to cause HIV reactivation [269,383]. Specific killing of HIV-eGFP-infected cells by SM-AEG40730 by gating dual eGFP -positive and Annexin-V+ MDMs revealed that SM-AEG40730 killed significantly higher number of intensely eGFP+ HIV-infected cells compared to the DMSO-treated HIV-infected cells **(Fig. 18B, left panel).** It may also be noted that the number of intensely eGFP positive cells following SM treatment is low because of a relatively smaller number of SM-activated eGFP+ cells **(Fig. 18B right panel).** Representative histogram showing killing of total eGFP+ and eGFP- **MDMs (Fig. 18A right panel)** and intensely eGFP+, HIV-eGFP-infected cells **(Fig. 18B, right panel)** by SM-AEG40730 is shown.

Figure 18. SM specifically induces cell death of HIV-eGFP-infected MDMs

A. Primary human MDMs were *in vitro* infected with HIV-eGFP for 7 days. Cells were treated with DMSO or AEG40730 for 72 hours. The cell death of the total population of HIV-eGFP-infected MDMs was detected by Annexin-V-BV711 and flowcytometry (left panel). Representative histogram shows HIV-eGFP-infected cells (middle panel) and cell death of total eGFP+ and eGFP- HIV-infected cells (right panel). **B.** Intensely eGFP-positive HIV-infected cells were gated and analyzed for apoptosis by Annexin-V-BV711 staining and flow cytometry (left panel). Representative histogram showing intensely positive HIV-eGFP-infected cells (middle panel) and cell death of high eGFP+ cells (right panel). The p values were calculated using Mann Whitney U test (n=4).

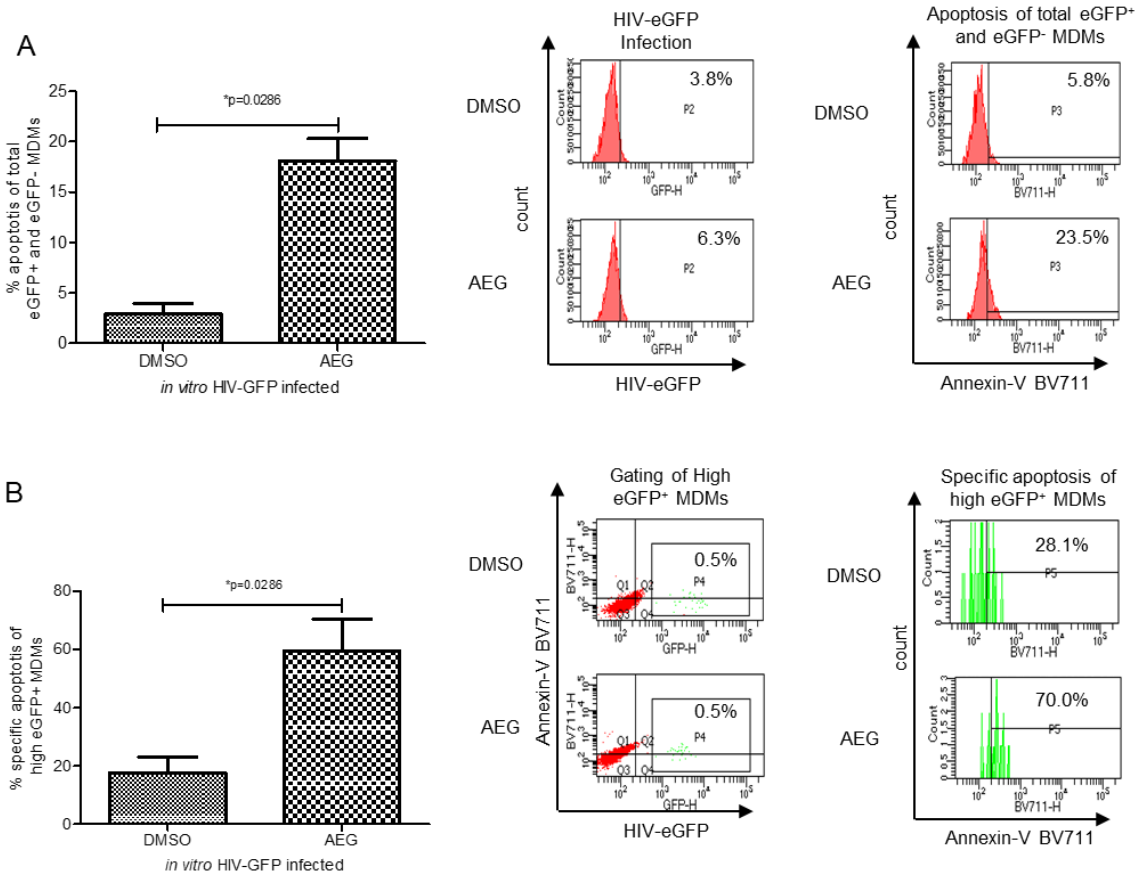
A
*p=0.0286
% apoptotis of total eGFP+ and eGFP- MDMs
25
20
15
10
5
0
DMSO
AEG
in vitro HIV-GFP infected
HIV-eGFP Infection
DMSO
AEG
3.8%
6.3%
P2
GFP-H
count
HIV-eGFP
Apoptosis of total eGFP+ and eGFP- MDMs
5.8%
23.5%
P3
BV711-H
Annexin-V BV711
B
*p=0.0286
% specific apoptotis of high eGFP+ MDMs
80
60
40
20
0
DMSO
AEG
in vitro HIV-GFP infected
Gating of High eGFP+ MDMs
0.5%
0.5%
Q1
Q2
Q3
Q4
P4
Annexin-V BV711
HIV-eGFP
Specific apoptosis of high eGFP+ MDMs
28.1%
70.0%
P5

2.4 Knocking down IAPs results in specific killing of HIV-infected MDMs

To confirm the involvement of IAPs in SM-mediated killing of HIV-infected MDMs, we employed IAP1/2 siRNAs as shown previously [272,274,377]. MDMs generated from PBMCs from healthy donors were infected with HIV-Bal-HSA for 7 days followed by treatment with either non-targeting siRNA or IAP siRNAs for 72 hours. Killing of total HIV-HSA-infected cells in the presence of IAP siRNA transfected cells was analyzed by staining with Annexin-V labelled with BV711 as above. The gating strategy is similar to as shown in **Fig. 16B.** To rule out non-specific low-level fluorescence by dead cells/debris, highly intense FITC positive HSA-expressing cells were gated. Specific killing of intensely FITC-positive HSA-expressing (HIV-infected) cells by IAP siRNAs was quantified by counter staining with Annexin-V labelled with BV711. The gating strategy is similar to as shown in **Fig. 16C.**

Quantification of Annexin-V positive total HSA+ and HSA- MDMs revealed that knocking down IAPs by siRNAs killed significantly higher number of total HIV-HSA+ and HSA- (HIV-infected) MDMs **(Fig. 19A, left panel).** Similarly, quantification of dual Annexin-V positive and intensely HSA+ MDMs show that knocking down IAPs by siRNAs killed significantly high numbers of intensely stained HSA+ MDMs **(Fig. 19B, left panel)** compared to the control HIV-HSA-infected cells treated with non-targeting siRNAs. Representative histogram showing killing of total HSA+ and HSA- **(Fig. 19A, right panel)** and intensely HSA positive **(Fig. 19B, right panel)** MDMs is shown.

Figure 19. IAP siRNA specifically induces cell death of HIV-HSA-infected MDMs

A. Primary human MDMs were *in vitro* infected with HIVNL4.3-Bal-HSA for 9 days. The cells were transfected with non-targeting control siRNA or cIAP1/2 siRNA. After 72 hours of transfection, cell death of the total population of HIV-HSA-infected MDMs was detected by Annexin-V-BV711 and flow cytometry (left panel). Representative histogram showing HIV-HSA-infected cells (middle panel) and cell death of total (HSA+ and HSA-) HIV-infected cells (right panel). **B.** Intensely HIV-HSA positive HIV-infected cells were gated and analyzed for apoptosis by Annexin-V-BV711 staining and flow cytometry (left panel). Representative histogram showing intensely positive HIV-HSA-infected cells (middle panel) and cell death of high HSA+ cells (right panel). The p values were calculated using Mann Whitney U test (n=4).

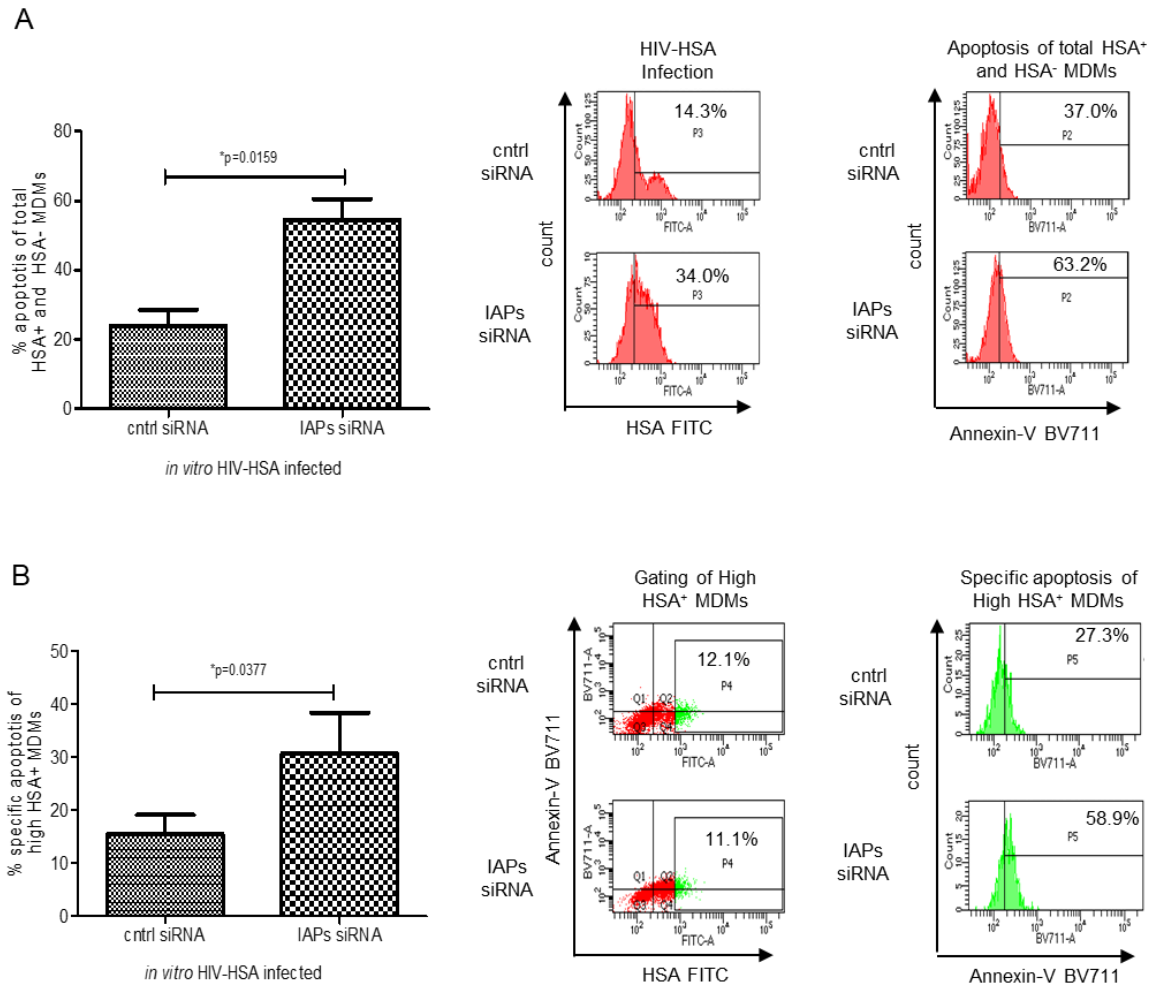
A
% apoptotis of total HSA+ and HSA- MDMs
*p=0.0159
cntrl siRNA
IAPs siRNA
in vitro HIV-HSA infected
HIV-HSA Infection
cntrl siRNA
IAPs siRNA
14.3%
34.0%
count
HSA FITC
Apoptosis of total HSA+ and HSA- MDMs
37.0%
63.2%
Annexin-V BV711
B
% specific apoptotis of high HSA+ MDMs
*p=0.0377
cntrl siRNA
IAPs siRNA
in vitro HIV-HSA infected
Gating of High HSA+ MDMs
12.1%
11.1%
Annexin-V BV711
HSA FITC
Specific apoptosis of High HSA+ MDMs
27.3%
58.9%
count
Annexin-V BV711

2.5 TNF-α mediates SM-induced apoptosis in U1 cells but not in HIV-infected MDMs

SM-induced cell death of various tumor cells is mediated by endogenously produced TNF-α following SM treatment through the activation of the non-canonical NFκB pathway [384,385]. To determine if SM-induced apoptosis in HIV-infected MDMs is due to endogenous TNF-α production, SM-LCL161-treated U937, U1 cells and *in vitro* HIV-infected primary MDMs were analyzed for TNF-α secretion. SM-LCL161 treatment resulted in low level although significant TNF-α production in undifferentiated and differentiated U937 and U1 cells **(Fig. 20A-D)** in contrast to both *in vitro* mock- and HIV-infected MDMs **(Fig. 20E).** Similarly, *ex vivo* derived MDMs from HIV-infected patients did not produce significantly higher levels of TNF-α following SM-LCL161 treatment compared to the untreated negative controls **(Fig. 20F).**

To evaluate the impact of TNF-α in SM-induced apoptosis of primary MDMs, SM-LCL161-treated MDMs were stimulated with Recombinant Tumor Necrosis Factor-alpha (rTNF-α) followed by analysis of cell death by PI staining. Treatment of MDMs with SM-LCL161 and TNF-α did not result in cell death **(Fig. 20G).** In contrast, rTNF-α either alone or in combination with SM-LCL161 induced significant cell death in U937 and U1 cells **(Fig. 20H, I)** similar to that observed in various tumor cells [386,387]. These results suggest that SM-mediated killing of HIV-infected MDMs is independent of TNF-α.

Figure 20. TNF-α mediates SM-induced apoptosis in U1 cells but not in HIV-infected MDMs

SM induced cell death in U1 cells is regulated by rTNFa. SM induce TNF-α secretion in undifferentiated and differentiated U937 and U1 cells (A-D). Cells were treated with various concentrations of SM-LCL161 for 48 hours. The supernatants were analyzed for TNF-α production by ELISA. **A.** Undifferentiated U 937, **B.** undifferentiated U1, **C.** differentiated U937, **D.** differentiated U1. **E.** SM treatment of HIV-infected MDMs does not induce TNF-α production. Human MDMs were *in vitro* infected with HIV_{CS204} (100 ng p24/well) for 7 days followed by the addition of SM-LCL161 for 48 hours (n=3). **F.** MDMs derived from HIV-patients were treated with SM-LCL161 for 48 hours (n=4). Supernatants were analyzed for TNF-α production by ELISA. U 937 (**G.**) and U1 (**H.**) were treated with either SM-LCL161 alone, rTNF-α alone or with SM-LCL161 and various concentrations of rTNF-α for 48 hours followed by analysis of cell death by PI staining and flow cytometry. **I.** MDMs were treated with SM-LCL161 for 2 hours followed by the addition of rTNF-α for 48 hours. Intracellular PI staining and flow cytometry were used to assessed levels of cell death (n=3). The p values were calculated using paired t test or Mann-Whitney U test *(These experiments were performed by Ramon Edwin Caballero)*.

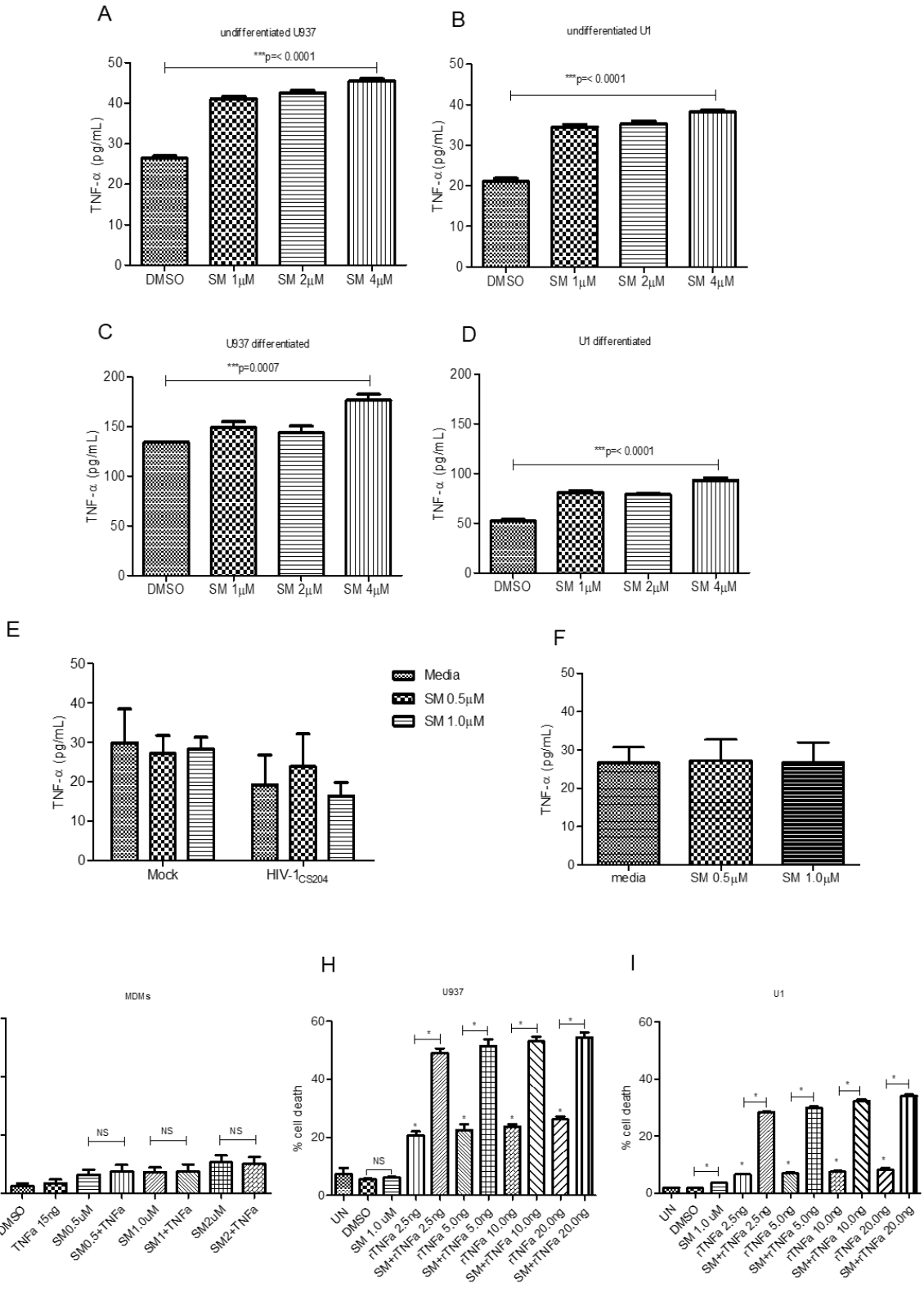
A
undifferentiated U937
***p=< 0.0001
TNF-α (pg/mL)
DMSO
SM 1μM
SM 2μM
SM 4μM
B
undifferentiated U1
***p=< 0.0001
C
U937 differentiated
***p=0.0007
D
U1 differentiated
***p=< 0.0001
E
Media
SM 0.5μM
SM 1.0μM
Mock
HIV-1CS204
F
media
G
MDMs
% cell death
NS
DMSO
TNFa 15ng
SM0.5μM
SM0.5+TNFa
SM1.0uM
SM1+TNFa
SM2uM
SM2+TNFa
H
U937
UN
SM 1.0 uM
rTNFa 2.5ng
SM+rTNFa 2.5ng
rTNFa 5.0ng
SM+rTNFa 5.0ng
rTNFa 10.0ng
SM+rTNFa 10.0ng
rTNFa 20.0ng
SM+rTNFa 20.0ng
I
U1

2.6 HIV-infected MDMs do not develop M1 phenotype before or after SM treatment

Macrophages polarized with IFN-γ develop a M1 phenotype which is highly susceptible to SM-induced cell death **(Fig. 21).** Therefore, it is possible that SM-induced cell death of HIV-infected MDMs is due to the development of M1 phenotype following HIV infection. To determine whether HIV-infected MDMs develop M1 phenotype before or after SM treatment, cytokine array analysis for the following cytokines was performed: IL-17F, GM-CSF, IFN-γ, IL-10, CCL20/MIP3a, IL-12p70, IL-13, IL-15, IL-17a, IL-22, IL-9, IL-1β, IL-33, IL-21, IL-23, IL-5, IL-6, IL-17ε/IL-25, IL-27, IL-31, TNF-α, TNF-β, and IL-28A. HIV-infected MDMs secreted significantly high levels of CCL20/MIP3α, IL-6, and TNF-α compared to the mock control. There was no significant difference in the secretion of IL-10, IL-21, IL-13, and IL-23 between the HIV-infected and mock-infected controls **(Fig. 22).** Remaining cytokines were not detected in either group suggesting that HIV infection of MDMs does not result in the upregulation of cytokines related to M1 phenotype. SM treatment did not affect the secretion of above mentioned cytokines including CCL20/MIP3α, IL-6, IL-23, IL-10, IL-21, IL-13, and TNF-α in *in vitro* HIV-infected MDMs **(Fig. 23A-G)** or in *ex vivo* derived MDMs from HIV-infected patients **(Fig. 23H).** These results suggest that *in vitro* HIV-infected MDMs either before or after SM treatment did not express M1 phenotype and SM-mediated apoptosis of HIV-infected MDMs is independent of M1 polarization.

Figure 21. SM induces cell death in M1 macrophages

A. M_0 and M_1 MDMs were treated with increasing concentration of SM-LCL161 48 hours (n=3). Cell death was assessed by intracellular PI staining and flow cytometry. The p values were calculated using Mann-Whitney U test. **B.** Representative histograms for cell death in M1 macrophages is shown *(These experiments were performed by Ramon Edwin Caballero)*.

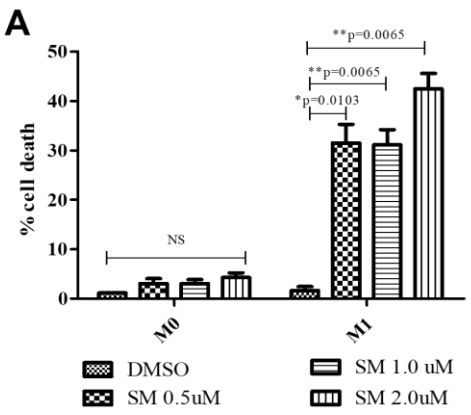
A
% cell death
50
40
30
20
10
0
NS
**p=0.0065
**p=0.0065
*p=0.0103
M0
M1
DMSO
SM 0.5uM
SM 1.0 uM
SM 2.0uM

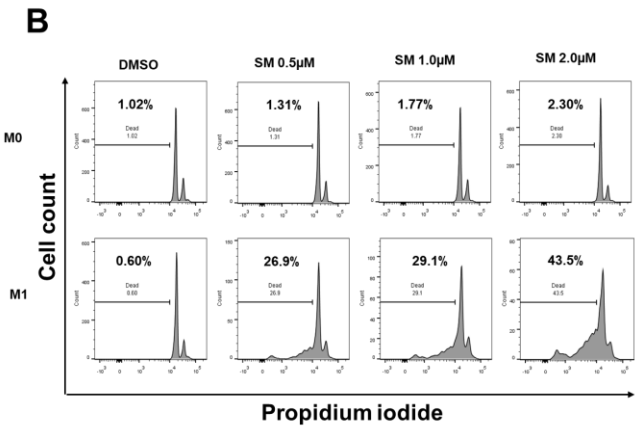
B
DMSO
SM 0.5μM
SM 1.0μM
SM 2.0μM
M0
M1
1.02%
1.31%
1.77%
2.30%
0.60%
26.9%
29.1%
43.5%
Cell count
Propidium iodide

Figure 22. HIV infection of MDMs does not result in the upregulation of cytokines related to M1 phenotype

Primary human MDMs were *in vitro* infected with mock or HIV_{CS204}. The supernatants collected after 7 days of infection were analyzed for the secretion of cytokines using human Th17 magnetic panel cytokine array kit for 22 different cytokines (n=6). The p values were calculated using Mann-Whitney U test *(These experiments were performed by Ramon Edwin Caballero)*.

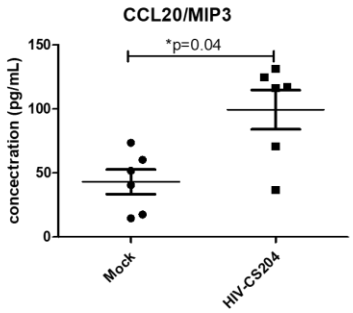
CCL20/MIP3
*p=0.04
concectration (pg/mL)
150
100
50
0
Mock
HIV-CS204

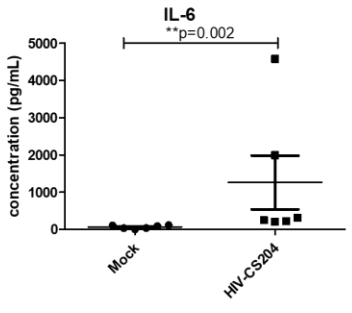
IL-6
**p=0.002
concentration (pg/mL)
5000
4000
3000
2000
1000
0
Mock
HIV-CS204

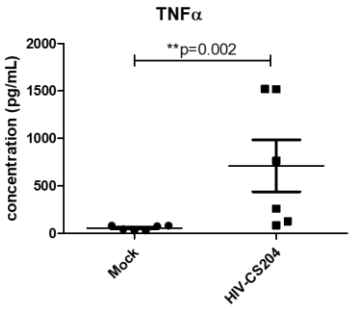
TNFα
**p=0.002
concentration (pg/mL)
2000
1500
1000
500
0
Mock
HIV-CS204

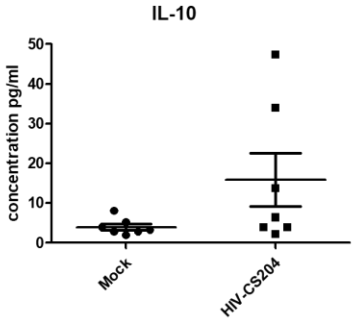
IL-10
concentration pg/ml
50
40
30
20
10
0
Mock
HIV-CS204

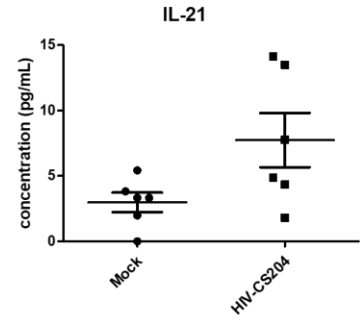
IL-21
concentration (pg/mL)
15
10
5
0
Mock
HIV-CS204

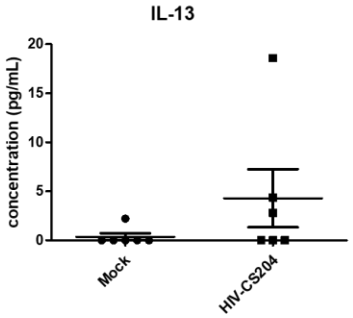
IL-13
concentration (pg/mL)
20
15
10
5
0
Mock
HIV-CS204

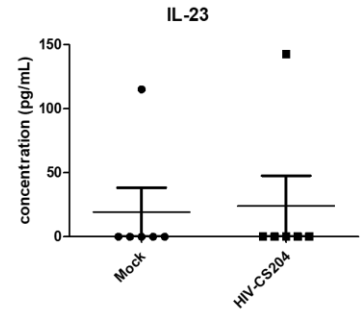
IL-23
concentration (pg/mL)
150
100
50
0
Mock
HIV-CS204

Figure 23. SM does not induce aberrant production of M1 cytokines in mock and HIV-infected MDMs.

A-G. The *in vitro* mock and HIV_{CS204}-infected primary MDMs for 7 days were treated with SM-LCL161 for 48 hours. Supernatants were collected, and cytokine profile was analyzed through Human Th17 magnetic panel cytokine array kit (n=3); **H.** SM does not induce cytokine production in primary MDMs generated from HIV-infected individuals. PBMC from ART-treated HIV+ patients were differentiated into macrophages for 7-days and subsequently treated with SM-LCL161 for 48 hours. The supernatants were analyzed for cytokines through human Th17 magnetic panel cytokine array. The p values were calculated using paired t test (n=3) *(These experiments were performed by Ramon Edwin Caballero)*.

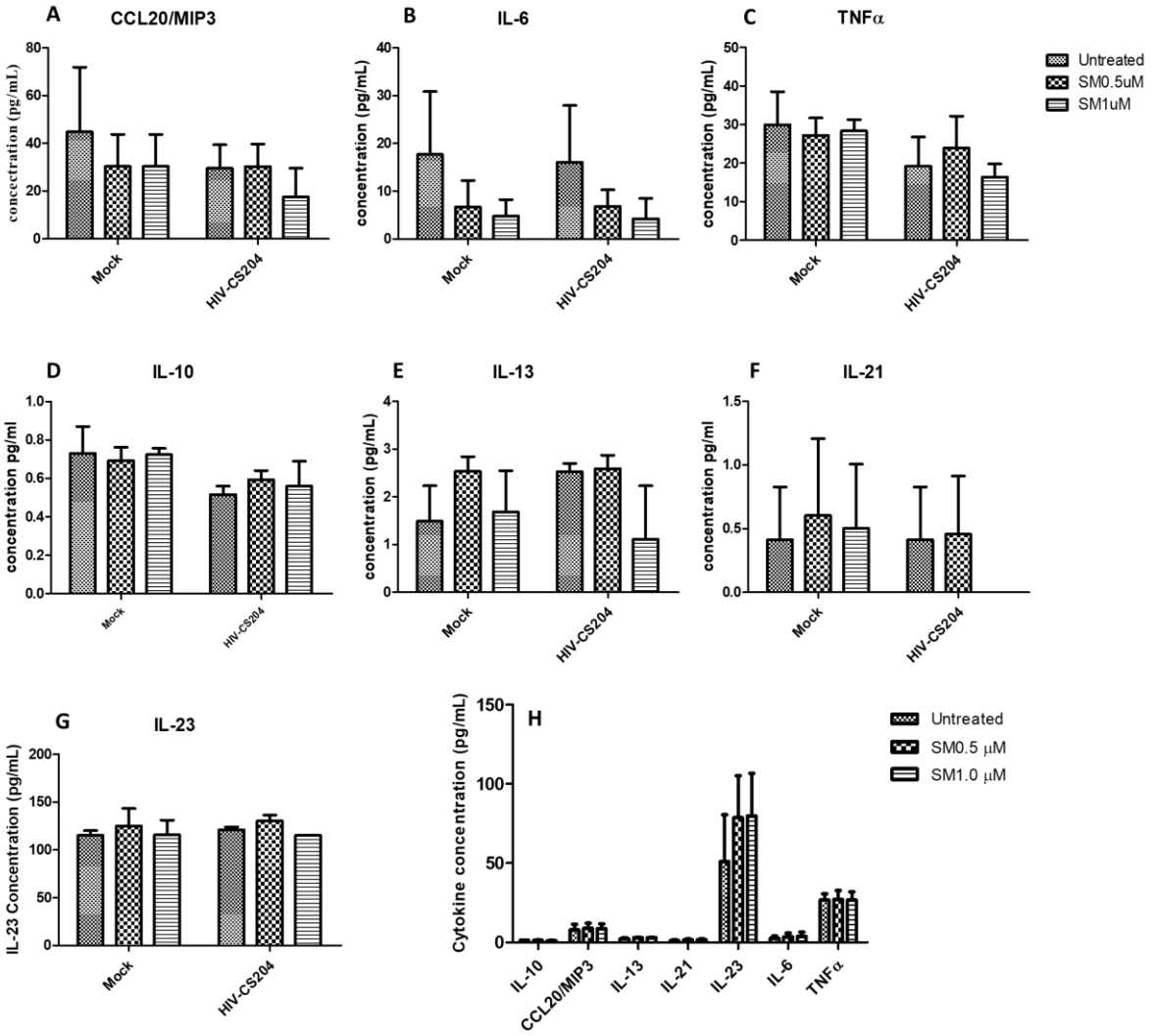
A
CCL20/MIP3
concecetration (pg/mL)
Mock
HIV-CS204
B
IL-6
concentration (pg/mL)
C
TNFα
Untreated
SM0.5uM
SM1uM
D
IL-10
concentration pg/ml
E
IL-13
F
IL-21
G
IL-23
IL-23 Concentration (pg/mL)
H
Cytokine concentration (pg/mL)
Untreated
SM0.5 μM
SM1.0 μM
IL-10
CCL20/MIP3
IL-13
IL-21
IL-23
IL-6
TNFα

2.7 HIV-infection downregulates the expression of RIPK1 in MDMs

SM-induced apoptosis of HIV-infected macrophages may be ascribed to the impaired expression of IAP-associated signalling kinases such as RIPK1 [388,389]. RIPK1 plays a key role in the regulation of various cellular processes such as NFκB signalling and apoptosis [390]. Moreover, RIPK1 is a target substrate for HIV protease, a viral protein that is synthesized late in the viral life cycle and inactivates RIPK1 in HIV-infected primary CD4+ T cells [391]. To determine whether RIPK1 is similarly cleaved and inactivated in HIV-infected MDMs, *in vitro* mock and HIV_{CS204}-infected MDMs for 7 days were treated with SM-LCL161 for 2 days followed by immunoprobing for RIPK1. HIV infection resulted in the downregulation of RIPK1 in the presence and absence of SM-LCL161 compared to the mock-infected controls **(Fig. 24A).** This was also demonstrated by *in vitro* infection of MDMs with HIV_{CS204} for 2-8 days. Infection with HIV_{CS204} resulted in cleavage of RIPK1 with a relative decrease in full length RIPK1 while the cleaved RIPK1 product gradually increased over time **(Fig. 24B).**

To confirm the downregulation of RIPK1 in HIV-infected MDMs, MDMs were infected with HIV-Bal-HSA. After 9 days of infection, HIV-infected HSA-expressing MDMs were harvested by magnetic column separation based on HSA expression followed by immunoblotting for RIPK1 analysis [294]. The negative fraction represents HIV-exposed uninfected cells that do not express HSA on their surface, and hence get eluted after the first passing of the labelled cells. Waste fraction represents cells that are eluted during the column wash prior to the collection of the HSA-selected MDMs. The positive fraction represents the HIV-infected HSA-expressing cells retained in the magnetic column that are eluted at the end of the HSA selection protocol. The gating strategy for detection of HIV-HSA-infected macrophages is

shown in **Fig. 24C** left panel. The positively selected MDMs infected with HIV-HSA showed ~70% purity while the negatively selected HIV-uninfected cells and waste fractions had ~7% and ~10% contaminating HSA expressing MDMs, respectively **(Fig. 24C, right panel)**. The results show that RIPK1 was downregulated in the positively selected HIV-HSA enriched fraction compared to the mock-infected and negatively selected HIV-uninfected MDMs **(Fig. 24D)**. These results indicate that RIPK1 degradation is a consequence of HIV infection of primary MDMs.

2.8 SM treatment of HIV-infected MDMs downregulates apoptosis-associated signalling molecules TRAF1 and BID

In addition to RIPK1, **t**he process of apoptosis requires the fine-tuned functionality of several signalling molecules including TRAF1/2, as well as proteins that regulate homeostasis of mitochondria such as BID and BAX [390,392–394]. We determined the expression of these signalling molecules in response to SM-LCL161 treatment of *in vitro* HIV_{CS204}-infected MDMs. HIV infection resulted in the downregulation of TRAF1 **(Fig. 24E, lanes 1 and 4).** Treatment of HIV-infected MDMs with SM-LCL161 also resulted in the downregulation of TRAF1 compared to the mock-infected and SM-treated MDMs **(Fig. 24E, lanes 2, 3 and 5).** However, *TRAF2* and *Bax* did not show a significant change in their expression in mock- and HIV-infected MDMs as well as between SM-LCL161 treated mock and HIV-infected MDMs **(Fig. 24E).** *Bid* was down-regulated with increasing concentration of SM-LCL161 in HIV-infected MDMs but not in mock-infected MDMs **(Fig. 24E).** Overall, these results suggest that SM dysregulates the expression of apoptosis-associated *TRAF1* and *Bid* in HIV-infected MDMs.

Figure 24. HIV infection results in downregulation of RIPK1 in MDMs

A. Human MDMs were *in vitro* infected with HIV_{CS204} (100ng p24/well) for 7 days followed by the addition of SM-LCL161 for 48 hours (n=4). **B.** Human MDMs were *in vitro* infected with HIV_{CS204} (100ng p24/well) and cells were harvested on day 0, 2, 4, 6, and 8. Cell lysates were subjected to Western immunoblotting for RIPK1. **C.** Gating strategy for detection of HIV-HSA-infected macrophages. HIV-infected bulk MDMs were gated as singlets followed by staining for live cells using E450 live/dead staining kit (Invitrogen). HIV-HSA-infected cells were detected within the live cell population by using FITC-labelled anti-CD24 antibodies (left panel). MDMs were *in vitro* infected with R5 tropic HIV-Bal-HSA as above for 11 days following which cells were subjected to magnetic column separation using CD24 (HSA)-biotin conjugated antibodies. The % of HIV-HSA-infected MDMs in isolated unsorted, negative, waste and positive fractions as assessed by flow cytometry is shown (right panel). **D.** Isolated fractions of HIV-HSA, namely negative fraction (negative sort), waste fraction and positively isolated fraction (positive sort) were subjected to Western immunoblotting for analysis of RIPK1 and pRIPK1. **E.** Human MDMs were *in vitro* infected with HIV_{CS204} (100ng p24/well) for 7 days followed by the addition of SM-LCL161 for 48 hours. Cell lysates were analyzed for TRAF1, TRAF2, BID and BAX by Western immunoblotting. The results shown are a representative of two (upper panel) and 4 (lower panel) experiments respectively *(These experiments were performed by Ramon Edwin Caballero)*.

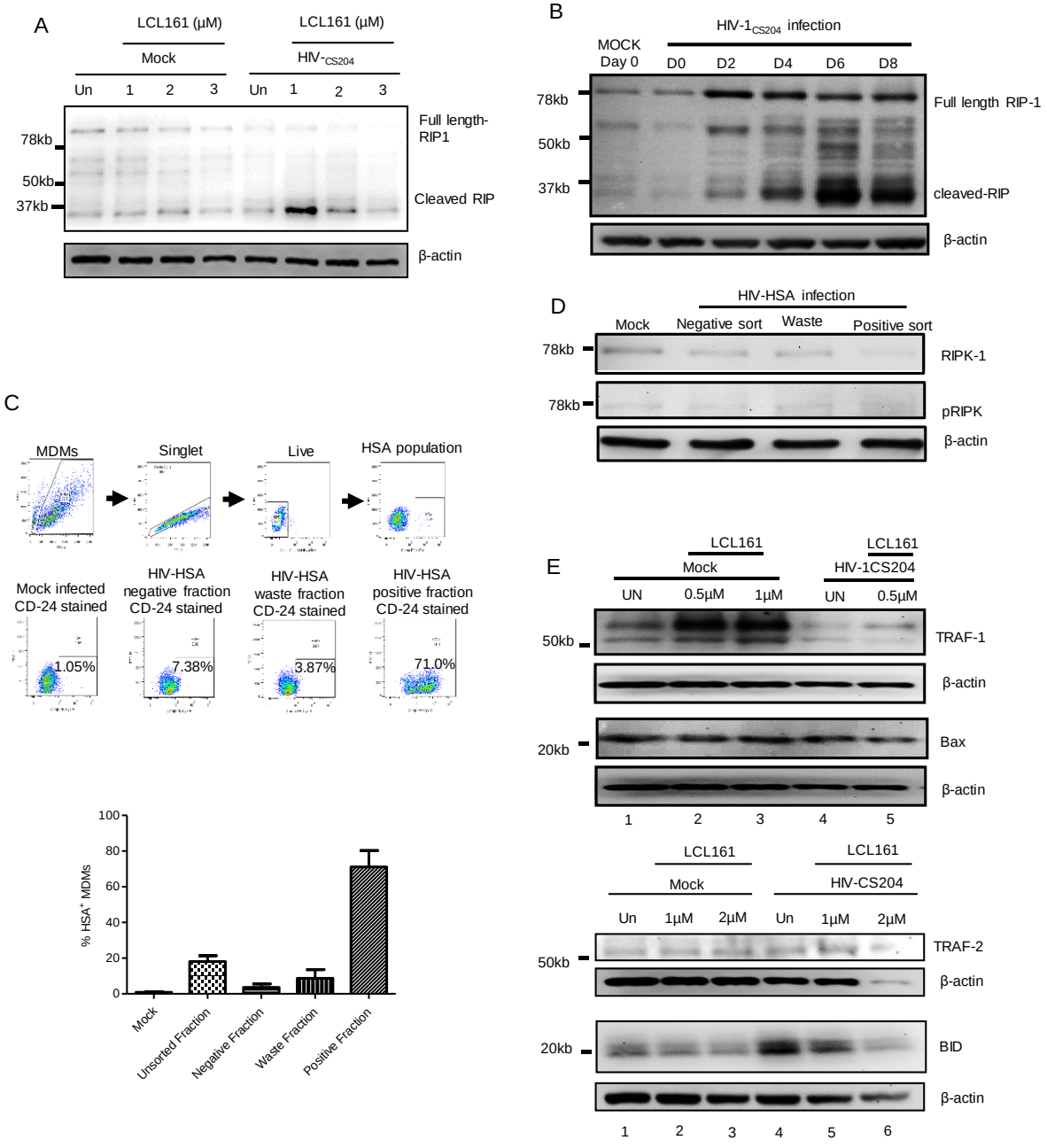
A
LCL161 (μM)
LCL161 (μM)
Mock
HIV-CS204
Un 1 2 3 Un 1 2 3
78kb
50kb
37kb
Full length-RIP1
Cleaved RIP
β-actin
B
HIV-1CS204 infection
MOCK Day 0
D0 D2 D4 D6 D8
78kb
50kb
37kb
Full length RIP-1
cleaved-RIP
β-actin
C
MDMs
Singlet
Live
HSA population
Mock infected CD-24 stained
HIV-HSA negative fraction CD-24 stained
HIV-HSA waste fraction CD-24 stained
HIV-HSA positive fraction CD-24 stained
1.05%
7.38%
3.87%
71.0%
% HSA+ MDMs
100
80
60
40
20
0
Mock
Unsorted Fraction
Negative Fraction
Waste Fraction
Positive Fraction
D
HIV-HSA infection
Mock
Negative sort
Waste
Positive sort
78kb
78kb
RIPK-1
pRIPK
β-actin
E
LCL161
LCL161
Mock
HIV-1CS204
UN 0.5μM 1μM UN 0.5μM
50kb
TRAF-1
β-actin
20kb
Bax
β-actin
1 2 3 4 5
LCL161
LCL161
Mock
HIV-CS204
Un 1μM 2μM Un 1μM 2μM
50kb
TRAF-2
β-actin
20kb
BID
β-actin
1 2 3 4 5 6

2.9 cIAP1/2 and RIPK1 are essential for survival of HIV-infected MDMs

The above results showing inactivation of RIPK1 in settings where cIAPs are absent, may affect the viability of MDMs. To determine the combined impact of knockdown of cIAPs and RIPK1 in the survival of MDMs, MDMs from healthy donors were pretreated with Necrostatin-1, a specific RIPK1 inhibitor, for 2 hours followed by treatment with SM-LCL161 and analysis for cell death. Treatment with SM-LCL161 or Necrostatin-1 alone did not induce significant cell death of normal primary MDMs. However, combination treatment of SM-LCL161 and Necrostatin-1 resulted in significant increase in cell death of primary MDMs **(Fig. 25A, B).** Moreover, treatment with Necrostatin-1 alone did not show cleavage of PARP or caspases-8 and 9 although treatment with SM-LCL161 alone did show their minimal cleavage **(Fig. 25C).** However, treatment with both Necrostatin-1 and SM-LCL161 revealed significantly enhanced cleavage of the three caspases as well as PARP **(Fig. 25C)**. These results suggest that cIAP1/2 and RIPK1 play an important role in regulating viability of primary human MDMs. Since HIV infection down regulates RIPK1 in MDMs and degradation of IAPs with SM-LCL161 results in death of HIV-infected MDMs suggest that RIPK1 and IAPs play crucial roles in SMs-induced cell death of HIV-infected MDMs.

Figure 25. Concomitant downregulation of cIAP1/2 and RIPK1 in MDMs derived from healthy donors results in activation of apoptosis

A. MDMs were treated with 10μM Necrostatin-1 for 2 hours followed by the addition of increasing concentration of SM-LCL161 for 48 hours. Cell death was assessed by intracellular PI staining and flow cytometry. The p values were calculated using Mann-Whitney U test (n=4). **B.** Representative histograms of the four experiments is shown. **C.** MDMs treated as above with Necrostatin-1 and SM-LCL161 were harvested and subjected to western immunoblotting for caspase-3, -8, and -9, PARP, and β-actin. The blots shown is a representative of three experiments *(These experiments were performed by Ramon Edwin Caballero)*.

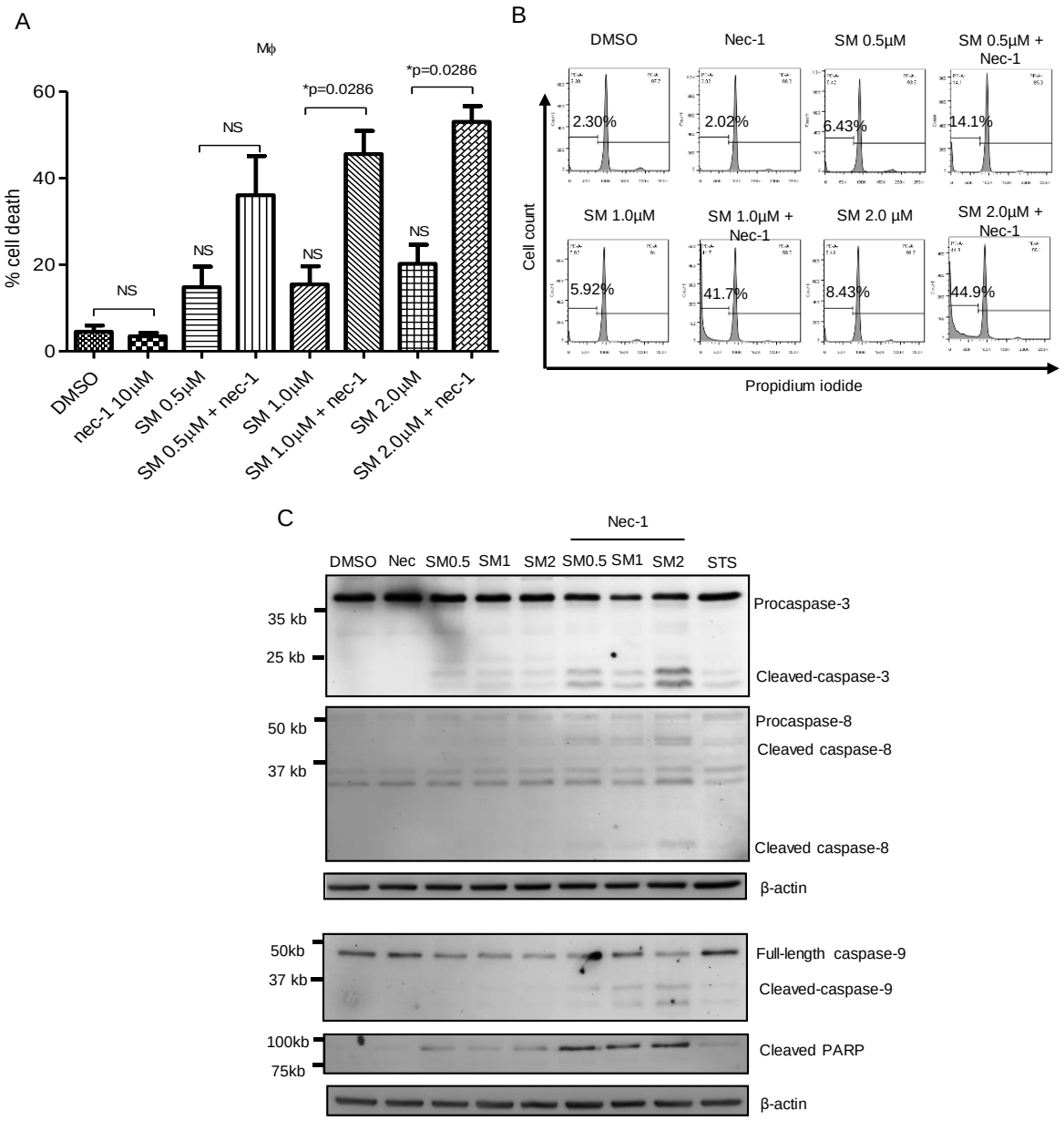
A
Mϕ
% cell death
60
40
20
0
NS
NS
NS
*p=0.0286
NS
*p=0.0286
NS
DMSO
nec-1 10μM
SM 0.5μM
SM 0.5μM + nec-1
SM 1.0μM
SM 1.0μM + nec-1
SM 2.0μM
SM 2.0μM + nec-1
B
DMSO
Nec-1
SM 0.5μM
SM 0.5μM + Nec-1
2.30%
2.02%
6.43%
14.1%
SM 1.0μM
SM 1.0μM + Nec-1
SM 2.0 μM
SM 2.0μM + Nec-1
5.92%
41.7%
8.43%
44.9%
Cell count
Propidium iodide
C
Nec-1
DMSO
Nec
SM0.5
SM1
SM2
SM0.5
SM1
SM2
STS
35 kb
25 kb
Procaspase-3
Cleaved-caspase-3
50 kb
37 kb
Procaspase-8
Cleaved caspase-8
Cleaved caspase-8
β-actin
50kb
37 kb
Full-length caspase-9
Cleaved-caspase-9
100kb
75kb
Cleaved PARP
β-actin

3. Discussion

In this study, we investigated the role of IAPs in resistance to apoptosis of HIV-infected macrophages. We show that although cIAP1/2 are dispensable host factors for the viability of macrophages, it plays a critical role in the survival of HIV-infected macrophages. This is illustrated by the observation that SMs induce apoptosis of chronically HIV-infected U1 cell line, *in vitro* HIV-infected MDMs, and *ex vivo* derived MDMs from naïve and ART-treated HIV patients. SMs were shown to specifically kill HIV-infected MDMs by employing an HSA expressing R5-laboratory strain, HIV-Bal-HSA, and eGFP-expressing, HIV-eGFP. The involvement of IAPs was confirmed by employing IAP siRNAs that resulted in killing of HIV-infected MDMs. Our data suggests that SM-induced apoptosis of HIV-infected macrophages is mediated by apoptosis, is independent of TNF-α and the establishment of M1 polarization. Furthermore, SM-induced apoptosis of HIV-infected macrophages may be due to RIPK1 degradation which in concert with IAP1/2 degradation results in apoptosis of HIV-infected macrophages.

To achieve eradication of HIV-1 in patients undergoing suppressive ART, it is imperative to devise strategies to eliminate HIV reservoirs in cell targets other than T cells such as macrophages. Recently, IAPs were shown as a potent negative regulator of LTR-dependent HIV-1 transcription and leading to the reversal of HIV latency in JLat latency model system and primary T cells [269]. In addition, IAP1/2 and Survivin, another member of the IAP family were suggested to be involved in survival of HIV-infected CD4+ T cells [271,375]. SMs activate the non-canonical NFκB pathway by virtue of RelA:p50 and RelB:p52 transcription factors which bind to the HIV-1 LTR region and results in the induction of virus transcription in latently infected

JLat cell lines [269,395]. In addition, XIAP down regulation by Flavopiridol, a cyclin-dependent kinase 9 (CDK-9) inhibitor, resulted in increased apoptosis of ACH2 cells (a chronically HIV-infected T cell line) [268]. Additionally, ablation of cIAP1/2 by SMs cleared hepatitis B virus in immune competent mouse models [269]. We and others have previously shown that ablation of cIAP1/2 by SMs does not affect survival of normal primary human macrophages [377,396]. However, resistance of macrophages to apoptogenic HIV-Vpr was attributed to cIAP1/2 [377]. These observations suggest that targeting of IAPs may represent a possible strategy for killing of HIV-infected macrophages. Herein, we show that *in vitro* HIV-infected MDMs and MDMs generated *ex vivo* from ART-treated or naïve HIV-infected patients were highly susceptibility to SM-mediated cell death. Induction of apoptosis was confirmed by using monomeric (LCL161) and dimeric (AEG40730) SMs as well as IAP-siRNAs and three different M-tropic strains including HIV_{cs204} (clinical), HIV-eGFP and HIV-Bal-HSA. The high variability in the degree of SM-mediated killing of *ex vivo* generated MDMs in ART-treated and naïve untreated groups may be due to the effects of antiretroviral drugs on mitochondrial function and highly variable percentage of HIV-infected monocytes in the patients [153,397]. The CD16+ monocytes in the ART-treated patients are significantly higher compared to the untreated group and CD16+ monocytes are more permissive to infection and preferentially harbors HIV-1 *in vivo* [341].

The number of HIV-infected macrophages in *in vitro* infected MDMs is around 5-10% due partly to a milieu of HIV restriction factors that limit the virus life cycle [294,363,398,399]. However, some of our experiments show killing of around 30% of macrophages suggesting that SM may cause non-specific killing of bystander MDMs. Since SM did not significantly inhibit virus replication, it is possible that HIV proteins

such as Vpr secreted in the supernatants may prime bystander MDMs to SM-mediated killing [400]. By employing HIV-Bal-HSA and HIV-eGFP strains, our results show that SMs are specifically killing HIV-infected macrophages. Although SM are killing relatively higher number of HIV-HSA-negative MDMs compared to mock-infected MDMs, the differences were not significant. Moreover, SMs killed significantly higher number of HIV-HSA-infected MDMs compared to the HIV-HSA-negative MDMs further suggests the specificity of SMs towards killing of HIV-infected macrophages. cIAP1 was shown to be a negative regulator of LTR-dependent HIV-1 transcription in latently infected primary memory T cells [269]. However, SM did not affect HIV transcription in U1 cells and *in vitro* HIV-infected MDMs. We have previously shown that SM treatment alone did not activate either classical or alternative NFκB pathways in macrophages that may explain SMs' inability to impact virus replication in macrophages [380].

Our results suggest that the mechanism of SM-mediated killing of HIV-infected MDMs is independent of endogenous TNF-α. SM-mediated killing has been attributed to endogenous TNF-α in cancer cells [384,385]; however, it has been reported to be independent of TNF-α in some cancer cells [401]. Given that macrophages produce high levels of TNF-α, the possibility that SM-mediated killing of HIV-1-infected MDMs could be attributed to TNF-α was investigated. TNF-α mediated SM-induced killing of myeloid U1 and U937 undifferentiated and PMA-differentiated cells in contrast to that of primary MDMs. Although the *in vitro* HIV-infected MDMs produced significant amounts of TNF-α compared to the mock-infected MDMs, SM treatment did not affect TNF-α secretion in either uninfected or HIV-infected MDMs. Moreover, rTNF-α failed

to induce cell death in SM-treated MDMs suggesting that SM-induced cell death in macrophages contrary to the cancer cells is independent of TNF-α further displaying dichotomy in the effects of SMs on leukemic myeloid cells and primary macrophages.

HIV infection results in dysregulation of cytokine profile *in vivo* and *in vitro* [402] and can possibly affect the polarization state of macrophages**.** Since IFN-γ-generated M1 macrophages are highly susceptible to SM-mediated cell death, the possibility of *in vitro* HIV-1 infection to polarize macrophages into M1 phenotype making these cells susceptible to SM-induced apoptosis was studied. We show that *in vitro* infected and *ex vivo* derived MDMs exposed to SM were not polarized into M1 phenotype suggesting that SM-mediated killing of HIV-infected macrophages was not due to M1 polarization.

Our results suggest that the mechanism of SM-mediated selective killing of U1 cells and primary MDMs infected with the clinical strain, HIV_{cs204} is via apoptosis. The pathways of apoptosis are regulated by RIPK1 [390,394]. In TNF-α-mediated signalling, RIPK1 is recruited in a multiprotein complex I along with TRADD, TRAF2, and cIAP1/2 to promote transcription of genes with anti-apoptotic properties such as cIAP1/2 [394]. RIPK1 is also recruited in a protein complex composed of TRADD, FADD, and caspase 8, which depending on additional proteins recruited, can induce apoptosis or necroptosis [394]. Recently, HIV infection of primary activated $CD4^+$ T cells was shown to downregulate RIPK1 through HIV-1 protease [391]. RIPK1 modification in response to human rhinovirus and Newcastle disease virus infection has also been reported [403,404]. Herein, we show that infection of MDMs with HIV_{CS204} or with HIV-Bal-HSA caused downregulation and cleavage of RIPK1. Given

that down regulation of *IAPs* alone by SM-LCL161 or of RIPK1 alone by Necrostatin did not induce cell death in uninfected MDMs, suggests that RIPK1 and IAP1/2 are dispensable in survival of macrophages. However, inactivation of RIPK1 by Necrostatin-1 following IAP degradation by SM resulted in a dramatic increase in cell death, cleavage of caspases and PARP in normal MDMs suggesting that RIPK1 may play a key role in SM-induced killing of HIV-infected macrophages. The role of RIPK1 degradation during HIV-1 infection of macrophages needs further investigation.

TRAF1 is an important receptor interacting protein that forms a complex with TRAF2 to transduce TNF-α-induced MAPK and NFκB activation [405]. TRAF2 is also a key determinant for SM-induced degradation of *cIAP1/2* [405]. Our results show that *in vitro* HIV infection as well as SM treatment of HIV-infected MDMs resulted in downregulation of TRAF1 but not of TRAF2. In addition, Bid, a proapoptotic protein, is downregulated in SM-treated MDMs. Bid is localized in an inactive form in the cytosol which becomes activated by proteolytic cleavage of active caspase 8 [393]. Upon activation, cleaved Bid translocates to mitochondria and forms a complex with BAX to disrupt its integrity resulting in the release of apoptogenic factors, caspase 3 activation and cell death. How SMs cause down regulation of *Bid* and *TRAF1* in HIV-infected macrophages is not clear. We have shown previously that HIV-Vpr targets BID, TRAF1 and TRAF2 for proteosomal degradation leading ultimately to mitochondrial outer membrane depolarization and apoptosis [272]. Since SMs did not inhibit virus replication and that HIV-Vpr is one of the early genes expressed in virus life cycle, and HIV-Vpr is released following *in vitro* infection of macrophages, the interplay between Vpr and SM-mediated effect may lead to down regulation of *Bid* and *TRAF1* and cell death of HIV-infected macrophages. The functional relevance of the

modulation of apoptosis related genes in response to SM-treatment of HIV-infected macrophages needs further investigation.

In summary, the results of this study suggest the potential significance of SM in killing of HIV-infected macrophages *in vivo*. In the event SMs can kill HIV-infected macrophages *in vivo,* they have the potential to be translated into clinical interventions aimed at eradicating HIV infection by directly targeting HIV-infected macrophages.

Chapter 6.3: A genome-wide screen identified novel gene targets to selectively induce the apoptosis of HIV-infected macrophages

1. Introduction

The eradication of HIV viruses from HIV-infected patients is one of the major medical problems today, primarily due to HIV reservoir formation [16,162]. Macrophages have been identified to be an early target for the virus and one of three major cellular reservoirs of HIV [142,151,406]. Once infected, macrophages are not like CD4+ T cells, which are characterized by a fast and irreversible depletion [108], but become more resistant to HIV cytopathic effects and may live longer than uninfected macrophages [152,156]. After infection, the viruses hide themselves in the host cellular genome as “pro-viruses” [56]. During antiretroviral therapy, the infected cells are not actively producing new viruses, their phenotype can be the same as uninfected macrophages, and the viral load in blood is too low to be detectable [407]. However, once treatments are interrupted or stopped, the pro-viruses may be re-activated, and infected cells start to produce and release infectious HIV particles again, resulting in a rapid viral rebound in blood [16].

Notably, macrophages have a long life span from months to years, and they are distributed all over the body [154,155]. Significantly, a subset of tissue resident macrophages are derived from embryonic progenitors before birth and independently maintain the macrophage pool without being superseded by bone marrow-derived or blood monocyte-derived cells [157]. Because they are long-lived and self-renewable, once infected, they are more likely to maintain HIV persistence and chronic infections than blood monocyte-derived macrophages [160]. Consequently, infected

macrophages become a source of HIV virus and can release infectious particles for a long period of time [199]. Cattin et al found that HIV virus is rarely detected in blood and colon myeloid cells during anti-retroviral therapy [408], and macrophages protect the virus against host anti-viral immune responses, and help to spread viruses and establish infection in anatomically protected sites [164]. For a complete cure of this disease, it is essential to selectively induce cell death of HIV-infected macrophages [195].

Numerous studies have reported that selective induction of apoptosis in HIV-infected macrophages could be achieved. Xue et al reported that Galectin-3, a potent apoptosis-inducing protein that regulates diverse cellular activities, selectively induced the apoptosis of HIV-infected macrophages by promoting caspase-independent cell death [262]. Perez and colleagues specifically killed HIV-infected CD4+ T cells with Motexafin Gadolinium (Gd-Tex), which is a compound that promotes intracellular oxidative stress [260]. Although their study was not focused on macrophages, their research discovered that specific eradication of HIV-infected cells was possible. Cunyat et al found that Colony-Stimulating Factor 1 Receptor (CSF-1R) antagonists selectively induced the cell death of HIV-infected macrophages *in vitro* [261]. In addition, targeting TRAIL selectively induced the apoptosis of *in vitro* infected macrophages [263,264,266,409]; however, targeting TRAIL did not show a significant survival benefit in the clinic [267]. Moreover, Pache et al discovered that cIAP1 negatively regulated the early transcription of HIV-1, and targeting cIAP by Smac Mimetics could reactivate the provirus and synergize with HDAC inhibitors to reverse latency in T cells [269]. A recent study in our lab discovered that targeting IAPs by SMs, or an siRNA mixture of *IAP* Genes (*xIAP*, *cIAP1* and *cIAP2*), also selectively

induced the apoptosis of HIV-infected macrophages *in vitro* [Chapter II]. Despite these promising results, gene products of *IAPs* are the last defence of normal cells against the death and therefore, targeting IAPs as a therapeutic treatment is controversial and may have detrimental consequences for immunity to infection [276,277].

Previous studies indicate that HIV infections substantially alter the gene expressions of host cells [206,207,265]. Our lab demonstrated that HIV-Tat significantly inhibited p38 MAPK and PI3K, which were implicated in HIV-Tat mediated inhibition of LPS-induced IL-23 and IL-27 production of macrophages [303]. Badley et al postulated that a possible mechanism for the resistance of macrophages to the cytopathic effects of HIV-1 might be that HIV infection dysregulated a variety of NFκB dependent apoptosis inhibitors, including Bcl2, cFLIP, xIAP and cIAP1/2 [209]. These studies suggest that HIV infection dysregulates the expression of many host genes essential for the survival of infected cells, and that targeting these genes may selectively induce the apoptosis of HIV-infected macrophages. I hypothesize that we may take advantage of this alteration to search for novel targets for this disease by a genome-wide screen.

Unfortunately, it is estimated that there are approximately 19,000 genes in a complete haploid set of human genome [278], making the screening process for target genes a big challenge. Encouragingly, siRNA and shRNA technologies, which have been widely used to be an efficient loss-of-function tool to study genes in recent years [324,325,410], made a high-throughput screening of target genes possible [279]. A couple of existing studies using these technologies have successfully identified many host factors that play important roles in HIV-1 infection [280–283], demonstrating that

siRNA and shRNA technologies may be applied to a fast, cost saving, and genome-wide screen of novel target genes to eradicate the HIV reservoir in macrophages.

Herein I selected a shRNA lentivirus-based gene silencing technology, 90k shRNA lentivirus pool technology, to screen novel genes that can be targeted to selectively induce apoptosis of HIV-infected macrophages. This technology is an RNAi consortium library containing a pool of 90,408 unique shRNA targeting 18,000 genes in the human genome, allowing for a high-throughput screen of a large number of genes simultaneously. This novel idea was applied to successfully screen target genes for breast cancer therapies in 2013 [285]. I applied this unbiased, pooled shRNA-based screening strategy [284,285] and identified four potential target genes, *Cox7a2*, *Znf484*, *Cstf2t*, and *Cdk2*. Our findings may help to understand the pathogenesis of AIDS, delineate the mechanisms underlying HIV reservoir formation in macrophages, and design effective therapeutic strategies for the complete eradication of HIV infections.

Note: all the experiments in this chapter were performed by Simon Xin Min Dong.

2. Results

2.1 Undifferentiated and differentiated U937 and U1 cells can be effectively infected with the 90k shRNA lentivirus pool

In order to screen genes that can be targeted to eradicate HIV-infected macrophages, I selected the 90k shRNA lentivirus pool to be my key strategy. Following the manufacturer protocol for this pool technology, I first determined which myeloid lineage cells could be used, as well as all the parameters essential for the application of this lentivirus pool.

Puromycin is the selection marker for the 90k shRNA lentivirus pool [411]. Hence, I first determined the optimal dose of puromycin required for killing a maximum number of myeloid lineage cells, namely U937, U1, THP-1, and primary Monocyte Derived Macrophages (MDMs). Puromycin effectively killed undifferentiated and PMA-differentiated U937, U1 and THP-1 cells, and primary MDMs **(Fig. 26)**. However, the dose of puromycin required to kill PMA-differentiated U1, THP-1 and U-937 cells was 4-5 times higher than that required for undifferentiated cells. Moreover, the dose required to kill HIV-infected primary MDMs was the highest (~20 µg/ml); requiring twice the amount used to kill the PMA-differentiated cells **(Tab. 1).**

Polybrene is commonly used to enhance the transduction rate of lentiviruses as previously reported [411]. I determined the concentration of polybrene that kills a minimal number of U937, U1, THP-1, and primary MDMs. I found that polybrene at concentrations of 5-10µg/ml killed minimal numbers of U937, U1 and THP-1 cells (Fig. 27A-F; Tab. 3). However, polybrene at the lowest working concentration (5 µg/ml) markedly changed the morphology of primary MDMs, indicating that it was toxic to primary MDMs and unsuitable for this cell type **(Fig. 27G, H; Tab. 2)**.

Figure 26. Puromycin sensitivity of U937, U1, THP-1 and primary MDMs

Undifferentiated and differentiated cells were treated with various doses of puromycin for 48 hours, harvested and stained with PI to track dead cells. The percentage of dead cells was detected by Flow Cytometry. The mean values and standard deviations were calculated by Excel (n=3). **A.** U937 Undifferentiated; **B**. U937 Differentiated 7 days; **C.** U1 Undifferentiated; **D.** U1 Differentiated 7 days; **E.** THP-1 Undifferentiated; **F.** THP-1 Differentiated 4 days; **G.** 16-day-old primary MDMs.

A: U937 Undifferentiated

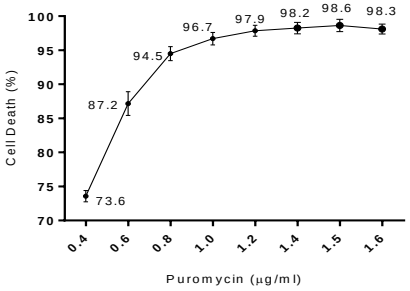

B: U937 Differentiated 7 days

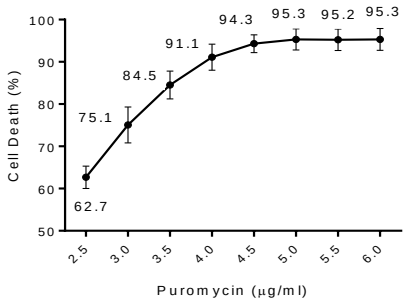

C: U1 Undifferentiated

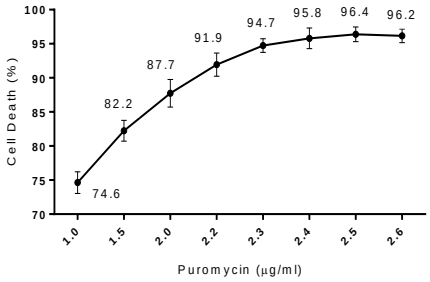

D: U1 Differentiated 7 days

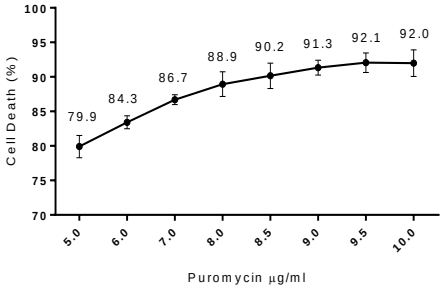

E: THP-1 Undifferentiated

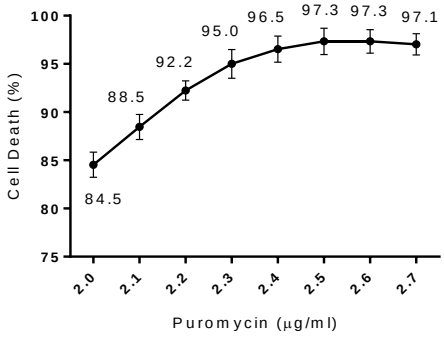

F: THP-1 Differentiated 4 days

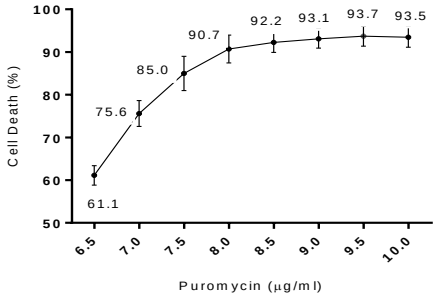

G: 16-day-old primary MDMs

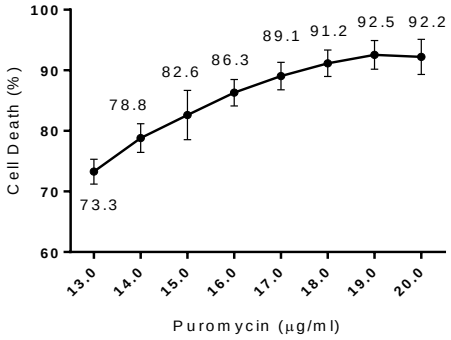

Table 1. Calculating the number of days for puromycin selection and puromycin sensitivity of myeloid linages cells

All results in Figure 26 were summarized into the last column in this table. Following the protocol of applying 90k shRNA lentivirus pool, days of PMA or M-CSF differentiation, the 90K shRNA lentivirus pool infection, and puromycin treatments were taken into consideration to determine the lowest puromycin concentration to reach the plateau of cell death.

Cells	Calculating days for Puromycin selection			Results
	Days of Differentiation	90K Pool Infection	Puromycin Treatment	Puromycin concentration to reach the plateau of cell death
U937 undifferentiated	N/A	2 days	2 days	1.5µg/ml
U937 differentiated	PMA, 5 days	2 days	2 days	5.0µg/ml
U1 undifferentiated	N/A	2 days	2 days	2.5µg/ml
U1 differentiated	PMA, 5 days	2 days	2 days	9.5µg/ml
THP-1 undifferentiated	N/A	2 days	2 days	2.5µg/ml
THP-1 differentiated	PMA, 2 days	2 days	2 days	9.5µg/ml
Primary MDMs	14 days (M-CSF 7 days , HIV infection 7 days)	2 days	2 days	19.0µg/ml

Figure 27. Polybrene tolerance of U937, U1, THP-1 and primary MDMs

Myeloid lineage cells were treated with various doses of polybrene for 48 hours. Cells were harvested and stained with PI to track dead cells. The percentage of dead cells was detected by Flow Cytometry. The mean values and standard deviations were calculated by Excel (n=3). **A.** undifferentiated U937; **B.** PMA-differentiated U937 5 days; **C.** undifferentiated U1; **D.** PMA-differentiated U1 5 days; **E.** undifferentiated THP-1; **F.** PMA-differentiated THP-1, 2 days old.; **G.** 14-day-old primary MDMs without treatment; **H.** 14-day-old primary MDMs 5 μg/ml polybrene treated for 48 hours.

A: U937 undifferentiated

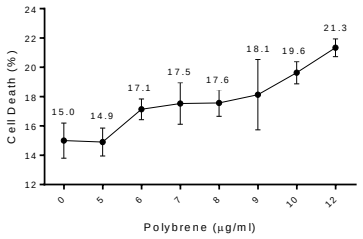

B: U937 differentiated 5 days

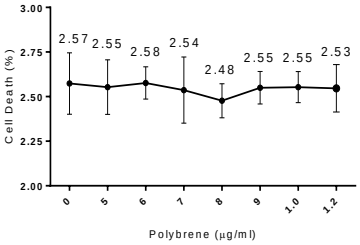

C: U1 undifferentiated

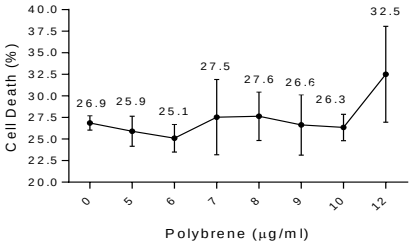

D: U1 differentiated 5 days

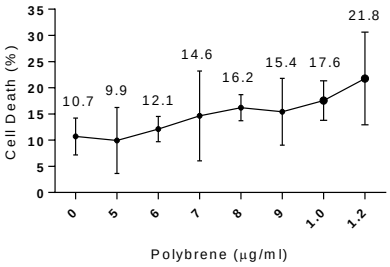

E: THP-1 undifferentiated

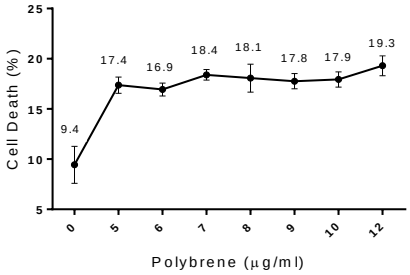

F: THP-1 differentiated 2 days

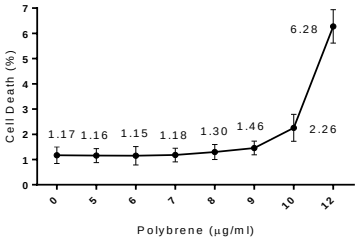

G: 14-day-old primary MDMs without treatment

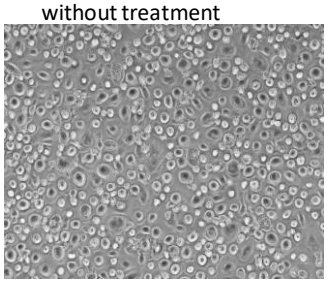

H: 14-day-old primary MDMs 5µg/ml polybrene treated

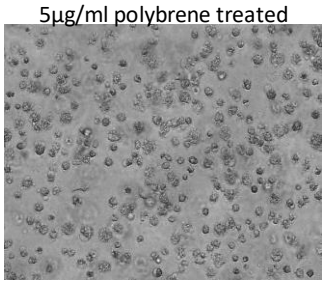

Table 2. Summary of Polybrene tolerance of undifferentiated and differentiated U937, U1, THP-1, and primary human MDMs

The results in Figure 27 were summarized into this table. Positively charged polybrene reduces the electrostatic repulsion forces between negatively charged cells and lentiviral particles, resulting in an enhanced transduction efficiency.

Cells	Polybrene concentration recommended
U937 undifferentiated	5-8µg/ml
U937 differentiated 5 days	5-10µg/ml
U1 undifferentiated	5-10µg/ml
U1 differentiated 5 days	5-10µg/ml
THP-1 undifferentiated	5-10µg/ml
THP-1 differentiated 2 days	5-10µg/ml
Primary MDMs	N/A

Since I intended to use the 90k shRNA lentivirus pool, I determined whether undifferentiated myeloid cells could be infected with lentiviruses using lentivirus-eGFP viruses. I show that 2 MOI of lentivirus-eGFP infected 30-40% of undifferentiated U937 cells (**Fig 28A**) whereas undifferentiated THP-1 cells were resistant to this infection (data not shown). As per the protocol, the infection rate of 90k shRNA lentivirus pool should be controlled to 30-40%. For this, U937 cells were infected with various concentrations of the 90K shRNA library followed by treatment with puromycin for 48 hours and assessed for cell viability. I also used lentivirus-eGFP as a reference virus to indirectly determine the optimal amount of 90k shRNA lentivirus pool to infect 0.5 million U937 cells. I found that 200 µl of 90k shRNA lentivirus pool or 2MOI lentivirus-eGFP infected 30-40% of U937 cells **(Fig 28A)**.

To determine if differentiated cells could be infected with the 90k shRNA lentivirus pool, U937 and THP-1 cells were infected with various volumes of the 90k shRNA lentivirus pool in the presence of polybrene followed by puromycin treatment. The results show that differentiated U937 could be effectively infected with 200 µl of the 90k shRNA lentivirus pool **(Fig. 28B)**. However, differentiated THP-1 cells could not be infected with the lentivirus pool **(Fig. 28C)**. Furthermore, the 90k shRNA lentivirus pool alone changed the morphology of primary MDMs leading to cell detachment and eventual cell death **(Fig. 28D)**, suggesting that the 90k shRNA lentivirus pool is toxic for primary MDMs. These results show that of all the myeloid lineage cells I examined, only U937 cells can be infected with the 90k shRNA lentivirus pool.

Several HIV-1 proteins, including Nef, Vpu, and Env, down-regulate CD4 expression in macrophages to avoid super-infection [151,412]. As a result,

macrophages are resistant to secondary viral infection. It is possible that U1 cells, a well characterized cellular model of chronically HIV-1 infected U937 cells [413], may be resistant to infection with the 90k shRNA lentivirus pool. Therefore, I investigated if U1 cells could be infected with lentiviruses by employing lentivirus-eGFP as a reference virus. Interestingly, the results show that U1 cells could be efficiently infected a second time by lentivirus-eGFP **(Fig. 28E)**.

Overall, these results suggest that of all the myeloid lineage cells examined, only U937 and U1 cells were suitable for the application of the shRNA lentiviral system to screen target genes to selectively induce apoptosis of HIV-infected macrophages. Furthermore, the infection rate of the 90k shRNA lentivirus pool could be controlled to be 30-40% to avoid duplicate infections.

2.2 Application of 90k shRNA lentivirus pool to screen target genes

Armed with the appropriate cell line model and controls, I next designed our screening strategy to induce cell death of HIV-infected macrophages. The workflow of the lentivirus-based pooled screen is described in **Fig. 29**. I applied the 90k shRNA lentivirus pool to uninfected undifferentiated and PMA-differentiated U937 and U1 cells simultaneously as per the method previously described [284], and genomic DNA was extracted for micro-array deconvolution analysis. This library uses the RNA Pol III promoter U6 to express shRNA that contain a 21-nt double-stranded stem and a 6-nt loop. The pre-miRNA-like shRNA are then processed into functional siRNAs in cells. In short, following the infection of U937 and U1 cells, gene knockdowns that caused lethality were identified by loss of the associated barcodes on microarrays as described in **Fig. 3**.

Figure 28. Infecting U937, THP-1, MDMs and U1 cells with 90k shRNA lentivirus pool

A. Differentiated U937 cells infected with 90K shRNA lentivirus for 48 hours and then selected with puromycin for 48 hours; **B.** Differentiated THP-1 cells infected with 90K shRNA lentivirus for 48 hours and then selected with puromycin for 48 hours; **C.** Primary MDMs infected with 90K shRNA Lentivirus Pool for 48 hours; **D.** U1 (HIV infected U937) cells infected with lentivirus-eGFP for 24 hours. **E.** The infection rate of 90K shRNA Lentivirus Pool was controlled to be 30~40%. Trypan Blue was used to distinguish live and dead cells; when 200µl 90K shRNA Lentivirus Pool and 2MOI lentivirus-eGFP were used to infect U937 cells and after puromycin selection for 48 hours, the same number of live cells could be counted under microscopy. By this way, the infection rate of 90K shRNA Lentivirus Pool was controlled to be 34.6%.

A: Differentiated U937 cells: infection with 90K shRNA lentivirus

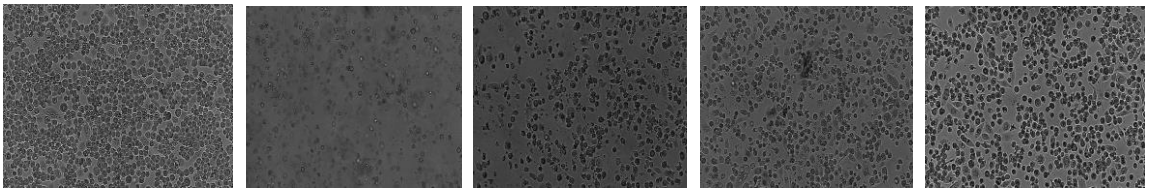

No virus; no Puromycin | No virus + Puromycin | 100µl 90K virus + Puromycin | 150µl 90K virus + Puromycin | 200µl 90K virus + Puromycin

B: Differentiated THP-1 cells: infection with 90K shRNA lentivirus

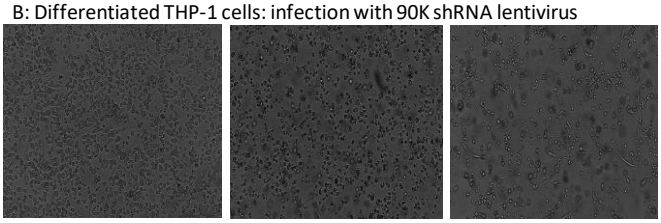

No virus; no Puromycin | No virus + Puromycin | 200µl 90K virus + Puromycin

C: Primary MDMs infected with 90K shRNA lentivirus

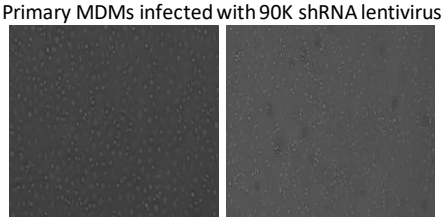

No virus | 200µl 90K virus

D: Differentiated U1: Infection with Lentivirus-eGFP

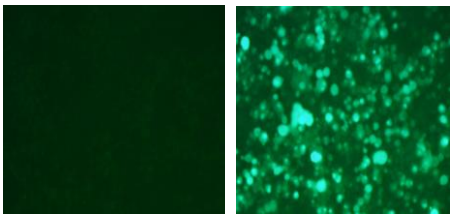

No virus | Lentivirus-eGFP (3MOI)

E: Controlling the infection rate of 90K lentivirus pool

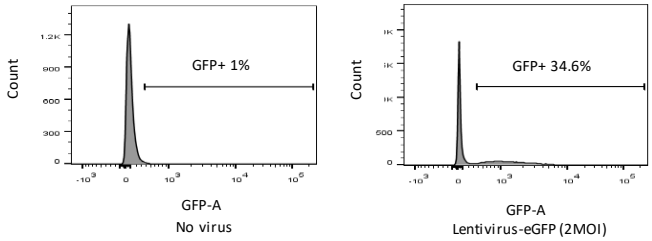

Figure 29. Workflow of the application of the 90k shRNA lentivirus pool

The application of the 90k shRNA lentivirus pool includes 7 steps: **1.** Infecting cells with the 90k shRNA lentivirus pool and selecting infected cells with puromycin; **2.** Collecting cells at different time point; **3.** Extracting genomic DNA of cell pellets; **4.** Amplification of shRNA sequence; **5.** Micro-array deconvolution; **6.** Data analysis on computer; **7.** Reporting results.

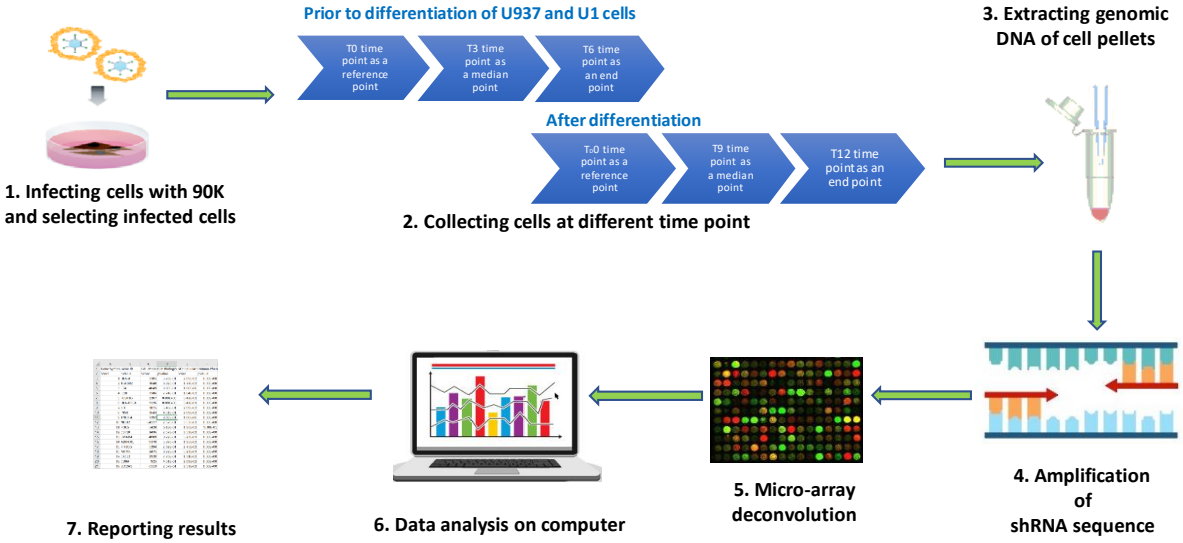
Prior to differentiation of U937 and U1 cells
T0 time point as a reference point
T3 time point as a median point
T6 time point as an end point
After differentiation
T0 time point as a reference point
T9 time point as a median point
T12 time point as an end point
1. Infecting cells with 90K and selecting infected cells
2. Collecting cells at different time point
3. Extracting genomic DNA of cell pellets
4. Amplification of shRNA sequence
5. Micro-array deconvolution
6. Data analysis on computer
7. Reporting results

The abundance of each shRNA in the mixture can be measured by custom barcode microarrays [284,285]. I used the GMAP arrays to de-convolute our pooled screen to identify genes whose loss of function caused selective lethality **(Fig. 30A)**. The loss of specific shRNA sequences within the HIV-infected U1 population as compared to the U937 population identifies shRNA targets that selectively cause the lethality of U1 cells. The overall quality of the screen was measured by the published framework that depends on a reference set of essential genes as well as non-essential genes and providing a Bayesian classifier of gene essentiality [414]. By this approach, I found our screens recorded a performance score of F-measure 0.69 and 0.52 **(Fig. 30B, C)**. Screens were analyzed taking into account 4 different timelines as both U937 and U1 cells differentiate after six days in culture. First, hits were identified that caused selective lethality prior to differentiation (T0 and T6 alone) or after differentiation (taking T6 and T12 time points into consideration). I also identified hits irrespective of the differentiation status by either analyzing all the time points (T0, T6 and T12) or analyzing as an end-point assay (taking T0 and T12 time points alone). I found 28 genes that were consistently identified in all possible analyses **(Fig. 30D)**, suggesting they may play key roles in the survival of U1 cells, and indicating these 28 genes as the most promising gene targets to kill HIV-infected macrophages.

Figure 30. Application of 90k shRNA lentivirus pool for a genome-wide screen

A. Schematic representation of the genome-wide screen. **B.** Volcano plot representing the hits from the screening. The X-axis represents the fitness score and the Y-axis represents the p value significance. Magenta color dots represent the final selected hits while the dark yellow represents all the significant hits from the screen. **C.** Precision-Recall curve evaluating quality of the screen as described in Hart et al 2013 [414]. Higher the F-measure, lower is the error rate. Usually F>0.5 is reliable screen. **D.** Cytoscape representation of the hits from the screen. Since the macrophages differentiate during the screening, the key nodes are arranged such that the hits prior to differentiation (T0-T6) and after differentiation (T6-T12) are presented in the context of overall hits. Nodes with gene names are those that were picked up in all possible conditions.

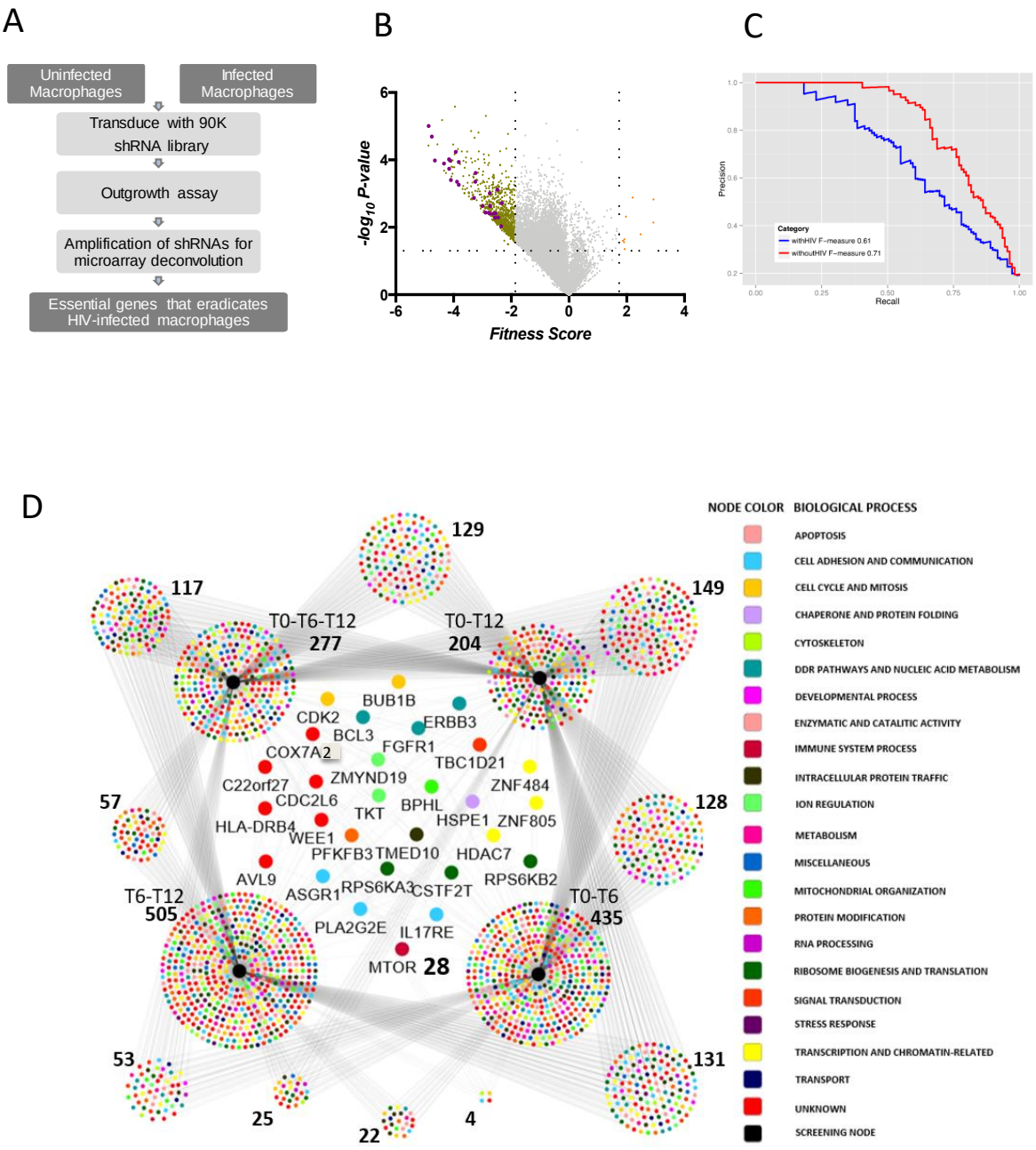
A
Uninfected Macrophages
Infected Macrophages
Transduce with 90K shRNA library
Outgrowth assay
Amplification of shRNAs for microarray deconvolution
Essential genes that eradicates HIV-infected macrophages
B
-log10 P-value
Fitness Score
C
Precision
Recall
Category
withHIV F-measure 0.61
withoutHIV F-measure 0.71
D
NODE COLOR
BIOLOGICAL PROCESS
APOPTOSIS
CELL ADHESION AND COMMUNICATION
CELL CYCLE AND MITOSIS
CHAPERONE AND PROTEIN FOLDING
CYTOSKELETON
DDR PATHWAYS AND NUCLEIC ACID METABOLISM
DEVELOPMENTAL PROCESS
ENZYMATIC AND CATALITIC ACTIVITY
IMMUNE SYSTEM PROCESS
INTRACELLULAR PROTEIN TRAFFIC
ION REGULATION
METABOLISM
MISCELLANEOUS
MITOCHONDRIAL ORGANIZATION
PROTEIN MODIFICATION
RNA PROCESSING
RIBOSOME BIOGENESIS AND TRANSLATION
SIGNAL TRANSDUCTION
STRESS RESPONSE
TRANSCRIPTION AND CHROMATIN-RELATED
TRANSPORT
UNKNOWN
SCREENING NODE
129
117
149
T0-T6-T12
277
T0-T12
204
BUB1B
CDK2
ERBB3
BCL3
FGFR1
COX7A2
TBC1D21
C22orf27
ZMYND19
ZNF484
57
CDC2L6
TKT
BPHL
128
HLA-DRB4
HSPE1
ZNF805
WEE1
PFKFB3
TMED10
HDAC7
AVL9
ASGR1
RPS6KA3
CSTF2T
RPS6KB2
T6-T12
505
T0-T6
435
PLA2G2E
IL17RE
MTOR
28
53
131
25
22
4

2.3 Screening of promising genes involved in apoptosis of HIV-infected macrophages with HIV-eGFP and HIV-HSA viruses

Subsequently, the 28 promising genes were assessed for their ability to induce death in HIV-infected macrophages by infecting primary MDMs with two different HIV-1 viruses, namely HIV-e-GFP and HIV-HSA, followed by transfection with siRNA of the 28 genes. The apoptosis of HIV-1 and mock-infected macrophages induced by siRNA transfection was analyzed by staining with Annexin-V followed by flow cytometry. The siRNA silencing of validated genes was verified by Western blotting.

To screen the promising genes for their ability to kill HIV-infected macrophages, I first studied the kinetics of two HIV-1 infection models namely HIV-eGFP- and HIV-HSA-infected human primary MDMs. Both viruses were produced from plasmid DNA and their Env proteins were mutated to be R5-tropic to increase the infection rate in myeloid cells [415]. Both viruses contain the entire HIV-1 genome and express all wild-type HIV-1 viral protein. However, the two viruses are distinct from each other. In the HIV-eGFP viral genome the eGFP gene is flanked by the viral Matrix (MA) and Capsid (Ca) proteins, making it easy to track active infections; however, this virus is as infectious as native HIV-1 only in single-round infectivity assays [293]. In the HIV-HSA genome an Internal Ribosome Entry Site (IRES) was constructed before the Tat gene to keep the infection active [305], and the cellular membrane-bound mouse Heat Stable Antigen (HSA, the murine CD24, 60aa) is expressed along with early viral genes upon productive infection. The presence of CD24 made it convenient to track active infections using commercially available anti-murine CD24 antibodies [294]. My results show that after infection with 150ng p24/well (12-well plate), the percentage of MDMs with eGFP signals peaked in approximately 50% within 24 hours but faded

quickly in the next couple of days **(Fig.31A)**; the percentage of MDMs with eGFP expression decreased to 5% within 5 days of infection, indicating the latency of HIV virus in macrophages. In contrast, for HIV-HSA virus, the percentage of MDMs with HSA expression was 5-10% in the first few days after infection, depending upon the donor, but infection rates increased steadily to 20-30 % by day 7-10 post-infection **(Fig.31B)**, suggesting active HIV infection.

The involvement of our promising genes in the killing of HIV-infected macrophages was examined by employing siRNAs for each of the 28 genes and infecting macrophages with HIV-eGFP. The MDMs generated from the PBMCs of healthy donors were infected with mock or HIV-eGFP viruses for 7 days, followed by transfection with either non-targeting siRNA or siRNA of each of the 28 genes for 72 hours. Cells were harvested, stained with Annexin-V labelled with BV-711, and analyzed by flow cytometry. The fold change of apoptotic cells (HIV-eGFP/mock infection) induced by each siRNA was calculated, and the results from four independent experiments were summarized **(Fig.31C)**. Each bar represents the results of a promising gene. As this was the first round of analysis, I arbitrarily selected genes with P≤0.1 (a star * over the bar) as the candidate genes that may selectively induce apoptosis of HIV-eGFP-infected macrophages. Based on this cut-off standard, 12 genes were selected for further analysis following infection of MDMs with HIV-HSA. The primary MDMs infected with mock or HIV-HSA viruses for 7 days were transfected with the siRNAs of each 12 selected genes for 72 hours followed by analysis of apoptosis by Annexin-V staining and flow cytometry. SMAC mimetic AEG40730 and a mixture of all siRNA of *xIAP*, *cIAP1* and *cIAP2* were selected to be the positive controls. The fold change (HIV-HSA/mock infection) of apoptotic cells induced by

each siRNA was calculated. The results from four independent experiments are summarized (**Fig. 31D**). The results show that four genes, namely *Cox7a2*, *Znf484*, *Cdk2* and *Cstf2t*, exhibited statistical significance (a star * over the bar indicated $p \leqslant 0.05$), suggesting that these four genes can be targeted to selectively induce apoptosis of HIV-HSA-infected MDMs.

Finally, I verified if the apoptosis of HIV-infected macrophages attributed to *Cox7a2*, *Znf484*, *Cdk2* and *Cstf2t* was due to their silencing by their specific siRNAs. Primary MDMs infected with HIV-HSA for 7 days were transfected with siRNA specific for the four selected genes for 48 hours followed by Western immunoblotting. The results show that siRNA effectively silenced all four selected genes in HIV-HSA-infected primary MDMs **(Fig. 31E)**. Interestingly, the basal expression of *Znf484* in uninfected primary MDMs was low, but expression was upregulated following HIV-HSA infection. The *Znf484* siRNA effectively silenced its expression in HIV-HSA-infected macrophages suggesting that the upregulation of *Znf484* may be essential for the survival of HIV-infected macrophages. Overall, the above results suggest that after two rounds of screening with 2 different HIV-1 viral strains, *Cox7a2*, *Znf484*, *Cdk2*, and *Cstf2t* genes can be targeted to selectively induce apoptosis of HIV-infected macrophages.

Figure 31. Validating promising genes with HIV-eGFP and HIV-HSA viruses using siRNA

A. Kinetics of HIV-eGFP infection. **B.** Kinetics of HIV-HSA infection. The mean values and SD of A and B were based on 3 independent experiments (n=3). **C.** Apoptosis of HIV-eGFP-infected MDMs induced by siRNA of 28 promising genes. **D.** Apoptosis of HIV-HSA-infected MDMs induced by siRNA of 12 candidate genes. The mean value and SD of C and D were based on 4 independent experiments (n=4) and the p values were calculated using Student's t test. **E.** siRNA transfection silenced the expression of all four identified genes in primary human MDMs.

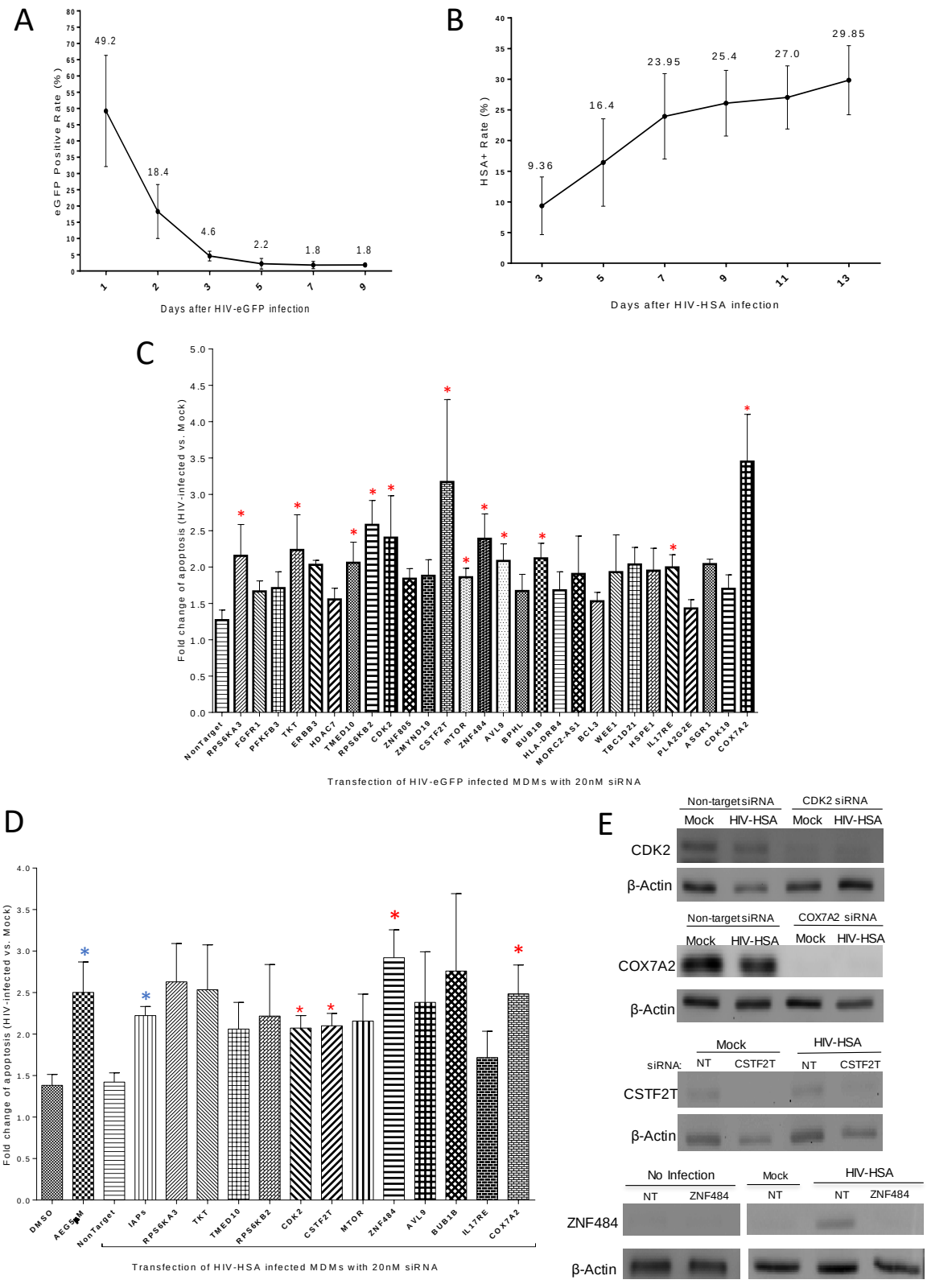
A
eGFP Positive Rate (%)
49.2
18.4
4.6
2.2
1.8
1.8
Days after HIV-eGFP infection
B
HSA+ Rate (%)
9.36
16.4
23.95
25.4
27.0
29.85
Days after HIV-HSA infection
C
Fold change of apoptosis (HIV-infected vs. Mock)
NonTarget
RPS6KA3
FGFR1
PFKFB3
TKT
ERBB3
HDAC7
TMED10
RPS6KB2
CDK2
ZNF805
ZMYND19
CSTF2T
mTOR
ZNF484
AVL9
BPHL
BUB1B
HLA-DRB4
MORC2-AS1
BCL3
WEE1
TBC1D21
HSPE1
IL17RE
PLA2G2E
ASGR1
CDK19
COX7A2
Transfection of HIV-eGFP infected MDMs with 20nM siRNA
D
Fold change of apoptosis (HIV-infected vs. Mock)
DMSO
AEG35a 5μM
NonTarget
IAPs
RPS6KA3
TKT
TMED10
RPS6KB2
CDK2
CSTF2T
MTOR
ZNF484
AVL9
BUB1B
IL17RE
COX7A2
Transfection of HIV-HSA infected MDMs with 20nM siRNA
E
Non-target siRNA
CDK2 siRNA
Mock
HIV-HSA
CDK2
β-Actin
Non-target siRNA
COX7A2 siRNA
COX7A2
β-Actin
Mock
HIV-HSA
siRNA:
NT
CSTF2T
CSTF2T
β-Actin
No Infection
Mock
HIV-HSA
ZNF484
ZNF484
β-Actin

2.4 Knocking down *Cox7a2*, *Znf484*, *Cdk2*, and *Cstf2t* results in specific killing of HIV-infected MDM

It has been suggested that the apoptosis of HIV-exposed uninfected bystander cells plays a critical role in the selective depletion of CD4+ T cells, leading to immunodeficiency, disease progression and AIDS [77]. Although macrophages survive after HIV infection, unlike depletion of CD4+ T cells [151,152], HIV-exposed uninfected bystander macrophages may play a role in HIV pathogenesis. Even though I observed significantly high levels of apoptosis in macrophages following transfection with siRNAs specific for the identified genes, it is possible that this may be at least in part due to the non-specific killing of uninfected macrophages. Notably, these dead cells, even though they are not HIV-infected, also emit weak GFP or FITC signals due to auto-fluorescence [416], falsely alluding to the killing of HIV-infected cells (GFP+ or HSA+) during flow cytometry analysis. Therefore, it is imperative to determine if siRNA silencing of the identified genes selectively induced apoptosis of HIV-infected macrophages or HIV-exposed uninfected bystander macrophages or both.

To determine if the silencing of four identified genes killed HIV-infected macrophages, I only gated the population that were eGFP or FITC (HSA) intensely positive to rule out non-specific low-level fluorescence by dead cells/debris. Only the cells in the eGFP or FITC (HSA) intensely positive population were taken into consideration for the analysis of specific killing of HIV-infected cells. The killing of HSA/eGFP intensely positive (HIV-infected) cells by siRNAs was quantified by Flow cytometry. The gating strategy for selecting HSA+ (mouse CD24+) cells is shown in **Fig. 32A**. Representative histogram from one blood donor showing killing of HSA intensely positive MDMs is displayed in **Fig. 32B**. Quantification of apoptotic cells and

HSA intensely positive MDMs indicated that knocking down *Cox7a2*, *Znf484*, *Cdk2*, and *Cstf2t* killed higher percentages of HSA+ MDMs compared to the HIV-HSA-infected cells treated with non-targeting siRNAs **(Fig.32C)**. Similar results were obtained with primary MDMs infected with HIV-eGFP. The gating strategy for selecting eGFP+ cells is shown in **Fig. 33A**, and the representative histogram reflecting the killing of eGFP intensely positive MDMs is displayed in **Fig. 33B**. siRNA for *Cox7a2*, *Znf484*, and *Cstf2t*, with the exception of *Cdk2*, selectively induced the apoptosis of HIV-eGFP-infected macrophages **(Fig. 33C)**. It may be noted that siRNA silencing of all four selected genes shifted HIV-infected macrophages upwards on the dot plots from the live quadrant to the apoptotic quadrant **(Fig. 32B & Fig. 33B)**, further suggesting that silencing the four identified genes induced apoptosis of HIV-infected macrophages.

Figure 32. siRNAs of the four identified genes selectively induced apoptosis of HIV-HSA-infected MDMs

A. Gating of HSA intensely positive MDMs. **B.** Representative histograms and dot plots for apoptosis of HSA intensely positive MDMs induced by siRNA transfection of 4 validated genes from one individual. **C.** Apoptosis of HSA intensely positive cells. The p values were calculated using Student's t test (n=4).

A: Gating strategy for specific killing of HSA+ cells

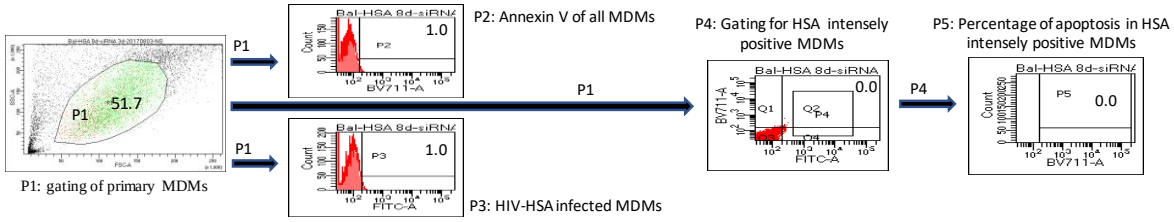

B: Representative histograms and dot plots for apoptosis (HSA)

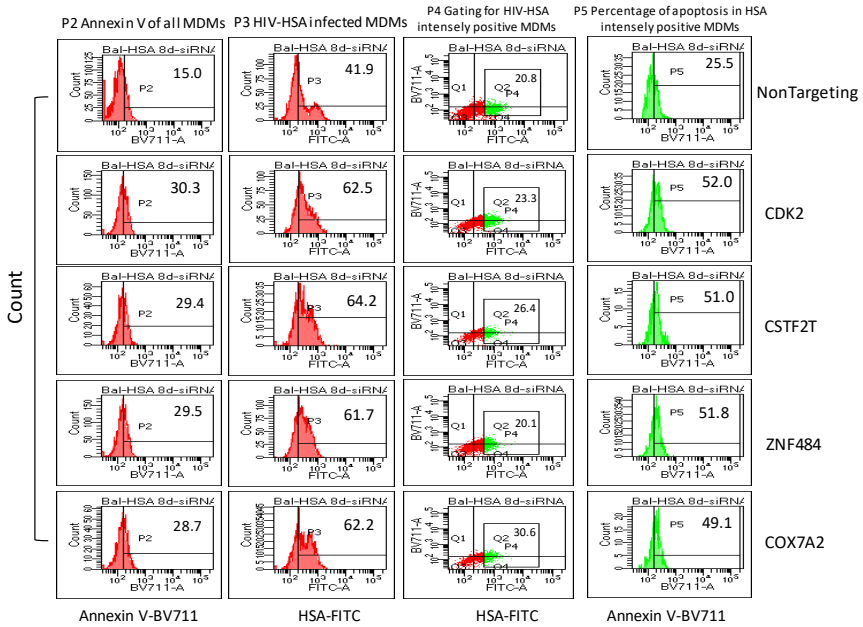

C: Apoptosis of HSA intensely positive cells

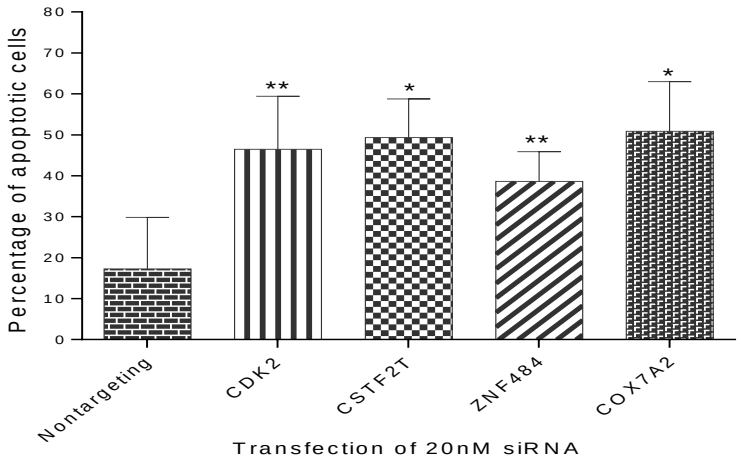

Figure 33. siRNAs of the four identified genes selectively induced the apoptosis of HIV-eGFP-infected MDMs

A. Gating of eGFP intensely positive MDMs. **B.** Representative histograms and dot plots for apoptosis of eGFP intensely positive MDMs induced by siRNA transfection of 4 validated genes from one individual. **C.** Apoptosis of eGFP intensely positive cells. The p values were calculated using Student's t test (n=4).

A: Gating strategy for specific killing of eGFP+ cells

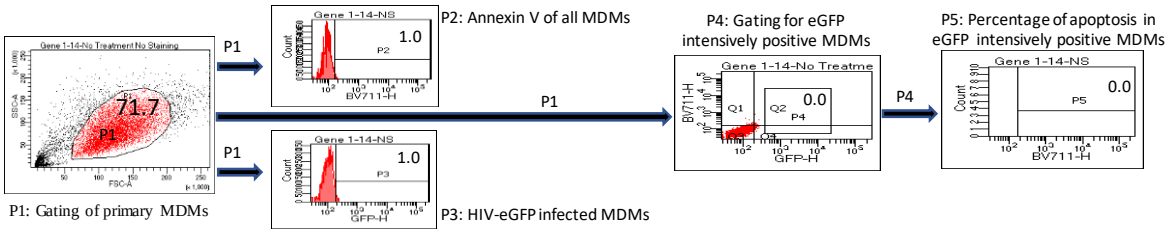

B: Representative histograms and dot plots for apoptosis (eGFP)

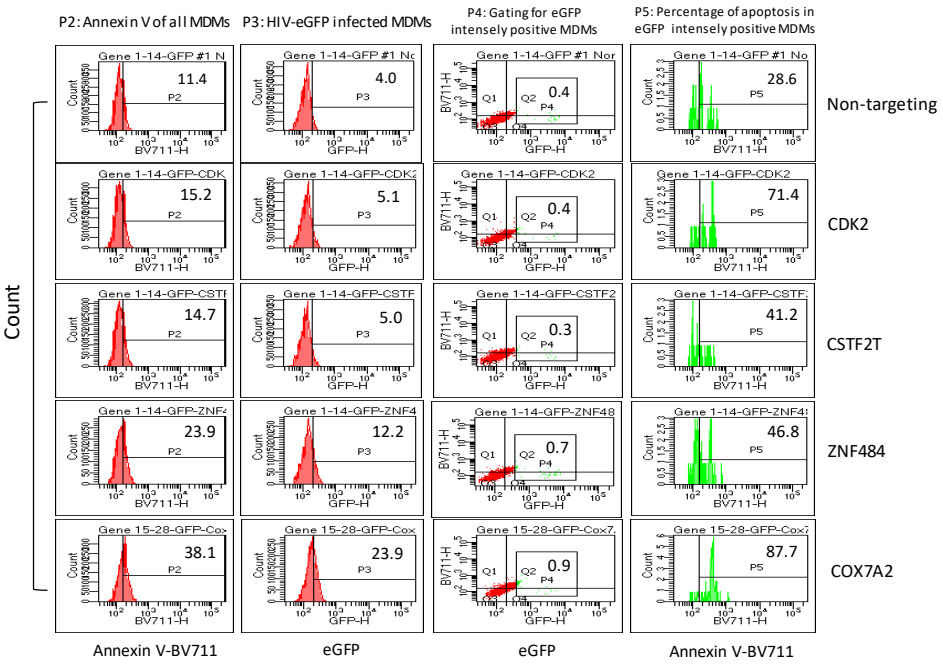

C: Apoptosis of eGFP intensely positive cells

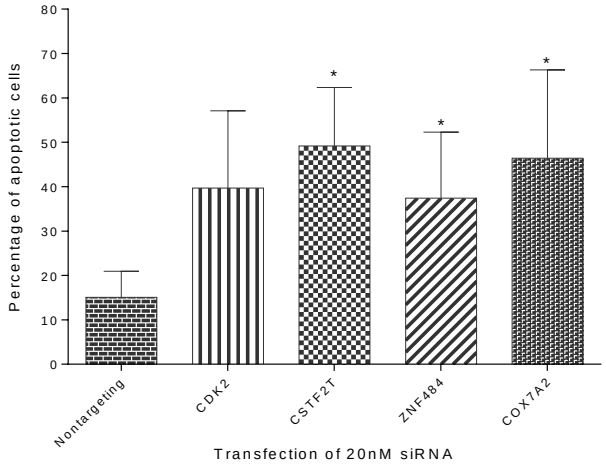

To determine if siRNA silencing of the four identified genes induced apoptosis of uninfected bystander macrophages, I further analyzed the flow cytometry data on targeting the four identified genes with siRNA transfection. The gating strategy for apoptosis of in HSA+ (HIV uninfected) and HSA- (HIV uninfected, bystander) cells is shown in **Fig. 34A**. *Cox7a2*, *Znf484*, *Cstf2t*, and *Cdk2* siRNAs killed significantly high numbers of HSA+ (HIV-infected) cells compared to either the mock or HSA- (uninfected bystander) cells (**Fig. 34B**). However, killing of uninfected bystander (HSA-, HIV-HSA exposed) was also significantly higher than the mock-infected cells, suggesting that siRNA silencing of the 4 identified specific genes also induces the apoptosis of uninfected bystander macrophages.

Similar results were obtained with MDMs infected with HIV-eGFP viruses. The gating strategy for the quantification of apoptosis in GFP+ and GFP- (uninfected bystander) cells is shown in **Fig. 35A**. The *Cox7a2*, *Znf484*, *Cstf2t*, and *Cdk2* siRNAs killed significantly high percentages of GFP+ (HIV-infected) cells compared to either the mock or GFP- (uninfected bystander, HIV-exposed) cells **(Fig. 35B)**, suggesting that *Cox7a2*, *Znf484*, *Cstf2t* and *Cdk2* siRNAs specifically kill HIV-infected macrophages. Notable, after studying the apoptotic effects of AEG40730 (targeting IAPs) and siRNAs for the four identified genes, I found that targeting a specific gene might not be able to induce the apoptosis of HIV-infected macrophages from all the blood donors **(Fig. 36)**, indicating the best gene targets to selectively induce the apoptosis of HIV-infected macrophages varied individually.

Figure 34. siRNA transfection of the four identified genes induced apoptosis of HIV-HSA-exposed but uninfected bystander MDMs

A. Gating strategy for the data analysis of HIV-HSA-uninfected bystander macrophages induced by siRNA transfection of the four identified genes. **B.** Apoptosis of HIV-HSA-uninfected bystander macrophages induced by siRNA transfection of the four identified genes. The p values were calculated using Student's t test (n=4).

A: Gating strategy for HIV-HSA-uninfected bystander macrophages

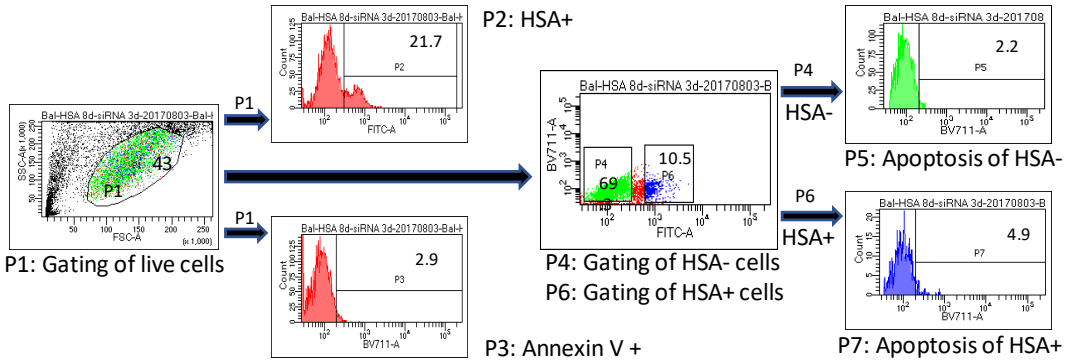

B: Apoptosis of HIV-HSA-uninfected bystander cells

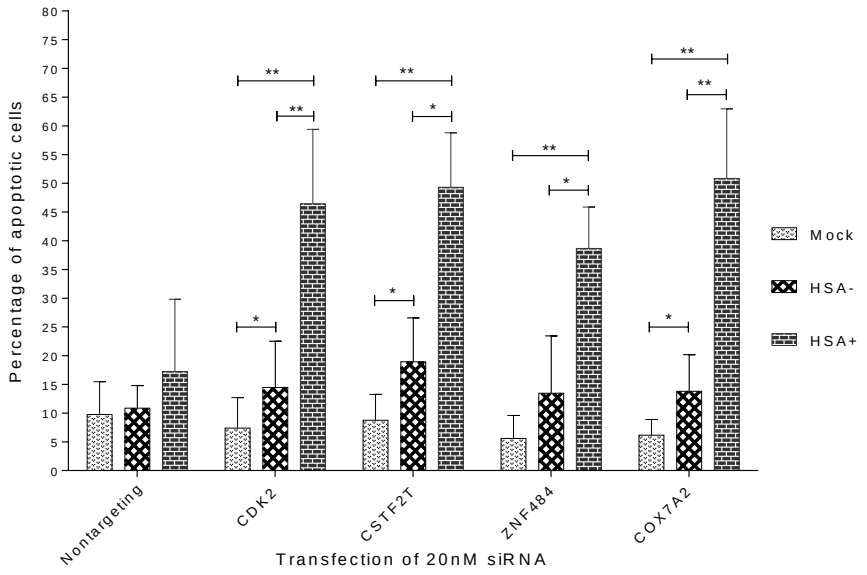

Figure 35. siRNA transfection of the four identified genes induced apoptosis of HIV-eGFP-exposed but uninfected bystander MDMs

A. Gating strategy for the data analysis of HIV-eGFP-uninfected bystander macrophages. **B.** Apoptosis of HIV-eGFP-uninfected bystander macrophages. The p values were calculated using Student's t test (n=4).

A: Gating strategy for HIV-eGFP-uninfected bystander macrophages

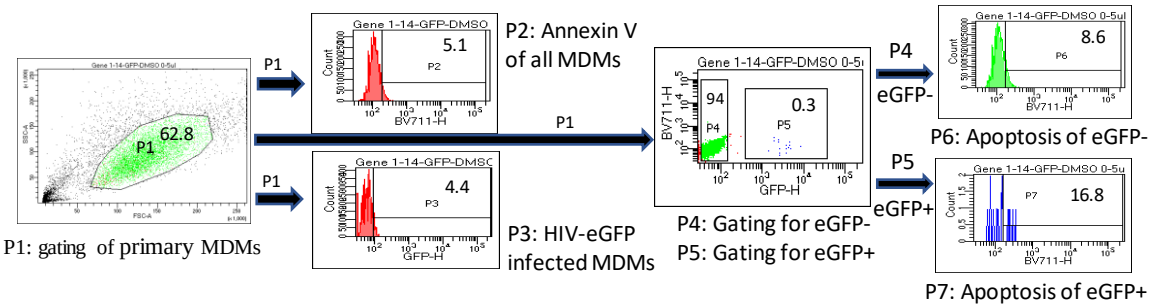

B: Apoptosis of HIV-eGFP-uninfected bystander cells

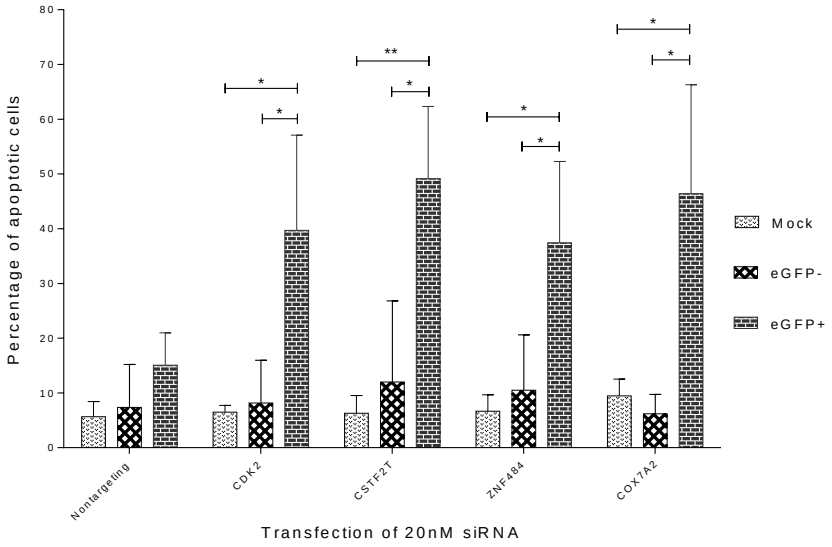

Figure 36. The best gene targets to induce apoptosis of HIV-infected MDMs varied individually

Six independent experiments were randomly selected to compare the apoptosis induced by SMAC Mimetics AEG40730 and siRNA silencing of the four identified. **A-C:** HIV-eGFP-infected primary MDMs from 3 individuals; **D-F:** HIV-HSA-infected primary MDMs from 3 individuals.

A: Donor 1

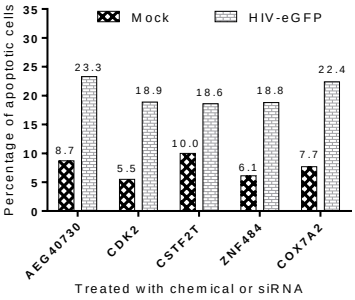

B: Donor 2

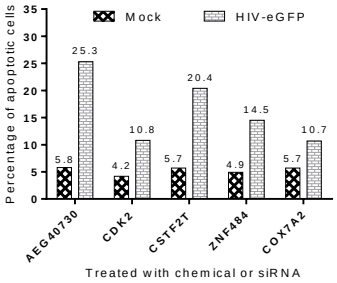

C: Donor 3

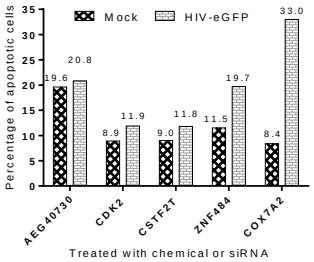

D: Donor 4

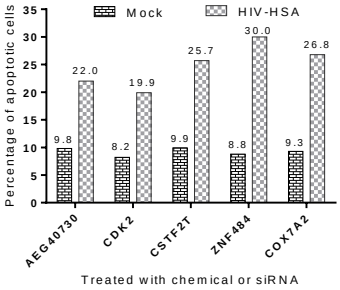

E: Donor 5

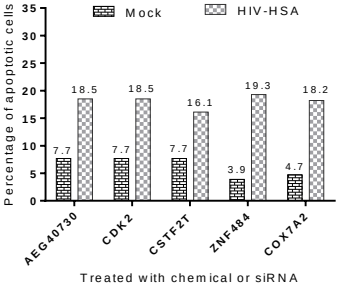

F: Donor 6

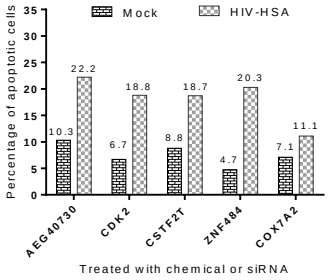

2.5 Pan-chemical inhibitors corresponding to *Cox7a2*, *Znf484*, *Cdk2* and *Cstf2t* selectively induced apoptosis of HIV-infected macrophages

To study if the identified genes can be therapeutically targeted to induce apoptosis of HIV-infected macrophages, through literature reviews, I found that sodium azide, azodicarbonamide, cordycepin, and inhibitor-II, which are commercially available, could be used to target the four identified genes, *Cox7a2*, *Znf484*, *Cstf2t*, and *Cdk2*, respectively. Unfortunately, all the commercially available chemical inhibitors targeting these genes are pan-inhibitors. The compound solutions were prepared as indicated in **Table 3**. Primary MDMs were infected with HIV-eGFP and HIV-HSA viruses for 7 days, then treated with chemicals for 24 hours before flow cytometry analysis. The gating strategy for HIV-eGFP and HIV-HSA-infected macrophages is shown in **Fig. 37A & 38A**. Representative histogram showing killing of intensely eGFP positive is shown in **Fig. 37B**. Quantification of Annexin-V-positive and HSA intensely positive MDMs show that similar to *Cox7a2*, *Znf484*, *Cstf2t* and *Cdk2* siRNAs, sodium azide, azodicarbonamide, inhibitor II and cordycepin, which inhibit COX7A2, ZNF484, CDK2, and CSTF2T, killed significantly high percentages of eGFP intensely positive MDMs (**Fig. 37C**) compared to the control HIV-eGFP-infected cells. Similar results were obtained for primary MDMs infected with HIV-HSA viruses and representative histogram showing killing of HSA intensely positive MDMs is shown in **Fig. 38B**. Sodium azide, azodicarbonamide, and inhibitor II also selectively induce apoptosis of HSA intensely positive primary MDMs **(Fig. 38C)**.

Table 3. Protocols to make inhibitor solutions for targeting the four identified genes

This table summarizes how the compound stock solutions were made and the working concentrations of the compound targeting the four identified genes.

Genes Targeted	Chemical Inhibitors	Working Concentration	Protocols to make stock solution
Cdk2	CDK2 inhibitor II (5 mg/ml in DMSO)	300 nM	1. For 10,000x: dissolve all in 0.843 ml DMSO. (MW:395.2; 1mg package) 2. Aliquot 10 µl and stored at -20°C. 3. For 100x, dilute 100x and aliquot into 50 µl before loading.
Cstf2t	Cordycepin (0.5 M in DMSO)	40 µg/ml 0.00016M	1. For 500x, all dissolved in 1.0 ml DMSO. (MW: 251.54; 10 mg package) 2. Aliquot 40 µl and stored at -20°C. 3. Dilute 5x for 100x working solution
Znf484	Azodicarbonamide (100 mM in DMSO)	1 mM	1. For 100x, weigh 11.6 mg. (MW: 116.08) 2. Dissolve in 1.0 ml DMSO. 3. Divide into 50 µl and store at -20 °C.
Cox7a2	Sodium Azide (1.0 M in H_20)	2 µl or 2 mM	1. For 100x, weigh 65mg. (MW: 65.01; 5g package) 2. Dissolve in 1.0 ml H_20. 3. Divide into 50 µl portions and store at -20°C.

Figure 37. Pan inhibitors of the four identified genes selectively induce apoptosis of HIV-eGFP-infected MDMs

A. Gating of eGFP intensely positive MDMs. **B.** Representative histograms and dot plots of apoptosis of eGFP intensely positive MDMs induced by CDK2 inhibitor II, Cordycepin (inhibitor of CSTF2T), Sodium Azide (inhibitors of respirasome complex IV, representing *Cox7a2*) and Azodicarbonamide (inhibitor of ZNF484) from one blood donor. **C.** Pan inhibitors selectively induce apoptosis of HIV-eGFP-infected MDMs (n=4). The p values were calculated using Student's t test.

A: Gating strategy for specific killing of eGFP+ cells induced by chemicals

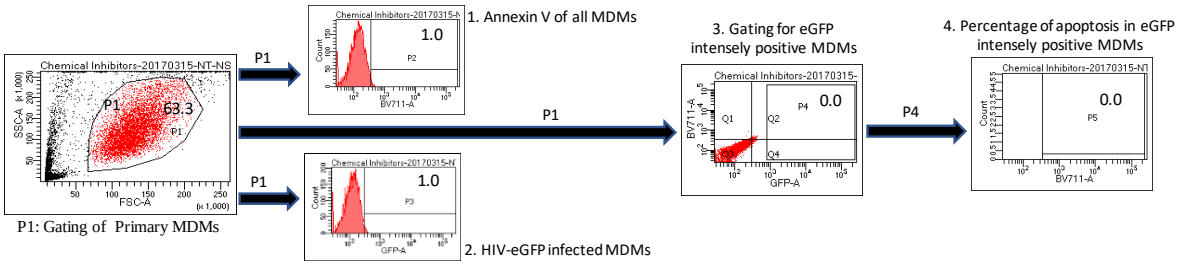

B: Representative histograms and dot plots for apoptosis induced by chemicals

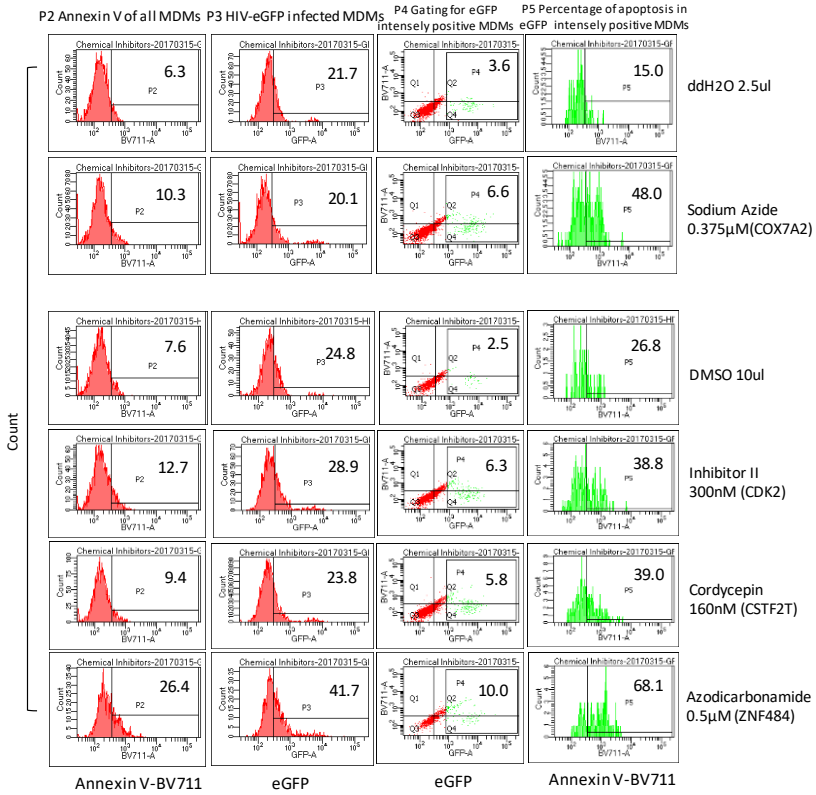

C: eGFP specific killing induced by chemicals

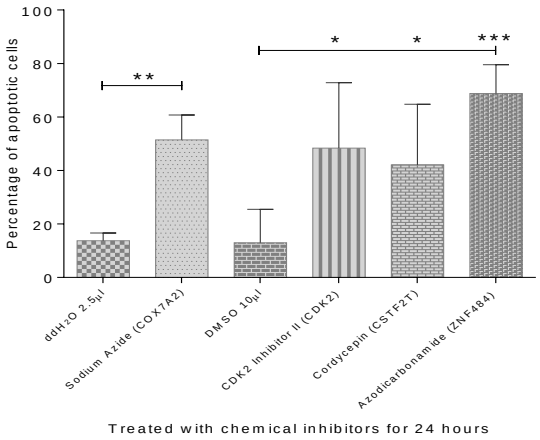

Figure 38. Pan inhibitors of the four identified genes selectively induce apoptosis of HIV-HSA-infected MDMs

A: gating of HSA intensely positive MDMs. **B.** Representative histograms and dot plots of apoptosis of HSA intensely positive MDMs induced by CDK2 inhibitor II, Cordycepin (inhibitor of CSTF2T), Sodium Azide (inhibitors of respirasome complex IV, representing *Cox7a2*) and Azodicarbonamide (inhibitor of ZNF484) from one blood donor. **C.** Pan inhibitors selectively induce apoptosis of HIV-HSA-infected MDMs (n=4). The p values were calculated using Student's t test.

A: Gating strategy for specific killing of HSA intensely positive cells

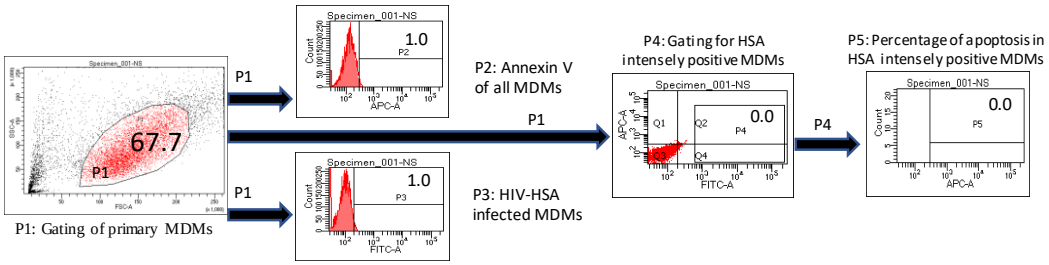

B: Representative histograms and dot plots for apoptosis induced by chemicals

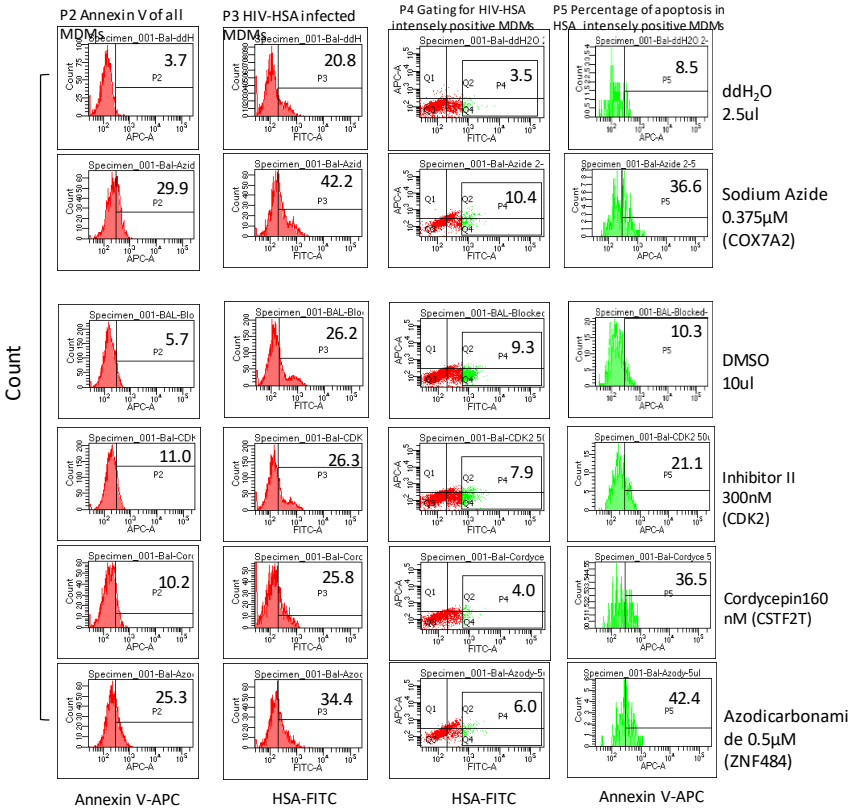

C: HSA Chemical Inhibitors Specificity

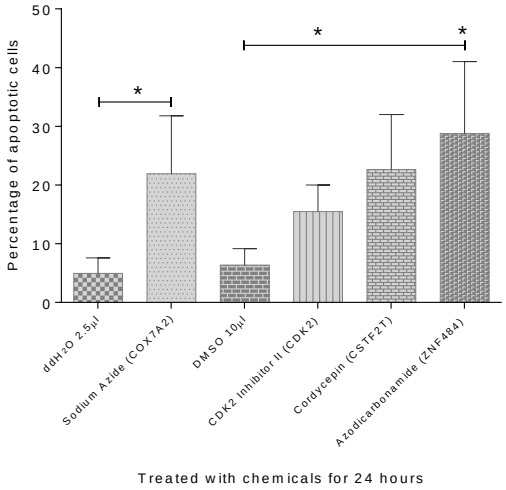

Subsequently, I determined if sodium azide, azodicarbonamide, cordycepin and inhibitor-II could induce apoptosis of HIV-exposed, uninfected bystander macrophages. MDMs were infected with HIV-eGFP and HIV-HSA for 7 days followed by treatment with sodium azide, azodicarbonamide, cordycepin and inhibitor-II for 24 hours. The apoptosis induced by chemical inhibitors was quantified by flow cytometer. The gating strategy for the quantification of apoptosis is the same as shown in **Fig. 35A and Fig. 34A**. Sodium azide, azodicarbonamide, cordycepin and inhibitor-II killed significantly high numbers of eGFP and HSA intensively positive (HIV-infected) cells compared to either the mock or HIV-exposed but uninfected bystander cells **(Fig. 39 A&B).** After treatment with the inhibitors, killing of eGFP- (HIV-eGFP-exposed but uninfected bystander) cells was significantly higher than the mock-infected cells **(Fig. 39A)**. However, killing of HSA- (HIV-HSA-exposed but uninfected bystander) cells was similar to the mock-infected cells except treated with sodium azide (**Fig. 39B**).

Overall, my results suggest that the chemical inhibitor of the four identified genes sodium azide, azodicarbonamide, cordycepin and CDK2 inhibitor-II can selectively induce the apoptosis of HIV-eGFP or HIV-HSA-infected macrophages. Treatment with these chemical inhibitors also induced the apoptosis of HIV-eGFP-exposed but uninfected bystander macrophages.

Figure 39. Pan inhibitors of the four identified genes induce apoptosis of HIV-exposed but uninfected bystander MDMs

A. Pan inhibitors of the four identified genes induce apoptosis of HIV-eGFP-exposed but uninfected bystander MDMs (n=4); the gating strategy is the same as **Figure 35**. **B.** Pan inhibitors of the four identified genes induce apoptosis of HIV-HSA exposed but uninfected bystander MDMs (n=4); the gating strategy is the same as **Figure 34**. The p values were calculated using Student's t test.

A: Apoptosis of HIV-eGFP-uninfected bystander cells induced by pan-inhibitors

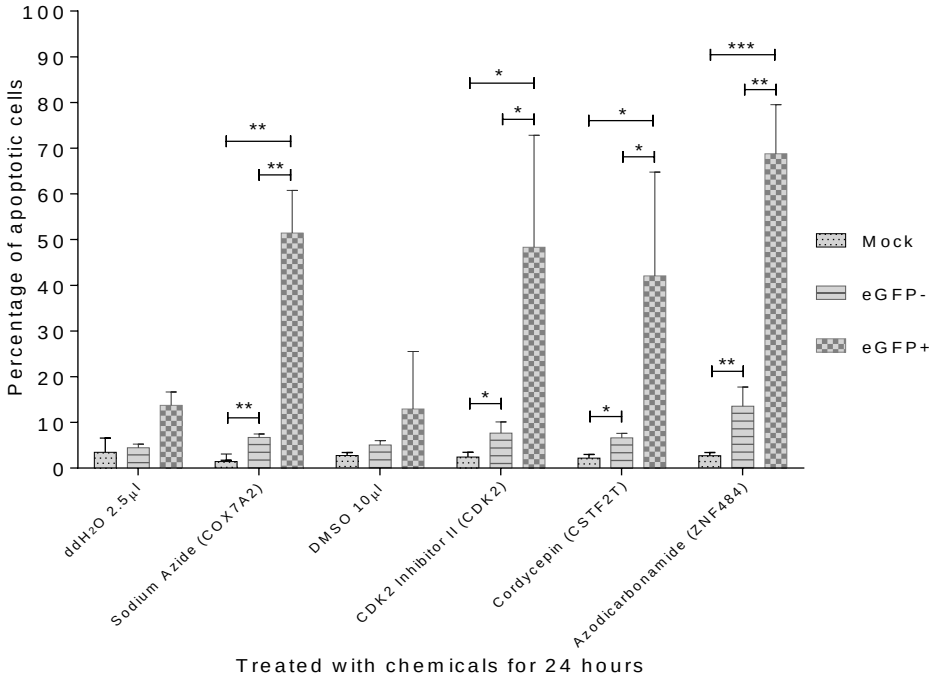

B: Apoptosis of HIV-HSA-uninfected bystander cells induced by pan-inhibitors

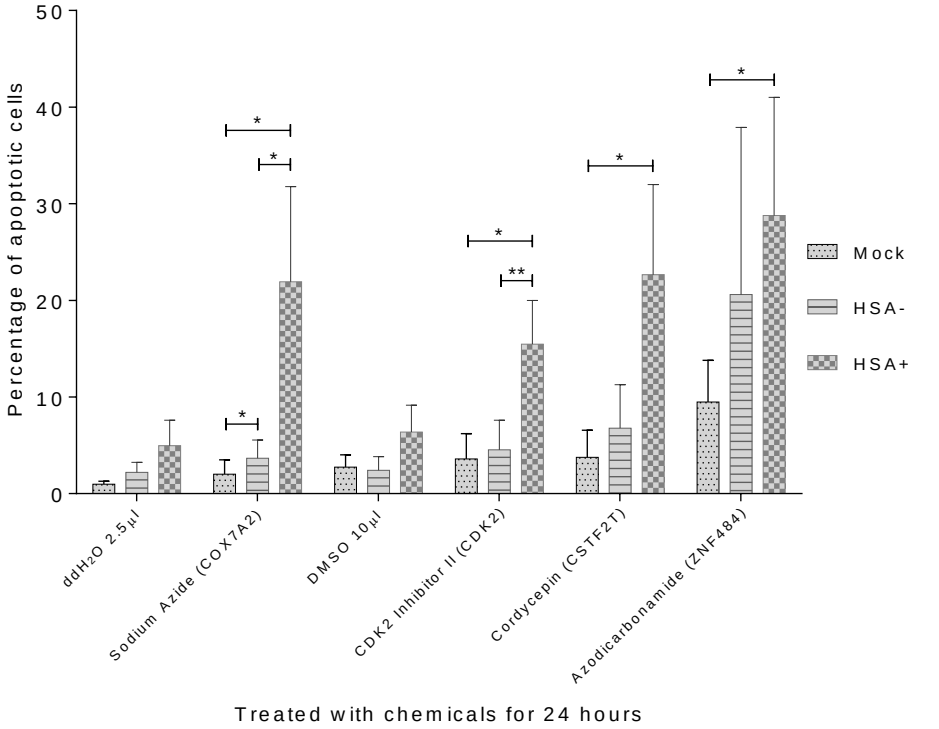

3. Discussion

Currently, the key problem in Anti-HIV therapy is HIV reservoir formation, and macrophages are one of three major cellular reservoirs. Thus, selective induction of apoptosis in HIV-infected macrophages is indispensable for a complete cure of this disease. Previous studies indicated that dysregulation of gene expression was essential for the survival of HIV-infected macrophages, making it possible to search for novel gene targets to remove macrophage-based HIV reservoirs. Herein by employing an unbiased, pooled shRNA-based screening strategy, 90k shRNA lentivirus pool technology, I identified 4 genes that could be targeted to selectively induce the apoptosis of HIV-infected macrophages.

When determining the parameters for the application of 90K lentivirus shRNA pool, I discovered several characteristics of myeloid lineage cells, which have rarely been reported in the literature. I found that for all myeloid lineage cells I tried, the longer time of differentiation, the more resistant to puromycin induced cell death they were. To keep the consistency and accuracy of the results, all our experiments were conducted punctually at the exact number of days as indicated. Moreover, the U1 cell line, which is HIV-1 infected U937 cell line, was found to be more resistant to puromycin-induced cell death than uninfected U937, supporting previous findings that HIV-1 infection made macrophages more resistant to apoptosis [417]. Furthermore, even though higher concentrations of PMA were used to differentiate U1 cells, many of them remained suspended in the supernatant, indicating the gene expression of adherent molecules might be dysregulated due to HIV infection. I suggest that all these characteristics should be taken into consideration in the studies related to macrophages.

In general, screening target genes is a long-term, laborious and costly process. In 90k shRNA lentivirus pool technology, siRNA and shRNA silencing were applied to knockdown a large number of genes simultaneously, making a fast, high-throughput, and cost-effective gene screening strategy viable. Although this technology was originally designed to screen target genes for cancer therapy, our study confirmed that it could also be customized to screen novel gene targets for selective induction of apoptosis in HIV-infected macrophages. Notably, macrophage is not the only HIV cellular reservoir and our research may also be repeated and customized to eradicate the other HIV cellular reservoirs. My results indicate that targeting multiple individual genes could selectively induce the apoptosis of HIV-infected macrophages. That may also arise in other HIV cellular reservoirs. It is likely that targeting some genes can selectively induce the apoptosis of all HIV cellular reservoirs, including memory T cells and astrocytes. Unequivocally, the application of this technology may uncover promising therapeutic targets for a complete cure of HIV infection and help to understand the mechanism of HIV reservoir formation. Significantly, the dysregulation of multiple genes arises not only after HIV infection, but also in many other diseases. Thus, the customization in this study may be repeated for a fast screening of novel gene targets to treat other diseases and provide new insights in understanding many human diseases.

On the other hand, macrophages are well-known to be hard-to-handle cells [418], causing many technical issues during the validation of promising genes in this study. This could be due to differences in individual donors, restriction factors, and multiple subsets of macrophages. For example, I found that the optimal time to analyze the apoptosis of HIV-infected primary MDMs induced by siRNA silencing varied

individually from 48 to 72 hours, causing the failure of many experiments if cells were not harvested at the appropriate time, which was unknown before flow cytometry analysis. Moreover, although CCR5-tropic HIV viruses were applied, the infection rate of primary MDMs was usually low (~20%). As a result, there was not much difference between mock and HIV-infected samples. Furthermore, I found that primary MDMs from many donors were not sensitive to siRNA transfection. Consequently, no result was obtained from many blood donors. Despite all these difficulties, the macrophages from many donors could still be transfected with siRNA for the validation purposes in this study. In addition, macrophages are known to be a cell type resistant to anti-retroviral treatments, primarily due to the compartmentalization of HIV-infected cells [419], or the altered cellular milieu after HIV-1 infection [420]. Consequently, herein when I was targeting the four identified genes of HIV-infected MDMs by chemical inhibitors, of all 12 blood donors I tested, the primary MDMs from only 4 individuals are sensitive to the chemical inhibitors we selected.

Although HAART efficiently reduces viral replication, it cannot eradicate viruses from the human body due to HIV reservoir formation [2], indicating the fight against HIV is not over and this battle might be a long-term campaign. This study shows that the eradication of HIV reservoir in macrophages is possible, but the best gene targets vary individually, reinforcing the complexity of HIV reservoir formation. Conceivably, gene expression varies from individual to individual, or even from cell to cell. Accordingly, once infected with HIV, the anti-HIV and survival mechanisms at the molecular level also vary from individual to individual, or even from cell to cell. As a result, the upregulation of a specific validated gene might be essential for the survival of HIV-infected macrophages from many individuals, but not all. Fortunately, my

results showed that we could have multiple “benched” gene targets, and I believe that, more and more genes, which can be targeted to selectively induce the apoptosis of HIV-infected macrophages, might be identified in the future. Silencing one of the validated genes could not specifically induce the apoptosis of HIV-infected macrophages from all the individuals, indicating that we may have to treat HIV-infected patients with individualized therapies.

In conclusion, 90k shRNA lentivirus pool technology is a powerful tool for a fast screen of target genes. Four genes, *Cox7a2*, *Znf484*, *Cdk2*, and *Cstf2t*, can be targeted to eradicate HIV reservoirs in macrophages. Interestingly, my results indicate that the best gene targets to induce the apoptosis of HIV-infected macrophages varied from individual to individual, indicating personalized treatment might be essential for a complete cure of HIV infections.

Chapter 6.4: The mechanism of targeting *Cox7a2* induced apoptosis of HIV-infected macrophages

1. Introduction

The results above indicate that *Cdk2*, *Cstf2t*, *Znf484* and *Cox7a2* are the four identified genes that can be targeted to selectively induce the apoptosis of HIV-infected macrophages. To understand the mechanisms of selective induction of apoptosis, herein I briefly reviewed the general information, biological functions, associated diseases, and relationship to HIV infection of the four genes.

CDK2 is the official designation for Cyclin-Dependent Kinase 2, which is a member of a family of serine/threonine protein kinases involved in cell cycle regulation [421]. The gene product of *Cdk2* is a 33kDa enzyme, a catalytic subunit of the cyclin-dependent protein kinase complex, which regulates progression through the cell cycle [422]. CDK2 protein is associated with and regulated by Cyclin A or E [423]. The function of CDK2 is especially critical for G1 to S phase transition. Molenaar et al discovered that CDK2 was a vital regulator of S phase progression. They found that siRNA silencing of CDK2 induced apoptosis of neuroblastoma cells, and suggested that this protein could be an anti-cancer target [424]. Shapiro also found that the signalling pathways of CDK2 could be targeted for cancer treatments [425]. Ammosova et al reported that CDK2/Cyclin E phosphorylates HIV-1 Tat *in vitro*, which is required to promote HIV-1 transcription and to activate integrated provirus [426]. Moreover, siRNA of *Cdk2* had no effect on cell cycle progression, but increased TNF-a induced apoptosis of OM10.1 cells (cloned from HL-60 promyelocyte cells that survived an acute HIV-1 infection) [427]. These observations suggest that CDK2 may serve as a therapeutic target for cancer and HIV infections [427]. The most commonly

used chemical inhibitor of CDK2 is CDK2 Inhibitor II, which is cell permeable, reversible and ATP-competitive [428,429].

CSTF2T, Cleavage Stimulation Factor subunit 2 tau variant, is a ~64kDa glycoprotein associated with internal oligo-adenylation and it directly binds to pre-mRNAs with its RNA Recognition Motif (RRM) [430]. Thus, it was identified to be one of 307 genes on the mRNA splicing major pathway and mRNA surveillance pathway [431]. CSTF2T binds to many RNAs, including histone RNAs, snoRNAs and snRNAs, resulting in shortened snRNA isoforms subject to rapid degradation [432]. Moreover, CSTF2T was found to control the splicing of RNAs, including ANK2, and play critical roles in tumorigenesis and cardiac function [432]. Aragaki performed a genome-wide screen to search for therapeutic targets, finding that siRNA silencing CSTF2 suppressed lung cancer cell growth, whereas exogenous expression of CSTF2 promoted growth and invasion of mammalian cells, suggesting this protein plays an important role in lung carcinogenesis and might be a prognostic biomarker in patients [433]. CSTF2 was also identified to be an HIV-1 Rev interacting protein by *in vitro* binding experiments involving cytosolic or nuclear extracts from Hela cells [434]. Cordycepin, a compound originated from Chinese Traditional Medicine, has been used to inhibit CSTF2T activity in many studies [435].

Znf484 gene encodes a 124.6kDa Zinc Finger protein 484, which is a sequence-specific DNA binding protein with transcription activity and may be involved in transcriptional regulation. Zinc finger proteins serve as zinc sensors to control activation domain function [436]. *Znf484* is a member of the Zinc Finger Family, which includes a large variety of proteins that exist widely in nature and are found in 3% of the genes of the human genome [437]. Accordingly, their functions are extraordinarily

diverse, including gene transcription, translation, mRNA trafficking, cytoskeleton organization, epithelial development, cell adhesion, protein folding, chromatin remodeling, and zinc ion sensing [438]. *Znf484* has also been identified as a cancer-associated gene and is involved in hepatic tumorigenesis [439]. Due to the diverse functions of zinc finger domains, inhibition of this motif may have drastic effects on a variety of viruses, including HIV [440], and zinc finger inhibitors are believed to be promising anti-HIV drugs when other therapies fail due to drug resistance or interruption of treatments [441]. Azodicarbonamide is one of the *Znf484* inhibitors, which inhibits HIV-1 replication by targeting the nucleocapsid protein [442,443].

COX7A2, Cytochrome C Oxidase Subunit 7A2, is a nuclear gene coded protein expressed in all tissues. Its molecular weight in muscle is 9kDa and in lung is 14kDa. The mitochondrial respiratory chain consists of five multi-subunit complexes named complex I, complex II, complex III, complex IV and complex V as presented in **Figure 40** [444]. *Cox7a2* is the terminal component of complex IV (cytochrome c oxidase), which catalyzes the electron transfer from reduced cytochrome c to oxygen [445]. Knockout of *Cox7a2* causes cytochrome c oxidase deficiency, resulting in the increase of ROS production [446]. Elsner's study found that *Cox7a2* expression could be used as a marker for monitoring cancer development, predicting regional lymph node metastasis, and disease outcome [447]. In 2001, Perez et al discovered that Motexafin Gadolinium (Gd-Tex), a compound that promotes intracellular oxidative stress, selectively induces apoptosis of HIV-1 infected CD4+ T cells in IL-2 stimulated cultures of PBMCs infected *in vitro* with HIV-1 [260], indicating targeting *Cox7a2*-induced apoptosis of HIV-infected macrophages may also be due to enhanced oxidative stress. Cyanide, azide, and carbon monoxide inhibit electron transfer in Complex IV [448]. Unfortunately, the reports on the relationship between HIV-1 infection and Cox7a2 are rare. Richard et al found that Cox7a2 is one of many genes most strongly affected after HIV-1 infection [449].

Figure 40. Structure and function of respiratory chain in mitochondrion

The respiratory chain in mitochondrion consists of five multi-subunit complexes named complex I, complex II, complex III, complex IV and complex V. Complex I is NADH/ubiquinone oxidoreductase; Complex II is succinate dehydrogenase; Complex III is cytochrome c reductase; Complex IV is cytochrome c oxidase; Complex V is the mitochondrial ATP synthase [450].

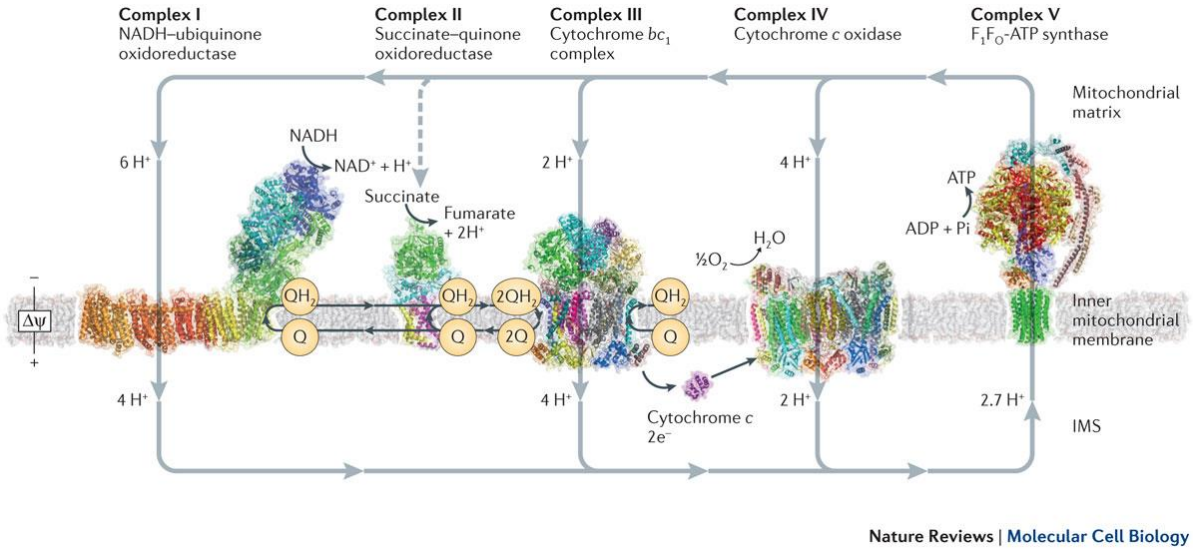

Sazanov LA. A giant molecular proton pump: structure and mechanism of respiratory complex I. Nat Rev Mol Cell Biol. 2015 Jun 20;16(6):375–88. Available from: http://dx.doi.org/10.1038/nrm3997 (Appendix 10.4).

Thus, each one of the validated gene is crucial for the survival of cells as summarized in **Table 4**. That may explain their involvement in apoptosis of HIV-infected macrophages due to siRNA silencing. Interestingly, all the four genes played important role in cancer development and might be targeted for cancer treatments. Notably, the results herein show for the first time that they can be targeted to selectively induce the apoptosis of HIV-infected macrophages. Subsequently, to understand the apoptosis of HIV-infected macrophages induced by targeting these genes, I focused on only one gene, *Cox7a2*, due to its significance in cell survival.

Further literature review was conducted, trying to understand the possible mechanisms of targeting *Cox7a2* induced apoptosis of HIV-infected macrophages. I found that both HIV infections and siRNA silencing of *Cox7a2* increases ROS production and the accumulated ROS products may account for the apoptosis of HIV-infected macrophages induced by targeting *Cox7a2*.

First, HIV infection increases ROS in infected macrophages. Ivanov reviewed numerous studies before 2016, finding that HIV infection triggered obvious oxidative stress in both *in vitro* and *in vivo* infections [451]. Elbim et al found enhanced ROS production in monocytes of HIV-infected individuals [452]. The possible mechanism of increased ROS might be because free radical defense was compromised by HIV infection. For example, in HIV-infected patients, Glutathione is depleted in plasma, lymphocytes, monocytes and lung epithelial lining [26–29], causing increased GSSG (glutathione disulfide) in plasma of HIV-positive patients [453,454]. Treitinger et al found that the levels of Superoxide Dismutase (SOD), an enzyme that helps to break down potentially harmful oxygen molecules in cells, preventing damages to tissues, is reduced in the plasma and monocytes of HIV-infected patients [455].

Table 4. Summary of literature review on the four identified genes

To study the mechanism of selective induction of apoptosis in HIV-infected macrophages, literatures were reviewed on the general information, biological functions, associated diseases, and relationship to HIV infection of these 4 genes, and the information was summarized into this table.

Gene Hits	Characteristics and Functions
Cdk2	Cyclin-dependent kinase 2: a 33kDa enzyme and a member of serine/ threonine protein kinase family. A catalytic subunit of the cyclin-dependent protein kinase complex, which is associated with and regulated by cyclin A or E, critical for G1 to S phase transition. Targeting this gene induced the apoptosis of neuroblastoma cells; the signalling pathways could be targeted for cancer treatments and it was believed to be a potential therapeutic target of HIV infections.
Cstf2t	Cleavage stimulation factor subunit 2 tau variant: an approximately 64kDa glycoprotein associated with internal oligo-adenylation and directly binds to pre-mRNAs with RNA recognition motif (RRM). The protein is on the mRNA splicing major pathway and mRNA surveillance pathway. Targeting this gene suppresses lung cancer cell growth, suggesting its important role in lung carcinogenesis. The gene product is an HIV-1 Rev interacting protein.
Znf484	Zinc Finger Protein 484: 124.6kDa; a member of the Zinc Finger Family, a sequence-specific DNA binding protein with transcription activity and may be involved in transcriptional regulation; a cancer-associated gene and involved in methylation during hepatic tumorigenesis; inhibition of zinc finger motif may have drastic effects on a variety of viruses, including HIV.
Cox7a2	Cytochrome c Oxidase Subunit 7A2: 9kDa in muscle and 14kDa in lung; a nuclear gene coded protein which is the terminal components of mitochondrial respirasome complex IV; catalyzes the electron transfer from reduced cytochrome c to oxygen; a marker for monitoring cancer development.

Second, knockout or silencing *Cox7a2* also significantly increases ROS level by interfering with the respiratory chain [446], resulting in apoptosis of HIV-infected macrophages. Numerous studies reported that ROS induced apoptosis under physiologic and pathologic conditions [456]. For example, Kasahara et al found that H_2O_2 induced both spontaneous and Fas-mediated apoptosis of neutrophils, which could be prevented by catalase [457]. A compound, Motexafin Gadolinium (Gd-Tex), which promotes intracellular oxidative stress, also selectively induces the apoptosis of HIV-infected CD4+ T cells [260].

Either HIV infection alone or targeting *Cox7a2* alone does not induce death in macrophages, suggesting that ROS production caused by HIV infection alone or by silencing *Cox7a2* alone is not enough to trigger apoptosis. However, silencing *Cox7a2* selectively induced the apoptosis of HIV-infected macrophages, and previous studies indicated that promoting intracellular oxidative stress (Gd-Tex) selectively induced the apoptosis of HIV-1 infected T cells [260]. Thus, I hypothesize that when ROS stress induced by HIV infection and siRNA silencing of *Cox7a2* reaches a threshold, the apoptotic program will be triggered to kill macrophages. This hypothesis is supported by the observation that anti-cancer agent 2-methoxyestradiol selectively induced apoptosis of cancer cells and improved photodynamic treatment effects, because it inhibits O_2^- eliminating enzyme SOD, leading to the accumulation of superoxide radical in cancer cells [458]. Therefore, targeting *Cox7a2* induced apoptosis of HIV-infected macrophages might be based on Superposition Mechanism as previously described [459]. Targeting *Cox7a2* induced apoptosis of HIV-infected macrophages also reflects the concept of “synthetic lethality”, which might be an important theoretical basis of selective killing of abnormal cells [284]: both HIV infection and

silencing *Cox7a2* are the two pre-conditions to kill cells. As a result, silencing *Cox7a2* selectively induced apoptosis of HIV-infected macrophages.

Based on this mechanism, I hypothesize that any factor that significantly enhances cellular ROS stress may selectively induce apoptosis of HIV-infected macrophages. Targeting any one of the respirasome complex may increase ROS production [460–463], thus possibly inducing apoptosis of HIV-infected macrophages. Hence, I studied if targeting any one of the respirasome complex could selectively induce apoptosis of HIV-infected macrophages. My results suggest that targeting complex II and IV is most likely to selectively induce apoptosis of HIV-infected MDMs. Moreover, I investigated if HIV-HSA infection or siRNA silencing respirasome complex II and IV enhanced ROS production in MDMs.

Note: all the experiments in this chapter were performed by Simon Xin Min Dong.

2. Results

2.1 Targeting respirasome complex II & IV selectively induces apoptosis of HIV-infected MDMs

To test the hypothesis on the mechanism of *Cox7a2* inhibition- induced apoptosis of HIV-infected macrophages, I first studied if targeting the subunit of each respirasome complex could induce apoptosis of HIV-infected macrophages. The existing literature indicates that targeting *NDUFA11* [464], *SDHA* [464], *UQCRQ* [465], *Cox7a2*, and *ATP5a1* [466] is most likely to interfere complex I, II, III, IV, and V, respectively. Thus, the siRNAs for these genes were selected to block the functions of these complexes. Results showed that targeting the subunit of Complex II and IV respectively was most likely to selectively induce apoptosis of both HIV-eGFP and HIV-HSA-infected MDMs. The apoptosis of total primary macrophages was shown in **Fig. 41A and 41B**, and the apoptosis of eGFP or HSA intensely positive macrophages was shown in **Fig. 42A and 42B**. I also studied if pan-chemical inhibitors of respirasome complexes I~V could selectively induced apoptosis of HIV-infected primary MDMs. The protocols for preparation of pan chemical inhibitors were listed in **Table 5.** My results indicated that pan-inhibitors that target complex II, III and IV were most like to selectively induce the apoptosis of HIV-infected macrophages. The apoptosis of total primary macrophages induced by chemical inhibitors was shown in **Fig. 41C**, and the apoptosis of eGFP or HSA intensely positive macrophages induced by chemical inhibitors was shown in **Fig. 42C**. Western blotting results indicated that siRNA successfully silenced the proteins I selected to interfere the functions of respirasome complex I-V **(Fig. 42D)**.

Table 5. Protocols to make compound solutions for targeting respirasome complexes

This table summarizes the protocol to make compound stock solutions and the working concentrations of the compounds used in this study to target the respirasome Complex I-V.

Gene	Inhibitors	Working Concentration	Protocols
Complex I inhibitor	**Rotenone (1mM in 99.9% ethanol) (Light sensitive)**	**10µM (100X) 10µl or 10µM**	**1. For 1000X, weigh 3.944mg; dissolve in 1 ml of ethanol, add 250 water to 800X; (MW: 394.4; 1g package) 2. Aliquot 37.5µl and store at -20 °C; 10x dilute by adding 270µl ethanol.**
Complex II inhibitor	**Carboxin (2mg/ml in 99.9% ethanol)**	**2µg/ml (1000X) 10µl or 2µg/ml**	**1. For 1000X, weigh 2mg; (MW: 235.3; 250mg package); dissolve in 1 ml of ethanol (99.9%). 2. Aliquots 30µl store at -20 °C; 10x dilute before use**
Complex III inhibitor	**Antimycin A 5mM in 99.9% ethanol**	**10µM (500X) 5µl or 5µM**	**1. For 1000X, weigh 2.7 in 1ml ethanol absolute (MW; 540; 25mg pack; hygroscopic). 2. Aliquot 60µl, store at -20 °C; 5x dilute before use.**
Complex IV Inhibitor	**Sodium Azide (1M in H_20)**	**10mM (100X) 2µl or 2mM**	**1. For 100X, weigh 65mg (MW: 65.01; 5g package) 2. Dissolve in 1 ml H20. 3. Divide into 50µl portions and store at -20 °C.**
Complex V inhibitor	**Oligomycin A 5mM in 99.9% ethanol**	**12.5µM (400X) 2µl or 10µM**	**1. For 1000X, dissolve ALL in 0.5 ml ethanol (MW: 791.06; 5mg package). 2. Aliquot 30µl and store at -20 °C; 10x dilute before use.**

Figure 41. Targeting respirasome complexes induced apoptosis of HIV-infected MDMs

The apoptosis of mock and HIV-infected cells treated with siRNA and chemical inhibitors was analyzed by flow cytometer. The percentages of apoptosis in HIV-infected cells were normalized with mock infections and then compared with that of nontargeting siRNA or Ethanol. **A.** siRNA of complex I-V treated HIV-eGFP-infected primary macrophages. **B.** siRNA of complex I-V treated HIV-HSA-infected primary macrophages. **C.** Pan-inhibitors of complex I-V treated HIV-eGFP-infected primary macrophages. The p values were calculated using Student t test (n=4). **D.** Western Blotting of siRNA silencing respirasome complex I-V.

A: HIV-eGFP + siRNA (Total)

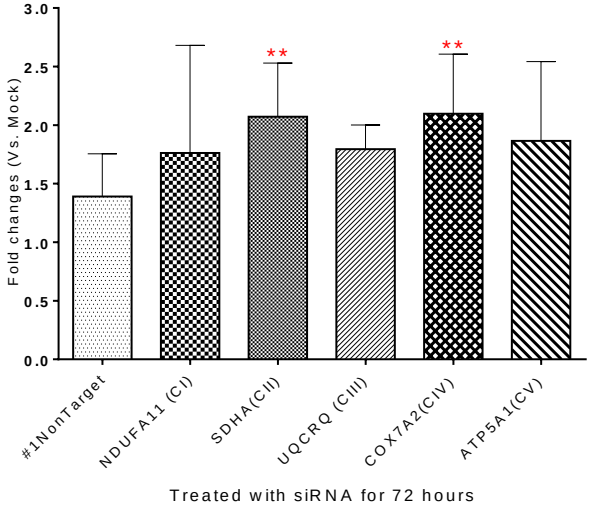

B: HIV-HSA + siRNA (Total)

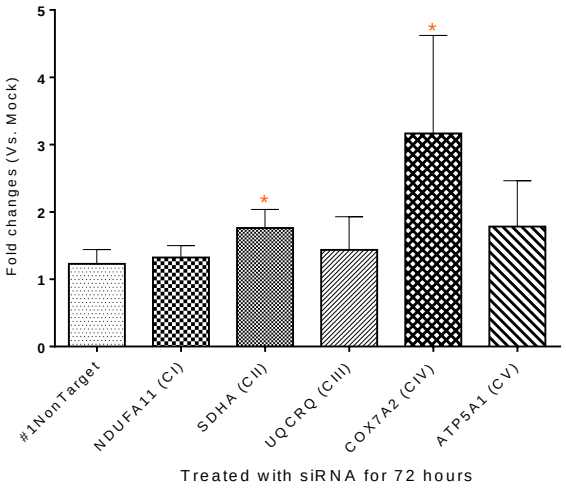

C: HIV-eGFP + Pan-Inhibitors (Total)

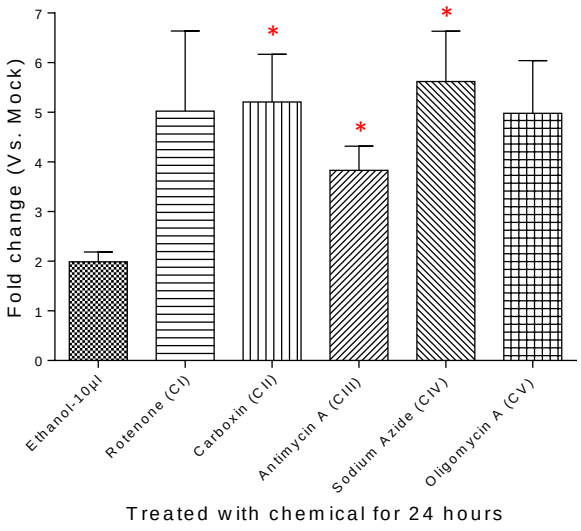

D: siRNA silencing of complex genes

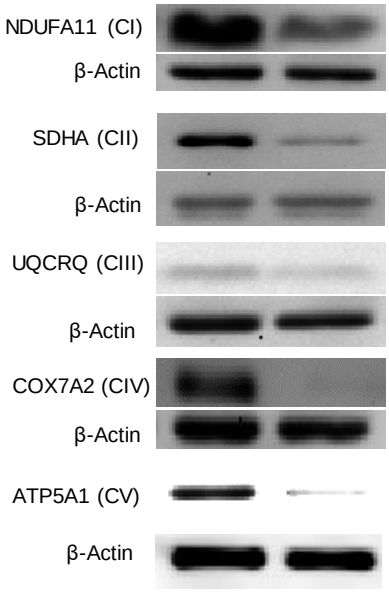

Figure 42. Targeting Complex II & IV selectively induced apoptosis of HIV-infected MDMs

The apoptosis of mock and HIV-infected cells treated with siRNA and chemical inhibitors was analyzed by flow cytometer. The percentages of eGFP+ or HSA+ cells were compared with that of nontargeting siRNA or Ethanol/ddH2O. **A.** siRNA of complex I-V treated HIV-eGFP-infected primary macrophages. **B.** siRNA of complex I-V treated HIV-HSA-infected primary macrophages. **C.** Pan-inhibitors of complex I-V treated HIV-eGFP-infected primary macrophages. P values were calculated using Student t test (n=4).

A: HIV-eGFP + siRNA (specificity)

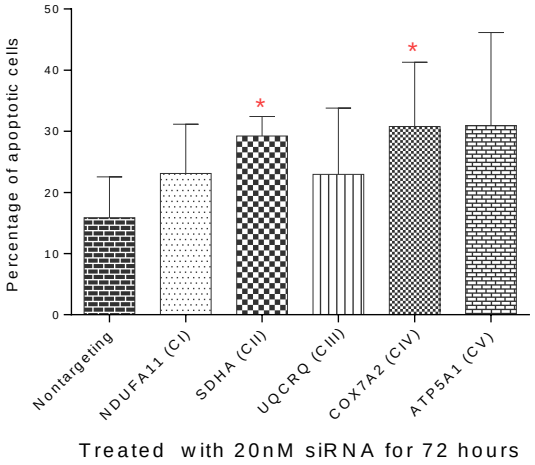

Treated with 20nM siRNA for 72 hours

B: HIV-HSA + siRNA (specificity)

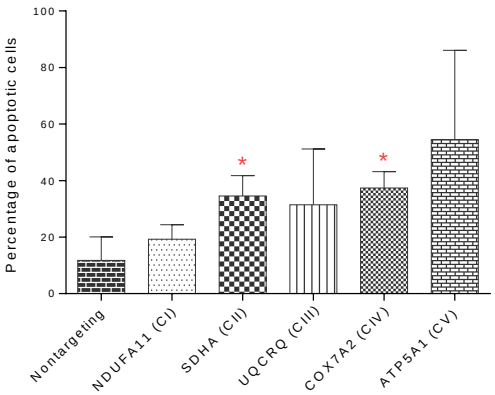

Treated with 20nM siRNA for 72 hours

C: HIV-eGFP + chemical inhibitors (specificity)

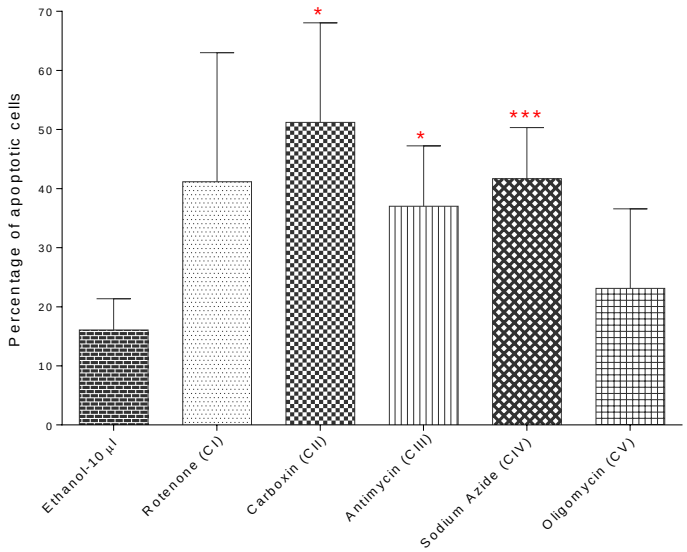

Treated with chemicals for 24 hours

2.2 HIV infection and targeting respirasome complex II & IV enhance ROS production in MDMs

Subsequently, it was confirmed whether HIV-HSA infection and interference with respirasome complex II and IV enhanced ROS production in macrophages. Primary human MDMs were infected with HIV-HSA for 9 days or treated with siRNA of *SDHA* (complex II) and *Cox7a2* (complex IV) for 48 hours, and then stained with CellROX® and/or mouse CD24 antibody. Cells were analyzed with flow cytometry. Results showed that both HIV-HSA infection and siRNA silencing of *SDHA* (complex II) and *Cox7a2* (complex IV) significantly enhanced ROS production in macrophages (**Figure 43A & 43B**). Attempts were also made to detect ROS production in HIV-infected macrophages treated with siRNA of *SDHA* (complex II) or *Cox7a2* (complex IV). However, targeting *SDHA* (complex II) or *Cox7a2* (complex IV) induced apoptosis of HIV-infected macrophages and the apoptotic cells turned into debris, resulting in direct removal of most of the HIV-infected macrophages from samples during the staining process, especially during the 3 washes/centrifugations steps. Therefore, interfering with complex II and IV-induced ROS production in HIV-infected macrophages was undetectable.

In summary, my results suggest that both HIV-HSA infection and interfering with respirasome complexes II and IV enhanced the ROS production in macrophages. Taking in account that both Gd-Tex [260] and ROS stress selectively induced apoptosis [456]in HIV-infected macrophages, I have elucidated that the mechanism of targeting *Cox7a2* induced apoptosis of HIV-infected macrophages is due to the superposition of ROS production induced by HIV-HSA infection and targeting *Cox7a2* as described in **Figure 44**.

Figure 43. HIV infection or silencing respirasome complex II and IV increases ROS stress of MDMs

Seven-day-old primary MDMs were infected with HIV-HSA for 9 days, or primary MDMs were infected with mock virus for 7 days and then treated with siRNA for 2 days. Then MDMs were harvested and stained for the detection of ROS production by flow cytometry on APC channel. **A:** ROS production induced by HIV-HSA infection. The p values were calculated using Student t test (n=4). **B:** ROS production induced by siRNA silencing of *SDHA* (complex II) and *Cox7a2* (complex IV) The p values were calculated using Student t test (n=8).

A: HIV-HSA infection increases ROS stress

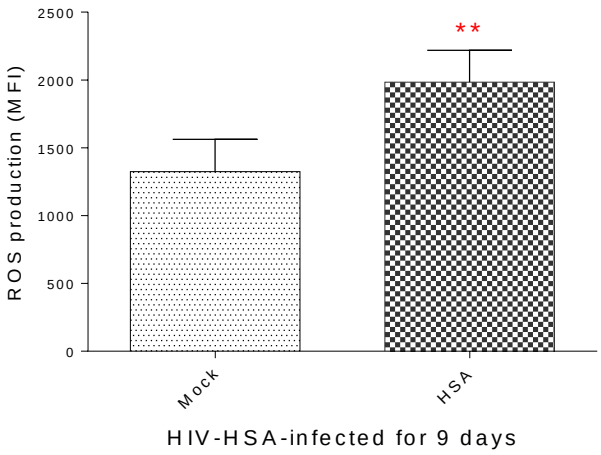

B: siRNA of Complex II & IV increases ROS stress

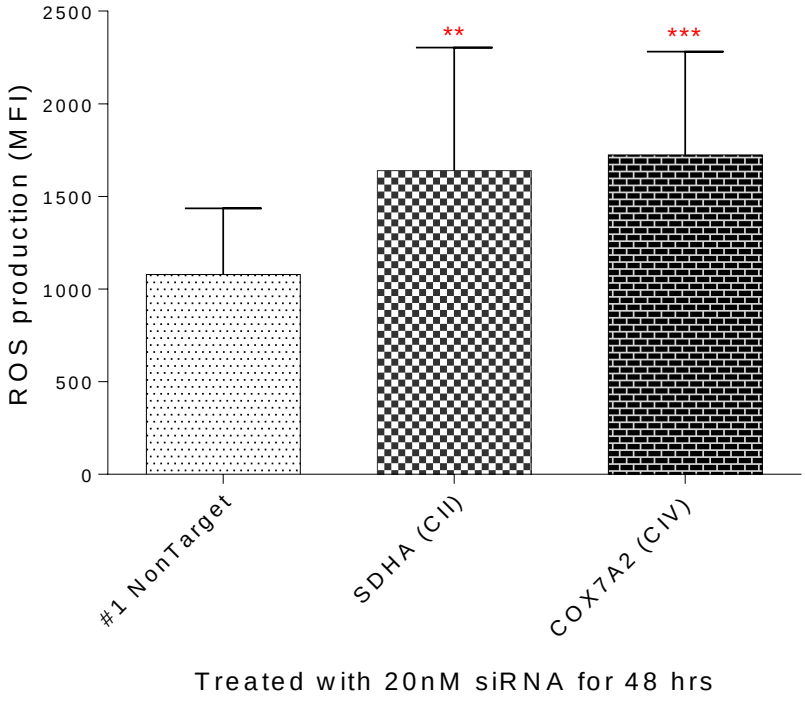

Figure 44. Mechanism of targeting COX7A2 induced apoptosis of HIV-infected MDMs

Superposition mechanism explains the targeting *Cox7a2* induced apoptosis of HIV-infected macrophages. Only when the ROS production reaches the threshold (dash line), do the cells undergo apoptosis. Without HIV infection and without *Cox7a2* knockdown, the ROS induced by the cells themselves cannot induce apoptosis. HIV infection induced ROS production, but infection alone cannot reach the threshold; therefore, the cell survives. Targeting *Cox7a2* alone induces ROS production, but cannot reach the threshold; therefore, the cell survives. When targeting *Cox7a2* in HIV-infected macrophages, the superposition of ROS production induced by both the HIV infection and *Cox7a2* inhibition reaches the threshold; therefore, macrophages undergo apoptosis.

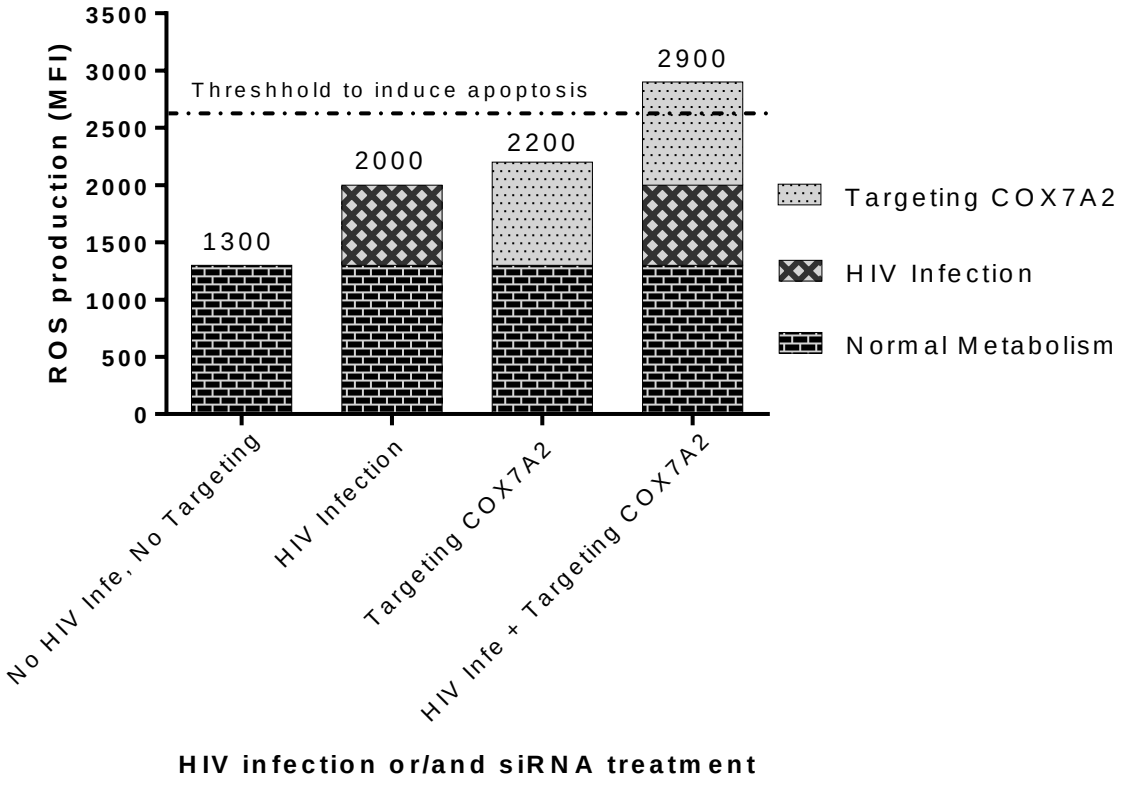
3500
3000
2500
2000
1500
1000
500
0
ROS production (MFI)
Threshhold to induce apoptosis
1300
2000
2200
2900
Targeting COX7A2
HIV Infection
Normal Metabolism
No HIV Infe, No Targeting
HIV Infection
Targeting COX7A2
HIV Infe + Targeting COX7A2
HIV infection or/and siRNA treatment

3. Discussion

This study identified that targeting four genes, *Cox7a2*, *Znf484*, *Cdk2*, and *Cstf2t* could selectively induce the apoptosis of HIV-infected macrophages. Existing data suggests that all these genes play crucial roles in the survival of host cells. During this study, I observed that targeting these genes killed HIV-infected, but not mock-infected macrophages, indicating they might be therapeutically targeted to eradicate HIV-infected macrophages from HIV-infected patients.

Interestingly, our literature review found that all 4 validated genes are associated with cancer development, and the compounds targeting these genes are anti-cancer drugs and may selectively induce the apoptosis of HIV-infected macrophages. Numerous previous studies also support this observation. For example, Sadaie et al discovered that many anticancer drugs had potential to inhibit HIV replication, and thus exhibited therapeutic effects in patients [467]. Clinical doctors also reported that anti-cancer drugs may be used to eradicate HIV reservoirs in HIV-infected patients [468]. Accordingly, Chow et al found that HIV protease inhibitors also had anti-cancer effects, and they believed that other anti-HIV drugs could also be used as anti-cancer drugs [469]. All the information indicates that the pathogeneses of cancer and AIDS are correlated although the mechanisms remain unclear.

This study also discovered the mechanisms of targeting *Cox7a2* and *Znf484* induced apoptosis of HIV-infected macrophages. My results indicate that targeting respirasome complex II also causes apoptotic effects similar to targeting COX7A2, and if we take the Gd-Tex-induced apoptosis of HIV-infected cells and other previous studies [260] into consideration, I confirmed that the factors, which effectively enhanced intracellular ROS production, could selectively induce the apoptosis of HIV-

infected macrophages, and targeting respirasome complex induced apoptosis of HIV-infected cells were due to the Superposition Mechanism [459] (**Figure 44**). In addition, similar to *IAPs*, HIV infection upregulates the gene expression of *Znf484*, which might be essential for the survival of HIV-infected macrophages. Thus, targeting *Znf484* also selectively induced the apoptosis of HIV-infected macrophages (**Figure 45**). The mechanisms of apoptosis induced by targeting *Cdk2* and *Znf484* need further studies.

This study has presented two ways to selectively induce the apoptosis of HIV-infected macrophages: 1) *Znf484* and *IAPs* represent a class of target genes, whose upregulations are essential to the survival of infected cells. Thus, targeting this class of genes selectively induces the apoptosis of HIV-infected macrophages; 2) *Cox7a2,* although HIV infection does not upregulate its gene expression, represents a class of target genes where the total damage due to HIV infection and gene silencing exceeds the limits that the cell can tolerate. Therefore, targeting this class of genes also selectively induces apoptosis of HIV-infected macrophages by superposition mechanism as previously described [459]. Targeting *Cox7a2*-induced apoptosis also confirmed that “Synthetic Lethality (only when two factors work simultaneously, cell death can be induced)” [284] may represent an important concept for the eradication of HIV reservoirs. Further studies on the mechanisms of apoptosis induced by the other two validated genes, *Cdk2* and *Cstf2t*, may discover other ways to selectively induce the apoptosis of HIV-infected macrophages.

In summary, herein I discovered that targeting *Cox7a2* induced apoptosis of HIV-infected macrophages is based on superposition mechanism, and any other factor capable of increasing intracellular ROS levels may selectively induce the apoptosis of HIV-infected macrophages.

Figure 45. Mechanism of targeting IAPs & ZNF484 induced apoptosis of HIV-infected MDMs

A: The upregulation of *IAPs* or *Znf484* is essential for the survival of HIV-infected macrophages. **B:** Targeting *IAPs* or *Znf484* induces the apoptosis of HIV-infected macrophages.

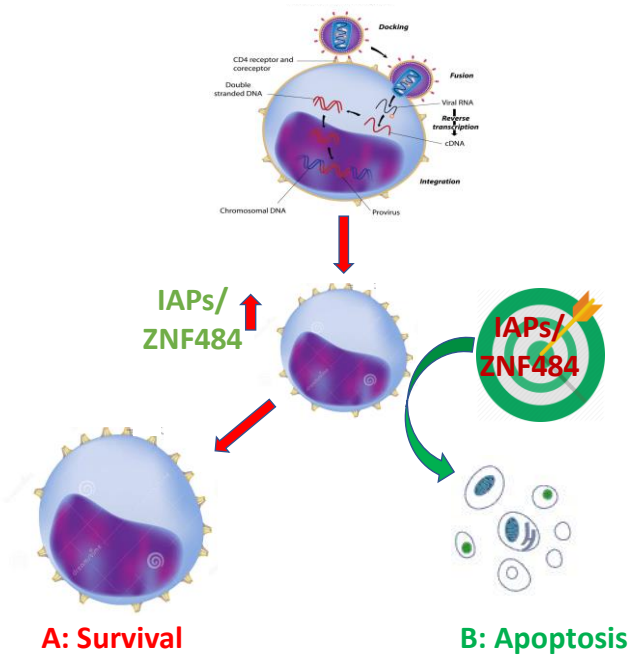
Docking
CD4 receptor and coreceptor
Fusion
Double stranded DNA
Viral RNA
Reverse transcription
cDNA
Integration
Chromosomal DNA
Provirus
IAPs/
ZNF484
IAPs/
ZNF484
A: Survival
B: Apoptosis

7. Concluding Remarks and Future Directions

Studies on the topic of selective induction of apoptosis in HIV-infected macrophages were rare. My results suggest that the eradication of HIV reservoir in macrophages is possible by targeting host genes. I believe that further study on the apoptosis of HIV-infected macrophages induced by targeting IAPs and all the 4 validated genes, will help to understand HIV reservoir formation and propose promising therapeutic targets for a cure of HIV infections.

7.1 Questions raised by this study for anti-HIV research

To reach the goal of this study, I first proposed a fast, easy-to-do, and cost-saving method for the selection of optimal transfection reagents for primary human macrophages. Other labs may customize our protocol to meet the facilities available to them or optimize the procedure to make it easier and more convenient under their circumstances for many other adherent cells. After all, IncuCyte® is very costly and may not be available to every lab. In this study, I selected the optimal transfection reagents for macrophages by *Bax* siRNA. I propose that, many other genes, such as eGFP, or many other genes which is easy for function test data analysis, can be employed for the selection of optimal siRNA transfection reagent.

I showed that both SMAC Mimetics AEG40730 and *IAPs* siRNA could selectively induce the apoptosis of HIV-infected macrophages. Therefore, SMAC Mimetics AEG40730 and *IAPs* siRNA were set as positive controls for the validation of promising target genes. I believe that targeting *IAPs* is a good research model to study specific killing of HIV-infected macrophages, although each gene may exert its own action to eradicate HIV reservoirs in macrophages. Moreover, targeting *Cox7a2* induced specific killing of HIV-infected macrophages due to the superposition of ROS

production caused by HIV-infection and interfering with the function of COX7A2. Our western blotting results suggest that the expression level of *Znf484* in normal macrophages is usually low, but HIV infection upregulates its expression for the survival of infected macrophages; as a result, targeting *Znf484* selectively induced the apoptosis of HIV-infected macrophages. However, how HIV infection upregulates the expression of *Znf484* has never been reported. In addition, the possible mechanisms of targeting *Cdk2* and *Cstf2t* induced apoptosis of HIV-infected macrophages also need further studies. Elucidating the signaling pathway of the apoptosis in HIV-infected macrophages induced by silencing these genes will help to understand the mechanism of HIV reservoir formation and the pathogenesis of AIDS, which are essential to find a complete cure for HIV infections.

The results of these studies raised many other questions as well. For example, whether targeting these genes affects HIV replication will help to understand HIV infections, and whether targeting these genes could selectively induce the apoptosis of HIV-infected memory T cells and astrocytes is also an interesting topic. In addition, there might be many other genes that can be targeted to selectively induce the apoptosis of HIV-infected macrophages. Another interesting topic is whether we can customize 90k shRNA lentivirus pool technology for a genome-wide screen of novel gene targets to selectively induce the apoptosis of other HIV reservoirs, such as memory T cells and astrocytes. It is possible that targeting one gene or a couple of genes could eradicate all 3 major cellular reservoirs. Furthermore, the apoptosis of uninfected bystander CD4+ Tells was believed to be the primary cause of immunodeficiency [77]; in this study, the apoptosis of uninfected bystander macrophages was also frequently observed. The impacts of the apoptosis of

uninfected bystander macrophages and the mechanisms behind this phenomenon need further studies.

7.2 Establishing a target gene pool for individualized therapy

Unequivocally, AIDS caused by HIV infection is one of the major medical issues of our time, and currently there is no complete cure for this disease. Previous studies have discovered that HIV infection substantially alters the gene expressions of host cells [206,208,257,470], and the dysregulations of some genes were crucial to the survival of infected cells [152,156]. Centering on this finding, I launched this study to search for novel gene targets for the eradication of HIV-infected macrophages.

Indeed, my results confirmed that HIV infection caused extensive biological effects, and we can use this to our advantage for the eradication of the HIV reservoir in macrophages. After the application of 90k shRNA lentivirus pool technology, our micro-array results suggested that thousands of host genes were upregulated (data not shown) after HIV infection. However, my validation study found that not all genes could be targeted to selectively induce the apoptosis of HIV-infected macrophages, indicating the upregulated genes could be categorized into two groups. One group is crucial for the survival of HIV-infected macrophages and targeting these genes will cause the death of infected cells. Another group is responsively upregulated due to infection or the dysregulation of other genes and targeting these genes cannot kill infected cells. *IAPs* and *ZNF484*, which was identified in this study, belong to the first group, and there might be many other genes that could also be targeted to selectively induce the cell death of HIV-infected macrophages but were not studied due to fundamental differences between individual donors or technical limitations. For example, targeting the 12 candidate genes resulting from HIV-eGFP virus-based

validation could selectively induce the apoptosis of HIV-infected macrophages in some, but not all individuals. As a result, they were not validated as target genes due to individual variation but targeting these genes might be specifically effective in some individuals. In addition, my results indicate that a validated gene could not specifically induce the apoptosis of HIV-infected macrophages from all individuals, and the macrophages from a randomly selected individual were only sensitive to certain specific genes. After all, the sample size from a single lab is quite limited and all the individuals studied herein were from a local population. If this study was repeated by other labs, more novel gene targets might be identified for Anti-HIV treatments. In that case, the establishment of a target gene pool, which covers all the effective targets to remove the HIV reservoirs in HIV-infected patients, might be an efficient way for a complete cure of this disease. For a specific HIV-infected patient, we may have to target the genes to which this individual is sensitive for effective eradication of HIV reservoirs. In that case, individual variations determined that individualized treatments [471] might be the way towards a complete cure of HIV infections.

7.3 Multigene regulation might be essential for a complete cure

This study confirmed that targeting the four identified genes could selectively induce the apoptosis of HIV-infected macrophages, and it is possible to remove HIV reservoirs in macrophages from HIV-infected patients. Undoubtedly, we are moving forward in the search for novel cure of HIV infections. However, existing data indicates that any one of the validated genes is crucial for the survival of not only HIV-infected macrophages, but also other types of cells in the human body. Consequently, similar to IAPs [276,277], targeting any one of these 4 genes may cause serious side-effects

to patients as well. The existing literature indicates multigene regulations might be the future direction for a complete cure without side-effects.

As mentioned above, HIV infections cause extensive biological effects in host cells, one of which is ROS stress. Yan et al induced ROS stress in cultured retinal neurons by low concentration H_2O_2, and studied the protective effects of a specific reagent, XY99-5038, which has been proven to have no side effects [472]. They found that XY99-5038 protected cultured retinal neurons from cell death induced by H_2O_2. Their microarray results suggested that, to protect cultured retinal neurons from the stress caused by H_2O_2, of all 1176 genes they evaluated, the expression of 72 genes were upregulated, and 77 genes were downregulated [473]. The damage caused by HIV infection is much more complex than ROS stress induced by H_2O_2; conceivably, to provide a complete cure of HIV infections, it is indispensable to upregulate or downregulate many more host genes. Yan's clinical observations and ongoing studies also found that patients with cancer can be cured without noticeable side effects, and that is also based on multigene regulations. For example, to induce the apoptosis of small-cell lung cancer cells, they identified that 39 genes were "hyper-variable genes" [474]. In fact, multigene regulation is a natural mechanism to protect human body from viral invasion. Another example is IFNs, which activate extremely powerful antiviral responses to control a great varieties of viral infections in the absence of adaptive immunity [196,475]. The protective effects of IFNs were demonstrated to be due to the intercellular signaling cascades, which upregulate and downregulate hundreds of genes simultaneously [196,475].

All above studies indicate that multigene regulation might be the future direction of Anti-HIV therapy. Although currently multigene regulation is rare, I believe that, as

science and medicine advance, the science community will overcome all the technical difficulties of multigene regulations and provide a novel cure without side-effects in the future.

7.4 Conclusions

This study provides novel gene targets and mechanistic insights of HIV infections. I concluded that 1) of many current commercially available reagents, DharmaFect 3 from Dharmacon is one of the optimal siRNA transfection reagents for primary human macrophages; 2) targeting *IAPs* either by SMAC Mimetics or *IAPs* siRNA could selectively induce the apoptosis of HIV-infected macrophages; 3) 90k shRNA lentivirus pool is a powerful tool for a fast, cost saving, and genome-wide screening of target genes; 4) four genes, *Cox7a2*, *Znf484*, *Cdk2*, and *Cstf2t* can be targeted to selectively induce the apoptosis of HIV-infected macrophages; 5) targeting these genes also induced the apoptosis of uninfected bystander macrophages; 6) the best gene targets to eradicate HIV reservoir in macrophages vary individually; 7) siRNA silencing of *Cox7a2* induced apoptosis of HIV-infected macrophages due to the superposition of ROS stress caused by HIV infection and silencing *Cox7a2*; 8) targeting respirasome complex II also selectively induced the apoptosis of HIV-infected macrophages; 9) HIV-infection upregulates the expression of *IAPs* and *Znf484* for the survival of infected macrophages from many individuals; therefore, targeting this gene could selectively induce the apoptosis of HIV-infected macrophages. Our further analysis based on this research suggests that the establishment of a target gene pool for individualized therapy and multigene regulation might be the future direction for a complete cure of HIV infections.

8. References

[1] Centers for Disease Control (CDC), Pneumocystis Pneumonia in Los Angeles, MMWR Wkly. Rep. 30 (1981) 250–2. https://stacks.cdc.gov/view/cdc/50022.

[2] F.P. Siegal, C. Lopez, G.S. Hammer, A.E. Brown, S.J. Kornfeld, J. Gold, J. Hassett, S.Z. Hirschman, C. Cunningham-Rundles, B.R. Adelsberg, D.M. Parham, M. Siegal, S. Cunningham-Rundles, D. Armstrong, Severe Acquired Immunodeficiency in Male Homosexuals, Manifested by Chronic Perianal Ulcerative Herpes Simplex Lesions, N. Engl. J. Med. 305 (1981) 1439–1444. https://doi.org/10.1056/NEJM198112103052403.

[3] H. Masur, M.A. Michelis, J.B. Greene, I. Onorato, R.A. Vande Stouwe, R.S. Holzman, G. Wormser, L. Brettman, M. Lange, H.W. Murray, S. Cunningham-Rundles, An Outbreak of Community-Acquired Pneumocystis carinii Pneumonia, N. Engl. J. Med. 305 (1981) 1431–1438. https://doi.org/10.1056/NEJM198112103052402.

[4] Centers for Disease Control (CDC), Current trends update on Acquired Immune Deficiency Syndrome (AIDS) – United States, Mmwr Morb Mortal Wkly Rep. 31 (1982) 507–8, 513–4.

[5] A.A. Okoye, L.J. Picker, CD4 + T-cell depletion in HIV infection: mechanisms of immunological failure, Immunol. Rev. 254 (2013) 54–64. https://doi.org/10.1111/imr.12066.

[6] F. Barre-Sinoussi, J. Chermann, F. Rey, M. Nugeyre, S. Chamaret, J. Gruest, C. Dauguet, C. Axler-Blin, F. Vezinet-Brun, C. Rouzioux, W. Rozenbaum, L. Montagnier, Isolation of a T-lymphotropic retrovirus from a patient at risk for acquired immune deficiency syndrome (AIDS), Science (80-.). 220 (1983) 868–871. https://doi.org/10.1126/science.6189183.

[7] R. Gallo, P. Sarin, E. Gelmann, M. Robert-Guroff, E. Richardson, V. Kalyanaraman, D. Mann, G. Sidhu, R. Stahl, S. Zolla-Pazner, J. Leibowitch, M. Popovic, Isolation of human T-cell leukemia virus in acquired immune deficiency syndrome (AIDS), Science (80-.). 220 (1983) 865–867. https://doi.org/10.1126/science.6601823.

[8] A.H. JOHN COFFIN, N. JAY A. LEVY, Luc MONTAGNIER, STEVEN OROSZLAN, et al TEICH, What to call the AIDS virus?, Nature. 321 (1986) 10–10. https://doi.org/10.1038/321010a0.

[9] Social Security, Disability Insurance., U . S . Federal Funding for HIV / AIDS : Trends Over Time, 2017.

[10] J.R. Minor, M.A. Hamburg, The AIDS Research Agenda at the National Institutes of Health, 2019. https://doi.org/10.1093/ajhp/48.12.2662.

[11] T.A. Schwetz, A.S. Fauci, The Extended Impact of Human Immunodeficiency Virus/AIDS Research, J. Infect. Dis. 219 (2018) 6–9. https://doi.org/10.1093/infdis/jiy441.

[12] Y. Li, H. Hui, B.H. Hahn, G.M. Shaw, C.J. Burgess, P.M. Sharp, R.W. Price, Complete nucleotide sequence, genome organization, and biological properties of human immunodeficiency virus type 1 in vivo: Evidence for limited defectiveness and complementation, J. Virol. 66 (1992) 6587–6600.

[13] K.J. Metzner, HIV Whole-Genome Sequencing Now: Answering Still-Open Questions, J. Clin. Microbiol. 54 (2016) 834–835.

https://doi.org/10.1128/JCM.03265-15.
[14] J.P.S. Manuel A. Navia, Paula M. D. Fitzgerald, Brian M. McKeever, Chih-Tai Leu, Jill C. Heimbach, Wayne K. Herber, Irving S. Sigal, Paul L. Darke, Three-dimensional structure of aspartyl protease from human immunodeficiency virus HIV-1, Nature. 337 (1989) 615–620. https://doi.org/10.1016/S0140-6736(14)60384-6.
[15] DHHS Panel on Antiretroviral Guidelines for Adults and Adolescents, Guidelines for the Use of Antiretroviral Agents in Adults and Adolescents Living with HIV, 2018. https://aidsinfo.nih.gov/contentfiles/lvguidelines/adultandadolescentgl.pdf.
[16] V. Dahl, L. Josefsson, S. Palmer, HIV reservoirs, latency, and reactivation: prospects for eradication., Antiviral Res. 85 (2010) 286–94. https://doi.org/10.1016/j.antiviral.2009.09.016.
[17] S.R. Lewin, S.G. Deeks, F. Barré-Sinoussi, Towards a cure for HIV--are we making progress?, Lancet (London, England). 384 (2014) 209–11. https://doi.org/10.1016/S0140-6736(14)61181-8.
[18] El Programa Conjunto de las Naciones Unidas sobre el VIH/SIDA (ONUSIDA)., Fact sheet - WORLD AIDS DAY 2018. 2017 Global HIV Statistics, 2018. http://www.unaids.org/sites/default/files/media_asset/UNAIDS_FactSheet_en.pdf.
[19] Public Health Agency of Canada., Summary: Estimates of HIV incidence, prevalence and Canada's progress on meeting the 90-90-90 HIV targets, 2016. Government of Canada, Ottawa: ON., (2018).
[20] C. Kuiken, B. Korber, R.W. Shafer, HIV sequence databases, AIDS Rev. 5 (2003) 52–61.
[21] N. Aidsmap, HIV-1 and HIV-2, (n.d.). http://www.aidsmap.com/HIV-1-and-HIV-2/page/1322970/.
[22] G. Maartens, C. Celum, S.R. Lewin, HIV infection: Epidemiology, pathogenesis, treatment, and prevention, Lancet. 384 (2014) 258–271. https://doi.org/10.1016/S0140-6736(14)60164-1.
[23] D. Cunningham, Impact of Genetic Variation within the HIV-1 LTR and Tat on Transcription; MMS Presentation; Department of Microbiology and Immunology Center for Molecular Virology and Translational Neuroscience Drexel University College of Medicine, April 25. (2012). https://www.slideshare.net/davemc528/mms-presentation-april-25-2012.
[24] B.E.P. Klaver, B.E.N. Berkhout, Comparison of 5' and 3' Long Terminal Repeat Promoter Function in Human Immunodeficiency Virus, J. Virol. 68 (1994) 3830–3840.
[25] A.D. Frankel, J.A.T. Young, HIV-1: Fifteen Proteins and an RNA, Annu. Rev. Biochem. 67 (1998) 1–25. https://doi.org/10.1146/annurev.biochem.67.1.1.
[26] H. Göttlinger, HIV-1 Gag: a molecular machine driving viral particle assembly and release, HIV Seq. Compend. (2001) 2–28.
[27] M.S. Johnson, M.A. McClure, D.F. Feng, J. Gray, R.F. Doolittle, Computer analysis of retroviral pol genes: assignment of enzymatic functions to specific sequences and homologies with nonviral enzymes., Proc. Natl. Acad. Sci. 83 (1986) 7648–7652. https://doi.org/10.1073/pnas.83.20.7648.
[28] R. Wyatt, P.D. Kwong, W. a Henrickson, J.G. Sodroski, Structure of the Core of

the HIV-1 gp120 Exterior Envelope Glycoprotein, Los Alamos Rev. (1999) 1–7.
[29] O.M.Z. Howard, A.-K. Shirakawa, J.A. Turpin, A. Maynard, G.J. Tobin, M. Carrington, J.J. Oppenheim, M. Dean, Naturally Occurring CCR5 Extracellular and Transmembrane Domain Variants Affect HIV-1 Co-receptor and Ligand Binding Function, J. Biol. Chem. 274 (1999) 16228–16234. https://doi.org/10.1074/jbc.274.23.16228.
[30] U. Stanford, Genomic Organization of HIV-1, (2005). https://web.stanford.edu/group/virus/retro/2005gongishmail/HIV-1.jpg.
[31] A.T. Das, A. Harwig, B. Berkhout, The HIV-1 Tat Protein Has a Versatile Role in Activating Viral Transcription, J. Virol. 85 (2011) 9506–9516. https://doi.org/10.1128/JVI.00650-11.
[32] M.E. Gonzalez, The HIV-1 vpr protein: A multifaceted target for therapeutic intervention, Int. J. Mol. Sci. 18 (2017) 1–21. https://doi.org/10.3390/ijms18010126.
[33] A.R. Lifson, Do Alternate Modes for Transmission of Human Immunodeficiency Virus Exist?, JAMA. 259 (1988) 1353. https://doi.org/10.1001/jama.1988.03720090043032.
[34] J.A. Levy, Pathogenesis of human immunodeficiency virus infection., Microbiol. Rev. 57 (1993) 183–289. http://www.ncbi.nlm.nih.gov/pubmed/8464405.
[35] D.D. Ho, T. Moudgil, M. Alam, Quantitation of Human Immunodeficiency Virus Type 1 in the Blood of Infected Persons, N. Engl. J. Med. 321 (1989) 1621–1625. https://doi.org/10.1056/NEJM198912143212401.
[36] R.L. Stoneburner, M.A. Chiasson, I.B. Weisfuse, P.A. Thomas, The epidemic of AIDS and HIV-1 infection among heterosexuals in New York City, AIDS. 4 (1990) 99–106. https://doi.org/10.1097/00002030-199002000-00001.
[37] R. Pearce-Pratt, D.M. Phillips, Studies of Adhesion of Lymphocytic Cells: Implications for Sexual Transmission of Human Immunodeficiency Virus1, Biol. Reprod. 48 (1993) 431–445. https://doi.org/10.1095/biolreprod48.3.431.
[38] R. Shen, H.E. Richter, P.D. Smith, Early HIV-1 Target Cells in Human Vaginal and Ectocervical Mucosa, Am. J. Reprod. Immunol. 65 (2011) 261–267. https://doi.org/10.1111/j.1600-0897.2010.00939.x.
[39] F. Hladik, P. Sakchalathorn, L. Ballweber, G. Lentz, M. Fialkow, D. Eschenbach, M.J. McElrath, Initial Events in Establishing Vaginal Entry and Infection by Human Immunodeficiency Virus Type-1, Immunity. 26 (2007) 257–270. https://doi.org/10.1016/j.immuni.2007.01.007.
[40] E.C. Study, Children born to women with HIV-1 infection: natural history and risk of transmission, Lancet. 337 (1991) 253–260. https://doi.org/10.1016/0140-6736(91)90866-N.
[41] S. Blanche, C. Rouzioux, M.-L.G. Moscato, F. Veber, M.-J. Mayaux, C. Jacomet, J. Tricoire, A. Deville, M. Vial, G. Firtion, A. de Crepy, D. Douard, M. Robin, C. Courpotin, N. Ciraru-Vigneron, F. le Deist, C. Griscelli, A Prospective Study of Infants Born to Women Seropositive for Human Immunodeficiency Virus Type 1, N. Engl. J. Med. 320 (1989) 1643–1648. https://doi.org/10.1056/NEJM198906223202502.
[42] M. Burgard, M.-J. Mayaux, S. Blanche, A. Ferroni, M.-L. Guihard-Moscato, M.-C. Allemon, N. Ciraru-Vigneron, G. Firtion, C. Floch, F. Guillot, E. Lachassine, M. Vial, C. Griscelli, C. Rouzioux, The Use of Viral Culture and p24 Antigen

Testing to Diagnose Human Immunodeficiency Virus Infection in Neonates, N. Engl. J. Med. 327 (1992) 1192–1197. https://doi.org/10.1056/NEJM199210223271702.
[43] G.C. John, J. Kreiss, Mother-to-child transmission of human immunodeficiency virus type 1., Epidemiol. Rev. 18 (1996) 149–57. https://doi.org/10.1093/oxfordjournals.epirev.a017922.
[44] A. Immune, D. Syndr, Report of a Consensus Workshop, Siena, Italy, January 17-18, 1992. Maternal factors involved in mother-to-child transmission of HIV-1., J. Acquir. Immune Defic. Syndr. 5 (1992) 1019–29. http://www.ncbi.nlm.nih.gov/pubmed/1453317.
[45] D. Klatzmann, F. Barre-Sinoussi, M. Nugeyre, C. Danquet, E. Vilmer, C. Griscelli, F. Brun-Veziret, C. Rouzioux, J. Gluckman, J. Chermann, A. Et, Selective tropism of lymphadenopathy associated virus (LAV) for helper-inducer T lymphocytes, Science (80-.). 225 (1984) 59–63. https://doi.org/10.1126/science.6328660.
[46] E.G. Cormier, T. Dragic, An overview of HIV-1 co-receptor function and its inhibitors, HIV Seq. Compend. (2000) 19-34.
[47] J.P. Moore, A. Trkola, T. Dragic, Co-receptors for HIV-1 entry, Curr. Opin. Immunol. 9 (1997) 551–562. https://doi.org/10.1016/S0952-7915(97)80110-0.
[48] J.F. Berson, R.W. Doms, Structure–function studies of the HIV-1 coreceptors, Semin. Immunol. 10 (1998) 237–248. https://doi.org/10.1006/smim.1998.0130.
[49] J. Novembre, A.P. Galvani, M. Slatkin, The Geographic Spread of the CCR5 Δ32 HIV-Resistance Allele, PLoS Biol. 3 (2005) e339. https://doi.org/10.1371/journal.pbio.0030339.
[50] R.J. Pratt CBE FRCN, HIV & AIDS, 5Ed, CRC Press, 2003. https://doi.org/10.1201/b13504.
[51] M. Moulard, H. Lortat-Jacob, I. Mondor, G. Roca, R. Wyatt, J. Sodroski, L. Zhao, W. Olson, P.D. Kwong, Q.J. Sattentau, Selective Interactions of Polyanions with Basic Surfaces on Human Immunodeficiency Virus Type 1 gp120, J. Virol. 74 (2000) 1948–1960. https://doi.org/10.1128/JVI.74.4.1948-1960.2000.
[52] E.O. Freed, D.J. Myers, R. Risser, Characterization of the fusion domain of the human immunodeficiency virus type 1 envelope glycoprotein gp41., Proc. Natl. Acad. Sci. 87 (1990) 4650–4654. https://doi.org/10.1073/pnas.87.12.4650.
[53] I. Le Blanc, P.-P. Luyet, V. Pons, C. Ferguson, N. Emans, A. Petiot, N. Mayran, N. Demaurex, J. Fauré, R. Sadoul, R.G. Parton, J. Gruenberg, Endosome-to-cytosol transport of viral nucleocapsids, Nat. Cell Biol. 7 (2005) 653–664. https://doi.org/10.1038/ncb1269.
[54] F.H. Epstein, F.H. Epstein, W.C. Greene, The Molecular Biology of Human Immunodeficiency Virus Type 1 Infection, N. Engl. J. Med. 324 (1991) 308–317. https://doi.org/10.1056/NEJM199101313240506.
[55] Y. Vaishnav, The Biochemistry Of Aids, Annu. Rev. Biochem. 60 (1991) 577–630. https://doi.org/10.1146/annurev.biochem.60.1.577.
[56] S. Aquaro, R. Caliò, J. Balzarini, M.C. Bellocchi, E. Garaci, C.F. Perno, Macrophages and HIV infection: therapeutical approaches toward this strategic virus reservoir, Antiviral Res. 55 (2002) 209–225. https://doi.org/10.1016/S0166-3542(02)00052-9.
[57] R. Craigie, F.D. Bushman, HIV DNA Integration, Cold Spring Harb. Perspect.

Med. 2 (2012) a006890–a006890. https://doi.org/10.1101/cshperspect.a006890.
[58] R.D. Sloan, M.A. Wainberg, The role of unintegrated DNA in HIV infection, Retrovirology. 8 (2011) 52. https://doi.org/10.1186/1742-4690-8-52.
[59] M.S. Dahabieh, E. Battivelli, E. Verdin, Understanding HIV latency: the road to an HIV cure., Annu. Rev. Med. 66 (2015) 407–21. https://doi.org/10.1146/annurev-med-092112-152941.
[60] Y. Zhou, H. Zhang, J.D. Siliciano, R.F. Siliciano, Kinetics of Human Immunodeficiency Virus Type 1 Decay following Entry into Resting CD4+ T Cells, J. Virol. 79 (2005) 2199–2210. https://doi.org/10.1128/JVI.79.4.2199-2210.2005.
[61] and D.B. Sunyoung Kim, Kenji Ikeuchi, Jerome Groopman, Factors affecting cellular tropism of human immunodeficiency virus, J. Virol. 64 (1990) 5600–5604.
[62] J.R. Munis, R.S. Kornbluth, J.C. Guatelli, D.D. Richman, Ordered appearance of human immunodeficiency virus type 1 nucleic acids following high multiplicity infection of macrophages, J. Gen. Virol. 73 (1992) 1899–1906. https://doi.org/10.1099/0022-1317-73-8-1899.
[63] L.W. GREENE, Adrenal Insufficiency as a Complication of the Acquired Immunodeficiency Syndrome, Ann. Intern. Med. 101 (1984) 497. https://doi.org/10.7326/0003-4819-101-4-497.
[64] S.Y. Kim, R. Byrn, J. Groopman, D. Baltimore, Temporal aspects of DNA and RNA synthesis during human immunodeficiency virus infection: evidence for differential gene expression., J. Virol. 63 (1989) 3708–13. http://www.ncbi.nlm.nih.gov/pubmed/2760980%0Ahttp://www.pubmedcentral.nih.gov/articlerender.fcgi?artid=PMC250962.
[65] P.A. Luciw, S.J. Potter, K. Steimer, D. Dina, Molecular cloning of AIDS-associated retrovirus, Nature. 312 (1984) 760.
[66] A.G. Fisher, M.B. Feinberg, S.F. Josephs, M.E. Harper, L.M. Marselle, G. Reyes, M.A. Gonda, A. Aldovini, C. Debouk, R.C. Gallo, F. Wong-Staal, The trans-activator gene of HTLV-III is essential for virus replication, Nature. 320 (1986) 367–371. https://doi.org/10.1038/320367a0.
[67] A. Dayton, J.G. Sodroski, C.A. Rosen, A. Wei Chun Goh, W.A. Haseltine, The trans-activator gene of the human T cell lymphotropic virus type III is required for replication, Cell. 44 (1986) 941–947. https://doi.org/10.1016/0092-8674(86)90017-6.
[68] P. Dubey, U.S. Dubey, B. Dubey, Modeling the role of acquired immune response and antiretroviral therapy in the dynamics of HIV infection, Math. Comput. Simul. 144 (2018) 120–137. https://doi.org/10.1016/j.matcom.2017.07.006.
[69] J.M. Costin, Cytopathic Mechanisms of HIV-1, Virol. J. 4 (2007) 100. https://doi.org/10.1186/1743-422X-4-100.
[70] T.G. VOSS, P.J. GATTI, C.D. FERMIN, R.F. GARRY, Reduction of Human Immunodeficiency Virus Production and Cytopathic Effects by Inhibitors of the Na+/K+/2Cl−Cotransporter, Virology. 219 (1996) 291–294. https://doi.org/10.1006/viro.1996.0249.
[71] R.F. Garry, Potential mechanisms for the cytopathic properties of HIV, AIDS. 3

(1989) 683–694. https://doi.org/10.1097/00002030-198911000-00001.
[72] P. Klenerman, R.E. Phillips, C.R. Rinaldo, L.M. Wahl, G. Ogg, R.M. May, A.J. McMichael, M.A. Nowak, Cytotoxic T lymphocytes and viral turnover in HIV type 1 infection, Proc. Natl. Acad. Sci. 93 (1996) 15323–15328. https://doi.org/10.1073/pnas.93.26.15323.
[73] C.L. Althaus, R.J. De Boer, Implications of CTL-Mediated Killing of HIV-Infected Cells during the Non-Productive Stage of Infection, PLoS One. 6 (2011) e16468. https://doi.org/10.1371/journal.pone.0016468.
[74] A. Smalls-Mantey, M. Connors, Q.J. Sattentau, Comparative Efficiency of HIV-1-Infected T Cell Killing by NK Cells, Monocytes and Neutrophils, PLoS One. 8 (2013) e74858. https://doi.org/10.1371/journal.pone.0074858.
[75] A. Smalls-Mantey, N. Doria-Rose, R. Klein, A. Patamawenu, S.A. Migueles, S.-Y. Ko, C.W. Hallahan, H. Wong, B. Liu, L. You, J. Scheid, J.C. Kappes, C. Ochsenbauer, G.J. Nabel, J.R. Mascola, M. Connors, Antibody-Dependent Cellular Cytotoxicity against Primary HIV-Infected CD4 + T Cells Is Directly Associated with the Magnitude of Surface IgG Binding, J. Virol. 86 (2012) 8672–8680. https://doi.org/10.1128/JVI.00287-12.
[76] M. Rogers, C.-Y. Ou, M. Rayfield, P. Thomas, E. Schoenbaum, E. Abrams, K. Krasinski, P. Selwyn, J. Moore, A. Kaul, K. Grimm, M. Bamji, G. Schochetman, Use of the polymerase chain reaction for early detection of the proviral sequences of human immunodeficiency virus in infants born to seropositive mothers, Int. J. Gynecol. Obstet. 31 (1990) 99–99. https://doi.org/10.1016/0020-7292(90)90234-C.
[77] H. Garg, J. Mohl, A. Joshi, HIV-1 induced bystander apoptosis., Viruses. 4 (2012) 3020–43. https://doi.org/10.3390/v4113020.
[78] C.O.. Byer, G. Galliano, S.P. Shriver, Dimensions of human sexuality. McGraw-Hill Humanities Social, 2002.
[79] M.-L. Gougeon, To kill or be killed: how HIV exhausts the immune system, Cell Death Differ. 12 (2005) 845–854. https://doi.org/10.1038/sj.cdd.4401616.
[80] B. Ahr, V. Robert-Hebmann, C. Devaux, M. Biard-Piechaczyk, Apoptosis of uninfected cells induced by HIV envelope glycoproteins, Retrovirology. 1 (2004) 1–12. https://doi.org/10.1186/1742-4690-1-12.
[81] J. Blanco, J. Barretina, K.F. Ferri, E. Jacotot, A. Gutiérrez, M. Armand-Ugón, C. Cabrera, G. Kroemer, B. Clotet, J.A. Esté, Cell-Surface-Expressed HIV-1 Envelope Induces the Death of CD4 T Cells during GP41-Mediated Hemifusion-like Events, Virology. 305 (2003) 318–329. https://doi.org/10.1006/viro.2002.1764.
[82] M. Tateyama, N. Oyaizu, T.W. McCloskey, S. Than, S. Pahwa, CD4 T lymphocytes are primed to express Fas ligand by CD4 cross-linking and to contribute to CD8 T-cell apoptosis via Fas/FasL death signaling pathway., Blood. 96 (2000) 195–202. http://www.ncbi.nlm.nih.gov/pubmed/10891451.
[83] F. Cottrez, F. Manca, A.G. Dalgleish, F. Arenzana-Seisdedos, A. Capron, H. Groux, Priming of human CD4+ antigen-specific T cells to undergo apoptosis by HIV-infected monocytes. A two-step mechanism involving the gp120 molecule., J. Clin. Invest. 99 (1997) 257–266. https://doi.org/10.1172/JCI119154.
[84] T.T. Murooka, M. Deruaz, F. Marangoni, V.D. Vrbanac, E. Seung, U.H. von

Andrian, A.M. Tager, A.D. Luster, T.R. Mempel, HIV-infected T cells are migratory vehicles for viral dissemination, Nature. 490 (2012) 283–287. https://doi.org/10.1038/nature11398.
[85] M. Castedo, G. Kroemer, Mitotic catastrophe: a special case of apoptosis., J. Soc. Biol. 198 (2004) 97–103. http://www.ncbi.nlm.nih.gov/pubmed/15368957.
[86] A. Sylwester, S. Murphy, D. Shutt, D.R. Soll, HIV-induced T cell syncytia are self-perpetuating and the primary cause of T cell death in culture., J. Immunol. 158 (1997) 3996–4007. http://www.ncbi.nlm.nih.gov/pubmed/9103471.
[87] J.-L. Perfettini, T. Roumier, M. Castedo, N. Larochette, P. Boya, B. Raynal, V. Lazar, F. Ciccosanti, R. Nardacci, J. Penninger, M. Piacentini, G. Kroemer, NF-κB and p53 Are the Dominant Apoptosis-inducing Transcription Factors Elicited by the HIV-1 Envelope, J. Exp. Med. 199 (2004) 629–640. https://doi.org/10.1084/jem.20031216.
[88] I. Spijkerman, F. de Wolf, M. Langendam, H. Schuitemaker, R. Coutinho, Emergence of Syncytium-Inducing Human Immunodeficiency Virus Type 1 Variants Coincides with a Transient Increase in Viral RNA Level and Is an Independent Predictor for Progression to AIDS, J. Infect. Dis. 178 (1998) 397–403. https://doi.org/10.1086/515627.
[89] K. Andreau, Contagious apoptosis facilitated by the HIV-1 envelope: fusion-induced cell-to-cell transmission of a lethal signal, J. Cell Sci. 117 (2004) 5643–5653. https://doi.org/10.1242/jcs.01486.
[90] S. Bär, M. Alizon, Role of the ectodomain of the gp41 transmembrane envelope protein of human immunodeficiency virus type 1 in late steps of the membrane fusion process., J. Virol. 78 (2004) 811–20. https://doi.org/10.1128/JVI.78.2.811.
[91] X.M. Wang, P.E. Nadeau, Y.-T. Lo, A. Mergia, Caveolin-1 Modulates HIV-1 Envelope-Induced Bystander Apoptosis through gp41, J. Virol. 84 (2010) 6515–6526. https://doi.org/10.1128/JVI.02722-09.
[92] H. Garg, R. Blumenthal, HIV gp41-induced apoptosis is mediated by caspase-3-dependent mitochondrial depolarization, which is inhibited by HIV protease inhibitor nelfinavir, J. Leukoc. Biol. 79 (2006) 351–362. https://doi.org/10.1189/jlb.0805430.
[93] A. Ashkenazi, M. Viard, Y. Wexler-Cohen, R. Blumenthal, Y. Shai, Viral envelope protein folding and membrane hemifusion are enhanced by the conserved loop region of HIV-1 gp41., FASEB J. 25 (2011) 2156–66. https://doi.org/10.1096/fj.10-175752.
[94] L. V. Chernomordik, M.M. Kozlov, Membrane Hemifusion: Crossing a Chasm in Two Leaps, Cell. 123 (2005) 375–382. https://doi.org/10.1016/j.cell.2005.10.015.
[95] J. Blanco, J. Barretina, G. Henson, G. Bridger, E. De Clercq, B. Clotet, J.A. Este, The CXCR4 Antagonist AMD3100 Efficiently Inhibits Cell-Surface-Expressed Human Immunodeficiency Virus Type 1 Envelope-Induced Apoptosis, Antimicrob. Agents Chemother. 44 (2000) 51–56. https://doi.org/10.1128/AAC.44.1.51-56.2000.
[96] H. Garg, A. Joshi, E.O. Freed, R. Blumenthal, Site-specific Mutations in HIV-1 gp41 Reveal a Correlation between HIV-1-mediated Bystander Apoptosis and Fusion/Hemifusion, J. Biol. Chem. 282 (2007) 16899–16906. https://doi.org/10.1074/jbc.M701701200.

[97] HIV.gov, What Are HIV and AIDS?, (2019). https://www.hiv.gov/hiv-basics/overview/about-hiv-and-aids/what-are-hiv-and-aids (accessed August 18, 2019).
[98] C.A. Sabin, J.D. Lundgren, The natural history of HIV infection, Curr. Opin. HIV AIDS. 8 (2013) 1. https://doi.org/10.1097/COH.0b013e328361fa66.
[99] E.W. Fiebig, D.J. Wright, B.D. Rawal, P.E. Garrett, R.T. Schumacher, L. Peddada, C. Heldebrant, R. Smith, A. Conrad, S.H. Kleinman, M.P. Busch, Dynamics of HIV viremia and antibody seroconversion in plasma donors: implications for diagnosis and staging of primary HIV infection., AIDS. 17 (2003) 1871–9. https://doi.org/10.1097/00002030-200309050-00005.
[100] B.P. Konrad, D. Taylor, J.M. Conway, G.S. Ogilvie, D. Coombs, On the duration of the period between exposure to HIV and detectable infection, Epidemics. 20 (2017) 73–83. https://doi.org/10.1016/j.epidem.2017.03.002.
[101] S. Lindbäck, A.C. Karlsson, J. Mittler, A. Blaxhult, M. Carlsson, G. Briheim, A. Sönnerborg, H. Gaines, Viral dynamics in primary HIV-1 infection. Karolinska Institutet Primary HIV Infection Study Group., AIDS. 14 (2000) 2283–91. https://doi.org/10.1097/00002030-200010200-00009.
[102] K. Porter, A.M. Johnson, A.N. Phillips, J.H. Darbyshire, The practical significance of potential biases in estimates of the AIDS incubation period distribution _in the UK Register of HIV Seroconverters, AIDS. 13 (1999) 1943–1951. https://doi.org/10.1097/00002030-199910010-00018.
[103] J.N. Blankson, Control of HIV-1 replication in elite suppressors., Discov. Med. 9 (2010) 261–6. http://www.ncbi.nlm.nih.gov/pubmed/20350494.
[104] E. Buenz, A. Badley, Impact of mitochondrial regulation of apoptosis on the pathogenesis and treatment of HIV-1-induced immunodeficiency, Mitochondrion. 4 (2004) 235–254. https://doi.org/10.1016/j.mito.2004.05.017.
[105] V. Appay, L. Papagno, C.A. Spina, P. Hansasuta, A. King, L. Jones, G.S. Ogg, S. Little, A.J. McMichael, D.D. Richman, S.L. Rowland-Jones, Dynamics of T Cell Responses in HIV Infection, J. Immunol. 169 (2002) 607.2-607. https://doi.org/10.4049/jimmunol.169.1.607-a.
[106] H.E. Gendelman, Efficient isolation and propagation of human immunodeficiency virus on recombinant colony-stimulating factor 1-treated monocytes, J. Exp. Med. 167 (1988) 1428–1441. https://doi.org/10.1084/jem.167.4.1428.
[107] G. Herbein, U. Mahlknecht, F. Batliwalla, P. Gregersen, T. Pappas, J. Butler, W.A. O'Brien, E. Verdin, Apoptosis of CD8+ T cells is mediated by macrophages through interaction of HIV gp120 with chemokine receptor CXCR4, Nature. 395 (1998) 189–194. https://doi.org/10.1038/26026.
[108] Z. Grossman, M. Meier-Schellersheim, A.E. Sousa, R.M.M. Victorino, W.E. Paul, CD4+ T-cell depletion in HIV infection: Are we closer to understanding the cause?, Nat. Med. 8 (2002) 319–323. https://doi.org/10.1038/nm0402-319.
[109] C. Chu, P.A. Selwyn, Complications of HIV infection: A systems-based approach, Am. Fam. Physician. 83 (2011) 395–406. https://doi.org/21322514.
[110] M. Vogel, C. Schwarze-Zander, J.-C. Wasmuth, U. Spengler, T. Sauerbruch, J.K. Rockstroh, The Treatment of Patients With HIV, Dtsch. Aerzteblatt Online. 107 (2010) 507–516. https://doi.org/10.3238/arztebl.2010.0507.
[111] C.A. Sabin, Do people with HIV infection have a normal life expectancy in the

era of combination antiretroviral therapy?, BMC Med. 11 (2013) 251. https://doi.org/10.1186/1741-7015-11-251.
[112] H.M. Naif, Pathogenesis of HIV infection, Infect. Dis. Rep. 5 (2013) 6. https://doi.org/10.4081/idr.2013.s1.e6.
[113] S. Broder, The development of antiretroviral therapy and its impact on the HIV-1/AIDS pandemic, Antiviral Res. 85 (2010) 1–18. https://doi.org/10.1016/j.antiviral.2009.10.002.
[114] J.M. McNicholl, Combining biomedical preventions for HIV: Vaccines with pre-exposure prophylaxis, microbicides or other HIV preventions, Hum. Vaccines Immunother. 12 (2016) 3202–3211. https://doi.org/10.1080/21645515.2016.1231258.
[115] A.R. Sedaghat, D.A. Rastegar, K.A. O'Connell, J.B. Dinoso, C.O. Wilke, J.N. Blankson, T Cell Dynamics and the Response to HAART in a Cohort of HIV-1–Infected Elite Suppressors, Clin. Infect. Dis. 49 (2009) 1763–1766. https://doi.org/10.1086/648081.
[116] World Health Organization, Guideline on When To Start Antiretroviral Therapy and on Pre-Exposure Prophylaxis for HIV, 2015.
[117] A. Edmonds, M. Yotebieng, J. Lusiama, Y. Matumona, F. Kitetele, S. Napravnik, S.R. Cole, A. Van Rie, F. Behets, The Effect of Highly Active Antiretroviral Therapy on the Survival of HIV-Infected Children in a Resource-Deprived Setting: A Cohort Study, PLoS Med. 8 (2011) e1001044. https://doi.org/10.1371/journal.pmed.1001044.
[118] S.M. Andrews, S. Rowland-Jones, Recent advances in understanding HIV evolution, F1000Research. 6 (2017) 597. https://doi.org/10.12688/f1000research.10876.1.
[119] J.M. Cuevas, R. Geller, R. Garijo, J. López-Aldeguer, R. Sanjuán, Extremely High Mutation Rate of HIV-1 In Vivo, PLOS Biol. 13 (2015) e1002251. https://doi.org/10.1371/journal.pbio.1002251.
[120] W.-S. Hu, S.H. Hughes, HIV-1 Reverse Transcription, Cold Spring Harb. Perspect. Med. 2 (2012) 1–22. https://doi.org/10.1101/cshperspect.a006882.
[121] D.D. Richman, S.C. Morton, T. Wrin, N. Hellmann, S. Berry, M.F. Shapiro, S.A. Bozzette, The prevalence of antiretroviral drug resistance in the United States, Aids. 18 (2004) 1393–1401. https://doi.org/10.1097/01.aids.0000131310.52526.c7.
[122] C. Pereira, J. Paridaen, Anti-HIV Drug Development - An Overview, Curr. Pharm. Des. 10 (2004) 4005–4037. https://doi.org/10.2174/1381612043382459.
[123] A.F. Feder, S.-Y. Rhee, S.P. Holmes, R.W. Shafer, D.A. Petrov, P.S. Pennings, More effective drugs lead to harder selective sweeps in the evolution of drug resistance in HIV-1, Elife. 5 (2016) 1–22. https://doi.org/10.7554/eLife.10670.
[124] L.K. Schrager, Cellular and Anatomical Reservoirs of HIV-1 in Patients Receiving Potent Antiretroviral Combination Therapy, JAMA. 280 (1998) 67. https://doi.org/10.1001/jama.280.1.67.
[125] L. Bertrand, M. Nair, M. Toborek, Solving the Blood-Brain Barrier Challenge for the Effective Treatment of HIV Replication in the Central Nervous System, Curr. Pharm. Des. 22 (2016) 5477–5486. https://doi.org/10.2174/1381612822666160726113001.
[126] A. Mujugira, R.W. Coombs, R. Heffron, C. Celum, A. Ronald, N. Mugo, J.M.

Baeten, Seminal HIV-1 RNA Detection in Heterosexual African Men Initiating Antiretroviral Therapy, J. Infect. Dis. 214 (2016) 212–215. https://doi.org/10.1093/infdis/jiw131.
[127] M.-A. Jenabian, C.T. Costiniuk, V. Mehraj, F.M. Ghazawi, R. Fromentin, J. Brousseau, P. Brassard, M. Bélanger, P. Ancuta, R. Bendayan, N. Chomont, J.-P. Routy, Immune tolerance properties of the testicular tissue as a viral sanctuary site in ART-treated HIV-infected adults, AIDS. 30 (2016) 2777–2786. https://doi.org/10.1097/QAD.0000000000001282.
[128] G. Darcis, R.W. Coombs, C. Van Lint, Exploring the anatomical HIV reservoirs, AIDS. 30 (2016) 2891–2893. https://doi.org/10.1097/QAD.0000000000001281.
[129] Y. Ganor, F. Real, A. Sennepin, C.A. Dutertre, L. Prevedel, L. Xu, D. Tudor, B. Charmeteau, A. Couedel-Courteille, S. Marion, A.R. Zenak, J.P. Jourdain, Z. Zhou, A. Schmitt, C. Capron, E.A. Eugenin, R. Cheynier, M. Revol, S. Cristofari, A. Hosmalin, M. Bomsel, HIV-1 reservoirs in urethral macrophages of patients under suppressive antiretroviral therapy, Nat. Microbiol. 4 (2019) 633–644. https://doi.org/10.1038/s41564-018-0335-z.
[130] H.F. Günthard, D. V. Havlir, S. Fiscus, Z. Zhang, J. Eron, J. Mellors, R. Gulick, S.D.W. Frost, A.J.L. Brown, W. Schleif, F. Valentine, L. Jonas, A. Meibohm, C.C. Ignacio, R. Isaacs, R. Gamagami, E. Emini, A. Haase, D.D. Richman, J.K. Wong, Residual Human Immunodeficiency Virus (HIV) Type 1 RNA and DNA in Lymph Nodes and HIV RNA in Genital Secretions and in Cerebrospinal Fluid after Suppression of Viremia for 2 Years, J. Infect. Dis. 183 (2001) 1318–1327. https://doi.org/10.1086/319864.
[131] T. Chun, D.C. Nickle, J.S. Justement, J.H. Meyers, G. Roby, C.W. Hallahan, S. Kottilil, S. Moir, J.M. Mican, J.I. Mullins, D.J. Ward, J.A. Kovacs, P.J. Mannon, A.S. Fauci, Persistence of HIV in Gut-Associated Lymphoid Tissue despite Long-Term Antiretroviral Therapy, J. Infect. Dis. 197 (2008) 714–720. https://doi.org/10.1086/527324.
[132] R.S. Veazey, M. Demaria, L. V Chalifoux, D.E. Shvetz, D.R. Pauley, H.L. Knight, M. Rosenzweig, R.P. Johnson, C. Ronald, R.S. Veazey, M. Demaria, L. V Chalifoux, D.E. Shvetz, D.R. Pauley, H.L. Knight, M. Rosenzweig, R.P. Johnson, R.C. Desrosiers, A.A. Lacknerk, Gastrointestinal Tract as a Major Site of CD4+ T Cell Depletion and Viral Replication in SIV Infection, Sci. New Ser. 280 (1998) 427–431.
[133] H. Sierra, M. Cordova, C.-S.J. Chen, M. Rajadhyaksha, Confocal Imaging–Guided Laser Ablation of Basal Cell Carcinomas: An Ex Vivo Study, J. Invest. Dermatol. 135 (2015) 612–615. https://doi.org/10.1038/jid.2014.371.
[134] H. Xu, X. Wang, R.S. Veazey, Mucosal immunology of HIV infection, Immunol. Rev. 254 (2013) 10–33. https://doi.org/10.1111/imr.12072.
[135] D.P. Kotler, T. Shimada, G. Snow, G. Winson, W. Chen, M. Zhao, Y. Inada, F. Clayton, Effect of combination antiretroviral therapy upon rectal mucosal HIV RNA burden and mononuclear cell apoptosis, AIDS. 12 (1998) 597–604. https://doi.org/10.1097/00002030-199806000-00008.
[136] S. Mehandru, M.A. Poles, K. Tenner-Racz, P. Jean-Pierre, V. Manuelli, P. Lopez, A. Shet, A. Low, H. Mohri, D. Boden, P. Racz, M. Markowitz, Lack of mucosal immune reconstitution during prolonged treatment of acute and early HIV-1 infection, PLoS Med. 3 (2006) 2335–2348.

https://doi.org/10.1371/journal.pmed.0040484.
[137] M. Guadalupe, S. Sankaran, M.D. George, E. Reay, D. Verhoeven, B.L. Shacklett, J. Flamm, J. Wegelin, T. Prindiville, S. Dandekar, Viral Suppression and Immune Restoration in the Gastrointestinal Mucosa of Human Immunodeficiency Virus Type 1-Infected Patients Initiating Therapy during Primary or Chronic Infection, J. Virol. 80 (2006) 8236–8247. https://doi.org/10.1128/JVI.00120-06.
[138] L.A. McNamara, K.L. Collins, Hematopoietic stem/precursor cells as HIV reservoirs, Curr. Opin. HIV AIDS. 6 (2011) 43–48. https://doi.org/10.1097/COH.0b013e32834086b3.
[139] H. Spiegel, H. Herbst, G. Niedobitek, H.D. Foss, H. Stein, Follicular dendritic cells are a major reservoir for human immunodeficiency virus type 1 in lymphoid tissues facilitating infection of CD4+ T-helper cells., Am. J. Pathol. 140 (1992) 15–22. http://www.ncbi.nlm.nih.gov/pubmed/1530997.
[140] A. Valentin, M. Rosati, D.J. Patenaude, A. Hatzakis, L.G. Kostrikis, M. Lazanas, K.M. Wyvill, R. Yarchoan, G.N. Pavlakis, Persistent HIV-1 infection of natural killer cells in patients receiving highly active antiretroviral therapy, Proc. Natl. Acad. Sci. 99 (2002) 7015–7020. https://doi.org/10.1073/pnas.102672999.
[141] J.B. Sundstrom, D.M. Little, F. Villinger, J.E. Ellis, A.A. Ansari, Signaling through Toll-Like Receptors Triggers HIV-1 Replication in Latently Infected Mast Cells, J. Immunol. 172 (2004) 4391–4401. https://doi.org/10.4049/jimmunol.172.7.4391.
[142] A. Alexaki, Y. Liu, B. Wigdahl, Cellular reservoirs of HIV-1 and their role in viral persistence., Curr. HIV Res. 6 (2008) 388–400. https://doi.org/http://www.cadence.com/products/cic/spectre_circuit/pages/default.aspx.
[143] M. Sgarbanti, A. Battistini, Therapeutics for HIV-1 reactivation from latency, Curr. Opin. Virol. 3 (2013) 394–401. https://doi.org/10.1016/j.coviro.2013.06.001.
[144] R.T. Davey, N. Bhat, C. Yoder, T.-W. Chun, J.A. Metcalf, R. Dewar, V. Natarajan, R.A. Lempicki, J.W. Adelsberger, K.D. Miller, J.A. Kovacs, M.A. Polis, R.E. Walker, J. Falloon, H. Masur, D. Gee, M. Baseler, D.S. Dimitrov, A.S. Fauci, H.C. Lane, HIV-1 and T cell dynamics after interruption of highly active antiretroviral therapy (HAART) in patients with a history of sustained viral suppression, Proc. Natl. Acad. Sci. 96 (1999) 15109–15114. https://doi.org/10.1073/pnas.96.26.15109.
[145] D. Finzi, J. Blankson, J.D. Siliciano, J.B. Margolick, K. Chadwick, T. Pierson, K. Smith, J. Lisziewicz, F. Lori, C. Flexner, T.C. Quinn, R.E. Chaisson, E. Rosenberg, B. Walker, S. Gange, J. Gallant, R.F. Siliciano, Latent infection of CD4+ T cells provides a mechanism for lifelong persistence of HIV-1, even in patients on effective combination therapy, Nat. Med. 5 (1999) 512–517. https://doi.org/10.1038/8394.
[146] T.-W. Chun, D. Engel, M.M. Berrey, T. Shea, L. Corey, A.S. Fauci, Early establishment of a pool of latently infected, resting CD4+ T cells during primary HIV-1 infection, Proc. Natl. Acad. Sci. 95 (1998) 8869–8873. https://doi.org/10.1073/pnas.95.15.8869.
[147] T.-W. Chun, L. Carruth, D. Finzi, X. Shen, J.A. DiGiuseppe, H. Taylor, M.

Hermankova, K. Chadwick, J. Margolick, T.C. Quinn, Y.-H. Kuo, R. Brookmeyer, M.A. Zeiger, P. Barditch-Crovo, R.F. Siliciano, Quantification of latent tissue reservoirs and total body viral load in HIV-1 infection, Nature. 387 (1997) 183–188. https://doi.org/10.1038/387183a0.
[148] D. Finzi, Identification of a Reservoir for HIV-1 in Patients on Highly Active Antiretroviral Therapy, Science (80-.). 278 (1997) 1295–1300. https://doi.org/10.1126/science.278.5341.1295.
[149] T.-W. Chun, L. Stuyver, S.B. Mizell, L.A. Ehler, J.A.M. Mican, M. Baseler, A.L. Lloyd, M.A. Nowak, A.S. Fauci, Presence of an inducible HIV-1 latent reservoir during highly active antiretroviral therapy, Proc. Natl. Acad. Sci. 94 (1997) 13193–13197. https://doi.org/10.1073/pnas.94.24.13193.
[150] J.B. Honeycutt, W.O. Thayer, C.E. Baker, R.M. Ribeiro, S.M. Lada, Y. Cao, R.A. Cleary, M.G. Hudgens, D.D. Richman, J.V. Garcia, HIV persistence in tissue macrophages of humanized myeloid-only mice during antiretroviral therapy, Nat. Med. 23 (2017) 638–643. https://doi.org/10.1038/nm.4319.
[151] A. Kumar, G. Herbein, The macrophage: a therapeutic target in HIV-1 infection, Mol. Cell. Ther. 2 (2014) 10. https://doi.org/10.1186/2052-8426-2-10.
[152] Z. Zhang, Sexual Transmission and Propagation of SIV and HIV in Resting and Activated CD4+ T Cells, Science (80-.). 286 (1999) 1353–1357. https://doi.org/10.1126/science.286.5443.1353.
[153] C. Gavegnano, R.F. Schinazi, Antiretroviral Therapy in Macrophages: Implication for HIV Eradication, Antivir. Chem. Chemother. 20 (2009) 63–78. https://doi.org/10.3851/IMP1374.
[154] A. Parihar, T.D. Eubank, A.I. Doseff, Monocytes and Macrophages Regulate Immunity through Dynamic Networks of Survival and Cell Death, J. Innate Immun. 2 (2010) 204–215. https://doi.org/10.1159/000296507.
[155] D.A. Ovchinnikov, Macrophages in the embryo and beyond: Much more than just giant phagocytes, Genesis. 46 (2008) 447–462. https://doi.org/10.1002/dvg.20417.
[156] P. Castellano, L. Prevedel, E.A. Eugenin, HIV-infected macrophages and microglia that survive acute infection become viral reservoirs by a mechanism involving Bim, Sci. Rep. 7 (2017) 12866. https://doi.org/10.1038/s41598-017-12758-w.
[157] F. Ginhoux, S. Jung, Monocytes and macrophages: Developmental pathways and tissue homeostasis, Nat. Rev. Immunol. 14 (2014) 392–404. https://doi.org/10.1038/nri3671.
[158] S. Epelman, K.J. Lavine, G.J. Randolph, Origin and Functions of Tissue Macrophages, Immunity. 41 (2014) 21–35. https://doi.org/10.1016/j.immuni.2014.06.013.
[159] A. Shapouri-Moghaddam, S. Mohammadian, H. Vazini, M. Taghadosi, S.-A. Esmaeili, F. Mardani, B. Seifi, A. Mohammadi, J.T. Afshari, A. Sahebkar, Macrophage plasticity, polarization, and function in health and disease, J. Cell. Physiol. 233 (2018) 6425–6440. https://doi.org/10.1002/jcp.26429.
[160] K.L. Clayton, V. Garcia, J.E. Clements, B.D. Walker, HIV Infection of Macrophages: Implications for Pathogenesis and Cure, Pathog. Immun. 2 (2017) 179. https://doi.org/10.20411/10.20411/pai.v2i2.204.
[161] A.D. Badley, D. Dockrell, M. Simpson, R. Schut, D.H. Lynch, P. Leibson, C. V.

Paya, Macrophage-dependent Apoptosis of CD4 + T Lymphocytes from HIV-infected Individuals Is Mediated by FasL and Tumor Necrosis Factor, J. Exp. Med. 185 (1997) 55–64. https://doi.org/10.1084/jem.185.1.55.
[162] T.W. Chun, A.S. Fauci, HIV reservoirs: Pathogenesis and obstacles to viral eradication and cure, Aids. 26 (2012) 1261–1268. https://doi.org/10.1097/QAD.0b013e328353f3f1.
[163] A. Lafeuillade, Eliminating the HIV Reservoir, Curr. HIV/AIDS Rep. 9 (2012) 121–131. https://doi.org/10.1007/s11904-012-0115-y.
[164] J.H. Campbell, A.C. Hearps, G.E. Martin, K.C. Williams, S.M. Crowe, The importance of monocytes and macrophages in HIV pathogenesis, treatment, and cure, Aids. 28 (2014) 2175–2187. https://doi.org/10.1097/QAD.0000000000000408.
[165] R. Gaudin, S. Berre, B. Cunha de Alencar, J. Decalf, M. Schindler, F.-X. Gobert, M. Jouve, P. Benaroch, Dynamics of HIV-Containing Compartments in Macrophages Reveal Sequestration of Virions and Transient Surface Connections, PLoS One. 8 (2013) e69450. https://doi.org/10.1371/journal.pone.0069450.
[166] H. Chu, J.-J. Wang, M. Qi, J.-J. Yoon, X. Wen, X. Chen, L. Ding, P. Spearman, The Intracellular Virus-Containing Compartments in Primary Human Macrophages Are Largely Inaccessible to Antibodies and Small Molecules, PLoS One. 7 (2012) e35297. https://doi.org/10.1371/journal.pone.0035297.
[167] S.K. Cribbs, J. Lennox, A.M. Caliendo, L.A. Brown, D.M. Guidot, Healthy HIV-1-Infected Individuals on Highly Active Antiretroviral Therapy Harbor HIV-1 in Their Alveolar Macrophages, AIDS Res. Hum. Retroviruses. 31 (2015) 64–70. https://doi.org/10.1089/aid.2014.0133.
[168] M.A. Szaniawski, A.M. Spivak, A. Bosque, V. Planelles, Sex Influences SAMHD1 Activity and Susceptibility to Human Immunodeficiency Virus-1 in Primary Human Macrophages, J. Infect. Dis. 219 (2019) 777–785. https://doi.org/10.1093/infdis/jiy583.
[169] A.J. Kandathil, S. Sugawara, A. Goyal, C.M. Durand, J. Quinn, J. Sachithanandham, A.M. Cameron, J.R. Bailey, A.S. Perelson, A. Balagopal, No recovery of replication-competent HIV-1 from human liver macrophages, J. Clin. Invest. 128 (2018) 4501–4509. https://doi.org/10.1172/JCI121678.
[170] J.M. Orenstein, M.S. Meltzer, T. Phipps, H.E. Gendelman, Cytoplasmic assembly and accumulation of human immunodeficiency virus types 1 and 2 in recombinant human colony-stimulating factor-1-treated human monocytes: an ultrastructural study., J. Virol. 62 (1988) 2578–86. http://www.ncbi.nlm.nih.gov/pubmed/3260631%0Ahttp://www.pubmedcentral.nih.gov/articlerender.fcgi?artid=PMC253687.
[171] A. Pelchen-Matthews, B. Kramer, M. Marsh, Infectious HIV-1 assembles in late endosomes in primary macrophages, J. Cell Biol. 162 (2003) 443–455. https://doi.org/10.1083/jcb.200304008.
[172] J.F. Foley, C.-R. Yu, R. Solow, M. Yacobucci, K.W.C. Peden, J.M. Farber, Roles for CXC Chemokine Ligands 10 and 11 in Recruiting CD4 + T Cells to HIV-1-Infected Monocyte-Derived Macrophages, Dendritic Cells, and Lymph Nodes, J. Immunol. 174 (2005) 4892–4900. https://doi.org/10.4049/jimmunol.174.8.4892.

[173] F. Groot, S. Welsch, Q.J. Sattentau, Efficient HIV-1 transmission from macrophages to T cells across transient virological synapses, Blood. 111 (2008) 4660–4663. https://doi.org/10.1182/blood-2007-12-130070.
[174] C.J.A. Duncan, R.A. Russell, Q.J. Sattentau, High multiplicity HIV-1 cell-to-cell transmission from macrophages to CD4+ T cells limits antiretroviral efficacy, AIDS. 27 (2013) 2201–2206. https://doi.org/10.1097/QAD.0b013e3283632ec4.
[175] I.A. Abela, L. Berlinger, M. Schanz, L. Reynell, H.F. Günthard, P. Rusert, A. Trkola, Cell-Cell Transmission Enables HIV-1 to Evade Inhibition by Potent CD4bs Directed Antibodies, PLoS Pathog. 8 (2012) e1002634. https://doi.org/10.1371/journal.ppat.1002634.
[176] Y. Dong, E.N. Benveniste, Immune function of astrocytes, Glia. 36 (2001) 180–190. https://doi.org/10.1002/glia.1107.
[177] K. Takahashi, S.L. Wesselingh, D.E. Griffin, J.C. McArthur, R.T. Johnson, J.D. Glass, Localization of HIV-1 in human brain using polymerase chain reaction/in situ hybridization and immunocytochemistry, Ann. Neurol. 39 (1996) 705–711. https://doi.org/10.1002/ana.410390606.
[178] G. Trillo-Pazos, A. Diamanturos, L. Rislove, T. Menza, W. Chao, P. Belem, S. Sadiq, S. Morgello, L. Sharer, D.J. Volsky, Detection of HIV-1 DNA in Microglia/ Macrophages, Astrocytes and Neurons Isolated from Brain Tissue with HIV-1 Encephalitis by Laser Capture Microdissection, Brain Pathol. 13 (2006) 144–154. https://doi.org/10.1111/j.1750-3639.2003.tb00014.x.
[179] S. Dewhurst, K. Sakai, J. Bresser, M. Stevenson, M.J. Evinger-Hodges, D.J. Volsky, Persistent productive infection of human glial cells by human immunodeficiency virus (HIV) and by infectious molecular clones of HIV., J. Virol. 61 (1987) 3774–82. http://www.ncbi.nlm.nih.gov/pubmed/2446007.
[180] M.E. Dorf, M.A. Berman, S. Tanabe, M. Heesen, Y. Luo, Astrocytes express functional chemokine receptors, J. Neuroimmunol. 111 (2000) 109–121. https://doi.org/10.1016/S0165-5728(00)00371-4.
[181] M. Ma, J.D. Geiger, A. Nath, Characterization of a novel binding site for the human immunodeficiency virus type 1 envelope protein gp120 on human fetal astrocytes., J. Virol. 68 (1994) 6824–8. http://www.ncbi.nlm.nih.gov/pubmed/8084022.
[182] E. Lavi, D.L. Kolson, A.M. Ulrich, L. Fu, F. González-Scarano, Chemokine receptors in the human brain and their relationship to HIV infection., J. Neurovirol. 4 (1998) 301–11. http://www.embase.com/search/results?subaction=viewrecord&from=export&id=L28260714.
[183] P.R. Clapham, J.N. Weber, D. Whitby, K. McIntosh, A.G. Dalgleish, P.J. Maddon, K.C. Deen, R.W. Sweet, R.A. Weiss, Soluble CD4 blocks the infectivity of diverse strains of HIV and SIV for T cells and monocytes but not for brain and muscle cells, Nature. 337 (1989) 368–370. https://doi.org/10.1038/337368a0.
[184] Y. Liu, H. Liu, B.O. Kim, V.H. Gattone, J. Li, A. Nath, J. Blum, J.J. He, CD4-Independent Infection of Astrocytes by Human Immunodeficiency Virus Type 1: Requirement for the Human Mannose Receptor, J. Virol. 78 (2004) 4120–4133. https://doi.org/10.1128/JVI.78.8.4120-4133.2004.
[185] R. Brack-Werner, Astrocytes: HIV cellular reservoirs and important participants in neuropathogenesis., AIDS. 13 (1999) 1–22.

https://doi.org/10.1097/00002030-199901140-00003.
[186] R. Brack-Werner, A. Kleinschmidt, A. Ludvigsen, W. Mellert, M. Neumann, R. Herrmann, M.C. Khim, A. Burny, N. Müller-Lantzsch, D. Stavrou, Infection of human brain cells by HIV-1: restricted virus production in chronically infected human glial cell lines., AIDS. 6 (1992) 273–85. http://www.ncbi.nlm.nih.gov/pubmed/1373627.
[187] S. Kramer-Hämmerle, I. Rothenaigner, H. Wolff, J.E. Bell, R. Brack-Werner, Cells of the central nervous system as targets and reservoirs of the human immunodeficiency virus, Virus Res. 111 (2005) 194–213. https://doi.org/10.1016/j.virusres.2005.04.009.
[188] D. Carroll-Anzinger, L. Al-Harthi, Gamma Interferon Primes Productive Human Immunodeficiency Virus Infection in Astrocytes, J. Virol. 80 (2006) 541–544. https://doi.org/10.1128/JVI.80.1.541-544.2006.
[189] C. Tornatore, A. Nath, K. Amemiya, E.O. Major, Persistent human immunodeficiency virus type 1 infection in human fetal glial cells reactivated by T-cell factor(s) or by the cytokines tumor necrosis factor alpha and interleukin-1 beta., J. Virol. 65 (1991) 6094–100. http://www.ncbi.nlm.nih.gov/pubmed/1920627.
[190] C. Tornatore, K. Meyers, W. Atwood, K. Conant, E. Major, Temporal patterns of human immunodeficiency virus type 1 transcripts in human fetal astrocytes., J. Virol. 68 (1994) 93–102. http://www.ncbi.nlm.nih.gov/pubmed/8254781.
[191] J.N. Clarke, J.-A. Lake, C.J. Burrell, S.L. Wesselingh, P.R. Gorry, P. Li, Novel pathway of human immunodeficiency virus type 1 uptake and release in astrocytes, Virology. 348 (2006) 141–155. https://doi.org/10.1016/j.virol.2005.12.004.
[192] J. Ryoo, J. Choi, C. Oh, S. Kim, M. Seo, S.Y. Kim, D. Seo, J. Kim, T.E. White, A. Brandariz-Nuñez, F. Diaz-Griffero, C.H. Yun, J.A. Hollenbaugh, B. Kim, D. Baek, K. Ahn, The ribonuclease activity of SAMHD1 is required for HIV-1 restriction, Nat. Med. 20 (2014) 936–941. https://doi.org/10.1038/nm.3626.
[193] M.H. Malim, APOBEC proteins and intrinsic resistance to HIV-1 infection, Philos. Trans. R. Soc. B Biol. Sci. 364 (2009) 675–687. https://doi.org/10.1098/rstb.2008.0185.
[194] R. Craigie, F.D. Bushma, Host Factors in Retroviral Integration and the Selection of Integration Target Sites, in: Mob. DNA III, American Society of Microbiology, 2014: pp. 1035–1050. https://doi.org/10.1128/microbiolspec.MDNA3-0026-2014.
[195] A. Kumar, W. Abbas, G. Herbein, HIV-1 latency in monocytes/macrophages., Viruses. 6 (2014) 1837–60. https://doi.org/10.3390/v6041837.
[196] R.E. Randall, S. Goodbourn, Interferons and viruses: An interplay between induction, signalling, antiviral responses and virus countermeasures, J. Gen. Virol. 89 (2008) 1–47. https://doi.org/10.1099/vir.0.83391-0.
[197] A. Telesnitsky, S. Goff, Reverse Transcriptase and the Generation of Retroviral DNA, 1997. http://www.ncbi.nlm.nih.gov/pubmed/21433342.
[198] J.S. Nandi, Unintegrated viral DNA as a marker for human immunodeficiency virus 1 infection in vivo and in vitro., Acta Virol. 43 (1999) 367–72. http://www.ncbi.nlm.nih.gov/pubmed/10825926.
[199] J. Kelly, M.H. Beddall, D. Yu, S.R. Iyer, J.W. Marsh, Y. Wu, Human

macrophages support persistent transcription from unintegrated HIV-1 DNA, Virology. 372 (2008) 300–312. https://doi.org/10.1016/j.virol.2007.11.007.
[200] A. Brussel, P. Sonigo, Evidence for Gene Expression by Unintegrated Human Immunodeficiency Virus Type 1 DNA Species, J. Virol. 78 (2004) 11263–11271. https://doi.org/10.1128/JVI.78.20.11263-11271.2004.
[201] H. Koppensteiner, R. Brack-Werner, M. Schindler, Macrophages and their relevance in Human Immunodeficiency Virus Type I infection, Retrovirology. 9 (2012) 82. https://doi.org/10.1186/1742-4690-9-82.
[202] S.R. DiNapoli, V.M. Hirsch, J.M. Brenchley, Macrophages in Progressive Human Immunodeficiency Virus/Simian Immunodeficiency Virus Infections, J. Virol. 90 (2016) 7596–7606. https://doi.org/10.1128/JVI.00672-16.
[203] A.S. Perelson, A.U. Neumann, M. Markowitz, J.M. Leonard, D.D. Ho, HIV-1 Dynamics in Vivo: Virion Clearance Rate, Infected Cell Life-Span, and Viral Generation Time, Science (80-.). 271 (1996) 1582–1586. https://doi.org/10.1126/science.271.5255.1582.
[204] S. Crowe, T. Zhu, W.A. Muller, The contribution of monocyte infection and trafficking to viral persistence, and maintenance of the viral reservoir in HIV infection, J. Leukoc. Biol. 74 (2003) 635–641. https://doi.org/10.1189/jlb.0503204.
[205] J. Murphy, R. Summer, A.A. Wilson, D.N. Kotton, A. Fine, The prolonged life-span of alveolar macrophages, Am. J. Respir. Cell Mol. Biol. 38 (2008) 380–385. https://doi.org/10.1165/rcmb.2007-0224RC.
[206] M. Giralt, P. Domingo, J.P. Guallar, M.L. Rodriguez de la Concepción, M. Alegre, J.C. Domingo, F. Villarroya, HIV-1 infection alters gene expression in adipose tissue, which contributes to HIV-1/HAART-associated lipodystrophy., Antivir. Ther. 11 (2006) 729–40. http://www.ncbi.nlm.nih.gov/pubmed/17310817.
[207] S.M. Yeligar, J.M. Ward, F.L. Harris, L.A.S. Brown, D.M. Guidot, S.K. Cribbs, Dysregulation of Alveolar Macrophage PPARγ, NADPH Oxidases, and TGFβ 1 in Otherwise Healthy HIV-Infected Individuals, AIDS Res. Hum. Retroviruses. 33 (2017) 1018–1026. https://doi.org/10.1089/aid.2016.0030.
[208] N. Gajanayaka, S. O'Hara, Y. Konarski, J. Fernandes, K. Muthumani, M. Kozlowski, J.B. Angel, A. Kumar, HIV and HIV-Tat inhibit LPS-induced IL-27 production in human macrophages by distinct intracellular signaling pathways, J. Leukoc. Biol. 102 (2017) 925–939. https://doi.org/10.1189/jlb.4A0716-332RR.
[209] A.D. Badley, A. Sainski, F. Wightman, S.R. Lewin, Altering cell death pathways as an approach to cure HIV infection, Cell Death Dis. 4 (2013) e718-11. https://doi.org/10.1038/cddis.2013.248.
[210] M. Zhang, X. Li, X. Pang, L. Ding, O. Wood, K. Clouse, I. Hewlett, A.I. Dayton, Identification of a Potential HIV-Induced Source of Bystander-Mediated Apoptosis in T Cells: Upregulation of TRAIL in Primary Human Macrophages by HIV-1 Tat, J. Biomed. Sci. 8 (2001) 290–296. https://doi.org/10.1159/000054045.
[211] and B.B. Agne`s Vendeville, Fabienne Rayne, Anne Bonhoure, Nadir Bettache, Philippe Montcourrier, HIV-1 Tat Enters T Cells Using Coated Pits before Translocating from Acidified Endosomes and Eliciting, Mol. Biol. Cell. 15 (2004) 2347–2360. https://doi.org/10.1091/mbc.E03.
[212] S.R. Bartz, M. Emerman, Human immunodeficiency virus type 1 Tat induces

apoptosis and increases sensitivity to apoptotic signals by up-regulating FLICE/caspase-8, J. Virol. 73 (1999) 1956–63.
[213] A. Nicolini, M.A. Ajmone-Cat, A. Bernardo, G. Levi, L. Minghetti, Human immunodeficiency virus type-1 Tat protein induces nuclear factor (NF)-κB activation and oxidative stress in microglial cultures by independent mechanisms, J. Neurochem. 79 (2008) 713–716. https://doi.org/10.1046/j.1471-4159.2001.00568.x.
[214] J. de Mareuil, M. Carre, P. Barbier, G.R. Campbell, S. Lancelot, S. Opi, D. Esquieu, J.D. Watkins, C. Prevot, D. Braguer, V. Peyrot, E.P. Loret, HIV-1 Tat protein enhances microtubule polymerization, Retrovirology. 2 (2005) 1–11. https://doi.org/10.1186/1742-4690-2-5.
[215] M. Tanaka, T. Ueno, T. Nakahara, K. Sasaki, A. Ishimoto, H. Sakai, Downregulation of CD4 is required for maintenance of viral infectivity of HIV-1, Virology. 311 (2003) 316–325. https://doi.org/10.1016/S0042-6822(03)00126-0.
[216] C.R. Casella, E.L. Rapaport, T.H. Finkel, Vpu increases susceptibility of human immunodeficiency virus type 1-infected cells to fas killing., J. Virol. 73 (1999) 92–100. http://www.ncbi.nlm.nih.gov/pubmed/9847311%0Ahttp://www.pubmedcentral.nih.gov/articlerender.fcgi?artid=PMC103812.
[217] K. Strebel, HIV-1 Vpu — an ion channel in search of a job, Biochim. Biophys. Acta - Biomembr. 1838 (2014) 1074–1081. https://doi.org/10.1016/j.bbamem.2013.06.029.
[218] S. Verma, A. Ali, S. Arora, A.C. Banerjea, Inhibition of β-TrcP-dependent ubiquitination of p53 by HIV-1 Vpu promotes p53-mediated apoptosis in human T cells, Blood. 117 (2011) 6600–6607. https://doi.org/10.1182/blood-2011-01-333427.
[219] S. Debaisieux, F. Rayne, H. Yezid, B. Beaumelle, The Ins and Outs of HIV-1 Tat, Traffic. 13 (2012) 355–363. https://doi.org/10.1111/j.1600-0854.2011.01286.x.
[220] M. Kogan, J. Rappaport, HIV-1 Accessory Protein Vpr: Relevance in the pathogenesis of HIV and potential for therapeutic intervention, Retrovirology. 8 (2011) 1–20. https://doi.org/10.1186/1742-4690-8-25.
[221] W. Abbas, T-Cell Signaling in HIV-1 Infection, Open Virol. J. 7 (2013) 57–71. https://doi.org/10.2174/1874357920130621001.
[222] J.L. Andersen, E. Le Rouzic, V. Planelles, HIV-1 Vpr: Mechanisms of G2 arrest and apoptosis, Exp. Mol. Pathol. 85 (2008) 2–10. https://doi.org/10.1016/j.yexmp.2008.03.015.
[223] M.A. Khan, C. Aberham, S. Kao, H. Akari, R. Gorelick, S. Bour, K. Strebel, Human Immunodeficiency Virus Type 1 Vif Protein Is Packaged into the Nucleoprotein Complex through an Interaction with Viral Genomic RNA, J. Virol. 75 (2001) 7252–7265. https://doi.org/10.1128/JVI.75.16.7252-7265.2001.
[224] W. Zhang, G. Chen, A.M. Niewiadomska, R. Xu, X.-F. Yu, Distinct Determinants in HIV-1 Vif and Human APOBEC3 Proteins Are Required for the Suppression of Diverse Host Anti-Viral Proteins, PLoS One. 3 (2008) e3963. https://doi.org/10.1371/journal.pone.0003963.
[225] K. Sakai, J. Dimas, M.J. Lenardo, The Vif and Vpr accessory proteins independently cause HIV-1-induced T cell cytopathicity and cell cycle arrest,

Proc. Natl. Acad. Sci. 103 (2006) 3369–3374. https://doi.org/10.1073/pnas.0509417103.
[226] C.A. Stoddart, R. Geleziunas, S. Ferrell, V. Linquist-Stepps, M.E. Moreno, C. Bare, W. Xu, W. Yonemoto, P.A. Bresnahan, J.M. McCune, W.C. Greene, Human Immunodeficiency Virus Type 1 Nef-Mediated Downregulation of CD4 Correlates with Nef Enhancement of Viral Pathogenesis, J. Virol. 77 (2003) 2124–2133. https://doi.org/10.1128/JVI.77.3.2124-2133.2003.
[227] E. Olivetta, M. Federico, HIV-1 Nef protects human-monocyte-derived macrophages from HIV-1-induced apoptosis, Exp. Cell Res. 312 (2006) 890–900. https://doi.org/10.1016/j.yexcr.2005.12.003.
[228] R. Geleziunas, W. Xu, K. Takeda, H. Ichijo, W.C. Greene, HIV-1 Nef inhibits ASK1-dependent death signalling providing a potential mechanism for protecting the infected host cell, Nature. 410 (2001) 834–838. https://doi.org/10.1038/35071111.
[229] D. Wolf, V. Witte, B. Laffert, K. Blume, E. Stromer, S. Trapp, P. D'Aloja, A. Schürmann, A.S. Baur, HIV-1 Nef associated PAK and PI3-Kinases stimulate Akt-independent Bad-phosphorylation to induce anti-apoptotic signals, Nat. Med. 7 (2001) 1217. https://doi.org/10.1038/nm1101-1217.
[230] A. Rasola, D. Gramaglia, C. Boccaccio, P.M. Comoglio, Apoptosis Enhancement by the HIV-1 Nef Protein, J. Immunol. 166 (2001) 81–88. https://doi.org/10.4049/jimmunol.166.1.81.
[231] K. Muthumani, A.Y. Choo, D.J. Shedlock, D.J. Laddy, S.G. Sundaram, L. Hirao, L. Wu, K.P. Thieu, C.W. Chung, K.M. Lankaraman, P. Tebas, G. Silvestri, D.B. Weiner, Human Immunodeficiency Virus Type 1 Nef Induces Programmed Death 1 Expression through a p38 Mitogen-Activated Protein Kinase-Dependent Mechanism, J. Virol. 82 (2008) 11536–11544. https://doi.org/10.1128/JVI.00485-08.
[232] M. Laforge, F. Petit, J. Estaquier, A. Senik, Commitment to Apoptosis in CD4+ T Lymphocytes Productively Infected with Human Immunodeficiency Virus Type 1 Is Initiated by Lysosomal Membrane Permeabilization, Itself Induced by the Isolated Expression of the Viral Protein Nef, J. Virol. 81 (2007) 11426–11440. https://doi.org/10.1128/JVI.00597-07.
[233] K.T. Arrildt, S.B. Joseph, R. Swanstrom, The HIV-1 Env Protein: A Coat of Many Colors, Curr. HIV/AIDS Rep. 9 (2012) 52–63. https://doi.org/10.1007/s11904-011-0107-3.
[234] J.-L. Perfettini, M. Castedo, T. Roumier, K. Andreau, R. Nardacci, M. Piacentini, G. Kroemer, Mechanisms of apoptosis induction by the HIV-1 envelope, Cell Death Differ. 12 (2005) 916–923. https://doi.org/10.1038/sj.cdd.4401584.
[235] K.B. Schwarz, Oxidative stress during viral infection: A review, Free Radic. Biol. Med. 21 (1996) 641–649. https://doi.org/10.1016/0891-5849(96)00131-1.
[236] D. Arnoult, L. Carneiro, I. Tattoli, S.E. Girardin, The role of mitochondria in cellular defense against microbial infection, Semin. Immunol. 21 (2009) 223–232. https://doi.org/10.1016/j.smim.2009.05.009.
[237] S. Desagher, J.-C. Martinou, Mitochondria as the central control point of apoptosis, Trends Cell Biol. 10 (2000) 369–377. https://doi.org/10.1016/S0962-8924(00)01803-1.
[238] S. Selvaraj, M. Ghebremichael, M. Li, Y. Foli, A. Langs-Barlow, A. Ogbuagu, L.

Barakat, E. Tubridy, R. Edifor, W. Lam, Y.-C. Cheng, E. Paintsil, Antiretroviral Therapy–Induced Mitochondrial Toxicity: Potential Mechanisms Beyond Polymerase-γ Inhibition, Clin. Pharmacol. Ther. 96 (2014) 110–120. https://doi.org/10.1038/clpt.2014.64.
[239] C.-Y. Huang, S.-F. Chiang, T.-Y. Lin, S.-H. Chiou, K.-C. Chow, HIV-1 Vpr Triggers Mitochondrial Destruction by Impairing Mfn2-Mediated ER-Mitochondria Interaction, PLoS One. 7 (2012) e33657. https://doi.org/10.1371/journal.pone.0033657.
[240] D. Arnoult, F. Petit, J.-D. Lelièvre, J. Estaquier, Mitochondria in HIV-1-induced apoptosis, Biochem. Biophys. Res. Commun. 304 (2003) 561–574. https://doi.org/10.1016/S0006-291X(03)00629-6.
[241] M. Casula, I. Bosboom-Dobbelaer, K. Smolders, S. Otto, M. Bakker, M.P. de Baar, P. Reiss, A. de Ronde, Infection with HIV-1 Induces a Decrease in mtDNA, J. Infect. Dis. 191 (2005) 1468–1471. https://doi.org/10.1086/429412.
[242] C.G. Morse, J.G. Voss, G. Rakocevic, M. McLaughlin, C.L. Vinton, C. Huber, X. Hu, J. Yang, D.W. Huang, C. Logun, R.L. Danner, Z.G. Rangel, P.J. Munson, J.M. Orenstein, E.J. Rushing, R.A. Lempicki, M.C. Dalakas, J.A. Kovacs, HIV Infection and Antiretroviral Therapy Have Divergent Effects on Mitochondria in Adipose Tissue, J. Infect. Dis. 205 (2012) 1778–1787. https://doi.org/10.1093/infdis/jis101.
[243] T. Hulgan, M. Gerschenson, HIV and Mitochondria: More Than Just Drug Toxicity, J. Infect. Dis. 205 (2012) 1769–1771. https://doi.org/10.1093/infdis/jis105.
[244] R. Gaur, U. Timilsina, Modulation of apoptosis and viral latency – an axis to be well understood for successful cure of human immunodeficiency virus, J. Gen. Virol. 97 (2016) 813–824. https://doi.org/10.1099/jgv.0.000402.
[245] P.N. Fernández Larrosa, D.O. Croci, D.A. Riva, M. Bibini, R. Luzzi, M. Saracco, S.E. Mersich, G.A. Rabinovich, L. Peralta, Apoptosis resistance in HIV-1 persistently-infected cells is independent of active viral replication and involves modulation of the apoptotic mitochondrial pathway, Retrovirology. 5 (2008) 19. https://doi.org/10.1186/1742-4690-5-19.
[246] A. Ohta, Y. Nishiyama, Mitochondria and viruses, Mitochondrion. 11 (2011) 1–12. https://doi.org/10.1016/j.mito.2010.08.006.
[247] N. Selliah, T.H. Finkel, Biochemical mechanisms of HIV induced T cell apoptosis., Cell Death Differ. 8 (2001) 127–36. https://doi.org/10.1038/sj.cdd.4400822.
[248] S.A. Stewart, B. Poon, J.B. Jowett, I.S. Chen, Human immunodeficiency virus type 1 Vpr induces apoptosis following cell cycle arrest., J. Virol. 71 (1997) 5579–92. http://www.ncbi.nlm.nih.gov/pubmed/9188632%0Ahttp://www.pubmedcentral.nih.gov/articlerender.fcgi?artid=PMC191800.
[249] S.A. Stewart, B. Poon, J.Y. Song, I.S.Y. Chen, Human Immunodeficiency Virus Type 1 Vpr Induces Apoptosis through Caspase Activation, J. Virol. 74 (2000) 3105–3111. https://doi.org/10.1128/JVI.74.7.3105-3111.2000.
[250] S. Mahalingam, V. Ayyavoo, M. Patel, T. Kieber-Emmons, G.D. Kao, R.J. Muschel, D.B. Weiner, HIV-1 Vpr interacts with a human 34-kDa mov34 homologue, a cellular factor linked to the G2/M phase transition of the

mammalian cell cycle, Proc. Natl. Acad. Sci. 95 (1998) 3419–3424. https://doi.org/10.1073/pnas.95.7.3419.
[251] J.B. Jowett, V. Planelles, B. Poon, N.P. Shah, M.L. Chen, I.S. Chen, The human immunodeficiency virus type 1 vpr gene arrests infected T cells in the G2 + M phase of the cell cycle., J. Virol. 69 (1995) 6304–13. http://www.ncbi.nlm.nih.gov/pubmed/7474080%0Ahttp://www.pubmedcentral.nih.gov/articlerender.fcgi?artid=PMC189580.
[252] J. He, S. Choe, R. Walker, P. Di Marzio, D.O. Morgan, N.R. Landau, Human immunodeficiency virus type 1 viral protein R (Vpr) arrests cells in the G2 phase of the cell cycle by inhibiting p34cdc2 activity., J. Virol. 69 (1995) 6705–11. http://www.ncbi.nlm.nih.gov/pubmed/7474080%0Ahttp://www.pubmedcentral.nih.gov/articlerender.fcgi?artid=PMC189580.
[253] W.C. Goh, M.E. Rogel, C.M. Kinsey, S.F. Michael, P.N. Fultz, M.A. Nowak, B.H. Hahn, M. Emerman, HIV-1 Vpr increases viral expression by manipulation of the cell cycle: A mechanism for selection of Vpr in vivo, Nat. Med. 4 (1998) 65–71. https://doi.org/10.1038/nm0198-065.
[254] E. Jacotot, L. Ravagnan, M. Loeffler, K.F. Ferri, H.L.A. Vieira, N. Zamzami, P. Costantini, S. Druillennec, J. Hoebeke, J.P. Briand, T. Irinopoulou, E. Daugas, S.A. Susin, D. Cointe, Z.H. Xie, J.C. Reed, B.P. Roques, G. Kroemer, The HIV-1 Viral Protein R Induces Apoptosis via a Direct Effect on the Mitochondrial Permeability Transition Pore, J. Exp. Med. 191 (2000) 33–46. https://doi.org/10.1084/jem.191.1.33.
[255] J.S. Anderson, Using TRIM5α as an HIV therapeutic: the alpha gene?, Expert Opin. Biol. Ther. 13 (2013) 1029–1038. https://doi.org/10.1517/14712598.2013.779251.
[256] K. Muthumani, D.S. Hwang, B.M. Desai, D. Zhang, N. Dayes, D.R. Green, D.B. Weiner, HIV-1 Vpr Induces Apoptosis through Caspase 9 in T Cells and Peripheral Blood Mononuclear Cells, J. Biol. Chem. 277 (2002) 37820–37831. https://doi.org/10.1074/jbc.M205313200.
[257] J.L. Andersen, J.L. DeHart, E.S. Zimmerman, O. Ardon, B. Kim, G. Jacquot, S. Benichou, V. Planelles, HIV-1 Vpr-Induced Apoptosis Is Cell Cycle Dependent and Requires Bax but Not ANT, PLoS Pathog. 2 (2006) e127. https://doi.org/10.1371/journal.ppat.0020127.
[258] V. Ayyavoo, A. Mahboubi, S. Mahalingam, R. Ramalingam, S. Kudchodkar, W. V Williams, D.R. Green, D.B. Weiner, HIV-1 Vpr suppresses immune activation and apoptosis through regulation of nuclear factor kappa B., Nat. Med. 3 (1997) 1117–23. https://doi.org/10.1038/nm0797-730.
[259] P.K. Tungaturthi, B.E. Sawaya, S.P. Singh, B. Tomkowicz, V. Ayyavoo, K. Khalili, R.G. Collman, S. Amini, A. Srinivasan, Role of HIV-1 Vpr in AIDS pathogenesis: relevance and implications of intravirion, intracellular and free Vpr, Biomed. Pharmacother. 57 (2003) 20–24. https://doi.org/10.1016/S0753-3322(02)00328-1.
[260] O.D. Perez, G.P. Nolan, D. Magda, R.A. Miller, L.A. Herzenberg, L.A. Herzenberg, Motexafin gadolinium (Gd-Tex) selectively induces apoptosis in HIV-1 infected CD4+ T helper cells., Proc. Natl. Acad. Sci. U. S. A. 99 (2002) 2270–4. https://doi.org/10.1073/pnas.261711499.
[261] F. Cunyat, J.N. Rainho, B. West, L. Swainson, J.M. McCune, M. Stevenson,

Colony-Stimulating Factor 1 Receptor Antagonists Sensitize Human Immunodeficiency Virus Type 1-Infected Macrophages to TRAIL-Mediated Killing, J. Virol. 90 (2016) 6255–6262. https://doi.org/10.1128/JVI.00231-16.
[262] J. Xue, C. Fu, Z. Cong, L. Peng, Z. Peng, T. Chen, W. Wang, H. Jiang, Q. Wei, C. Qin, Galectin-3 promotes caspase-independent cell death of HIV-1-infected macrophages, FEBS J. 284 (2017) 97–113. https://doi.org/10.1111/febs.13955.
[263] J.J. Lum, A.A. Pilon, J. Sanchez-Dardon, B.N. Phenix, J.E. Kim, J. Mihowich, K. Jamison, N. Hawley-Foss, D.H. Lynch, A.D. Badley, Induction of Cell Death in Human Immunodeficiency Virus-Infected Macrophages and Resting Memory CD4 T Cells by TRAIL/Apo2L, J. Virol. 75 (2001) 11128–11136. https://doi.org/10.1128/JVI.75.22.11128-11136.2001.
[264] Y. Huang, N. Erdmann, H. Peng, S. Herek, J.S. Davis, X. Luo, T. Ikezu, J. Zheng, TRAIL-mediated apoptosis in HIV-1-infected macrophages is dependent on the inhibition of Akt-1 phosphorylation., J. Immunol. 177 (2006) 2304–13. http://www.ncbi.nlm.nih.gov/pubmed/16887991%5Cnhttp://www.pubmedcentral.nih.gov/articlerender.fcgi?artid=PMC1892167.
[265] L. Zheng, Y. Yang, L. Guocai, C.D. Pauza, M.S. Salvato, HIV Tat Protein Increases Bcl-2 Expression in Monocytes Which Inhibits Monocyte Apoptosis Induced by Tumor Necrosis Factor-Alpha-Related Apoptosis-Induced Ligand, Intervirology. 50 (2007) 224–228. https://doi.org/10.1159/000100565.
[266] D.J. Schnepple, B. Shepard, G.D. Bren, N.W. Cummins, S. Natesampillai, S. Trushin, A. Algeciras-Schimnich, X.W. Meng, A.M. Sainski, S.A. Rizza, S.H. Kaufmann, A.D. Badley, Isolation of a TRAIL Antagonist from the Serum of HIV-infected Patients, J. Biol. Chem. 286 (2011) 35742–35754. https://doi.org/10.1074/jbc.M111.274639.
[267] D. Mahalingam, E. Szegezdi, M. Keane, S. de Jong, A. Samali, TRAIL receptor signalling and modulation: Are we on the right TRAIL?, Cancer Treat. Rev. 35 (2009) 280–288. https://doi.org/10.1016/j.ctrv.2008.11.006.
[268] R. Berro, C. de la Fuente, Z. Klase, K. Kehn, L. Parvin, A. Pumfery, E. Agbottah, A. Vertes, S. Nekhai, F. Kashanchi, Identifying the Membrane Proteome of HIV-1 Latently Infected Cells, J. Biol. Chem. 282 (2007) 8207–8218. https://doi.org/10.1074/jbc.M606324200.
[269] L. Pache, M.S. Dutra, A.M. Spivak, J.M. Marlett, J.P. Murry, Y. Hwang, A.M. Maestre, L. Manganaro, M. Vamos, P. Teriete, L.J. Martins, R. König, V. Simon, A. Bosque, A. Fernandez-Sesma, N.D.P. Cosford, F.D. Bushman, J.A.T. Young, V. Planelles, S.K. Chanda, BIRC2/cIAP1 Is a Negative Regulator of HIV-1 Transcription and Can Be Targeted by Smac Mimetics to Promote Reversal of Viral Latency, Cell Host Microbe. 18 (2015) 345–353. https://doi.org/10.1016/j.chom.2015.08.009.
[270] M.R. López-Huertas, E. Mateos, M. Sánchez del Cojo, F. Gómez-Esquer, G. Díaz-Gil, S. Rodríguez-Mora, J.A. López, E. Calvo, G. López-Campos, J. Alcamí, M. Coiras, The Presence of HIV-1 Tat Protein Second Exon Delays Fas Protein-mediated Apoptosis in CD4 + T Lymphocytes, J. Biol. Chem. 288 (2013) 7626–7644. https://doi.org/10.1074/jbc.M112.408294.
[271] H.-H. Kuo, R. Ahmad, G.Q. Lee, C. Gao, H.-R. Chen, Z. Ouyang, M.J. Szucs, D. Kim, A. Tsibris, T.-W. Chun, E. Battivelli, E. Verdin, E.S. Rosenberg, S.A. Carr, X.G. Yu, M. Lichterfeld, Anti-apoptotic Protein BIRC5 Maintains Survival

of HIV-1-Infected CD4+ T Cells, Immunity. 48 (2018) 1183-1194.e5. https://doi.org/10.1016/j.immuni.2018.04.004.
[272] M.H. and A.K. Mansi Saxena, Aurelia Busca, Bacterial DNA-induced antiapoptotic cIAP2 protect human macrophages against HIV- Vpr-mediated mitochondrial membrane depolarization, (n.d.).
[273] A. Busca, M. Saxena, M. Kryworuchko, A. Kumar, Anti-Apoptotic Genes in the Survival of Monocytic Cells During Infection, Curr. Genomics. 10 (2009) 306–317. https://doi.org/10.2174/138920209788920967.
[274] M. Saxena, A. Busca, S. Pandey, M. Kryworuchko, A. Kumar, CpG Protects Human Monocytic Cells against HIV-Vpr–Induced Apoptosis by Cellular Inhibitor of Apoptosis-2 through the Calcium-Activated JNK Pathway in a TLR9-Independent Manner, J. Immunol. 187 (2011) 5865–5878. https://doi.org/10.4049/jimmunol.1100115.
[275] G. Ebert, C. Allison, S. Preston, J. Cooney, J.G. Toe, M.D. Stutz, S. Ojaimi, N. Baschuk, U. Nachbur, J. Torresi, J. Silke, C.G. Begley, M. Pellegrini, Eliminating hepatitis B by antagonizing cellular inhibitors of apoptosis, Proc. Natl. Acad. Sci. 112 (2015) 5803–5808. https://doi.org/10.1073/pnas.1502400112.
[276] M. Dougan, S. Dougan, J. Slisz, B. Firestone, M. Vanneman, D. Draganov, G. Goyal, W. Li, D. Neuberg, R. Blumberg, N. Hacohen, D. Porter, L. Zawel, G. Dranoff, IAP inhibitors enhance co-stimulation to promote tumor immunity, J. Exp. Med. 207 (2010) 2195–2206. https://doi.org/10.1084/jem.20101123.
[277] I.E. Gentle, I. Moelter, N. Lechler, S. Bambach, S. Vucikuja, G. Häcker, P. Aichele, Inhibitor of apoptosis proteins (IAPs) are required for effective T cell expansion/survival during anti-viral immunity in mice., Blood. 123 (2013) 659–669. https://doi.org/10.1182/blood-2013-01-479543.
[278] I. Ezkurdia, D. Juan, J.M. Rodriguez, A. Frankish, M. Diekhans, J. Harrow, J. Vazquez, A. Valencia, M.L. Tress, Multiple evidence strands suggest that there may be as few as 19,000 human protein-coding genes., Hum. Mol. Genet. 23 (2014) 5866–78. https://doi.org/10.1093/hmg/ddu309.
[279] N. Agrawal, P.V.N. Dasaradhi, A. Mohmmed, P. Malhotra, R.K. Bhatnagar, S.K. Mukherjee, RNA interference: mechanism and applications., Mikrobiyol. Bul. 38 (2004) 285–294. https://doi.org/10.1128/MMBR.67.4.657.
[280] M.L. Yeung, L. Houzet, V.S.R.K. Yedavalli, K.-T. Jeang, A Genome-wide Short Hairpin RNA Screening of Jurkat T-cells for Human Proteins Contributing to Productive HIV-1 Replication, J. Biol. Chem. 284 (2009) 19463–19473. https://doi.org/10.1074/jbc.M109.010033.
[281] R. König, Y. Zhou, D. Elleder, T.L. Diamond, G.M.C. Bonamy, J.T. Irelan, C. Chiang, B.P. Tu, P.D. De Jesus, C.E. Lilley, S. Seidel, A.M. Opaluch, J.S. Caldwell, M.D. Weitzman, K.L. Kuhen, S. Bandyopadhyay, T. Ideker, A.P. Orth, L.J. Miraglia, F.D. Bushman, J.A. Young, S.K. Chanda, Global Analysis of Host-Pathogen Interactions that Regulate Early-Stage HIV-1 Replication, Cell. 135 (2008) 49–60. https://doi.org/10.1016/j.cell.2008.07.032.
[282] F.D. Bushman, N. Malani, J. Fernandes, I. D'Orso, G. Cagney, T.L. Diamond, H. Zhou, D.J. Hazuda, A.S. Espeseth, R. König, S. Bandyopadhyay, T. Ideker, S.P. Goff, N.J. Krogan, A.D. Frankel, J.A.T. Young, S.K. Chanda, Host Cell Factors in HIV Replication: Meta-Analysis of Genome-Wide Studies, PLoS Pathog. 5 (2009) e1000437. https://doi.org/10.1371/journal.ppat.1000437.

[283] A.L. Brass, D.M. Dykxhoorn, Y. Benita, N. Yan, A. Engelman, R.J. Xavier, J. Lieberman, S.J. Elledge, Identification of Host Proteins Required for HIV Infection Through a Functional Genomic Screen, Science (80-.). 319 (2008) 921–926. https://doi.org/10.1126/science.1152725.
[284] J.M. Paul, B. Toosi, F.S. Vizeacoumar, K.K. Bhanumathy, Y. Li, C. Gerger, A. El Zawily, T. Freywald, D.H. Anderson, D. Mousseau, R. Kanthan, Z. Zhang, F.J. Vizeacoumar, A. Freywald, Targeting synthetic lethality between the SRC kinase and the EPHB6 receptor may benefit cancer treatment., Oncotarget. 7 (2016) 50027–50042. https://doi.org/10.18632/oncotarget.10569.
[285] F.J. Vizeacoumar, R. Arnold, F.S. Vizeacoumar, M. Chandrashekhar, A. Buzina, J.T.F. Young, J.H.M. Kwan, A. Sayad, P. Mero, S. Lawo, H. Tanaka, K.R. Brown, A. Baryshnikova, A.B. Mak, Y. Fedyshyn, Y. Wang, G.C. Brito, D. Kasimer, T. Makhnevych, T. Ketela, A. Datti, M. Babu, A. Emili, L. Pelletier, J. Wrana, Z. Wainberg, P.M. Kim, R. Rottapel, C.A. O'Brien, B. Andrews, C. Boone, J. Moffat, A negative genetic interaction map in isogenic cancer cell lines reveals cancer cell vulnerabilities, Mol. Syst. Biol. 9 (2013). https://doi.org/10.1038/msb.2013.54.
[286] H. Song, P.-C. Yang, Construction of shRNA lentiviral vector, N. Am. J. Med. Sci. 2 (2010) 598–601. https://doi.org/10.4297/najms.2010.2598.
[287] L. Zhang, Q. Zhou, CRISPR/Cas technology: a revolutionary approach for genome engineering, Sci. China Life Sci. 57 (2014) 639–640. https://doi.org/10.1007/s11427-014-4670-x.
[288] G. Herbein, A. Coaquette, D. Perez-Bercoff, G. Pancino, Macrophage activation and HIV infection: can the Trojan horse turn into a fortress?, Curr. Mol. Med. 2 (2002) 723–38. http://www.ncbi.nlm.nih.gov/pubmed/12462393.
[289] R.C. Wilson, J.A. Doudna, Molecular Mechanisms of RNA Interference, Annu. Rev. Biophys. 42 (2013) 217–239. https://doi.org/10.1146/annurev-biophys-083012-130404.
[290] S. Dokka, D. Toledo, X. Shi, J. Ye, Y. Rojanasakul, High-efficiency gene transfection of macrophages by lipoplexes., Int. J. Pharm. 206 (2000) 97–104. http://www.ncbi.nlm.nih.gov/pubmed/11058814.
[291] A.-A. Keller, M.B. Maeß, M. Schnoor, B. Scheiding, S. Lorkowski, Transfecting Macrophages, in: Methods Mol. Biol. B. Ser., 2018: pp. 187–195. https://doi.org/10.1007/978-1-4939-7837-3_18.
[292] J.M. Gottesfeld, J.M. Turner, P.B. Dervan, Chemical approaches to control gene expression., Gene Expr. 9 (2000) 77–91. http://www.ncbi.nlm.nih.gov/pubmed/11097426.
[293] W. Hübner, P. Chen, A. Del Portillo, Y. Liu, R.E. Gordon, B.K. Chen, W. Hubner, P. Chen, A.D. Portillo, Y. Liu, R.E. Gordon, B.K. Chen, Sequence of human immunodeficiency virus type 1 (HIV-1) Gag localization and oligomerization monitored with live confocal imaging of a replication-competent, fluorescently tagged HIV-1., J. Virol. 81 (2007) 12596–607. https://doi.org/10.1128/JVI.01088-07.
[294] M. Imbeault, R. Lodge, M. Ouellet, M.J. Tremblay, Efficient magnetic bead-based separation of HIV-1-infected cells using an improved reporter virus system reveals that p53 up-regulation occurs exclusively in the virus-expressing cell population, Virology. 393 (2009) 160–167.

https://doi.org/10.1016/j.virol.2009.07.009.
[295] M.D. Stuchell, J.E. Garrus, B. Müller, K.M. Stray, S. Ghaffarian, R. McKinnon, H.-G. Kräusslich, S.G. Morham, W.I. Sundquist, The Human Endosomal Sorting Complex Required for Transport (ESCRT-I) and Its Role in HIV-1 Budding, J. Biol. Chem. 279 (2004) 36059–36071. https://doi.org/10.1074/jbc.M405226200.
[296] B.M. Dale, G.P. McNerney, W. Hübner, T.R. Huser, B.K. Chen, Tracking and quantitation of fluorescent HIV during cell-to-cell transmission, Methods. 53 (2011) 20–26. https://doi.org/10.1016/j.ymeth.2010.06.018.
[297] S. Padilla-Parra, M. Marin, N. Gahlaut, R. Suter, N. Kondo, G.B. Melikyan, Fusion of Mature HIV-1 Particles Leads to Complete Release of a Gag-GFP-Based Content Marker and Raises the Intraviral pH, PLoS One. 8 (2013) e71002. https://doi.org/10.1371/journal.pone.0071002.
[298] C.U.T. Hellen, Internal ribosome entry sites in eukaryotic mRNA molecules, Genes Dev. 15 (2001) 1593–1612. https://doi.org/10.1101/gad.891101.
[299] R. Terrasse, M. Memmi, S. Palle, L. Heyndrickx, G. Vanham, B. Pozzetto, T. Bourlet, Visualization of X4- and R5-Tropic HIV-1 Viruses Expressing Fluorescent Proteins in Human Endometrial Cells: Application to Tropism Study, PLoS One. 12 (2017) e0169453. https://doi.org/10.1371/journal.pone.0169453.
[300] J.-F. Bolduc, M. Ouellet, L. Hany, M.J. Tremblay, Toll-Like Receptor 2 Ligation Enhances HIV-1 Replication in Activated CCR6 + CD4 + T Cells by Increasing Virus Entry and Establishing a More Permissive Environment to Infection, J. Virol. 91 (2017) 1–15. https://doi.org/10.1128/JVI.01402-16.
[301] S. Rao, R. Amorim, M. Niu, Y. Breton, M.J. Tremblay, A.J. Mouland, Host mRNA decay proteins influence HIV-1 replication and viral gene expression in primary monocyte-derived macrophages, Retrovirology. 16 (2019) 3. https://doi.org/10.1186/s12977-019-0465-2.
[302] F.R. Bertani, P. Mozetic, M. Fioramonti, M. Iuliani, G. Ribelli, F. Pantano, D. Santini, G. Tonini, M. Trombetta, L. Businaro, S. Selci, A. Rainer, Classification of M1/M2-polarized human macrophages by label-free hyperspectral reflectance confocal microscopy and multivariate analysis, Sci. Rep. 7 (2017) 8965. https://doi.org/10.1038/s41598-017-08121-8.
[303] N. Gajanayaka, S. O'Hara, Y. Konarski, J. Fernandes, K. Muthumani, M. Kozlowski, J.B. Angel, A. Kumar, HIV and HIV-tat inhibit LPS-induced IL-27 production in human macrophages by distinct intracellular signaling pathways, J. Leukoc. Biol. 102 (2017) 1–16. https://doi.org/10.1189/jlb.4A0716-332RR.
[304] J.R. Fernandes, T.K. Berthoud, A. Kumar, J.B. Angel, IL-23 signaling in Th17 cells is inhibited by HIV infection and is not restored by HAART: Implications for persistent immune activation, PLoS One. 12 (2017) e0186823. https://doi.org/10.1371/journal.pone.0186823.
[305] M. Imbeault, K. Giguère, M. Ouellet, M.J. Tremblay, Exon Level Transcriptomic Profiling of HIV-1-Infected CD4+ T Cells Reveals Virus-Induced Genes and Host Environment Favorable for Viral Replication, PLoS Pathog. 8 (2012). https://doi.org/10.1371/journal.ppat.1002861.
[306] O.L.C. Wijburg, G.P.J.M. van den Dobbelsteen, J. Vadolas, A. Sanders, R.A. Strugnell, N. van Rooijen, The role of macrophages in the induction and regulation of immunity elicited by exogenous antigens, Eur. J. Immunol. 28 (1998) 479–487. https://doi.org/10.1002/(SICI)1521-

4141(199802)28:02<479::AID-IMMU479>3.0.CO;2-R.
[307] S. Gordon, The role of the macrophage in immune regulation, Res. Immunol. 149 (1998) 685–688. https://doi.org/10.1016/S0923-2494(99)80039-X.
[308] S.-Y. Park, M.-Y. Jung, S.-J. Lee, K.-B. Kang, A. Gratchev, V. Riabov, J. Kzhyshkowska, I.-S. Kim, Stabilin-1 mediates phosphatidylserine-dependent clearance of cell corpses in alternatively activated macrophages, J. Cell Sci. 122 (2009) 3365–3373. https://doi.org/10.1242/jcs.049569.
[309] T.A. Wynn, K.M. Vannella, Macrophages in Tissue Repair, Regeneration, and Fibrosis, Immunity. 44 (2016) 450–462. https://doi.org/10.1016/j.immuni.2016.02.015.
[310] Y. Chen, X. Zhang, Pivotal regulators of tissue homeostasis and cancer: macrophages, Exp. Hematol. Oncol. 6 (2017) 23. https://doi.org/10.1186/s40164-017-0083-4.
[311] O. Krysko, G. Holtappels, N. Zhang, M. Kubica, K. Deswarte, L. Derycke, S. Claeys, H. Hammad, G.G. Brusselle, P. Vandenabeele, D. V. Krysko, C. Bachert, Alternatively activated macrophages and impaired phagocytosis of S. aureus in chronic rhinosinusitis, Allergy. 66 (2011) 396–403. https://doi.org/10.1111/j.1398-9995.2010.02498.x.
[312] R. Firszt, B. Vickery, An Interferon-Inducible Neutrophil-Driven Blood Transcriptional Signature in Human Tuberculosis, Pediatrics. 128 (2011) S145–S146. https://doi.org/10.1542/peds.2011-2107LLLL.
[313] D. Montoya, D. Cruz, R.M.B. Teles, D.J. Lee, M.T. Ochoa, S.R. Krutzik, R. Chun, M. Schenk, X. Zhang, B.G. Ferguson, A.E. Burdick, E.N. Sarno, T.H. Rea, M. Hewison, J.S. Adams, G. Cheng, R.L. Modlin, Divergence of Macrophage Phagocytic and Antimicrobial Programs in Leprosy, Cell Host Microbe. 6 (2009) 343–353. https://doi.org/10.1016/j.chom.2009.09.002.
[314] M. Quiding-Järbrink, S. Raghavan, M. Sundquist, Enhanced M1 Macrophage Polarization in Human Helicobacter pylori-Associated Atrophic Gastritis and in Vaccinated Mice, PLoS One. 5 (2010) e15018. https://doi.org/10.1371/journal.pone.0015018.
[315] J.-L. Mège, V. Mehraj, C. Capo, Macrophage polarization and bacterial infections, Curr. Opin. Infect. Dis. 24 (2011) 230–234. https://doi.org/10.1097/QCO.0b013e328344b73e.
[316] L.J. Thompson, S.J. Dunstan, C. Dolecek, T. Perkins, D. House, G. Dougan, N.T. Hue, T.T. Phi La, D.C. Du, L.T. Phuong, N.T. Dung, T.T. Hien, J.J. Farrar, D. Monack, D.J. Lynn, S.J. Popper, S. Falkow, Transcriptional response in the peripheral blood of patients infected with Salmonella enterica serovar Typhi, Proc. Natl. Acad. Sci. 106 (2009) 22433–22438. https://doi.org/10.1073/pnas.0912386106.
[317] L. Parisi, E. Gini, D. Baci, M. Tremolati, M. Fanuli, B. Bassani, G. Farronato, A. Bruno, L. Mortara, Macrophage Polarization in Chronic Inflammatory Diseases: Killers or Builders?, J. Immunol. Res. 2018 (2018) 1–25. https://doi.org/10.1155/2018/8917804.
[318] A. Shapouri-Moghaddam, S. Mohammadian, H. Vazini, M. Taghadosi, S.-A. Esmaeili, F. Mardani, B. Seifi, A. Mohammadi, J.T. Afshari, A. Sahebkar, Macrophage plasticity, polarization, and function in health and disease, J. Cell. Physiol. 233 (2018) 6425–6440. https://doi.org/10.1002/jcp.26429.

[319] M. Ponzoni, F. Pastorino, D. Di Paolo, P. Perri, C. Brignole, Targeting Macrophages as a Potential Therapeutic Intervention: Impact on Inflammatory Diseases and Cancer, Int. J. Mol. Sci. 19 (2018) 1953. https://doi.org/10.3390/ijms19071953.
[320] P. Hadji, R. Coleman, M. Gnant, J. Green, The impact of menopause on bone, zoledronic acid, and implications for breast cancer growth and metastasis, Ann. Oncol. 23 (2012) 2782–2790. https://doi.org/10.1093/annonc/mds169.
[321] A. Sica, A. Mantovani, Macrophage plasticity and polarization: in vivo veritas, J. Clin. Invest. 122 (2012) 787–795. https://doi.org/10.1172/JCI59643.
[322] M. Koren-Gluzer, M. Rosenblat, T. Hayek, Paraoxonase 2 Induces a Phenotypic Switch in Macrophage Polarization Favoring an M2 Anti-Inflammatory State, Int. J. Endocrinol. 2015 (2015) 1–9. https://doi.org/10.1155/2015/915243.
[323] F. Porcheray, S. Viaud, A.-C. Rimaniol, C. Léone, B. Samah, N. Dereuddre-Bosquet, D. Dormont, G. Gras, Macrophage activation switching: an asset for the resolution of inflammation., Clin. Exp. Immunol. 142 (2005) 481–9. https://doi.org/10.1111/j.1365-2249.2005.02934.x.
[324] W.A. Weiss, S.S. Taylor, K.M. Shokat, Recognizing and exploiting differences between RNAi and small-molecule inhibitors, Nat. Chem. Biol. 3 (2007) 739–744. https://doi.org/10.1038/nchembio1207-739.
[325] D. Ovcharenko, K. Kelnar, C. Johnson, N. Leng, D. Brown, Genome-Scale MicroRNA and Small Interfering RNA Screens Identify Small RNA Modulators of TRAIL-Induced Apoptosis Pathway, Cancer Res. 67 (2007) 10782–10788. https://doi.org/10.1158/0008-5472.CAN-07-1484.
[326] Y. Xia, B. Gates, Y. Yin, Building complex structures from monodisperse spherical colloids, Aust. J. Chem. 54 (2001) 287–290. https://doi.org/10.1071/CH01098.
[327] T. Stroh, U. Erben, A.A. Kühl, M. Zeitz, B. Siegmund, Combined Pulse Electroporation – A Novel Strategy for Highly Efficient Transfection of Human and Mouse Cells, PLoS One. 5 (2010) e9488. https://doi.org/10.1371/journal.pone.0009488.
[328] S. Spagnou, A.D. Miller, M. Keller, Lipidic Carriers of siRNA: Differences in the Formulation, Cellular Uptake, and Delivery with Plasmid DNA †, Biochemistry. 43 (2004) 13348–13356. https://doi.org/10.1021/bi048950a.
[329] M. Breunig, U. Lungwitz, R. Liebl, A. Goepferich, Breaking up the correlation between efficacy and toxicity for nonviral gene delivery, Proc. Natl. Acad. Sci. U. S. A. 104 (2007) 14454–14459. https://doi.org/10.1073/pnas.0703882104.
[330] A. Reynolds, Induction of the interferon response by siRNA is cell type- and duplex length-dependent, RNA. 12 (2006) 988–993. https://doi.org/10.1261/rna.2340906.
[331] P. Guha, A. Dey, R. Sen, M. Chatterjee, S. Chattopadhyay, S.K. Bandyopadhyay, Intracellular GSH Depletion Triggered Mitochondrial Bax Translocation to Accomplish Resveratrol-Induced Apoptosis in the U937 Cell Line, J. Pharmacol. Exp. Ther. 336 (2011) 206–214. https://doi.org/10.1124/jpet.110.171983.
[332] A. Single, H. Beetham, B.J. Telford, P. Guilford, A. Chen, A Comparison of Real-Time and Endpoint Cell Viability Assays for Improved Synthetic Lethal Drug

Validation, J. Biomol. Screen. 20 (2015) 1286–1293. https://doi.org/10.1177/1087057115605765.
[333] Y. Li, J. Yuan, Systematic Metrics Depicting Cell Death Kinetics, Cell Chem. Biol. 24 (2017) 785–786. https://doi.org/10.1016/j.chembiol.2017.07.006.
[334] L. Liu, N.M.M. Oliveira, K.M. Cheney, C. Pade, H. Dreja, A.-M.H. Bergin, V. Borgdorff, D.H. Beach, C.L. Bishop, M.T. Dittmar, Á. McKnight, A whole genome screen for HIV restriction factors, Retrovirology. 8 (2011) 94. https://doi.org/10.1186/1742-4690-8-94.
[335] M. Chemudupati, A.D. Kenney, S. Bonifati, A. Zani, T.M. McMichael, L. Wu, J.S. Yount, From APOBEC to ZAP: Diverse mechanisms used by cellular restriction factors to inhibit virus infections, Biochim. Biophys. Acta - Mol. Cell Res. 1866 (2019) 382–394. https://doi.org/10.1016/j.bbamcr.2018.09.012.
[336] S.M. Tietz, M. Berghoff, Gene silencing of MK2 in hard-to-transfect human U937 cells., J. Biomol. Tech. 23 (2012) 47–50. https://doi.org/10.7171/jbt.12-2302-005.
[337] S. Mehrotra, I. Lee, C. Chan, Multilayer mediated forward and patterned siRNA transfection using linear-PEI at extended N/P ratios, Acta Biomater. 5 (2009) 1474–1488. https://doi.org/10.1016/j.actbio.2009.01.004.
[338] E. Iorns, C.J. Lord, A. Ashworth, Parallel RNAi and compound screens identify the PDK1 pathway as a target for tamoxifen sensitization, Biochem. J. 417 (2009) 361–371. https://doi.org/10.1042/BJ20081682.
[339] R.C. Pink, P. Samuel, D. Massa, D.P. Caley, S.A. Brooks, D. Raul, F. Carter, The passenger strand, miR-21-3p, plays a role in mediating cisplatin resistance in ovarian cancer cells, Gynecol. Oncol. 137 (2015) 143–151. https://doi.org/http://dx.doi.org/10.1016/j.ygyno.2014.12.042.
[340] S.P. Tsofack, C. Garand, C. Sereduk, D. Chow, M. Aziz, D. Guay, H.H. Yin, M. Lebel, NONO and RALY proteins are required for YB-1 oxaliplatin induced resistance in colon adenocarcinoma cell lines, Mol. Cancer. 10 (2011) 145. https://doi.org/10.1186/1476-4598-10-145.
[341] P.J. Ellery, E. Tippett, Y.-L. Chiu, G. Paukovics, P.U. Cameron, A. Solomon, S.R. Lewin, P.R. Gorry, A. Jaworowski, W.C. Greene, S. Sonza, S.M. Crowe, The CD16 + Monocyte Subset Is More Permissive to Infection and Preferentially Harbors HIV-1 In Vivo, J. Immunol. 178 (2007) 6581–6589. https://doi.org/10.4049/jimmunol.178.10.6581.
[342] S. Sonza, H.P. Mutimer, R. Oelrichs, D. Jardine, K. Harvey, A. Dunne, D.F. Purcell, C. Birch, S.M. Crowe, Monocytes harbour replication-competent, non-latent HIV-1 in patients on highly active antiretroviral therapy, AIDS. 15 (2001) 17–22. https://doi.org/10.1097/00002030-200101050-00005.
[343] J.B. Honeycutt, A. Wahl, C. Baker, R.A. Spagnuolo, J. Foster, O. Zakharova, S. Wietgrefe, C. Caro-Vegas, V. Madden, G. Sharpe, A.T. Haase, J.J. Eron, J.V. Garcia, Macrophages sustain HIV replication in vivo independently of T cells, J. Clin. Invest. 126 (2016) 1353–1366. https://doi.org/10.1172/JCI84456.
[344] L. Redel, V. Le Douce, T. Cherrier, C. Marban, A. Janossy, D. Aunis, C. Van Lint, O. Rohr, C. Schwartz, HIV-1 regulation of latency in the monocyte-macrophage lineage and in CD4+ T lymphocytes, J. Leukoc. Biol. 87 (2010) 575–588. https://doi.org/10.1189/jlb.0409264.
[345] S.M. Crowe, S. Sonza, HIV-1 can be recovered from a variety of cells including

peripheral blood monocytes of patients receiving highly active antiretroviral therapy: a further obstacle to eradication., J. Leukoc. Biol. 68 (2000) 345–50. http://www.ncbi.nlm.nih.gov/pubmed/10985250.
[346] M. Araínga, B. Edagwa, R.L. Mosley, L.Y. Poluektova, S. Gorantla, H.E. Gendelman, A mature macrophage is a principal HIV-1 cellular reservoir in humanized mice after treatment with long acting antiretroviral therapy, Retrovirology. 14 (2017) 17. https://doi.org/10.1186/s12977-017-0344-7.
[347] S.A. Yukl, E. Sinclair, M. Somsouk, P.W. Hunt, L. Epling, M. Killian, V. Girling, P. Li, D. V. Havlir, S.G. Deeks, J.K. Wong, H. Hatano, A comparison of methods for measuring rectal HIV levels suggests that HIV DNA resides in cells other than CD4+ T cells, including myeloid cells, AIDS. 28 (2014) 439–442. https://doi.org/10.1097/QAD.0000000000000166.
[348] P.D. Smith, G. Meng, J.F. Salazar-Gonzalez, G.M. Shaw, Macrophage HIV-1 infection and the gastrointestinal tract reservoir, J. Leukoc. Biol. 74 (2003) 642–649. https://doi.org/10.1189/jlb.0503219.
[349] F. González-Scarano, J. Martín-García, The neuropathogenesis of AIDS, Nat. Rev. Immunol. 5 (2005) 69–81. https://doi.org/10.1038/nri1527.
[350] T. Igarashi, C.R. Brown, Y. Endo, A. Buckler-White, R. Plishka, N. Bischofberger, V. Hirsch, M.A. Martin, Macrophage are the principal reservoir and sustain high virus loads in rhesus macaques after the depletion of CD4+ T cells by a highly pathogenic simian immunodeficiency virus/HIV type 1 chimera (SHIV): Implications for HIV-1 infections of humans, Proc. Natl. Acad. Sci. 98 (2001) 658–663. https://doi.org/10.1073/pnas.98.2.658.
[351] S. Aquaro, P. Bagnarelli, T. Guenci, A. De Luca, M. Clementi, E. Balestra, R. Caliò, C.-F. Perno, Long-term survival and virus production in human primary macrophages infected by human immunodeficiency virus, J. Med. Virol. 68 (2002) 479–488. https://doi.org/10.1002/jmv.10245.
[352] P. Mlcochova, K.A. Sutherland, S.A. Watters, C. Bertoli, R.A. Bruin, J. Rehwinkel, S.J. Neil, G.M. Lenzi, B. Kim, A. Khwaja, M.C. Gage, C. Georgiou, A. Chittka, S. Yona, M. Noursadeghi, G.J. Towers, R.K. Gupta, A G1-like state allows HIV -1 to bypass SAMHD 1 restriction in macrophages , EMBO J. 36 (2017) 604–616. https://doi.org/10.15252/embj.201696025.
[353] C.M. Coleman, L. Wu, HIV interactions with monocytes and dendritic cells: Viral latency and reservoirs, Retrovirology. 6 (2009) 1–12. https://doi.org/10.1186/1742-4690-6-51.
[354] M.J. McElrath, R.M. Steinman, Z.A. Cohn, Latent HIV-1 infection in enriched populations of blood monocytes and T cells from seropositive patients, J. Clin. Invest. 87 (1991) 27–30. https://doi.org/10.1172/JCI114981.
[355] L. Gillim-Ross, A. Cara, M.E. Klotman, HIV-1 extrachromosomal 2-LTR circular DNA is long-lived in human macrophages, Viral Immunol. 18 (2005) 190–196. https://doi.org/10.1089/vim.2005.18.190.
[356] P. Delobel, K. Sandres-Sauné, M. Cazabat, F.E. L'Faqihi, C. Aquilina, M. Obadia, C. Pasquier, B. Marchou, P. Massip, J. Izopet, Persistence of distinct HIV-1 populations in blood monocytes and naive and memory CD4 T cells during prolonged suppressive HAART, Aids. 19 (2005) 1739–1750. https://doi.org/10.1097/01.aids.0000183125.93958.26.
[357] T. Zhu, D. Muthui, S. Holte, D. Nickle, F. Feng, S. Brodie, Y. Hwangbo, J.I.

Mullins, L. Corey, Evidence for Human Immunodeficiency Virus Type 1 Replication In Vivo in CD14+ Monocytes and Its Potential Role as a Source of Virus in Patients on Highly Active Antiretroviral Therapy, J. Virol. 76 (2002) 707–716. https://doi.org/10.1128/jvi.76.2.707-716.2002.
[358] S. Pang, Y. Koyanagi, S. Miles, C. Wiley, H. V. Vinters, I.S.Y. Chen, High levels of unintegrated HIV-1 DNA in brain tissue of AIDS dementia patients, Nature. 343 (1990) 85–89. https://doi.org/10.1038/343085a0.
[359] S.A. Watters, P. Mlcochova, R.K. Gupta, Macrophages: The neglected barrier to eradication, Curr. Opin. Infect. Dis. 26 (2013) 561–566. https://doi.org/10.1097/QCO.0000000000000014.
[360] J. Inlora, V. Chukkapalli, S. Bedi, A. Ono, Molecular Determinants Directing HIV-1 Gag Assembly to Virus-Containing Compartments in Primary Macrophages, J. Virol. 90 (2016) 8509–8519. https://doi.org/10.1128/JVI.01004-16.
[361] F. Graziano, E. Vicenzi, G. Poli, Immuno-Pharmacological Targeting of Virus-Containing Compartments in HIV-1-Infected Macrophages, Trends Microbiol. 24 (2016) 558–567. https://doi.org/10.1016/j.tim.2016.02.018.
[362] C.J.A. Duncan, J.P. Williams, T. Schiffner, K. Gartner, C. Ochsenbauer, J. Kappes, R.A. Russell, J. Frater, Q.J. Sattentau, High-Multiplicity HIV-1 Infection and Neutralizing Antibody Evasion Mediated by the Macrophage-T Cell Virological Synapse, J. Virol. 88 (2014) 2025–2034. https://doi.org/10.1128/JVI.03245-13.
[363] H. Koppensteiner, C. Banning, C. Schneider, H. Hohenberg, M. Schindler, Macrophage Internal HIV-1 Is Protected from Neutralizing Antibodies, J. Virol. 86 (2012) 2826–2836. https://doi.org/10.1128/JVI.05915-11.
[364] N. Sharova, C. Swingler, M. Sharkey, M. Stevenson, Macrophages archive HIV-1 virions for dissemination in trans, EMBO J. 24 (2005) 2481–2489. https://doi.org/10.1038/sj.emboj.7600707.
[365] C.R. Avalos, C.M. Abreu, S.E. Queen, M. Li, S. Price, E.N. Shirk, E.L. Engle, E. Forsyth, B.T. Bullock, F. Mac Gabhann, S.W. Wietgrefe, A.T. Haase, M.C. Zink, J.L. Mankowski, J.E. Clements, L. Gama, Brain macrophages in simian immunodeficiency virus-infected, antiretroviral-suppressed macaques: A functional latent reservoir, MBio. 8 (2017) 1–16. https://doi.org/10.1128/mBio.01186-17.
[366] J.J. Cenker, R.D. Stultz, D. McDonald, Brain Microglial Cells Are Highly Susceptible to HIV-1 Infection and Spread, AIDS Res. Hum. Retroviruses. 33 (2017) 1155–1165. https://doi.org/10.1089/aid.2017.0004.
[367] J. Hassan, K. Browne, C. De Gascun, HIV-1 in Monocytes and Macrophages: An Overlooked Reservoir?, Viral Immunol. 29 (2016) 532–533. https://doi.org/10.1089/vim.2016.0091.
[368] Q.J. Sattentau, M. Stevenson, Macrophages and HIV-1: An Unhealthy Constellation, Cell Host Microbe. 19 (2016) 304–310. https://doi.org/10.1016/j.chom.2016.02.013.
[369] C.R. Avalos, S.L. Price, E.R. Forsyth, J.N. Pin, E.N. Shirk, B.T. Bullock, S.E. Queen, M. Li, D. Gellerup, S.L. O'Connor, M.C. Zink, J.L. Mankowski, L. Gama, J.E. Clements, Quantitation of Productively Infected Monocytes and Macrophages of Simian Immunodeficiency Virus-Infected Macaques, J. Virol.

90 (2016) 5643–5656. https://doi.org/10.1128/jvi.00290-16.
[370] S.R. Dinapoli, A.M. Ortiz, F. Wu, K. Matsuda, H.L.T. Iii, V.M. Hirsch, K. Knox, J.M. Brenchley, Tissue-resident macrophages can contain replication-competent virus in macaques, JCI Insight. 2 (2017). https://doi.org/10.1172/jci.insight.91214.
[371] M. Stevenson, HIV persistence in macrophages, Nat. Med. 23 (2017) 538–539. https://doi.org/10.1038/nm.4337.
[372] K.M. Bruner, N.N. Hosmane, R.F. Siliciano, Towards an HIV-1 cure: measuring the latent reservoir, Trends Microbiol. 23 (2015) 192–203. https://doi.org/10.1016/j.tim.2015.01.013.
[373] A.J. Murray, K.J. Kwon, D.L. Farber, R.F. Siliciano, The Latent Reservoir for HIV-1: How Immunologic Memory and Clonal Expansion Contribute to HIV-1 Persistence, J. Immunol. 197 (2016) 407–417. https://doi.org/10.4049/jimmunol.1600343.
[374] J.D. Siliciano, R.F. Siliciano, HIV-1 eradication strategies: Design and assessment, Curr. Opin. HIV AIDS. 8 (2013) 318–325. https://doi.org/10.1097/COH.0b013e328361eaca.
[375] G.R. Campbell, R.S. Bruckman, Y.-L. Chu, R.N. Trout, S.A. Spector, SMAC Mimetics Induce Autophagy-Dependent Apoptosis of HIV-1-Infected Resting Memory CD4+ T Cells, Cell Host Microbe. 24 (2018) 689-702.e7. https://doi.org/10.1016/j.chom.2018.09.007.
[376] G. Ebert, S. Preston, C. Allison, J. Cooney, J.G. Toe, M.D. Stutz, S. Ojaimi, H.W. Scott, N. Baschuk, U. Nachbur, J. Torresi, R. Chin, D. Colledge, X. Li, N. Warner, P. Revill, S. Bowden, J. Silke, C.G. Begley, M. Pellegrini, Cellular inhibitor of apoptosis proteins prevent clearance of hepatitis B virus, Proc. Natl. Acad. Sci. 112 (2015) 5797–5802. https://doi.org/10.1073/pnas.1502390112.
[377] A. Busca, M. Saxena, A. Kumar, Critical Role for Antiapoptotic Bcl-xL and Mcl-1 in Human Macrophage Survival and Cellular IAP1/2 (cIAP1/2) in Resistance to HIV-Vpr-induced Apoptosis, J. Biol. Chem. 287 (2012) 15118–15133. https://doi.org/10.1074/jbc.M111.312660.
[378] R. Feltham, B. Bettjeman, R. Budhidarmo, P.D. Mace, S. Shirley, S.M. Condon, S.K. Chunduru, M.A. McKinlay, D.L. Vaux, J. Silke, C.L. Day, Smac Mimetics Activate the E3 Ligase Activity of cIAP1 Protein by Promoting RING Domain Dimerization, J. Biol. Chem. 286 (2011) 17015–17028. https://doi.org/10.1074/jbc.M111.222919.
[379] E.C. Dueber, A.J. Schoeffler, A. Lingel, J.M. Elliott, A. V. Fedorova, A.M. Giannetti, K. Zobel, B. Maurer, E. Varfolomeev, P. Wu, H.J.A. Wallweber, S.G. Hymowitz, K. Deshayes, D. Vucic, W.J. Fairbrother, Antagonists Induce a Conformational Change in cIAP1 That Promotes Autoubiquitination, Science (80-.). 334 (2011) 376–380. https://doi.org/10.1126/science.1207862.
[380] A. Busca, Y. Konarski, N. Gajanayaka, S. O'Hara, J. Angel, M. Kozlowski, A. Kumar, cIAP1/2–TRAF2–SHP-1–Src–MyD88 Complex Regulates Lipopolysaccharide-Induced IL-27 Production through NF-κB Activation in Human Macrophages, J. Immunol. (2018) ji1700199. https://doi.org/10.4049/jimmunol.1700199.
[381] M.S. Meltzer, D.R. Skillman, D.L. Hoover, B.D. Hanson, J.A. Turpin, D.C. Kalter, H.E. Gendelman, Macrophages and the human immunodeficiency virus.,

Immunol. Today. 11 (1990) 217–23. http://www.ncbi.nlm.nih.gov/pubmed/2191685.
[382] T.M. Folks, K.A. Clouse, J. Justement, A. Rabson, E. Duh, J.H. Kehrl, A.S. Fauci, Tumor necrosis factor alpha induces expression of human immunodeficiency virus in a chronically infected T-cell clone., Proc. Natl. Acad. Sci. 86 (1989) 2365–2368. https://doi.org/10.1073/pnas.86.7.2365.
[383] S.Z. Khan, N. Hand, S.L. Zeichner, Apoptosis-induced activation of HIV-1 in latently infected cell lines, Retrovirology. 12 (2015) 1–19. https://doi.org/10.1186/s12977-015-0169-1.
[384] S.L. Petersen, L. Wang, A. Yalcin-Chin, L. Li, M. Peyton, J. Minna, P. Harran, X. Wang, Autocrine TNFα Signaling Renders Human Cancer Cells Susceptible to Smac-Mimetic-Induced Apoptosis, Cancer Cell. 12 (2007) 445–456. https://doi.org/10.1016/j.ccr.2007.08.029.
[385] J.E. Vince, W.W.-L. Wong, N. Khan, R. Feltham, D. Chau, A.U. Ahmed, C.A. Benetatos, S.K. Chunduru, S.M. Condon, M. McKinlay, R. Brink, M. Leverkus, V. Tergaonkar, P. Schneider, B.A. Callus, F. Koentgen, D.L. Vaux, J. Silke, IAP Antagonists Target cIAP1 to Induce TNFα-Dependent Apoptosis, Cell. 131 (2007) 682–693. https://doi.org/10.1016/j.cell.2007.10.037.
[386] M. El-Mesery, M.E. Shaker, A. Elgaml, The SMAC mimetic BV6 induces cell death and sensitizes different cell lines to TNF-α and TRAIL-induced apoptosis, Exp. Biol. Med. 241 (2016) 2015–2022. https://doi.org/10.1177/1535370216661779.
[387] B.L. Probst, L. Liu, V. Ramesh, L. Li, H. Sun, J.D. Minna, L. Wang, Smac mimetics increase cancer cell response to chemotherapeutics in a TNF-α-dependent manner, Cell Death Differ. 17 (2010) 1645–1654. https://doi.org/10.1038/cdd.2010.44.
[388] S.T. Beug, H.H. Cheung, E.C. LaCasse, R.G. Korneluk, Modulation of immune signalling by inhibitors of apoptosis, Trends Immunol. 33 (2012) 535–545. https://doi.org/10.1016/j.it.2012.06.004.
[389] M.J.M. Bertrand, K. Doiron, K. Labbé, R.G. Korneluk, P.A. Barker, M. Saleh, Cellular Inhibitors of Apoptosis cIAP1 and cIAP2 Are Required for Innate Immunity Signaling by the Pattern Recognition Receptors NOD1 and NOD2, Immunity. 30 (2009) 789–801. https://doi.org/10.1016/j.immuni.2009.04.011.
[390] F. Humphries, S. Yang, B. Wang, P.N. Moynagh, RIP kinases: key decision makers in cell death and innate immunity, Cell Death Differ. 22 (2015) 225–236. https://doi.org/10.1038/cdd.2014.126.
[391] R.N. Wagner, J.C. Reed, S.K. Chanda, HIV-1 protease cleaves the serine-threonine kinases RIPK1 and RIPK2, Retrovirology. 12 (2015) 74. https://doi.org/10.1186/s12977-015-0200-6.
[392] J.E. Vince, D. Pantaki, R. Feltham, P.D. Mace, S.M. Cordier, A.C. Schmukle, A.J. Davidson, B.A. Callus, W.W.-L. Wong, I.E. Gentle, H. Carter, E.F. Lee, H. Walczak, C.L. Day, D.L. Vaux, J. Silke, TRAF2 Must Bind to Cellular Inhibitors of Apoptosis for Tumor Necrosis Factor (TNF) to Efficiently Activate NF-κB and to Prevent TNF-induced Apoptosis, J. Biol. Chem. 284 (2009) 35906–35915. https://doi.org/10.1074/jbc.M109.072256.
[393] S.J. Korsmeyer, M.C. Wei, M. Saito, S. Weiler, K.J. Oh, P.H. Schlesinger, Pro-apoptotic cascade activates BID, which oligomerizes BAK or BAX into pores

that result in the release of cytochrome c, Cell Death Differ. 7 (2000) 1166–1173. https://doi.org/10.1038/sj.cdd.4400783.
[394] J. Geng, Y. Ito, L. Shi, P. Amin, J. Chu, A.T. Ouchida, A.K. Mookhtiar, H. Zhao, D. Xu, B. Shan, A. Najafov, G. Gao, S. Akira, J. Yuan, Regulation of RIPK1 activation by TAK1-mediated phosphorylation dictates apoptosis and necroptosis, Nat. Commun. 8 (2017) 359. https://doi.org/10.1038/s41467-017-00406-w.
[395] Y. Kim, J.L. Anderson, S.R. Lewin, Getting the “Kill” into “Shock and Kill”: Strategies to Eliminate Latent HIV, Cell Host Microbe. 23 (2018) 14–26. https://doi.org/10.1016/j.chom.2017.12.004.
[396] N. Müller-Sienerth, L. Dietz, P. Holtz, M. Kapp, G.U. Grigoleit, C. Schmuck, H. Wajant, D. Siegmund, SMAC Mimetic BV6 Induces Cell Death in Monocytes and Maturation of Monocyte-Derived Dendritic Cells, PLoS One. 6 (2011) e21556. https://doi.org/10.1371/journal.pone.0021556.
[397] R. Azzam, L. Lal, S.-L. Goh, K. Kedzierska, A. Jaworowski, E. Naim, C.L. Cherry, S.L. Wesselingh, J. Mills, S.M. Crowe, Adverse Effects of Antiretroviral Drugs on HIV-1-infected and -uninfected Human Monocyte-derived Macrophages, JAIDS J. Acquir. Immune Defic. Syndr. PAP (2006) 19–28. https://doi.org/10.1097/01.qai.0000214809.83218.88.
[398] C. Tasker, S. Subbian, P. Gao, J. Couret, C. Levine, S. Ghanny, P. Soteropoulos, X. Zhao, N. Landau, W. Lu, T.L. Chang, IFN-ε protects primary macrophages against HIV infection, JCI Insight. 1 (2016) 1–17. https://doi.org/10.1172/jci.insight.88255.
[399] Y. Nitahara-Kasahara, M. Kamata, T. Yamamoto, X. Zhang, Y. Miyamoto, K. Muneta, S. Iijima, Y. Yoneda, Y. Tsunetsugu-Yokota, Y. Aida, Novel Nuclear Import of Vpr Promoted by Importin Is Crucial for Human Immunodeficiency Virus Type 1 Replication in Macrophages, J. Virol. 81 (2007) 5284–5293. https://doi.org/10.1128/JVI.01928-06.
[400] R. Mukerjee, J.R. Chang, L. Del Valle, A. Bagashev, M.M. Gayed, R.B. Lyde, B.J. Hawkins, E. Brailoiu, E. Cohen, C. Power, S.A. Azizi, B.B. Gelman, B.E. Sawaya, Deregulation of microRNAs by HIV-1 Vpr Protein Leads to the Development of Neurocognitive Disorders, J. Biol. Chem. 286 (2011) 34976–34985. https://doi.org/10.1074/jbc.M111.241547.
[401] M.A. Miles, C.J. Hawkins, Mutagenic assessment of chemotherapy and Smac mimetic drugs in cells with defective DNA damage response pathways, Sci. Rep. 8 (2018) 14421. https://doi.org/10.1038/s41598-018-32517-9.
[402] Y.S. Laura C Miller, Macrophage Polarization in Virus-Host Interactions, J. Clin. Cell. Immunol. 06 (2015). https://doi.org/10.4172/2155-9899.1000311.
[403] S.N. Croft, E.J. Walker, R. Ghildyal, Human Rhinovirus 3C protease cleaves RIPK1, concurrent with caspase 8 activation, Sci. Rep. 8 (2018) 1569. https://doi.org/10.1038/s41598-018-19839-4.
[404] Y. Liao, H.-X. Wang, X. Mao, H. Fang, H. Wang, Y. Li, Y. Sun, C. Meng, L. Tan, C. Song, X. Qiu, C. Ding, RIP1 is a central signaling protein in regulation of TNF-α/TRAIL mediated apoptosis and necroptosis during Newcastle disease virus infection, Oncotarget. 8 (2017) 43201–43217. https://doi.org/10.18632/oncotarget.17970.
[405] M. Rothe, M.-G. Pan, W.J. Henzel, T.M. Ayres, D. V. Goeddel, The TNFR2-

TRAF signaling complex contains two novel proteins related to baculoviral inhibitor of apoptosis proteins, Cell. 83 (1995) 1243–1252. https://doi.org/10.1016/0092-8674(95)90149-3.
[406] G. Zybarth, N. Reiling, H. Schmidtmayerova, B. Sherry, M. Bukrinsky, Activation-Induced Resistance of Human Macrophages to HIV-1 Infection In Vitro, J. Immunol. 162 (1999) 400–406. http://www.jimmunol.org/cgi/content/abstract/162/1/400.
[407] M.D. Marsden, J.A. Zack, Eradication of HIV: current challenges and new directions, J. Antimicrob. Chemother. 63 (2008) 7–10. https://doi.org/10.1093/jac/dkn455.
[408] A. Cattin, T.R. Wiche Salinas, A. Gosselin, D. Planas, B. Shacklett, E.A. Cohen, M.P. Ghali, J. Routy, P. Ancuta, HIV-1 is rarely detected in blood and colon myeloid cells during viral-suppressive antiretroviral therapy, AIDS. 33 (2019) 1293–1306. https://doi.org/10.1097/QAD.0000000000002195.
[409] S.G. Hymowitz, H.W. Christinger, G. Fuh, M. Ultsch, M. O'Connell, R.F. Kelley, A. Ashkenazi, A.M. de Vos, Triggering cell death: the crystal structure of Apo2L/TRAIL in a complex with death receptor 5., Mol. Cell. 4 (1999) 563–71. https://doi.org/10.1016/S1097-2765(00)80207-5.
[410] J. Mullenders, R. Bernards, Loss-of-function genetic screens as a tool to improve the diagnosis and treatment of cancer, Oncogene. 28 (2009) 4409–4420. https://doi.org/10.1038/onc.2009.295.
[411] A.S. Chuck, M.F. Clarke, B.O. Palsson, Retroviral infection is limited by Brownian Motion, Hum. GENE Ther. Y. 7 (1996) 1527–1534.
[412] K. Levesque, A. Finzi, J. Binette, E. Cohen, Role of CD4 Receptor Down-regulation During HIV-1 Infection, Curr. HIV Res. 2 (2004) 51–59. https://doi.org/10.2174/1570162043485086.
[413] M. Alfano, G. Vallanti, P. Biswas, C. Bovolenta, E. Vicenzi, B. Mantelli, T. Pushkarsky, R. Rappuoli, A. Lazzarin, M. Bukrinsky, G. Poli, The Binding Subunit of Pertussis Toxin Inhibits HIV Replication in Human Macrophages and Virus Expression in Chronically Infected Promonocytic U1 Cells, J. Immunol. 166 (2001) 1863–1870. https://doi.org/10.4049/jimmunol.166.3.1863.
[414] T. Hart, K.R. Brown, F. Sircoulomb, R. Rottapel, J. Moffat, Measuring error rates in genomic perturbation screens: gold standards for human functional genomics., Mol. Syst. Biol. 10 (2014) 733. https://doi.org/10.15252/msb.20145216.
[415] S. Rana, G. Besson, D.G. Cook, J. Rucker, R.J. Smyth, Y. Yi, J.D. Turner, H.H. Guo, J.G. Du, S.C. Peiper, E. Lavi, M. Samson, F. Libert, C. Liesnard, G. Vassart, R.W. Doms, M. Parmentier, R.G. Collman, Role of CCR5 in infection of primary macrophages and lymphocytes by macrophage-tropic strains of human immunodeficiency virus: resistance to patient-derived and prototype isolates resulting from the delta ccr5 mutation., J. Virol. 71 (1997) 3219–27.
[416] R. Dittmar, E. Potier, M. van Zandvoort, K. Ito, Assessment of Cell Viability in Three-Dimensional Scaffolds Using Cellular Auto-Fluorescence, Tissue Eng. Part C Methods. 18 (2012) 198–204. https://doi.org/10.1089/ten.tec.2011.0334.
[417] Z. Yuan, X. Fan, B. Staitieh, C. Bedi, P. Spearman, D.M. Guidot, R.T. Sadikot, HIV-related proteins prolong macrophage survival through induction of Triggering receptor expressed on myeloid cells-1, Sci. Rep. 7 (2017) 1–10.

https://doi.org/10.1038/srep42028.
[418] A. Troegeler, C. Lastrucci, C. Duval, A. Tanne, C. Cougoule, I. Maridonneau-Parini, O. Neyrolles, G. Lugo-Villarino, An efficient siRNA-mediated gene silencing in primary human monocytes, dendritic cells and macrophages, Immunol. Cell Biol. 92 (2014) 699–708. https://doi.org/10.1038/icb.2014.39.
[419] P.W. Denton, O.S. Søgaard, M. Tolstrup, Impacts of HIV Cure Interventions on Viral Reservoirs in Tissues, Front. Microbiol. 10 (2019) 1–7. https://doi.org/10.3389/fmicb.2019.01956.
[420] C. Gavegnano, R.F. Schinazi, Antiretroviral Therapy in Macrophages: Implication for HIV Eradication, Antivir. Chem. Chemother. 20 (2009) 63–78. https://doi.org/10.3851/IMP1374.
[421] K. Vermeulen, D.R. Van Bockstaele, Z.N. Berneman, The cell cycle: a review of regulation, deregulation and therapeutic targets in cancer., Cell Prolif. 36 (2003) 131–49. https://doi.org/10.1306/74D715D2-2B21-11D7-8648000102C1865D.
[422] M. Malumbres, M. Barbacid, Mammalian cyclin-dependent kinases, Trends Biochem. Sci. 30 (2005) 630–641. https://doi.org/10.1016/j.tibs.2005.09.005.
[423] E. Lees, B. Faha, V. Dulic, S.I. Reed, E. Harlow, Cyclin E/cdk2 and cyclin A/cdk2 kinases associate with p107 and E2F in a temporally distinct manner., Genes Dev. 6 (1992) 1874–1885. https://doi.org/10.1101/gad.6.10.1874.
[424] J.J. Molenaar, M.E. Ebus, D. Geerts, J. Koster, F. Lamers, L.J. Valentijn, E.M. Westerhout, R. Versteeg, H.N. Caron, Inactivation of CDK2 is synthetically lethal to MYCN over-expressing cancer cells, Proc. Natl. Acad. Sci. 106 (2009) 12968–12973. https://doi.org/10.1073/pnas.0901418106.
[425] G.I. Shapiro, Cyclin-dependent kinase pathways as targets for cancer treatment, J. Clin. Oncol. 24 (2006) 1770–1783. https://doi.org/10.1200/JCO.2005.03.7689.
[426] T. Ammosova, R. Berro, M. Jerebtsova, A. Jackson, S. Charles, Z. Klase, W. Southerland, V.R. Gordeuk, F. Kashanchi, S. Nekhai, Phosphorylation of HIV-1 Tat by CDK2 in HIV-1 transcription, Retrovirology. 3 (2006) 1–21. https://doi.org/doi.org/10.1186/1742-4690-3-78.
[427] T. Ammosova, R. Berro, F. Kashanchi, S. Nekhai, RNA interference directed to CDK2 inhibits HIV-1 transcription, Virology. 341 (2005) 171–178. https://doi.org/10.1016/j.virol.2005.06.041.
[428] S.T. Davis, Prevention of Chemotherapy-Induced Alopecia in Rats by CDK Inhibitors, Science (80-.). 291 (2001) 134–137. https://doi.org/10.1126/science.291.5501.134.
[429] T.M. Bigley, J.M. Reitsma, S.S. Terhune, Antagonistic Relationship between Human Cytomegalovirus pUL27 and pUL97 Activities during Infection, J. Virol. 89 (2015) 10230–10246. https://doi.org/10.1128/JVI.00986-15.
[430] J.M. Perez Canadillas, Recognition of GU-rich polyadenylation regulatory elements by human CstF-64 protein, EMBO J. 22 (2003) 2821–2830. https://doi.org/10.1093/emboj/cdg259.
[431] PathCards, mRNA Splicing - Major Pathway, Weizmann Inst. Sci. (2019). https://pathcards.genecards.org/card/mrna_splicing_-_major_pathway.
[432] Y. Kargapolova, M. Levin, K. Lackner, S. Danckwardt, sCLIP—an integrated platform to study RNA–protein interactomes in biomedical research:

identification of CSTF2tau in alternative processing of small nuclear RNAs, Nucleic Acids Res. 45 (2017) 6074–6086. https://doi.org/10.1093/nar/gkx152.
[433] M. Aragaki, K. Takahashi, H. Akiyama, E. Tsuchiya, S. Kondo, Y. Nakamura, Y. Daigo, Characterization of a Cleavage Stimulation Factor, 3′ pre-RNA, Subunit 2, 64 kDa (CSTF2) as a Therapeutic Target for Lung Cancer, Clin. Cancer Res. 17 (2011) 5889–5900. https://doi.org/10.1158/1078-0432.CCR-11-0240.
[434] S. Naji, G. Ambrus, P. Cimermančič, J.R. Reyes, J.R. Johnson, R. Filbrandt, M.D. Huber, P. Vesely, N.J. Krogan, J.R. Yates, A.C. Saphire, L. Gerace, Host Cell Interactome of HIV-1 Rev Includes RNA Helicases Involved in Multiple Facets of Virus Production, Mol. Cell. Proteomics. 11 (2012) M111.015313. https://doi.org/10.1074/mcp.M111.015313.
[435] A. Kondrashov, H.A. Meijer, A. Barthet-Barateig, H.N. Parker, A. Khurshid, S. Tessier, M. Sicard, A.J. Knox, L. Pang, C.H. de Moor, Inhibition of polyadenylation reduces inflammatory gene induction, RNA. 18 (2012) 2236–2250. https://doi.org/10.1261/rna.032391.112.
[436] A.J. Bird, K. McCall, M. Kramer, E. Blankman, D.R. Winge, D.J. Eide, Zinc fingers can act as Zn2+ sensors to regulate transcriptional activation domain function, EMBO J. 22 (2003) 5137–5146. https://doi.org/10.1093/emboj/cdg484.
[437] A. Klug, The Discovery of Zinc Fingers and Their Applications in Gene Regulation and Genome Manipulation, Annu. Rev. Biochem. 79 (2010) 213–231. https://doi.org/10.1146/annurev-biochem-010909-095056.
[438] J.H. Laity, B.M. Lee, P.E. Wright, Zinc finger proteins: New insights into structural and functional diversity, Curr. Opin. Struct. Biol. 11 (2001) 39–46. https://doi.org/10.1016/S0959-440X(00)00167-6.
[439] K. Wu, W. Wang, Y. Ye, J. Huang, Y. Zhou, Y. Zhang, X. Zhang, W. Wu, Integration of protein interaction and gene co-expression information for identification of melanoma candidate genes, Melanoma Res. 29 (2019) 126–133. https://doi.org/10.1097/CMR.0000000000000525.
[440] D.H. Hua, Zinc finger ejectors and methods of use thereof, 2008. https://doi.org/10.1016/j.(73).
[441] M.L. Schito, A. Goel, Y. Song, J.K. Inman, R.J. Fattah, W.G. Rice, J.A. Turpin, A. Sher, E. Appella, In vivo antiviral activity of novel human immunodeficiency virus type 1 nucleocapsid p7 zinc finger inhibitors in a transgenic murine model., AIDS Res. Hum. Retroviruses. 19 (2003) 91–101. https://doi.org/10.1089/088922203762688595.
[442] J. Tassignon, J. Ismaili, A. Le Moine, F. Van Laethem, O. Leo, M. Vandevelde, M. Goldman, Azodicarbonamide inhibits T-cell responses in vitro and in vivo, Nat. Med. 5 (1999) 947–950. https://doi.org/10.1038/11392.
[443] C. Soto, E.M. Sigurdsson, L. Morelli, R. Asok Kumar, E.M. Castaño, B. Frangione, β-sheet breaker peptides inhibit fibrillogenesis in a rat brain model of amyloidosis: Implications for Alzheimer's therapy, Nat. Med. 4 (1998) 822–826. https://doi.org/10.1038/nm0798-822.
[444] W. Kühlbrandt, Structure and function of mitochondrial membrane protein complexes, BMC Biol. 13 (2015) 89. https://doi.org/10.1186/s12915-015-0201-x.
[445] R. Guo, J. Gu, M. Wu, M. Yang, Amazing structure of respirasome: unveiling the secrets of cell respiration, Protein Cell. 7 (2016) 854–865.

https://doi.org/10.1007/s13238-016-0329-7.
[446] M. Rak, P. Benit, D. Chretien, J. Bouchereau, M. Schiff, R. El-Khoury, A. Tzagoloff, P. Rustin, Mitochondrial cytochrome c oxidase deficiency, Clin. Sci. 130 (2016) 393–407. https://doi.org/10.1042/CS20150707.
[447] M. Elsner, S. Rauser, S. Maier, C. Schöne, B. Balluff, S. Meding, G. Jung, M. Nipp, H. Sarioglu, G. Maccarrone, M. Aichler, A. Feuchtinger, R. Langer, U. Jütting, M. Feith, B. Küster, M. Ueffing, H. Zitzelsberger, H. Höfler, A. Walch, MALDI imaging mass spectrometry reveals COX7A2, TAGLN2 and S100-A10 as novel prognostic markers in Barrett's adenocarcinoma, J. Proteomics. 75 (2012) 4693–4704. https://doi.org/10.1016/j.jprot.2012.02.012.
[448] L.L. Pearce, E. Lopez Manzano, S. Martinez-Bosch, J. Peterson, Antagonism of Nitric Oxide Toward the Inhibition of Cytochrome c Oxidase by Carbon Monoxide and Cyanide, Chem. Res. Toxicol. 21 (2008) 2073–2081. https://doi.org/10.1021/tx800140y.
[449] R. Mitchell, C.-Y. Chiang, C. Berry, F. Bushman, Global analysis of cellular transcription following infection with an hiv-based vector, Mol. Ther. 8 (2003) 674–687. https://doi.org/10.1016/S1525-0016(03)00215-6.
[450] L.A. Sazanov, A giant molecular proton pump: structure and mechanism of respiratory complex I, Nat. Rev. Mol. Cell Biol. 16 (2015) 375–388. https://doi.org/10.1038/nrm3997.
[451] A. V. Ivanov, V.T. Valuev-Elliston, O.N. Ivanova, S.N. Kochetkov, E.S. Starodubova, B. Bartosch, M.G. Isaguliants, Oxidative Stress during HIV Infection: Mechanisms and Consequences, Oxid. Med. Cell. Longev. 2016 (2016) 1–18. https://doi.org/10.1155/2016/8910396.
[452] C. Elbim, S. Pillet, M.H. Prevost, A. Preira, P.M. Girard, N. Rogine, H. Matusani, J. Hakim, N. Israel, M.A. Gougerot-Pocidalo, Redox and activation status of monocytes from human immunodeficiency virus-infected patients: relationship with viral load., J. Virol. 73 (1999) 4561–6. http://www.ncbi.nlm.nih.gov/pubmed/10233914%0Ahttp://www.pubmedcentral.nih.gov/articlerender.fcgi?artid=PMC112496.
[453] P. Aukrust, a M. Svardal, F. Müller, B. Lunden, R.K. Berge, P.M. Ueland, S.S. Frøland, Increased levels of oxidized glutathione in CD4+ lymphocytes associated with disturbed intracellular redox balance in human immunodeficiency virus type 1 infection., Blood. 86 (1995) 258–67. http://www.ncbi.nlm.nih.gov/pubmed/7795231.
[454] R.M. López Galera, J.C. Juárez Giménez, J.B. Montoro Ronsano, R.M. Segura Cardona, M.A. Arbós Via, C. Altisent Roca, J.M. Tusell Puigbert, Glutathione and cysteine in HIV-infected hemophiliacs., Clin. Chim. Acta. 254 (1996) 63–72. http://www.ncbi.nlm.nih.gov/pubmed/28580453.
[455] Treitinger, Spada, Verdi, Miranda, Oliveira, Silveira, Moriel, Abdalla, Decreased antioxidant defence in individuals infected by the human immunodeficiency virus, Eur. J. Clin. Invest. 30 (2000) 454–459. https://doi.org/10.1046/j.1365-2362.2000.00642.x.
[456] H.U. Simon, A. Haj-Yehia, F. Levi-Schaffer, Role of reactive oxygen species (ROS) in apoptosis induction., Apoptosis. 5 (2000) 415–8. https://doi.org/10.1023/A:1009616228304.
[457] Y. Kasahara, K. Iwai, A. Yachie, K. Ohta, A. Konno, H. Seki, T. Miyawaki, N.

Taniguchi, Involvement of reactive oxygen intermediates in spontaneous and CD95 (Fas/APO-1)-mediated apoptosis of neutrophils., Blood. 89 (1997) 1748–53. http://www.ncbi.nlm.nih.gov/pubmed/9057659.
[458] H. Pelicano, L. Feng, Y. Zhou, J.S. Carew, E.O. Hileman, W. Plunkett, M.J. Keating, P. Huang, Inhibition of Mitochondrial Respiration, J. Biol. Chem. 278 (2003) 37832–37839. https://doi.org/10.1074/jbc.M301546200.
[459] S.X.M. Dong, C.C.Y. Chang, Philosophical Principles of Life Science, Wunan Culture Enterprise, Taipei, 2012.
[460] M. Ogawa, Y. Takemoto, S. Sumi, D. Inoue, N. Kishimoto, N. Takamune, S. Shoji, S. Suzu, S. Misumi, ATP generation in a host cell in early-phase infection is increased by upregulation of cytochrome c oxidase activity via the p2 peptide from human immunodeficiency virus type 1 Gag, Retrovirology. 12 (2015) 1–14. https://doi.org/10.1186/s12977-015-0224-y.
[461] I.P. Hargreaves, A.J. Duncan, L. Wu, A. Agrawal, J.M. Land, S.J.R. Heales, Inhibition of mitochondrial complex IV leads to secondary loss complex II-III activity: Implications for the pathogenesis and treatment of mitochondrial encephalomyopathies, Mitochondrion. 7 (2007) 284–287. https://doi.org/10.1016/j.mito.2007.02.001.
[462] L. Wang, Q. Duan, T. Wang, M. Ahmed, N. Zhang, Y. Li, L. Li, X. Yao, Mitochondrial Respiratory Chain Inhibitors Involved in ROS Production Induced by Acute High Concentrations of Iodide and the Effects of SOD as a Protective Factor, Oxid. Med. Cell. Longev. 2015 (2015) 1–14. https://doi.org/10.1155/2015/217670.
[463] E.J. Wolvetang, K.L. Johnson, K. Krauer, S.J. Ralph, a W. Linnane, Mitochondrial respiratory chain inhibitors induce apoptosis., FEBS Lett. 339 (1994) 40–4. http://www.ncbi.nlm.nih.gov/pubmed/8313978.
[464] S. Jang, S. Javadov, Elucidating the contribution of ETC complexes I and II to the respirasome formation in cardiac mitochondria, Sci. Rep. 8 (2018) 17732. https://doi.org/10.1038/s41598-018-36040-9.
[465] E. Fernandez-Vizarra, M. Bugiani, P. Goffrini, F. Carrara, L. Farina, E. Procopio, A. Donati, G. Uziel, I. Ferrero, M. Zeviani, Impaired complex III assembly associated with BCS1L gene mutations in isolated mitochondrial encephalopathy, Hum. Mol. Genet. 16 (2007) 1241–1252. https://doi.org/10.1093/hmg/ddm072.
[466] A.A. Baran, K.A. Silverman, J. Zeskand, R. Koratkar, A. Palmer, K. McCullen, W.J. Curran, T.B. Edmonston, L.D. Siracusa, A.M. Buchberg, The modifier of Min 2 (Mom2) locus: Embryonic lethality of a mutation in the Atp5a1 gene suggests a novel mechanism of polyp suppression, Genome Res. 17 (2007) 566–576. https://doi.org/10.1101/gr.6089707.
[467] M. SADAIE, R. MAYNER, J. DONIGER, A novel approach to develop anti-HIV drugs: adapting non-nucleoside anticancer chemotherapeutics, Antiviral Res. 61 (2004) 1–18. https://doi.org/10.1016/j.antiviral.2003.09.004.
[468] A. Guihot, A.-G. Marcelin, M.-A. Massiani, A. Samri, C. Soulié, B. Autran, J.-P. Spano, Drastic decrease of the HIV reservoir in a patient treated with nivolumab for lung cancer, Ann. Oncol. 29 (2018) 517–518. https://doi.org/10.1093/annonc/mdx696.
[469] W.A. Chow, C. Jiang, M. Guan, Anti-HIV drugs for cancer therapeutics: back to

the future?, Lancet Oncol. 10 (2009) 61–71. https://doi.org/10.1016/S1470-2045(08)70334-6.
[470] A.D. Badley, K. Parato, D.W. Cameron, S. Kravcik, B.N. Phenix, D. Ashby, A. Kumar, D.H. Lynch, J. Tschopp, J.B. Angel, Dynamic correlation of apoptosis and immune activation during treatment of HIV infection, Cell Death Differ. 6 (1999) 420–432. https://doi.org/10.1038/sj.cdd.4400509.
[471] M. Qian, S.A. Murphy, Performance guarantees for individualized treatment rules, Ann. Stat. 39 (2011) 1180–1210. https://doi.org/10.1214/10-AOS864.
[472] Y. Xin, Y.T. Fong, G. Wolf, D. Wolf, W. Cao, Protective effect of XY99-5038 on hydrogen peroxide induced cell death in cultured retinal neurons, Life Sci. 69 (2001) 289–299. https://doi.org/10.1016/S0024-3205(01)01122-5.
[473] and W.C. Yan, X., Y. T. Fong, G. Wolf, D. Brackett, M. Zaharia, D. Wolf, M. R. Lerner, G. D. Lee, Role of XY99-5038 in neuronal survival and protection, in: 4th World Conf. Mol. Biol. Cell Signaling, Transcr. Transl. as Ther. Targets, Luxemb., 2002.
[474] X. Yan, F. Li, I. Dozmorov, M.B. Frank, M. Dao, M. Centola, W. Cao, D. Hu, External Qi of Yan Xin Qigong induces cell death and gene expression alterations promoting apoptosis and inhibiting proliferation, migration and glucose metabolism in small-cell lung cancer cells, Mol. Cell. Biochem. 363 (2012) 245–255. https://doi.org/10.1007/s11010-011-1176-8.
[475] K. Schroder, P.J. Hertzog, T. Ravasi, D.A. Hume, Interferon- y : an overview of signals , mechanisms and functions, J. Leukoc. Biol. 75 (2004) 163–189. https://doi.org/10.1189/jlb.0603252.Journal.

9. Contributions of Collaborators

The experiments depicted in **Figure 15** were performed by Niranjala Gajanayaka; the experiments depicted in **Figure 12-14** and **Figure 20-25** were performed by Ramon Edwin Caballero.

Our lab also has experiments in collaboration with Dr. Franco Vizeacoumar's Lab, Department of Pathology, Cancer Cluster, College of Medicine, University of Saskatchewan, Saskatoon. Dr. Franco Vizeacoumar's Lab provided the protocol of the 90k shRNA lentivirus pool technology and prepared the 90k shRNA lentivirus pool. After customization of the protocol and application of 90k shRNA lentivirus pool to U937 and U1, we submitted the genomic DNA to Dr. Franco Vizeacoumar's Lab for micro-array and computer analysis, and they issued the report with 28 promising genes, **Figure 31**.

10. Appendices

10.1 Target sequences of siRNAs in this research

Note: Only BLOCK-iT™ Alexa Fluor™ Red Fluorescent Control was purchased from ThermoFisher Scientific Invitrogen; all other siRNAs were purchased from Dharmacon.

Gene	Catalogue #:	N0.	Target Sequences from 5' to 3'
Bax	E-003308-00-0005	1	GUGGCAGCUGACAUGUUUU
		2	GCGUUUUCCUUACGUGUCU
		3	GACCUUGACUUGAUUAGUG
		4	UGGAAUUGCUCAAGUUCAU
BLOCK-iT™ Alexa Fluor™ Red Fluorescent Control	ThermoFisher Scientific Invitrogen	1	UCGAGAAGAUGAUCUGACUGCCUGG
		2	UUAUCUCUCAGCUCCACGCCAUUGG
		3	AGACUCGGCAAAGUCGAGAUAGUCG
Accell Non-targeting	D-001950-01-05	1	UGGUUUACAUGUCGACUAA
xIAP	L-004098-00-0005	1	GUAGAUAGAUGGCAAUAUG
		2	GAACUGGGCAGGUUGUAGA
		3	GAAAGAGAUUAGUACUGAA
		4	GGACUCUACUACACAGGUA
cIAP1	L-004390-00-0005	1	UCGCAAUGAUGAUGUCAAA
		2	GAAUGAAAGGCCAAGAGUU
		3	GAAAUGCUGCGGCCAACAU
		4	UAUAGGACCUGGAGAUAGG
cIAP2	L-004099-00-0005	1	CAUGUGAACUGUACCGAAU
		2	UAACGAAAAUGCCAGAUUA
		3	GUUCAUCCGUCAAGUUCAA
		4	CUAACUGCCGGAAUUAUUA
Human NDUFA11 (Complex I)	L-018508-01-0005	1	GCUGGGAGGUGUUUGCAAA
		2	GGCUAAGGUUGGACAAUAC
		3	CUGCGUGUACUUUGGCAUA
		4	GAGCACGCACGCACAACUA
Human SDHA (Complex II)	L-009398-01-0005	1	AAAGGUUUAUGGAGCGAUA
		2	CGAAGGACCUGGCGUCUAG
		3	GGACUGGCCACGCGCUAUU
		4	GGUGCUGGUUGUCUCAUUA
Human UQCRQ (Complex III)	L-012517-01-0005	1	UGACAAAUGAGCAACGCAU
		2	GGGACUGAAGAGUUCGAGA
		3	CGGCAUGUGAUCAGCUACA
		4	GGUCUGCACUGUUGUGAUA
Human ATP5A1 (Complex V)	L-017064-01-0005	1	GCUGGGAGGUGUUUGCAAA
		2	GGCUAAGGUUGGACAAUAC
		3	CUGCGUGUACUUUGGCAUA
		4	GAGCACGCACGCACAACUA

RPS6KA3	L-003026-00	1	AUACAAUGCUUACCGGUUA
		2	CUACAUAGCCUGGGAAUAA
		3	CGUAAUCAGUCACCAGUUU
		4	GACAGCAAAUUAUGGAUGA
FGFR1	L-003131-00	1	GCCACACUCUGCACCGCUA
		2	CCACAGAAUUGGAGGCUAC
		3	CAAAUGCCCUUCCAGUGGG
		4	GAAAUUGCAUGCAGUGCCG
PFKFB3	L-006763-00	1	CGACGACCCUACAGUUGUG
		2	CAAGUACUAUUACCGCUAC
		3	GGACCUAACCCGCUCAUGA
		4	AAAGCUACCUGGCGAAAGA
TKT	L-004734-00	1	GGAACUAGCCGCCAAUACA
		2	CCGUGGAGGACCAUUAUUA
		3	GCAGUUAACCGGGUACCAA
		4	GAUAAGGAGUCUUGGCAUG
ERBB3	L-003127-00	1	GCGAUGCUGAGAACCAAUA
		2	AGAUUGUGCUCACGGGACA
		3	GCAGUGGAUUCGAGAAGUG
		4	UCGUCAUGUUGAACUAUAA
HDAC7	L-009330-00	1	GACAAGAGCAAGCGAAGUG
		2	GCAGAUACCCUCGGCUGAA
		3	GGUGAGGGCUUCAAUGUCA
		4	UGGCUGCUCUUCUGGGUAA
TMED10	L-003718-00	1	CCAAGAAAUUGAUUGAGUA
		2	CAAACACUCGGGUCCUAUA
		3	GGAAUGAGUUAUGCUGUUA
		4	AAUAAUCACUGUAGGAGUA
RPS6KB2	L-004671-00	1	GCGGAACAUUCUAGAGUCA
		2	GUUGAGGGCAGCUGGCCUA
		3	GGAAGAAAACCAUGGAUAA
		4	GGAACUGGCCUAUGCCUUC
CDK2	L-003236-00	1	GAGCUUAACCAUCCUAAUA
		2	GAAACAAGUUGACGGGAGA
		3	GGAGUUACUUCUAUGCCUG
		4	GGGCCUAGCUUUCUGCCAU
ZNF805	L-031184-02	1	ACUCAAUGUCUUUGUUCUA
		2	GUUAUUACGCACUUGGGAA
		3	GGAUUAUACAGGAUCGAGU
		4	ACUCACAUGGAUCAGGUAA
ZMYND19	L-021402-02	1	CCAAAUACACGCUGAUCGA
		2	CUUAAAUGGCAAACGGUCA
		3	CUAAAUGUGACCCGGUAUU

ZMYND19	L-021402-02	4	AAACUGUCCUGUUGUCGAA
CSTF2T	L-021449-02	1	GUUCAGUGGGAGAGCGCUU
		2	ACAAGGAGUCAGUAUACAA
		3	GAGGAUAACUCGCGUUUAC
		4	CCACUGGAGCGUCUUGAAA
MTOR	L-003008-00	1	GGCCAUAGCUAGCCUCAUA
		2	CAAAGGACUUCGCCCAUAA
		3	GCAGAAUUGUCAAGGGAUA
		4	CCAAAGCACUACACUACAA
ZNF484	L-026258-02	1	GGGAAAUAGUUCAUGUAAA
		2	CAUUAUGAGUGCAGUGAAU
		3	UGAUAAGACUAUUGGAGAU
		4	GAACAAACCUUUAAGUCGU
AVL9	L-025311-01	1	GGUCACAACUAGCCGGAAU
		2	ACAUCGUGGUGGUCGGAUU
		3	CAGUAUAGACCCCGGAAAA
		4	CUGGGAGGGAGGUGACGAA
BPHL	L-008262-00	1	GCAGAUGAAUUCAACAAGU
		2	GGGCAUAACCGCACUCAUU
		3	GCUACUUCCUGGGAUGUUA
		4	CAUGCCGACUUCAUUCAUA
BUB1B	L-004101-00	1	CAAUACAGCUUCACUGAUA
		2	GCAAUGAGCCUUUGGAUAU
		3	GAAACGGGCAUUUGAAUAU
		4	GAUGGUGAAUUGUGGAAUA
HLA-DRB4	L-013225-01	1	GGACGGAGCGAGUGUGGAA
		2	ACGGGGUUGUGGAGAGCUU
		3	GCGCUACAACAGUGACCUG
		4	GUAUGGCAGCGCUGACAGU
MORC2-AS1	R-016517-00	1	GCACUGGACUCGCCGUUAU
		2	CUGUUUCUGUGGAUGUUAA
		3	UGAGGUGGUUAGACAGGAU
		4	UCAAGUUACUGUGGUGAGA
BCL3	L-003874-00	1	AGACACGCCUCUCCAUAUU
		2	GGCCGGAGGCGCUUUACUA
		3	GCGCAAAUGUACUCCGGCA
		4	GCCGGGAGCUCGACAUCUA
WEE1	L-005050-00	1	AAUAGAACAUCUCGACUUA
		2	AAUAUGAAGUCCCGGUAUA
		3	GAUCAUAUGCUUAUACAGA
		4	CGACAGACUCCUCAAGUGA
TBC1D21	L-016748-02	1	UAACAUUGCACGUGACAUU
		2	GCAACGUCCUCAUCGACAA

TBC1D21	L-016748-02	3	GCAACAACCUCAUCGACCU
		4	CUUCAAGUCCUUCGAUGAU
HSPE1	L-019649-00	1	GGACAAGCGUUUAGAAAGU
		2	GCAAGCAACAGUAGUCGCU
		3	CCACUGAAGUUCUGAAAUC
		4	UGAAAUGGCAUCAACAUGA
IL17RE	L-007947-02	1	GCAAAGACCUCCCGAAUGC
		2	GAGGACGACUGGCCGAAAA
		3	GGAAUGAGCCUUCGACCCU
		4	GCAUGGAGGACCCGAGUUC
PLA2G2E	L-010283-00	1	CCGCAAAUAUGCCCAUUAU
		2	GCUACGGGCGUCUGGAGAA
		3	AGUCCGCCCUGCAGUACAA
		4	UGUCAGCGAACGUGGCAUU
ASGR1	L-013268-00	1	GGCAAUGGCUCAGAAAGGA
		2	GGGCUGACGCCGACAACUA
		3	GAGCGCAGCUGCUACUGGU
		4	GCAGAAAUUUGUCCAGCAC
CDK19	L-004689-00	1	GAGCAUGACUUGUGGCAUA
		2	GAUCGGAUAUUUAGUGUCA
		3	UAAAGCCACUAGCAGAUUU
		4	UAUGGCUGCUGUUUGAUUA
CSF1R	L-003109-00	1	GGAAGAUCAUCGAGAGCUA
		2	GGUGAAGGAUGGAUACCAA
		3	GUAACGUGCUGUUGACCAA
		4	CCAGCAGCGUUGAUGUUAA
COX7A2	L-011626-01	1	CAGAUUGGGCAGAGGACGA
		2	GUAUCUAAAGGGUGGGGUA
		3	CUGUAUAGAGCCACCAUGA
		4	UCCAGGAGGAUGAUGAAAU

10.2 Author Permission to use HIV Gag-iGFP(envJRFL) plasmid map

Figure 4A: pNL4.3 BAL IRES HSA plasmid map

Benjamin K. Chen

Subject: Re: Request for permission to use a plasmid map and DNA sequence in PhD Thesis
From: Chen, Benjamin
Sent: Tuesday, May 7, 2019 10:23 AM
To: Simon X.M Dong

Dear Mr. Dong,
You have my permission.
Good luck with your thesis.

Benjamin K. Chen
Professor of Icahn School of Medicine at Mount Sinai

On Monday, May 6, 2019 2:01 PM, Simon X. M. Dong wrote:

Subject: Request for permission to use a plasmid map and DNA sequence in PhD Thesis

Hi, Dr. Benjamin K. Chen,

I am a PhD student at the University of Ottawa, Children's Hospital of Eastern Ontario. My supervisor is Dr. Ashok Kumar. This email is to request your permission to use a plasmid map (HIV Gag-iGFP(envJRFL) and use this plasmid as the template to clone 6 HIV-1 single genes into lentivirus in my PhD Thesis.

A couple of years ago, we bought this Plasmid from NIH (Cat. #: 12456), and we downloaded all the related information including DNA sequence from NIH website. We were directed to cite your papers published in 2007 by NIH website. This plasmid DNA was used in my research to produce HIV-1 viruses for the topic "Selective induction of the apoptosis in HIV-infected macrophages". To further study the pathogenesis of HIV-1 infection, we also used this plasmid as templates to amplify 6 single genes: Vpr, Vpu, Tat, Vif, Nef, and Env.

Currently, I am writing my PhD thesis. The plasmid map and the sequences of these single HIV-1 genes from this plasmid are essential information to understand my project. I would like to use this map as important background information in the introduction part to help our readers. So, I hope I can get your permission to use the information in my PhD thesis.

Thank you very much, and I am looking forward to hearing from you soon.
Best Wishes,
Simon Xin Min Dong
PhD Candidate at the University of Ottawa

10.3 Author Permission to use pNL4.3 BAL IRES HSA plasmid map

Figure 4B: pNL4.3 BAL IRES HSA plasmid map

Michel J. Tremblay, PhD

Subject: Re: Request for permission to use a plasmid map in PhD Thesis

From: Michel J. Tremblay

Date: Wednesday, May 1, 2019 11:39 AM

To: Simon X.M. Dong

Dear Mr. Dong,

Yes, you have my permission.

Sincerely yours.

Michel J. Tremblay, Ph.D

Vice-recteur adjoint à la recherche, à la création et à l'innovation (VRRCI)

On May 1, 2019, at 11:12AM, Simon X. M. Dong wrote:

Dear Dr. Michel J. Tremblay,

I am a PhD student of Dr. Ashok Kumar at the University of Ottawa, Children's Hospital of Eastern Ontario. I am writing to request your permission to use a plasmid map (pNL4.3 BAL IRES HSA 15665bp) in my PhD Thesis.

A couple of years ago, under the request of Dr. Kumar, you send us this plasmid with the map and sequence. This plasmid DNA was used in my research to produce HIV-1 viruses for the topic "Selective induction of the apoptosis in HIV-infected macrophages".

Currently, I am writing my PhD thesis. The plasmid map from you is essential information to understand my project. I would like to use this map in the introduction part as an important background information to help my readers. So, I hope I can get your permission to use this figure in my thesis.

Thank you very much, and I am looking forward to hearing from you soon.

Best wishes,

Simon Xin Min Dong

PhD Candidate at the University of Ottawa

10.4 Author Permission to use a figure on the electron transport chain

Figure 40. Structure and function of respiratory chain in mitochondrion

Prof. Leonid Sazanov

Subject: **Re: Permission to use one of your figures in PhD thesis**

From: Leonid Sazanov

Date: Saturday, Sept. 14, 2019, 6:16 AM

To: Simon X.M Dong

Simon X.M. Dong,

Yes, ok.

Best

Prof. Leonid Sazanov FRS

IST Austria, Am Campus 1, A-3400 Klosterneuburg, Austria

On Sept. 13, 2019, at 12:13PM, Simon X. M. Dong wrote:

Dear Dr. Leonid A. Sazanov

I am a PhD student at the University of Ottawa, Canada. Currently, I am writing my PhD thesis. I would like to use your **Figure 1. The electron transport chain** in your Review Paper entitled "**A giant molecular proton pump: structure and mechanism of respiratory complex I**" in my PhD thesis. This figure will help my readers and audiences understand the background information of my research. So, I write you this email, wondering if I can get your permission to use this figure in my PhD thesis.

Thank you very much, have a nice weekend, and I am looking forward to hearing from you soon.

Simon Xin Min Dong
PhD Candidate at the University of Ottawa
451 Smyth Road, Ottawa, Ontario, K1H 8M5